

Mechanical Behaviour, Water Absorption and Morphology of Wheat Straw, Talc, Mica and Wollastonite filled Polypropylene Composites

by

Arathi Mohan Sharma

A thesis
presented to the University of Waterloo
in fulfillment of the
thesis requirement for the degree of
Master of Applied Science
in
Chemical Engineering

Waterloo, Ontario, Canada, 2012

© Arathi Mohan Sharma 2012

AUTHOR'S DECLARATION

I hereby declare that I am the sole author of this thesis. This is a true copy of the thesis, including any required final revisions, as accepted by my examiners.

I understand that my thesis may be made electronically available to the public.

ABSTRACT

Polypropylene continues to be the mainstream choice thermoplastic for automotive applications. In many applications PP is filled with mineral fillers for improvement of properties. Biobased natural fillers or fibres are attractive materials to reduce the weight because of the low specific gravity of the biobased materials compared to the mineral fillers.

Our group has done extensive research on the development of wheat straw fiber in thermoplastics in the past years. It is very important to understand the behaviour of single fillers on composites before studying the effects of mixing fillers or fibers (hybridization). The objective of this study is to evaluate and compare systematically the effects of wheat straw and mineral fillers in the polypropylene matrix. The study includes two types of wheat straw (WS) categorized based on their size (fine WS and medium WS) and three different types of natural minerals (Talc, Mica and Wollastonite). Three types of polypropylene (PP), Homopolymer PP, High Impact Copolymer PP and Homopolymer-Copolymer Blend PP, were investigated as the matrix. This study also evaluates the effect of combining two fillers (WS and mineral filler) in the hybrid composite. The fillers were formulated in three different percentages (20, 30 and 40wt %) and compounded via extrusion. Samples for all formulations were prepared by injection molding. The mechanical properties (flexural modulus and strength, tensile modulus and strength, impact strength), water absorption and density were measured. The properties of hybrid composites were evaluated by varying the amounts of two fillers at 10wt%-20wt%, 15wt%-15wt% and 20wt%-10wt% each, keeping the overall filler content constant at 30wt%.

The effect of type of filler, filler size and filler content were critical in this work. The results obtained from this study indicated that filler type and filler content greatly influenced the mechanical properties and water absorption characteristics of the composites. The flexural modulus increased with increasing filler content. It was interesting to observe that though the impact strength decreased with the addition of fillers, increasing the filler content from 20 to 40 wt% did not affect the property. With respect to all fillers, wollastonite improved the mechanical properties significantly. Increasing the amount of WS content reduced the composite's resistance to water absorption. Among mineral fillers, mica showed significantly higher percentage gain in weight with water absorption. Combination of fillers at varying percentages did not have any

synergy effect on the mechanical behaviour of the composite. The percentage increase in weight with water absorption was observed to be increasing with increasing WS content in hybrid composites, but significantly lower than pure WS composites. The morphological study on WS composites revealed improved interaction of filler with homopolymer and polypropylene blend.

ACKNOWLEDGEMENTS

I would like to express my sincere gratitude to my supervisor Dr. Leonardo C. Simon, for his valuable guidance, assistance and support rendered throughout my graduate program.

I would like to thank Dr. Ting Tsui and Dr. Aiping Yu, my thesis committee members, for accepting to be the readers for my thesis, and for all their help and guidance.

I would also like to thank Dr. Mehdi Tajvidi, visiting professor from Iran, for his valuable advice.

Thanks to all my friends and colleagues, especially Dr. C. Ravindra Reddy, Dr. Muhammad Arif and Zeinab Jahed for their time and assistance during my research work.

Indeed a special thanks to co-op students, Kelvin, Brent, Hasaan and Ambrose for their valuable help, encouragement, support and good humour all along the way.

Finally I would like to thank OMAFRA-Industrial Bioproducts Program and NSERC Discovery Program for their financial support. Also, sincere thanks to industrial partners A. Schulman Inc., Omtec Inc. and Braskem SA for offering raw materials needed for this work.

DEDICATION

I would like to dedicate this thesis to my beloved husband, Gautam, who has showered enormous love and supported me in all ways throughout my graduate studies.

TABLE OF CONTENTS

List of Figures	x
List of Tables	xiii
List of Abbreviations	xiv
1 Introduction	1
1.1 Motivation and Objectives	2
1.2 Organization of Thesis	3
1.3 Project Plan	4
2 Literature Review	6
2.1 Thermoplastic Composites in Automotive Applications	6
2.2 Polypropylene: Processing Techniques	11
2.3 Fillers	20
2.4 Polypropylene Composites	21
2.4.1 Natural Fibre Polypropylene Composites	23
2.4.2 Mineral Filler - Polypropylene Composites	27
2.4.3 Other Common Inorganic Fillers and Glass Fiber	31
2.5 Biocomposite Composition	33
2.5.1 Polypropylene Matrix	33
2.5.2 Mineral Fillers	35
2.5.3 Wheat Straw	37
2.5.4 Additives	40
2.6 Properties of Interest	43
2.6.1 Mechanical Properties	43
2.6.2 Differential Scanning Calorimetry	46
2.6.3 Scanning Electron Microscopy	47
2.6.4 Water Absorption	47
3 Materials and Methods	49
3.1 Materials	49

3.2	Processing Methods	50
3.2.1	Compounding via Extrusion	50
3.2.2	Injection Molding	51
3.3	Characterization Methods	51
3.3.1	Morphology.....	51
3.3.2	Particle Size Analysis.....	52
3.3.3	Differential Scanning Calorimetry (DSC).....	53
3.3.4	Melt Flow Index (MFI)	53
3.3.5	Water Absorption.....	53
3.3.6	Density	54
3.3.7	Moisture Content	54
3.3.8	Mechanical Properties.....	55
4	Results and Discussions: Polypropylene Resins.....	58
4.1	Formulations.....	58
4.2	Properties	58
4.2.1	Differential Scanning Calorimetry	58
4.2.2	Melt Flow Index.....	60
4.2.3	Water Absorption.....	61
5	Results and Discussions: Polypropylene-Filler Composites	62
5.1	Characterization of Wheat Straw.....	62
5.1.1	Particle Size Analysis.....	62
5.1.2	Moisture Content Analysis.....	65
5.2	Formulations and Properties: Polypropylene-Filler Composites	66
5.2.1	Flexural Strength	68
5.2.2	Flexural Modulus.....	71
5.2.3	Tensile Strength	73
5.2.4	Tensile Modulus	75
5.2.5	Impact Strength.....	77
5.2.6	Specific Flexural Modulus	79
5.2.7	SEM.....	81
5.2.8	Water Absorption.....	85
6	Results and Discussions: Polypropylene Hybrid Composites	90

6.1	Formulations and Properties	90
6.1.1	Flexural strength	93
6.1.2	Flexural Modulus.....	98
6.1.3	Tensile strength.....	102
6.1.4	Tensile Modulus	107
6.1.5	Impact strength.....	111
6.1.6	Specific Flexural Modulus	115
6.1.7	SEM.....	118
6.1.8	Water Absorption.....	125
7	Conclusions and Recommendations.....	134
	References	140
	Permissions Page.....	147
	Appendix.....	155

LIST OF FIGURES

Figure 1.1 Schematic Representation of the Work Plan	5
Figure 2.1 PP Compounds for Automobiles (Moritomi 2010)	10
Figure 2.2 Structure of Polypropylene.....	11
Figure 2.3 Stereoregularity in PP chain-Isotactic, Syndiotactic and Atactic	12
Figure 2.4 Processing methods for PP, USA, 1996 (Maier 1998)	13
Figure 2.5 Polypropylene extrusion processes, USA, 1996 (Maier 1998)	14
Figure 2.6 Schematic Diagram of an Extruder, Source: Tadmor, Klien 1970.....	15
Figure 2.7 Schematic Diagram of a Screw - Injection Molding Machine	16
Figure 2.8 Schematic of a Basic Extrusion Blow Molding Process (CustomPartNet 2008)	17
Figure 2.9 Basic Pressure Thermoforming Process (CustomPartNet 2008).....	19
Figure 2.10 (a) Disposable Products, (b) Blister Packaging	20
Figure 2.11 Fillers used in Thermoplastic Composites	23
Figure 2.12 Structure of Cellulose	24
Figure 2.13 Cellulose, Hemicellulose and Lignin (Sannigrahi 2010)	25
Figure 2.14 Consumption of Bio-fibers within Western Europe (Thomas, Pothan 2009)	27
Figure 2.15 Morphologies of Different Minerals	30
Figure 2.16 Crystalline Silica (Wypych 1993)	33
Figure 2.17 Two Phase Structure of Impact Modified Polypropylene (Calhoun 2006).....	34
Figure 2.18 WS in Flex 2010.....	39
Figure 2.19 Chain Breaking Antioxidant.....	41
Figure 2.20 Irganox 1010.....	42
Figure 2.21 Irgafos 168.....	42
Figure 2.22 Mechanism of MAPP Adhesion with Fiber Surface (Rowell 2007).....	43
Figure 3.1 Haake Minilab Microcompounder (left) and conical screws (right).	50
Figure 3.2 Best Fitting Ellipses for fWS Particles.....	52
Figure 4.1 Plot showing MFI Values for pure Resins	60
Figure 4.2 Water Absorption plots for hPP, icPP and bPP Resins	61
Figure 5.1 Optical Microscope Image of (a) fine WS and (b) medium WS.....	62
Figure 5.2 Plot Showing Length Distributions of Fine and Medium WS Particles.....	63
Figure 5.3 Plot Showing Width Distributions of Fine and Medium WS Particles	64
Figure 5.4 Plot Showing Aspect Ratio of Fine and Medium WS Particles	64
Figure 5.5 Flexural Strength of Single Filler (a) hPP, (b) icPP and (c) bPP Composites.....	70
Figure 5.6 Flexural Modulus of Single Filler (a) hPP, (b) icPP and (c) bPP Composites	72
Figure 5.7 Tensile Strength of Single Filler (a) hPP, (b) icPP and (c) bPP Composites	74
Figure 5.8 Tensile Modulus of Single Filler (a) hPP, (b) icPP and (c) bPP Composites	76
Figure 5.9 Impact Strength of Single Filler (a) hPP, (b) icPP and (c) bPP Composites.....	78

Figure 5.10 Specific Flexural Modulus of Single Filler (a) hPP, (b) icPP and (c) bPP Composites	80
Figure 5.11 SEM of 30 wt% fWS-hPP composite (1000X)	82
Figure 5.12 SEM of 30 wt% fWS-icPP composite (500X)	83
Figure 5.13 SEM of 30 wt% fWS-bPP composite (500X)	83
Figure 5.14 SEM of 30 wt% mWS-icPP composite (500X)	84
Figure 5.15 SEM of 30 wt% mWS-bPP Composite (300X)	84
Figure 5.16 Water Absorption Plot for WS filled (a) hPP, (b) icPP and (c) bPP Composites	86
Figure 5.17 Water Absorption Plot for Mineral filled hPP Composites.....	87
Figure 5.18 Water Absorption Plot for Mineral filled icPP Composites.....	87
Figure 5.19 Water Absorption Plot for Mineral filled bPP Composites.....	88
Figure 6.1 Flexural Strength of (a) Mineral/fWS (b) Mineral/mWS hPP Composites	93
Figure 6.2 Flexural Strength of (a) Mineral/fWS (b) Mineral/mWS icPP Composites.....	95
Figure 6.3 Flexural Strength of (a) Mineral/fWS (b) Mineral/mWS bPP Composites	96
Figure 6.4 Flexural Modulus of (a) Mineral/fWS (b) Mineral/mWS hPP Composites.....	98
Figure 6.5 Flexural Modulus of (a) Mineral/fWS (b) Mineral/mWS icPP Composites.....	99
Figure 6.6 Flexural Modulus of (a) Mineral/fWS (b) Mineral/mWS bPP Composites.....	101
Figure 6.7 Tensile Strength of (a) Mineral/fWS (b) Mineral/mWS hPP Composites.....	102
Figure 6.8 Tensile Strength of (a) Mineral/fWS (b) Mineral/mWS icPP Composites	104
Figure 6.9 Tensile Strength of (a) Mineral/fWS (b) Mineral/mWS bPP Composites	105
Figure 6.10 Tensile Modulus of (a) Mineral/fWS (b) Mineral/mWS hPP Composites	107
Figure 6.11 Tensile Modulus of (a) Mineral/fWS (b) Mineral/mWS icPP Composites	108
Figure 6.12 Tensile Modulus of (a) Mineral/fWS (b) Mineral/mWS bPP Composites	109
Figure 6.13 Impact Strength of (a) Mineral/fWS (b) Mineral/mWS hPP Composites.....	111
Figure 6.14 Impact Strength of (a) Mineral/fWS (b) Mineral/mWS icPP Composites.....	112
Figure 6.15 Impact Strength of (a) Mineral/fWS (b) Mineral/mWS bPP Composites.....	113
Figure 6.16 Specific Flexural Modulus of (a) Mineral/fWS (b) Mineral/mWS hPP Composites	115
Figure 6.17 Specific Flexural Modulus of (a) Mineral/fWS (b) Mineral/mWS icPP Composites	116
Figure 6.18 Specific Flexural Modulus of (a) Mineral/fWS (b) Mineral/mWS bPP Composites	117
Figure 6.19 SEM of 15% talc-15%fWS-hPP Composite (1000X).....	120
Figure 6.20 SEM of 15% mica-15%fWS-hPP Composite (500X).....	120
Figure 6.21 SEM of 15% talc-15%fWS-icPP Composite (1000X).....	121
Figure 6.22 SEM of 15% mica-15%fWS-icPP Composite (500X).....	121
Figure 6.23 SEM of 15% wollastonite-15%fWS-icPP Composite (500X).....	122
Figure 6.24 SEM of 15% talc-15%fWS-bPP Composite (1000X).....	122
Figure 6.25 SEM of 15% mica-15%fWS-bPP Composite (1000X).....	123
Figure 6.26 SEM of 15% talc-15%mWS-hPP Composite (500X).....	123

Figure 6.27 SEM of 15% talc-15% mWS-icPP Composite (500X)	124
Figure 6.28 SEM of 15% mica-15% mWS-icPP Composite (500X)	124
Figure 6.29 SEM of 15% talc-15% mWS-bPP Composite (500X)	125
Figure 6.30 Water Absorption Plots for Mineral/fWS hPP Composites	128
Figure 6.31 Water Absorption Plots for Mineral/mWS hPP Composites	129
Figure 6.32 Water Absorption Plots for Mineral/fWS icPP Composites	130
Figure 6.33 Water Absorption Plots for Mineral/mWS icPP Composites.....	131
Figure 6.34 Water Absorption Plots for Mineral/fWS bPP Composites	132
Figure 6.35 Water Absorption Plots for Mineral/mWS icPP Composites.....	133
Figure A.1 DSC Plot for Homopolymer PP without Antioxidant	155
Figure A.2 DSC Plot for Homopolymer PP with Antioxidant	156
Figure A.3 DSC Plot for Impact Copolymer PP without Antioxidant	156
Figure A.4 DSC Plot for Impact Copolymer PP with Antioxidant	157
Figure A.5 DSC Plot for Homopolymer-Copolymer Blend PP without Antioxidant	157
Figure A.6 DSC Plot for Homopolymer-Copolymer Blend PP with Antioxidant	158
Figure A.7 SEM of 30wt% mWS-hPP Composite (100X).....	159
Figure A.8 SEM of 15% wollastonite-15% fWS-hPP Composite (500X)	159
Figure A.9 SEM of 15% wollastonite-15% fWS-bPP Composite (500X)	160
Figure A.10 SEM of 15% mica-15% mWS-hPP Composite (500X)	160
Figure A.11 SEM of 15% mica-15% mWS-bPP Composite (500X)	161

LIST OF TABLES

Table 2.1 Thermoplastics and their Automotive Applications	7
Table 2.2 Merits and Demerits of PP for its Use in Automotive Industry.....	9
Table 2.3 PP Property Requirements	10
Table 2.4 Extrusion and Injection Blow Molding	18
Table 2.5 Particle Morphology of Fillers.....	21
Table 2.6 Mechanical Properties of some of the Organic and Inorganic fibres	26
Table 2.7 Mineral fillers used in Western Europe (Hancock, Rothon 2003)	28
Table 2.8 World Filler Consumption in 1999 (Zweifel 2001).....	29
Table 2.9 Properties of Wollastonite with different aspect ratios.....	37
Table 2.10 Composition of WS at Different Location of Cultivation (McKean, Jacobs 1997)	38
Table 3.1 Specimen Dimensions According to ASTM Standards.....	57
Table 4.1 Formulations for Pure Polypropylene Resins	58
Table 4.2 Results from DSC Analysis	59
Table 4.3 Melt Flow Index for PP Resins.....	60
Table 5.1 Moisture Content Results for Fillers.....	65
Table 5.2 Formulations and Properties Chart for Single Filler PP Composites	66
Table 6.1 Formulations and Properties Chart for Hybrid PP Composites.....	90
Table 7.1 Summary of Formulation-Property Relationship	136

LIST OF ABBREVIATIONS

%	Percentage
ε	Strain
σ	Stress
α	Alpha
ABS	Acrylonitrile butadiene styrene
AO	Antioxidant
ASTM	American Standard for Testing of Materials
β	Beta
bPP	Homopolymer-Copolymer Blend Polypropylene
cm	Centimeter
CA	Coupling agent
CaO	Calcium oxide
D	Diameter
DSC	Differential Scanning Calorimetry
E	Young's Modulus or Modulus of Elasticity
EPR	Ethylene-propylene rubber
fWS	Fine wheat straw
g	Grams
GPa	Gega Pascal
Hr	Hour
hPP	Homopolymer Polypropylene
icPP	High Impact Copolymer Polypropylene
J	Joules
Kg	Kilogram
L	Length
m	Meter
mg	Milligrams
min	minute
mm	Millimeter
MAPP	Maleic anhydride grafted poly-propylene
MFI	Melt Flow Index
MPa	Mega Pascal
mWS	Medium wheat straw
nm	Nanometer
PE	Polyethylene
PP	Polypropylene

PPO	Poly phenylene oxides
Psi	Pounds square inch
PU	Polyurethane
sec	Seconds
SEM	Scanning Electron Microscopy
SiO ₂	Silicon dioxide
Sp gr	Specific Gravity
T _{m2}	Melting temperature
T _c	Crystallization temperature
T _g	Glass Transition Temperature
TMI	Testing Machines Inc
TPO	Thermoplastic polyolefin rubbers
UV	Ultra-violet
Wnite	Wollastonite
wt	Weight
WS	Wheat Straw
°C	Degree Celsius
μm	Micro-meter
%C _{m2}	Percentage crystallinity at melting

1 INTRODUCTION

Researchers are aiming for exceptional low cost and durable materials for automotive applications. Plastics, due to their relative low cost, reduced weight, recyclability, corrosion resistance and good strength, have now revolutionized many industries and substituted the use of metals in many applications in the automobile industry. It is reported that a pound of plastic or plastic composites can replace 3-4 pounds of heavy metals, while retaining the properties (Racine, 2010). Thermoplastics such as polyethylene (PE), polypropylene (PP), polyurethane (PU), acrylonitrile butadiene styrene (ABS) and other polymers are used widely in the exterior, interior and under the bonnet applications. Polymer composites gained wide acceptance mainly due to their ability to reduce weight and enhance safety at low cost. Various types of organic and inorganic fillers are used in thermoplastic composites. Some of the synthetic fillers include glass fibre, carbon fibre, graphite and boron fibres.

The use of mineral particulate fillers has been thriving in the industries for many years and it still continues to attract researchers and scientists in various fields. Functional fillers are not only used to reduce cost of the bulk material but also serve as a means to improve the mechanical properties of composite materials. A large percentage of natural minerals are used with polyolefins although there are reports showing its use with other neat polymers as well (Švab 2005, Rothon 1999). The incorporation of mineral fillers is known to improve the strength, rigidity, stiffness, modulus, crystallinity and dimensional stability of polymer composite. The fillers also have adverse effect on impact strength of the composite. All these properties are highly influenced not only by size, type and concentration of fillers but also by the interaction between the matrix and the filler. Some of the particulate fillers used with polyolefins are calcium carbonate, talc, mica, kaolin, wollastonite and silica.

Due to environmental concerns, the urge to use more eco-friendly, renewable and compostable resources as fillers in composites is progressing at a higher rate. Researchers have investigated the use of several bio-fibres such as flax, hemp, jute, sisal and wood as filler or reinforcement for polymer composites. Low weight and low cost of these fibres make them even more attractive. Due to the depleting wood resources and the cost involved in manufacturing processes, the use of

agricultural byproducts as bio-based fillers in composites is gaining grounds in several industrial sectors. Agricultural residues such as wheat straw and rice straw are sustainable alternatives. Despite the inherent hydrophilicity, like other plant filler or fibres, wheat straw continues to be in high demand due to its availability, weight and cost effectiveness. Several physical and chemical modification methods have been developed to reduce the hydrophilic nature of WS and improve the interfacial interaction with hydrophobic polymer matrices.

1.1 MOTIVATION AND OBJECTIVES

Several attempts have been made earlier to study the mechanical behaviour and water absorption characteristics of single fillers in thermoplastics. No efforts are put forward to compare and analyze the properties of bio-based fibre such as wheat straw and mineral fillers such as talc, mica and wollastonite on polypropylene composites.

Hybridization is a result of combination of two or more fillers in a common matrix. The blending of bio-fibres and natural mineral fillers in composites seems to be an interesting alternative for reducing the water absorption characteristic of bio-fibre composites. Another added advantage is the synergistic effect on properties obtained by combining two fillers. Though there are several literature studies on the effect of hybridization of fillers in composites, limited study has been done on combination of wheat straw fibres and minerals in PP composites.

The present study aimed at doing a systematic comparison of the properties of fine wheat straw, medium wheat straw, talc, mica and wollastonite fillers on homopolymer, copolymer and polypropylene blend while evaluating the potential of weight savings in polypropylene thermoplastics. The second part of the work aimed at combining two fillers – wheat straw and mineral filler simultaneously to study the hybrid properties and synergy effect produced on PP composites.

1.2 ORGANIZATION OF THESIS

The thesis is organized in 7 chapters as described below:

Chapter 1 – **Introduction**: The chapter provides an introductory opening to the research thesis with emphasis on motivations, objectives and project plan.

Chapter 2 – **Literature Review**: This chapter covers a literature study carried out as part of the thesis, which mainly discusses various thermoplastics and thermoplastic composites used in automotive applications. It also covers topics such as polypropylene processing, bio-based and natural mineral fillers. The composite composition and characterization methods are also introduced in this section.

Chapter 3 – **Materials and Methods**: This chapter discusses the different types of polypropylene matrices and fillers used in the preparation of the composites. The processing methods and characterization techniques used to evaluate the properties of the composites are also discussed.

The results and discussions section is divided into three main chapters, as follows:

Chapter 4 - **Results and Discussions - Polypropylene Matrix**: The results of the composite preparation and characterization methods are presented. This chapter compares and analyzes the properties of pure PP resins (without any fillers) used in this research work.

Chapter 5 - **Results and Discussions – Polypropylene Filler Composites**: A discussion and systematic comparison of the results obtained for single filler PP composites are presented in this chapter.

Chapter 6 - **Results and Discussions - Polypropylene Hybrid Composites**: In this chapter, the graphical representations, along with the discussion of the results obtained for Polypropylene hybrid composites made of two different fillers at varying compositions are systematically presented.

Chapter 7 – **Conclusions and Recommendations**: This chapter summarizes the main conclusions derived from the previous three chapters and provides suggestions for future work.

1.3 PROJECT PLAN

Figure 1.1 represents a systematic approach for the study involving the initial process of composite preparation to testing their properties and comparing the results. The design reflects three different polypropylene resins and five different fillers used in the study. The formulations for the matrices, fillers, hybrid fillers, coupling agents and antioxidants are also included in the plan. The sample processing was carried out by compounding with twin screw extruder and by injection moulding for preparation of composite specimens. The various testing methods for measuring the physical properties of the composites are also illustrated in Figure1.1.

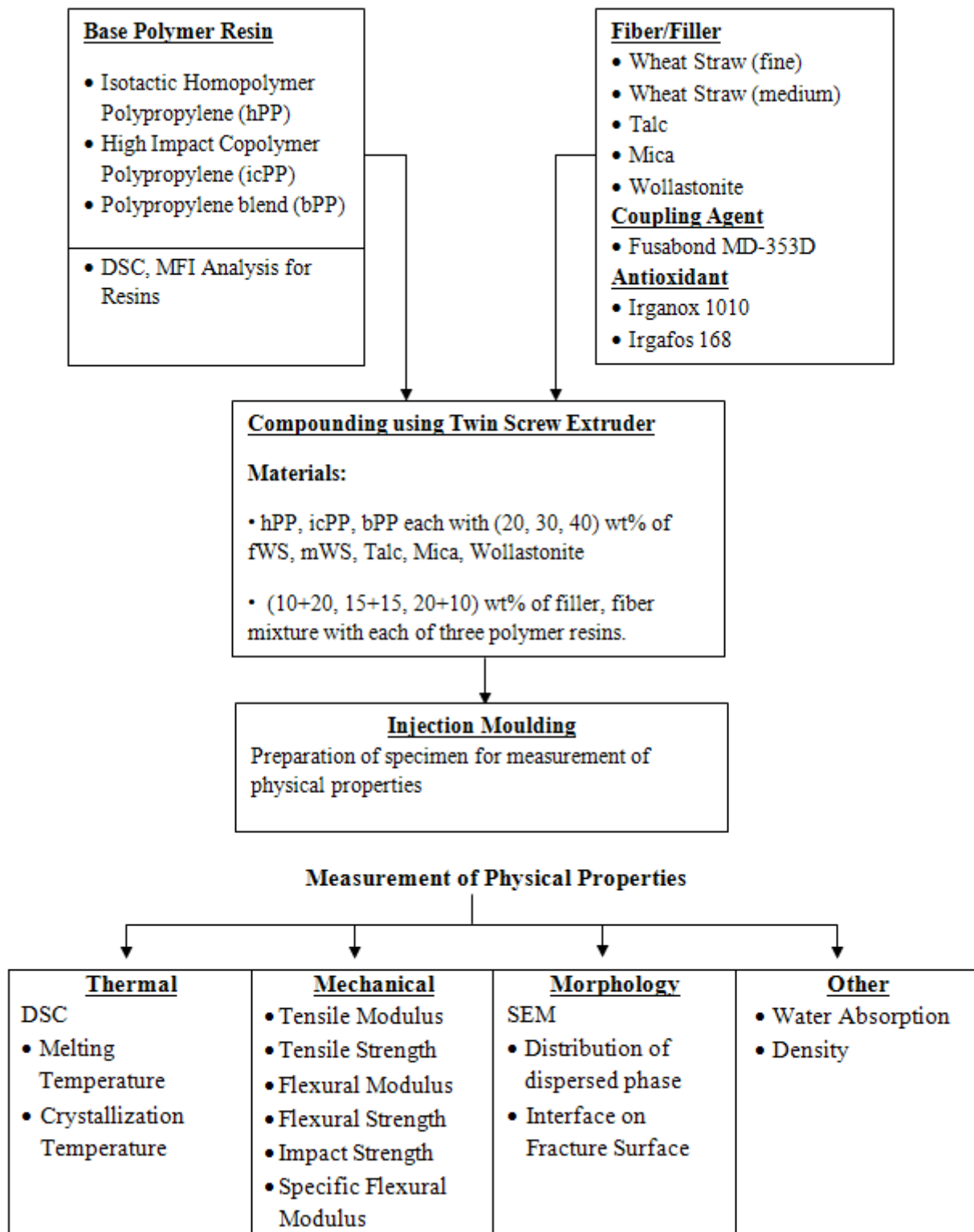


Figure 1.1 Schematic Representation of the Work Plan

2 LITERATURE REVIEW

2.1 THERMOPLASTIC COMPOSITES IN AUTOMOTIVE APPLICATIONS

A composite is a mixture of two or more differently distinct materials having different properties; such that the final combination has improved properties that cannot be achieved by the individual materials. Thermoplastics are those polymers that can be processed by using temperature, that is, which can be remelted and remolded into different shapes and yet retain their properties. On the contrary, thermosetting plastics cannot be reshaped further after the initial hardening. Thermoplastic materials are classified into four categories:

- Commodity thermoplastics
- Engineering thermoplastics
- Thermoplastic elastomers or rubbers
- Blends or alloys

Thermoplastic composites are those materials which are formed by the combination of a thermoplastic (component 1 in composite) which is the matrix (often called the continuous phase) and fillers or fibers (component 2 in composite) which is the dispersed phase. Some examples of mineral dispersed phase include glass fibers, talc, mica, wollastonite and calcium carbonate and bio-fiber dispersed phase (filler or fiber) include wood flour, wheat straw, jute, sisal, cotton, soy, paper etc.

Thermoplastic composites have a widespread application due to their enhanced properties such as good strength, thermal stability, chemical resistance, impact strength, good dimensional stability and relatively low cost. They are widely used in flexible and rigid packaging, automotive applications, sports goods, electrical insulations, building and constructions, medical applications, tools and toys, garden and other outdoor applications.

Various thermoplastics and their applications in automotive industry are listed in Table 2.1.

Table 2.1 Thermoplastics and their Automotive Applications

Thermoplastics	Automotive Applications
Polyethylene	Interior covering for dash boards, door panels, consoles, boot interiors, hand grips. PE foam adhesives for fixing spoilers, rear and front lights, body side protective mouldings. Crosslinked PE – sound deadening, carpeting, boot mats
Polypropylene/ Copolymer/ Elastomer modified blends	Accelerator pedals, Dome lights, Kick panels, Door frame parts, Car battery cases, Bumpers, Radiator grilles, Fascia panels
Polymethylmethacrylate	Steering wheel plaques Fascia paneling
Polyamides (Nylon 46)	Automatic gears, Gear boxes, Engine differentials, Clutch area, Car radiator parts
Polyacetals	Pump impellers Carburetor bodies
Injection molded polycarbonate, polycarbonate-ABS alloys	Decorative Bezels, Optical reflectors, Instrument panels, Air vents, Cowl panels, Wheel covers, Rear light chassis, Headlamp houses, Central electrical control boxes, Loudspeaker grilles, Window trim
Acrylonitrile Butadiene Styrene	Fascia panels, Door covers, Door handles, Radiator grilles, Ventilation system

	components, Heater housings, Seat belt fastenings, Console panels, Loudspeaker housings, Interior trim
Polyurethanes	Seat foam, Arm rest and head rests, Sound absorption and vibration dampening, Bumpers, Airbag covers, Window encapsulation
Polybutylene Terephthalate	Small interior mouldings – ashtrays, foot pedals, door handles, safety belt components, Exterior – windscreen wipe holders, exterior mirror housings
Thermoplastic polyolefin rubbers (TPO)	Convuluted bellows, flexible diaphragms, protective sleeving, steering gear boots, torque couplings and tubings, car bumpers, radiator grilles, door gaskets, headlight surrounds
Polyphenylene oxides (Styrenic modified PPO's)	Instrumental panels, steering column cladding, central consoles, loudspeaker housing, ventilator grilles, nozzles and parcel shelves

Plastics are now inevitable in the automotive industry. The ease of processing, reduced weight, resistance to chemicals, high heat and oil resistance, greater stiffness, high temperature performance, wear resistance, noise reduction, vibration dampening, high flowability and productivity are some of the properties which make polymers superior to metals in automobiles. A typical vehicle weighing around 1,200 kg contains approximately

10% to 15% of plastic components used for body parts, interior trim, instrument panels and headlamps. Seats, padded safety components for interiors and sound insulation wings are made up of polyurethane foams (thermosetting) which encompass another 2.6% of the polymer used in cars (Drake 1998). An additional 9% of plastic materials are used in surface coatings, undersealants, textiles and carpeting, rubbers for tyres, engine mountings, gaskets, drive belts and service fluids like break and antifreeze fluids. In the early 21th century, an average car contained around 75kg – 100kg of plastic components (Brydon 1999).

This chapter will focus on the automotive applications of polypropylene (PP) based thermoplastic composites. The principle objective of this project is to study and compare the properties of different types of polypropylene, types of straw fiber and types of mineral filler on the properties of thermoplastic composites manufactured by injection molding for use in the automotive industry.

Table 2.2 Merits and Demerits of PP for its Use in Automotive Industry

Merits	Demerits
Chemical resistance	Anisotropic shrinkage
Low density	Warp tendency
Environmental stress cracking resistance	Sink marks
Recyclability	Visibility of weld lines
Inline coloring	Scratch resistance
Broad processing window	Pretreatment for painting
Acoustics	
Low price	

Over recent years, polypropylene has been growing very rapidly and is now an indispensable choice in the automotive sector. A wide range of filled and unfilled PP makes their way to exterior, interior and under-the-bonnet automotive applications. Polypropylene is so demanding because of ease of processing, low cost (compared to poly[acrylonitrile-

butadiene-styrene], polyamide or polycarbonate), good balance of mechanical strength, low specific gravity, excellent weatherability, colorability, chemical resistance and thermal stability. Being 15-20% lighter than other polymers, it embodies a significant weight saving in car parts. Some of the advantages and disadvantages of PP for automobiles have been listed in Table 2.2 (SABIC Polypropylenes solution for automotive demands: Jan 2005).

Figure 2.1 shows the different grades of polypropylene compounds and their inherent properties for automotive applications (Moritomi 2010). Some of the requirements for PP to be used in automobiles have also been listed in Table 2.3.

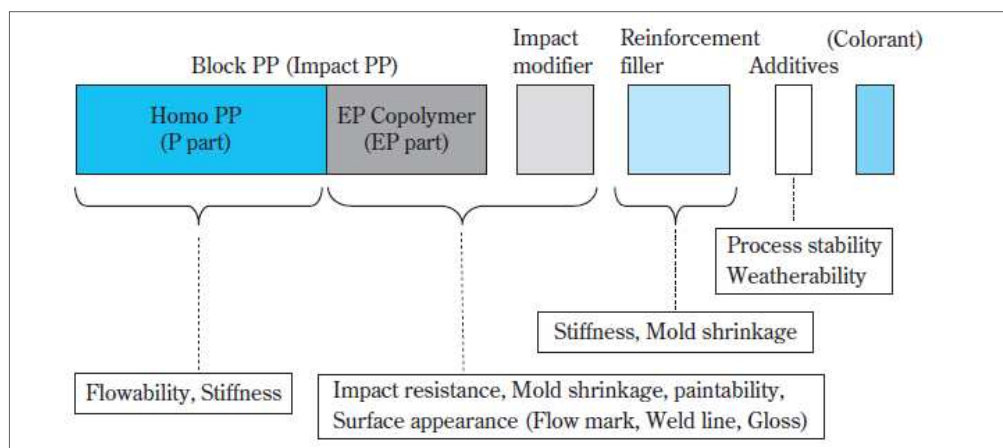


Figure 2.1 PP Compounds for Automobiles (Moritomi 2010)

Table 2.3 PP Property Requirements

Location	Application (car part)	Property requirements
Exterior	<ul style="list-style-type: none"> - Bumpers - Bumper spoilers - Lateral sidings - Body panels - Wheel arch liners 	<ul style="list-style-type: none"> - High flow - Good processability - No surface defects - Good paintability - Good thermal stability - Good dimensional stability - High UV resistance - High impact strength at low temperature - Damage tolerance

Interior	<ul style="list-style-type: none"> - Trim components - Dashboards - Glove box - Pillar claddings - Door pockets - Door panels - Console bins - Chairs 	<ul style="list-style-type: none"> - Good scratch resistance - Low smell - Low emission - Medium to high impact - Good dimensional stability - High flow - Low gloss - Sound-dampening
Under-the-Hood	<ul style="list-style-type: none"> - Battery cases - Electronic housings - Heating ventilation AC - Air ducts - Break fluid reservoirs - Engine covers - Water pump housings - Fuel rails 	<ul style="list-style-type: none"> - High temperature resistance - Chemical resistance - Wear resistance - Good shrink and warp control - Sound dampening - High strength - Toughness - Durability

2.2 POLYPROPYLENE: PROCESSING TECHNIQUES

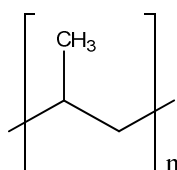


Figure 2.2 Structure of Polypropylene

Polypropylene is a semi-crystalline thermoplastic polyolefin resin invented in the early 1950's. It continues to be a fast growing commodity plastic in many markets today. It has a low density of 0.90g/cm³ compared to other thermoplastics. This is because of the type of crystallinity favored by the methyl group substituent on its backbone as shown in Figure 2.2.

The crystallinity and high molecular weight of the polymer is due to the use of a special type of polymerization catalyst invented by Natta and co-workers in 1955 (Moore 1996). With proper catalyst selection it is possible to control the stereoregularity during the polymerization. Polypropylene can be prepared in three different types of tacticity: namely isotacticity, syndiotacticity and atacticity. Isotactic polymer is formed when all the methyl groups arrange themselves on one side of the backbone due to stereoregular insertion of the propylene during polymerization. A polymer chain is said to be syndiotactic when the methyl groups arrange alternately above and below the plane of main chain backbone. When there is a random configuration of the methyl groups, they are known to be atactic. The different forms of stereoregularity are shown in Figure 2.3. The level of stereoregularity can be controlled by controlling the polymerization catalysts and polymerization conditions.

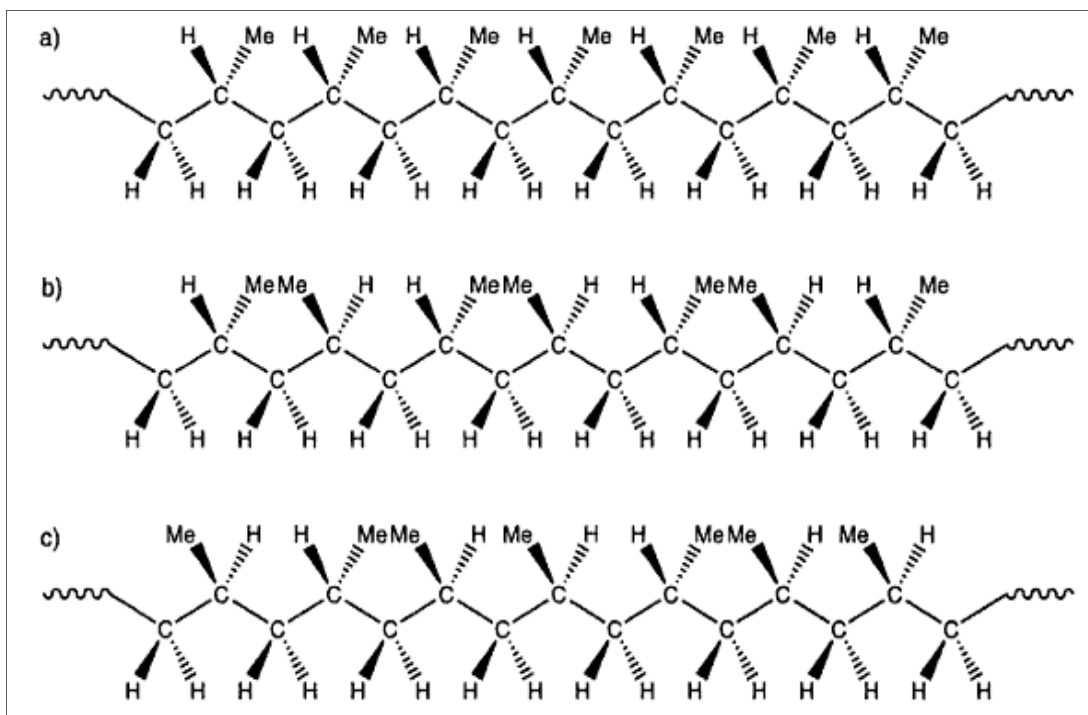


Figure 2.3 Stereoregularity in PP chain-Isotactic, Syndiotactic and Atactic

(Calhoun, Peacock 2006)

Polypropylene can be processed using a wide variety of manufacturing techniques such as injection molding, blow molding, profile extrusion and thermoforming (Maier 1998). Due to

its inherent nature of low density, good chemical resistance, broad processing window and excellent property balance, PP can be processed to suit different applications. Flow properties, thermal properties, shrinkage and warping are the main factors affecting the processing of a material.

Processing, in general, includes all the steps occurring between polymerization and formation of end products. There involves three steps in the processing of any thermoplastic polyolefin and they are: 1) Heating, 2) Forming/Molding and 3) Cooling. The division of various processing techniques is shown in Figure 2.4.

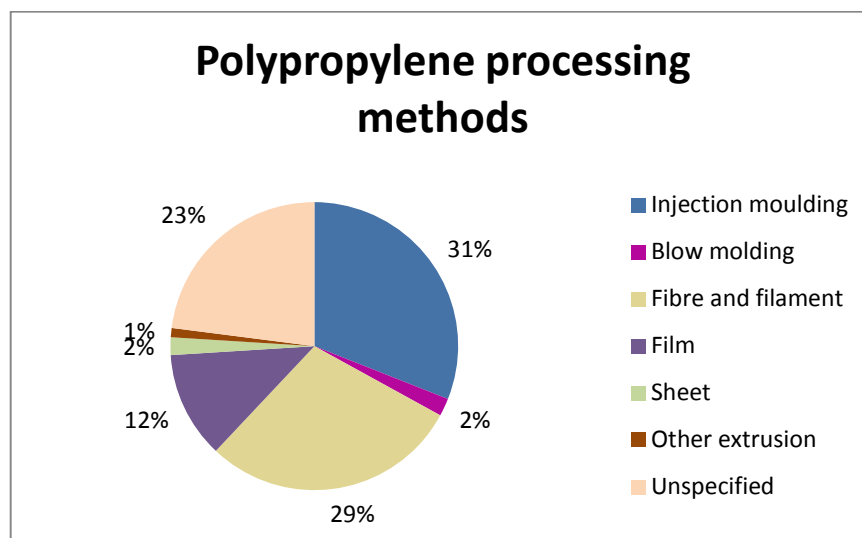


Figure 2.4 Processing methods for PP, USA, 1996 (Maier 1998)

EXTRUSION

Polypropylene, a versatile thermoplastic resin, can be formed into fibres, filaments, films, sheets etc. This is done through extrusion which is considered the single most accepted process for forming PP. Good melt strength, low processing temperature, broad processing window are some of the unique characteristics which enable PP to be extruded into various forms. Around 66% (Figure 2.5) of PP extrusion goes into the manufacturing of carpet yarns, upholstery fabrics, ropes, cords, strapping, etc. (Maier 1998).

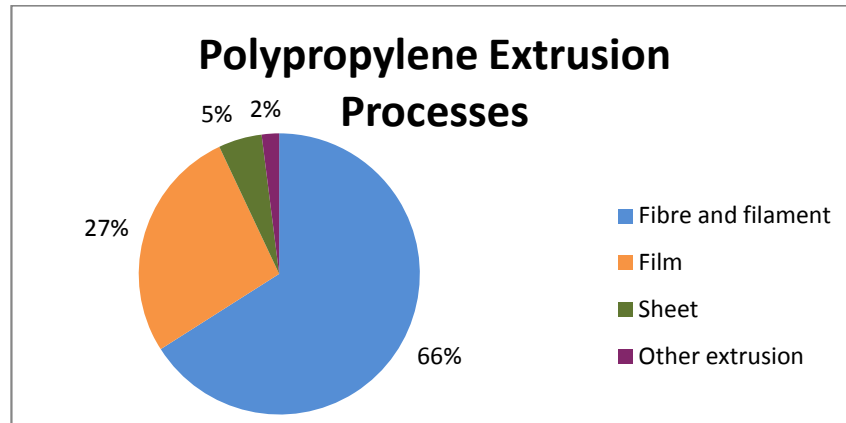


Figure 2.5 Polypropylene extrusion processes, USA, 1996 (Maier 1998)

Extrusion is a continuous process which results in a semi-finished product and needs to be processed yet again to make the end product. An extruder consists of a rotating screw (single screw or twin screws), which is motor driven, fitted into a barrel. At the inlet of the barrel is a feed throat provided to feed the material in the form of powder or pellets. As the material is conveyed through the screws, the mixing and shearing action of the screw and the heating devices inside the barrel heats and melts the material. There is a pressure build up at the die end of the extruder as the extrudate flows out and this extrusion pressure is typically in the range of 1000 to 5000 psi (Maier 1998). Screw speed, screw geometry and melt viscosity are the important parameters which determine the output rate of the extruder. The molten material pumped out through the die is then cooled in a water bath. It is then pelletized for further processing required. The temperature inside the barrel is set in the melting range of PP.

Twin screws are normally used when mixing or compounding and homogenization of the melt becomes crucial to the final product. In particular, they are used when additives or fillers need to be incorporated into the polymeric matrix to form composites. In general, there are three zones represented in a screw (Figure 2.6):

1. Feed zone - Material or thermoplastic resin is fed and conveyed through the extruder screws.
2. Melting and Compression zone – Friction, compression and the heating devices in the barrel completely melt the plastic material in this zone.

3. Metering zone - Further mixing takes place to ensure uniform temperature throughout the material.

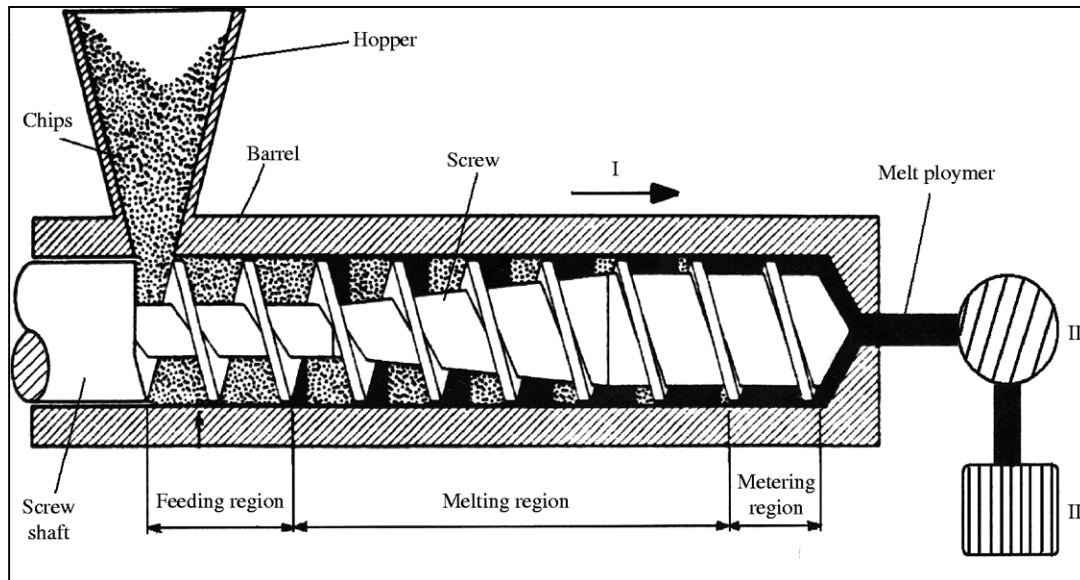


Figure 2.6 Schematic Diagram of an Extruder, Source: Tadmor, Klien 1970

(Koç 2009)

INJECTION MOLDING

Injection molding is one of the most widely used manufacturing methods for polypropylene products. In this process, polymer resin in the form of pellets or powder is fed and conveyed through a rotating screw where it mixes, softens and melts due to high temperature (above the melting point of the polymer). It is then injected into a mold (or cavity) under pressure. A ram pushes the molten material forward into the mold, the shot should fill the mold cavity and keep the pressure inside the mold until the polymer starts solidifying. The mold temperature is maintained below 65 °C (Frank 1968). The mold remains closed until the part solidifies. Adequate time is given before opening the mold. The mold is then cooled and opened for ejecting the rigid PP parts. There can be several mold cavities in a single mold enabling production of multiple parts at one shot. Uniformity of part thickness and part appearance are the two main challenges in injection molding. The main parameters that are

considered are ram pressure, polymer melt temperature, molding cycle and polymer processability. Polypropylene is an attractive choice of resin for injection molding. A schematic diagram for an injection mold is shown in Figure 2.7.

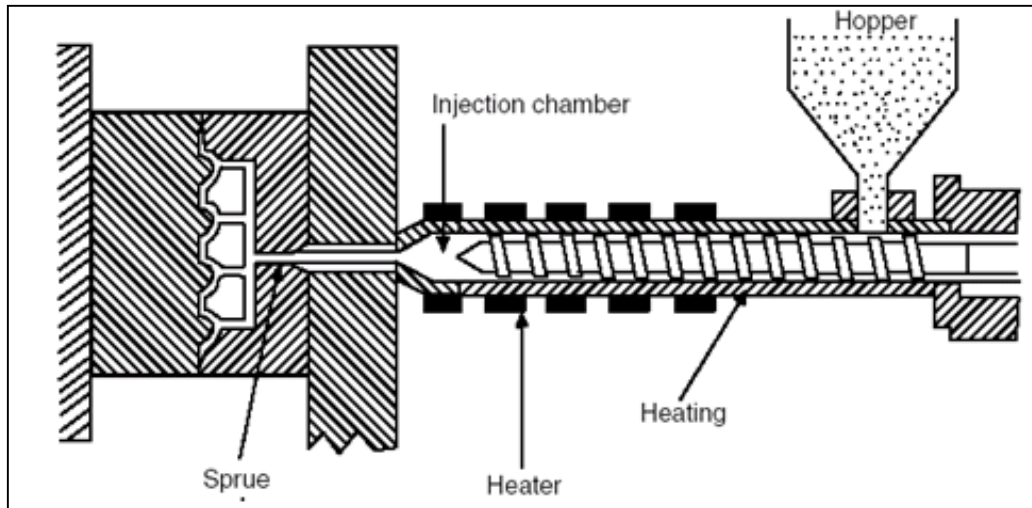


Figure 2.7 Schematic Diagram of a Screw - Injection Molding Machine
(LongMold Technology Co. Ltd 2009)

This technique is predominantly used for products that require an elaborate geometry. Aside from automotive, it is widely used in other applications like food storage containers, water bottles which come in different shapes, appliances, tools (like electric drills), luggages and furnitures (outdoor tables and chairs). Ease of molding, stiffness, durability, light weight, electrical properties and cost are the features that enable use of PP for such applications. Injection molded homopolymer/copolymer PP with a melt flow index (MFI) around 25g/10min (Karian 1999) are used in medical applications such as disposable syringes and medical vials. Injection molded PP with 20% long glass fibre has showcased its use in Ford cars instrument panel (Plastic News 2011).

BLOW MOLDING

Blow molding is a technique for manufacturing hollow thermoplastic articles. Polypropylene represents a share of about 3% of the overall blow molding market (Maier 1998). Blow

molding is a discontinuous process involving extrusion as well as blowing the molten polymer extrudate by air. It begins with the production of a molten tube of polymer called a parison or a pre-form, using an extruder or injection molding respectively. This parison is then placed between a split mold having a hollow cavity, as shown in the Figure 2.8. The mold is then closed while sealing the parison tube. An air blowing device is fitted at one of the parison end, which will blow air into the parison and inflate it into the mold cavity. Then the mold is cooled with water, solidifying the part inside, to form the end product. The mold is then opened and part is ejected and trimmed.

The 5 steps involved in blow molding process are summarized below,

1. Plasticizing the thermoplastic resin
2. Production of pre-form or tube shaped polymer
3. Blowing the pre-form in a mold
4. Cooling and ejection of the molded part
5. Trimming

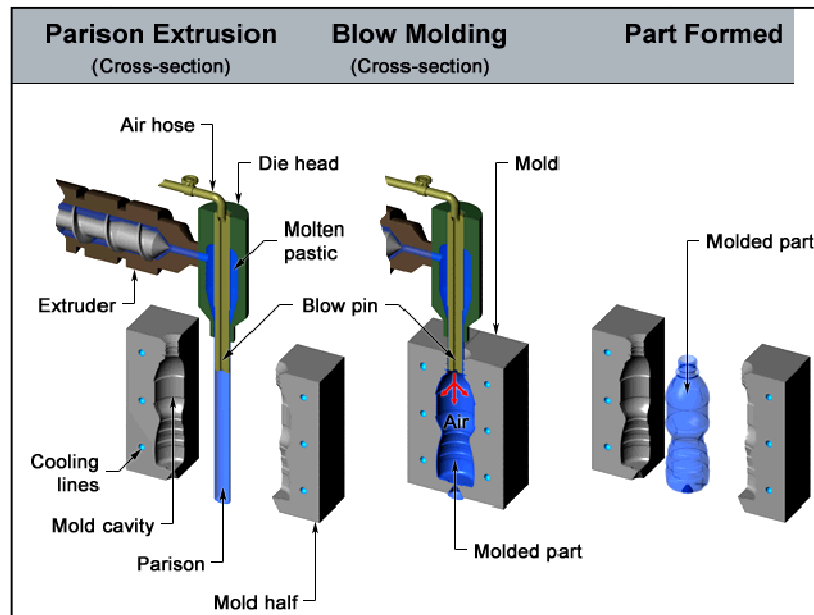


Figure 2.8 Schematic of a Basic Extrusion Blow Molding Process (CustomPartNet 2008)

Random copolymer grades of PP are increasingly finding their way into the blow molding market for production of bottles and containers. They also contribute to the automotive applications such as expansion tanks, fluid reservoirs, ducts and fenders and trims (Maier 1998). Increased transparency and melt strength are the characteristic features which make PP advantageous for such applications. Injection blow molding is the suitable process for manufacturing small, high production clear parts (Rosato 2004). Stretch blow molding has also been put forth for use with polypropylene. It is characterized by increased transparency, resistance to burst pressure and reduced permeability (Maier 1998). Some of the advantages and disadvantages of extrusion blow molding and injection blow molding are shown in Table 2.4

Table 2.4 Extrusion and Injection Blow Molding

Techniques	Advantages	Disadvantages
Extrusion Blow Molding	Lower tooling cost, Incorporation of blown handleware	Controlling parison swell, Producing scrap, Limited wall thickness control, Plastic distribution
Injection Blow Molding	No flash during processing, Wall thickness control, Plastic distribution control, Higher accuracy bottleneck finishes	High tooling cost, Longer start-up time, Incorporation of only solid handlewares, restriction to small products

THERMOFORMING

Thermoforming is a process in which thermoplastic sheets (pre-form) are formed into different shapes using heat and pressure. This is done by first clamping the sheet on to a

mold cavity (called female mold) and then drawing vacuum (basic vacuum forming process) so that the atmospheric air pressure pushes and deforms the sheet into the cavity. It is then cooled for its shape to be maintained, ejected and trimmed. Factors such as forming force, mold type, method of pre-stretching and material input forms greatly affect the performance of the final thermoformed product.

Other thermoforming processes include vacuum forming, basic pressure forming, drape thermoforming, plug assist thermoforming, and twin sheet thermoforming. Figure 2.9 shows a schematic representation of a basic pressure thermoforming processing technique.

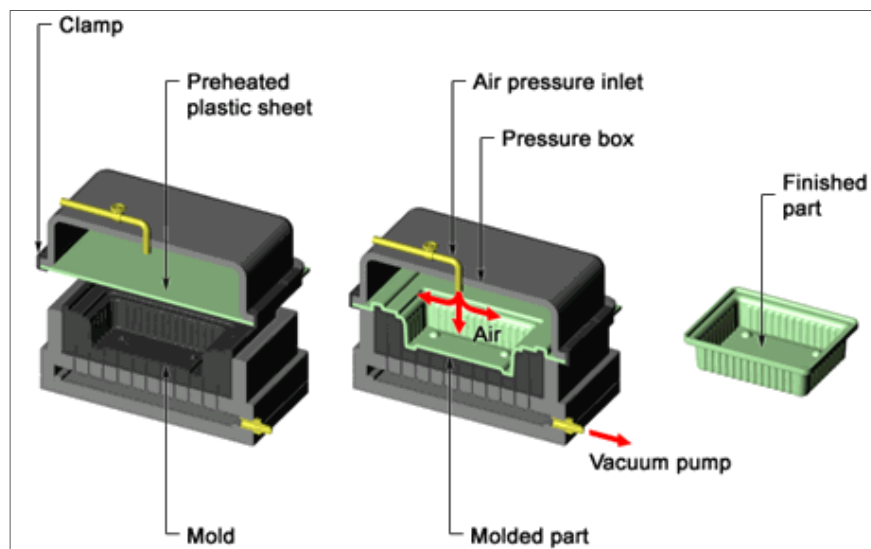


Figure 2.9 Basic Pressure Thermoforming Process (CustomPartNet 2008)

Very small amount of polypropylene was used for thermoforming a decade ago, due to low elasticity of semi crystalline polymers and low melt strength of PP sheets, causing processing complexities. With the recent developments in PP materials and thermoforming processes, a swift growth in this area is observed. Good oxygen barrier properties, chemical resistance, stress crack resistance, high softening point, excellent toughness are some of the useful properties of PP which make it exceptional material for thermoforming. Applications of thermoformed PP include food packaging like deli containers, cups for yogurt, chocolate

packaging, disposable cold drink cups etc. and other medical applications like blister packs and pharmaceutical packaging (Figure 2.10).



Figure 2.10 (a) Disposable Products, (b) Blister Packaging

2.3 FILLERS

Fillers are substances which are added to improve cost effectiveness of the base material. Initially it was only thought to reduce cost by reducing the amount of expensive base material but developments have brought forth its influence in the properties of base material as well. Those which help in reducing cost are called Extenders and those which aid in enhancing the properties are called Functional Fillers. The latter is incorporated for three vital reasons:

- Property enhancement
- Cost reduction
- Improving and controlling of processing characteristics

There are several classifications of fillers. One classification is based on the geometry of the filler namely fibers, flakes, spheres and particulates. In composites they are generally classified according to their reinforcing characteristics and are called reinforcing, semi-reinforcing and non-reinforcing fillers.

Fibres are usually distinguished by their long axis and high aspect ratio. The influence of fibers on polymer composites depends on its size or length, shape, orientation and composition. The optimum performance in composites is obtained if the load is acting along the longitudinal axis of the fibres (Pandey 2004). Professor Pandey also suggests that where a high concentration of fibers is expected it is best to create multidirectional orientation of fibres in the composite. There are natural and synthetic fibers. Synthetic fibres include glass fibres, carbon fibres, graphite fibres and boron fibres. They have high modulus and good thermal stability.

Particulate fillers can be organic or inorganic in nature. Some of these fillers are acicular, plate-like or fibrous in their morphology. See Table 2.5. The chemical nature of these fillers determines the structure of mineral and also the nature of interaction between polymer and filler (Rothon 2003). Many reports indicate the ability of particulate fillers to act as nucleating agents. This effect is typically shown with the addition of talc mineral at low concentrations in PP matrix (Karger-Kocsis 1995A).

Table 2.5 Particle Morphology of Fillers

Shape	Aspect Ratio	Example
Cube	1	Feldspar and Calcite
Sphere	1	Glass spheres
Block	1-4	Quartz, calcite, silica, and barite
Plate	4-30	Kaolin, talc, and hydrous alumina
Flake	50-200 ++	Mica, graphite and montmorillonite nanoclays
Fiber	20-200 ++	Wollastonite, glass fibres, carbon nanotubes, wood fibres, asbestos fibres, and carbon fibres

2.4 POLYPROPYLENE COMPOSITES

Polypropylene composites are a sub class of polyolefin composites. Additional functional materials are added to polypropylene in order to improve the mechanical properties in a cost

effective manner such that they can be suited for end-use applications. These materials are classified into different groups namely modifiers, property extenders and processing aids (Nwabunma 2008). Antioxidants, light stabilizers, UV absorbers, peroxide decomposers, nucleating agents, flame retardants, colorants, lubricants and blowing agents come under a class of additives which are dispersed in the polypropylene resin during several stages of processing to provide resistance and also to stabilize the base material. They also contribute by improving the mechanical properties to a certain extent.

Over the years several types of fillers have been in use with polypropylene. Minerals such as talc, calcium carbonate, mica, silica, glass fibres, carbon fibres, wollastonite and biobased fibres such as wood flour, wheat straw, coconut fibre, jute, sisal and kenaf have been favorably used with PP either as fillers or as reinforcements to provide better strength and modulus to the composite. Most of the fillers are polar in nature, so there arise a problem of reduced adhesion between the non polar matrix and the polar filler which can affect the final properties of the composite. As a solution, several types of coupling agents or compatibilizers were developed with the aim of improving the bonding. Literature studies have shown that maleic anhydride grafted polypropylene is the most widely used coupling agent for PP based composites (Jahani 2010, Reddy 2010 and Jahani 2011).

A large variety of filled propylene composites are found in vehicle's interior, exterior and under-the-bonnet applications. Long glass fibre reinforced PP have found its use as bumper beams. Talc filled impact copolymer composites are used in door and instrument panels (Karian 1999). Low cost, ease of processing and recyclability of PP composites are paving way to the rapid market growth in the automotive sector. Figure 2.11 shows some of the fillers used in automotive thermoplastic PP composites.

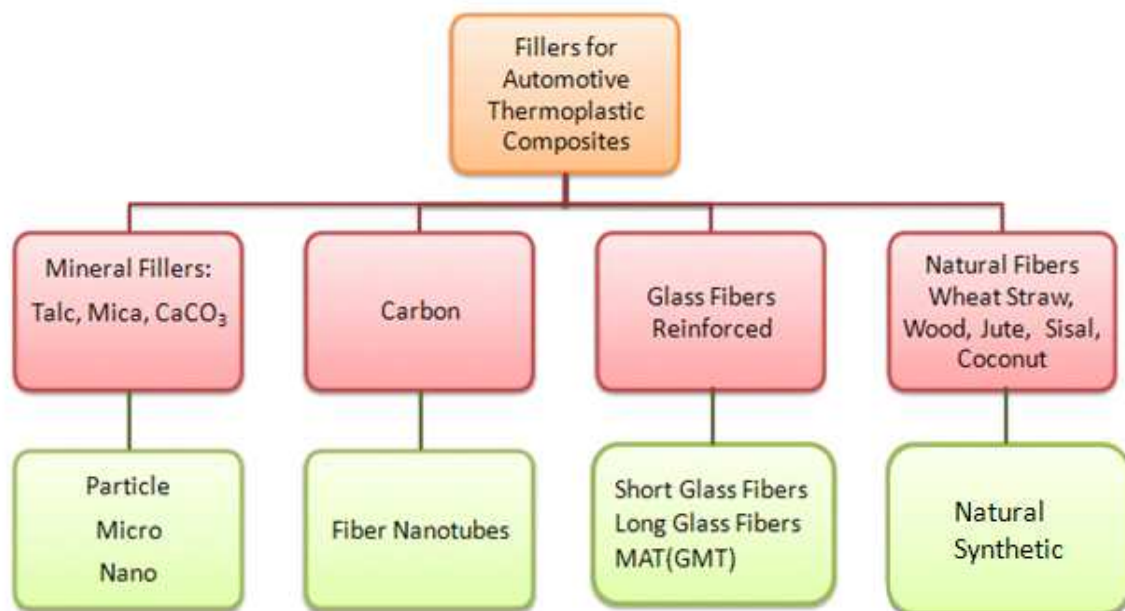


Figure 2.11 Fillers used in Thermoplastic Composites

2.4.1 NATURAL FIBRE POLYPROPYLENE COMPOSITES

The term natural fibre encompasses a wide range of animal (like wool or silk), plant (like hemp and sisal) or mineral (like asbestos) fibres. Natural fibres extracted from the stem or leaf part of a plant is the subject of interest in the composite world. They are often referred to as bio-based fibers.

Plant fibre comprises of three major constituents namely cellulose, hemicellulose and lignin, along with other small compounds like wax, pectin and lipids (Mussig 2010). The constituent composition can vary depending on the species and age of the plant (Mohanty, Misra et. al. 2005). The primary component cellulose is a linear polymer made up of 1,4- β anhydroglucose units, containing hydroxyl groups (See Figure 2.12 and 2.13 for the structure of cellulose and a schematic representation of plant cell wall). They interact and bond with adjacent molecules to form fibres. Being the major component of fibre, cellulose imparts good strength, stiffness and

structural stability. Hemicellulose is a branched polymer with molecular weight lower than that of cellulose but they contribute to the structural component of the fibre. Lignin is a high molecular weight phenolic compound (biochemical polymer) which acts as a structural support in plants. It is less polar than cellulose and improves adhesiveness between fibres. The polarity of bio-based fibres is one of the drawbacks when considering their use in composites with polypropylene but it has been overcome by the development of coupling agents.

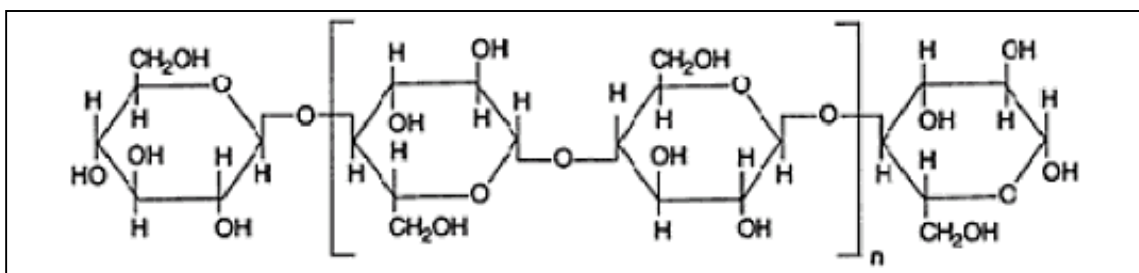


Figure 2.12 Structure of Cellulose

Depending on the species and climatic conditions the fibres can have different dimensions as well as physiochemical performances. The cellulose content in fibre is believed to provide good tensile and flexural property to the fibre. Strength and stiffness characteristics of the fibre directly depend on the internal structure and composition of the fibre. Plant fibres have the inherent advantage of being biodegradable and also possess low specific gravity. Besides, thermal recyclability, renewability and low energy consumption are the other favorable factors. All these characteristics of plant fibres prove advantageous for use in plastic composites providing significant reinforcement and performance improvement.

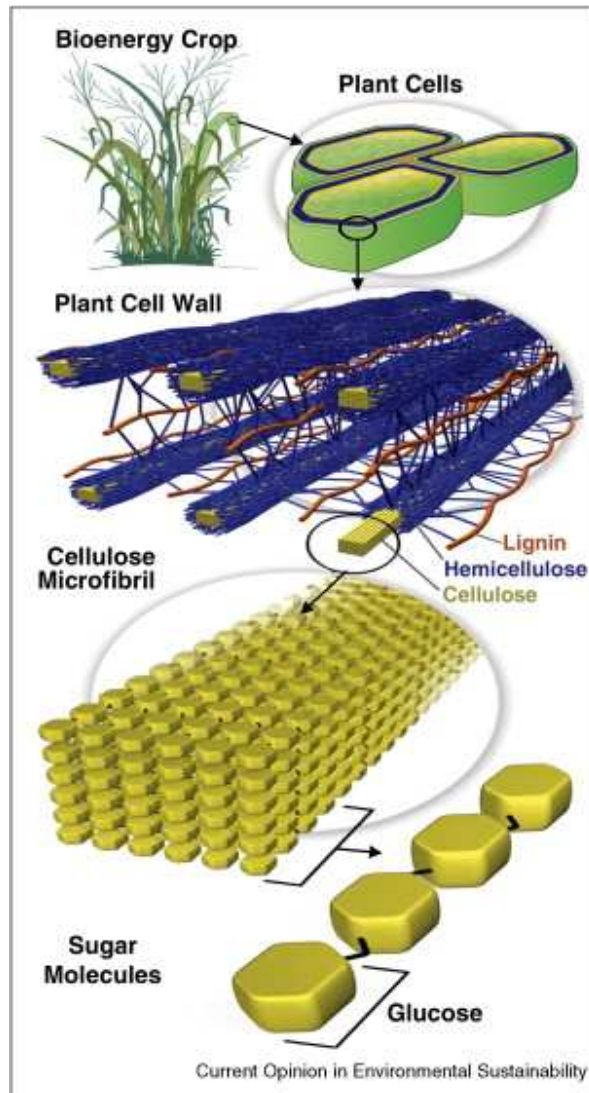


Figure 2.13 Cellulose, Hemicellulose and Lignin (Sannigrahi 2010)

With the recent motivation from many sectors in industry towards composites based on renewable materials, bio-based fibres are being used widely for PP composites to enhance the performance of polypropylene. Extensive studies have been done in this area and fibers like wood, wheat straw, hemp, flax, sisal, jute and bamboo have already found their application in many sector. Though the properties imparted by bio-based fibres are lower compared to synthetic ones such as glass fibers (Table 2.6), the overall specific property of bio-based fibers offer great advantages. The incorporation of natural fibers into the polypropylene matrix improves the stiffness, tensile strength and young's modulus (Reddy 2010, Tajvidi 2003). Further, improved

adhesion between the matrix and the lignocellulosic fibre with the addition of maleic anhydride grafted polypropylene (MAPP) have been reported in many work (Karnani 1997).

Table 2.6 Mechanical Properties of some of the Organic and Inorganic Fibers
(Clemons 2005)

Fiber/Fiber bundles	Density (g cm⁻³)	Stiffness (GPa)	Strength (MPa)	Strain (%)
Glass	2.49	70	2700	-
Kevlar	1.44	124	2800	2.5
Nylon-6	1.14	1.8-2.3	503-690	17-45
Polypropylene	0.91	1.6-2.4	170-325	80-100
Polyester (staple)	1.38	1.5-2.1	270-730	12-55
Flax	1.4 – 1.5	50-70	500-900	1.5-4.0
Hemp	1.48	30-60	300-son	2-4
Jute	1.3 – 1.5	20-55	200-500	2-3
Softwood	1.4	10-50	100-170	-
Harwood	1.4	10-70	90-180	-

There is a remarkable trend in the replacement of metals by plastic composites in the automotive industry. In the last decade, several European cars had door panels, seat backs, headliners, package trays, dashboards and trunk liners made out of bio-fiber composites (Figure 2.14). The trend has spread to the North American market as well (Thomas 2009). Interior trim components such as dashboard are made using PP, hemp and kenaf by Johnson Controls Inc., for Daimler Chrysler. The Adam Opal AG also uses flax filled PP composites for interior trim applications (Bledzki 2002). Other applications include buildings and constructions – decking, claddings and window frames using wood PP composite, furnitures and panels and aerospace applications.

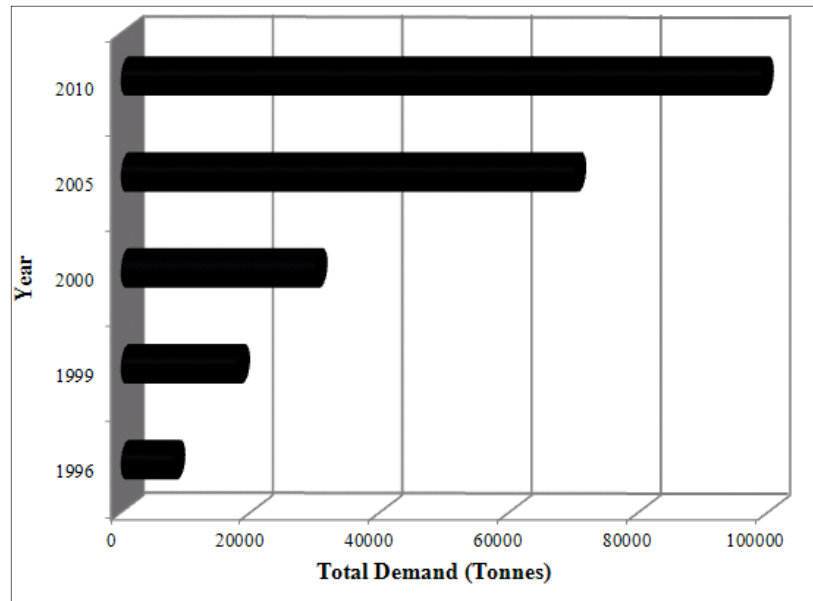


Figure 2.14 Consumption of Bio-fibers within Western Europe (Thomas, Pothan 2009)

2.4.2 MINERAL FILLER - POLYPROPYLENE COMPOSITES

Minerals are abundantly available in nature and they serve as an important class of filler for polymer composites. Most of the minerals are crystalline and possess a definite regular order of atomic arrangement in their structure. The inter-atomic force, atom distance and separation are critical for the crystalline atom arrangements. They are linked together in a three dimensional repeating network. All these factors determine the final properties such as density, optical properties, hardness and shape of the mineral. Table 2.7 lists the principal mineral fillers used in plastics in Europe.

Table 2.7 Mineral fillers used in Western Europe (Hancock 2003)

Some types of mineral fillers used in plastics in Europe			
Filler	Main mineral (crystalline phase)	Chemical composition (simplistic formulae used for the silicates, see individual entries for details)	Shape
Natural calcium carbonate	Calcite	CaCO_3	Aspect ratio about 3:1, blocky
Talc	Talc	MgSiO_3	Platy
China clay	Kaolinite	$\text{Al}_2\text{O}_3 \cdot 2\text{SiO}_2 \cdot 2\text{H}_2\text{O}$	Platy
Calcined clay	Metakaolinite	Al_2SiO_5	Low aspect ratio, platy
Calcined clay	Amorphous	Al_2SiO_5	Low aspect ratio, platy
Alumina trihydrate	Gibbsite	$\text{Al}(\text{OH})_3$	Low aspect ratio, platy
Magnesium hydroxide	Brucite	$\text{Mg}(\text{OH})_2$	Variable
Wollastonite	Wollastonite	CaSiO_3	Acicular
Mica	Muscovite	KFeMgAlSiO_n	Platy
Mica	Phlogopite	KFeMgAlSiO_n	Platy
Silica	Quartz	SiO_2	Cubic
Silica	Amorphous	SiO_2	Aggregated

Minerals originate from rocks - igneous, sedimentary or metamorphic rocks. Silicate minerals such as talc, mica, wollastonite and kaolin are found in igneous rocks. Large concentrations of limestone (calcium carbonate) are found in the sedimentary rocks. Magnesium hydroxide or brucite, feldspar and chlorite are found in metamorphic rocks. Traces of wollastonite mineral are also present in the metamorphic rocks. Hardness is one of the superior properties which distinguish minerals. It is a measure of mineral's resistance towards scratching. Among the 10 minerals whose hardness is known, talc has been identified to have the lowest hardness of 1 and diamond has the highest hardness of 10 in Mohr's scale (Wypych 1993). Calcite, widely used form of calcium carbonate has a Mohr's hardness of 3 and specific gravity of 2.7 g/cm³.

Hancock and Rothon points out the importance of mineral fillers in the polymer industry (Rothon 2003). In early 21st century the consumption of minerals as fillers in rubbers and plastics were estimated to be over 2.5 million tonnes per year in Western Europe (Hancock 2003). Carbonates and silicate minerals are the most widely used fillers in composites. It is estimated that calcium carbonate dominates the filler types used in PVC and polyolefins with over 80% in regards to volume consumption (Rothon 1999). Carbonate group of minerals are classified as calcite, aragonite, and dolomite according to their different crystal structure. Out of these, calcite which has a rhombohedral structure, plays an important role as fillers. Calcium carbonate has a great influence in reducing the cost of the base material when used as filler. Good dispersion characteristics, increased elastic modulus and impact strength, shrinkage reduction, good coloration and excellent surface finish are advantageous characteristics of CaCO₃ mineral filler. Rothon quotes that in most cases mineral fillers reduce the toughness or impact strength of the thermoplastic composite, whereas addition of calcium carbonate at 30 to 40 % loadings in polypropylene can significantly increase the toughness (Rothon 1999).

Table 2.8 World Filler Consumption in 1999 (Zweifel 2001)

Filler	Calcium Carbonate	Talc	Kaolin	Wollastonite	Others
Share	66%	6%	6%	3%	19%

About one-third of all minerals belong to the silicate family. Silicate minerals such as talc, mica, wollastonite and clay minerals are used as fillers on a wide scale.

Addition of minerals enhances the mechanical properties like stiffness and strength, thermal resistance and maintains good dimensional stability in composites. The reduction in toughness generally associated with addition of minerals is attributed to factors like filler size, shape distribution, filler surface treatment, polymer type and testing equipment (Rothon 1999). Kaolin clay, china clay, bentonite clay and few others belong to the class of clay minerals. It is known that clay, when homogeneously dispersed in the polymer matrix, can change the thermal and flame resistance, mechanical properties and gas permeability of the polymer (Sardhashti 2009). Previous study indicated that bentonite clay can be effectively used as reinforcement for PP

thermoplastic without the need of surface modification (Sarkar 2008). Significant increase in tensile strength and toughness at as low as 5 mass% clay was reported. Reports say that clay-PP nanocomposites are being used for structural seat backs in Honda Acura (Gao 2004). The surface morphologies of some of the minerals are shown in Figure 2.15.

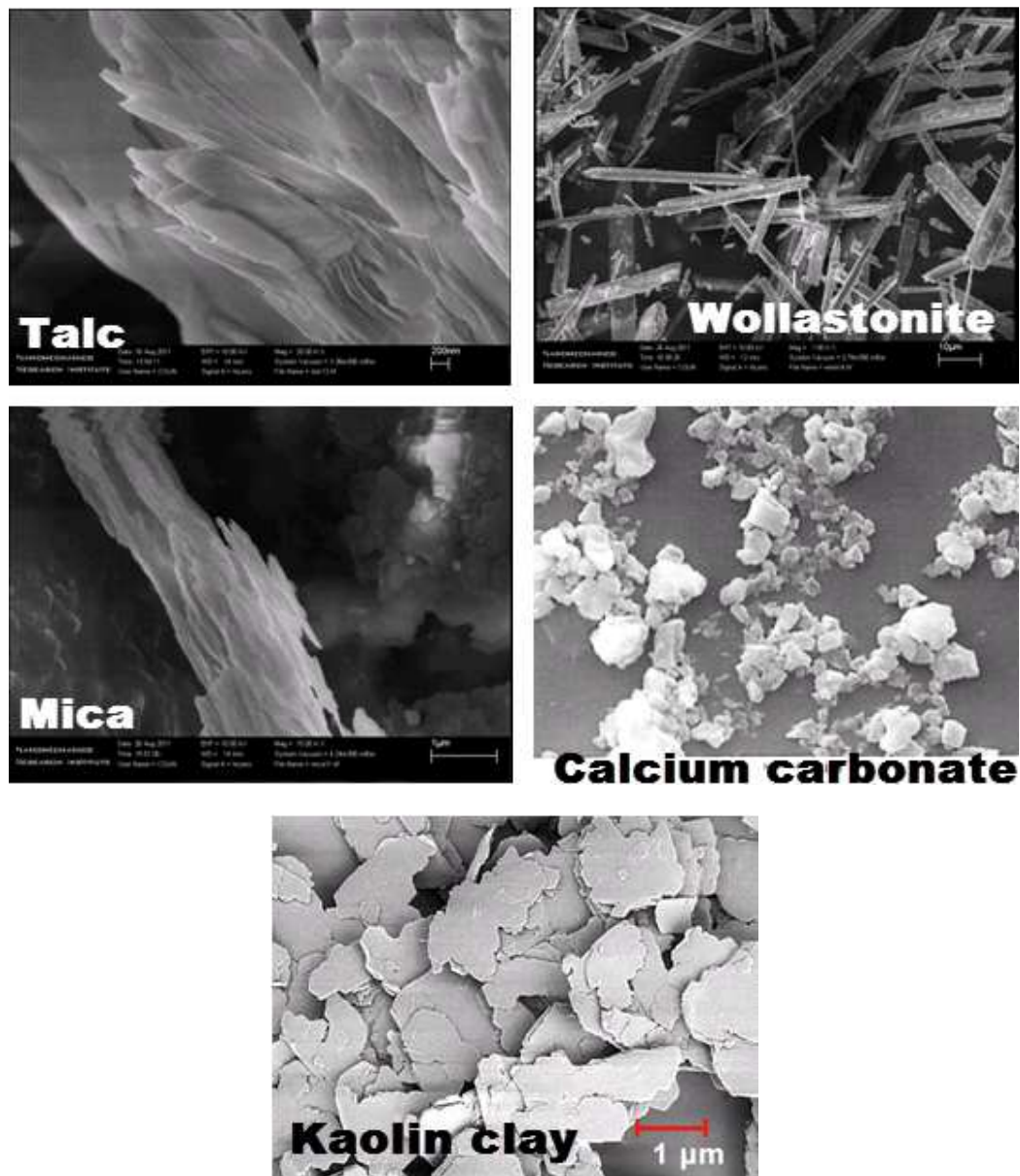


Figure 2.15 Morphologies of Different Minerals

2.4.3 OTHER COMMON INORGANIC FILLERS AND GLASS FIBER

GLASS FIBRE

Glass fibre is a class of fibrous fillers. They consist of numerous fine fibres made of glass comprising of silica oxide and traces of other oxides in their structure. E-glass and S-glass are two main types of glass fibres. They are classified according to their characteristics properties. E-glass shows good electrical properties whereas S-glass have good strength, stiffness and high temperature resistance which make them appropriate as a filler or reinforcement material for composites.

Glass fibres were used as an insulation material until the scope of it being used as reinforcing filler for polymer composites emerged. They are the most extensively used reinforcing filler in thermoplastics. Glass fibre improves rigidity, tensile strength, flexural modulus, heat deflection temperature and also provides good dimensional stability to the composite. The reinforcing effect depends on the type of fibre, size of fibre, coupling agent and the matrix used.

Chopped strands of glass fibres are generally used in polypropylene at a loading of 5-30 wt% in injection molding (Maier 1998). Glass mat reinforced thermoplastic (GMT) commonly consisting of PP as the base matrix shows enhanced toughness, good impact strength and excellent stiffness to toughness ratio. Poucke and James, in their work on long glass fibre PP composites reported the developing long fibre thermoplastics in automotive applications such as front end carriers, instrument panels, door modules and lower and overhead console reinforcements (Poucke 2006). Glass fiber reinforced PP are also used in fan mountings and shrouds, belt covers, air filters, spoilers and cooling system tanks (Maier 1998).

GLASS SPHERES

Glass beads or glass spheres are chemically composed of 50-60% silica, 25-30% alumina, 4-10% iron oxide with traces of other oxides (Wypych 1993). Small wall thickness of these spheres as low as 10% its diameter is likely to withstand pressure up to 10 MPa. There are hollow and solid glass spheres. Like in E and S glass fibres, the hollow glass spheres help in reducing weight and solid glass spheres provide good strength to the composite. The typical shape of the filler allows high loadings and hence increased stiffness at low viscosity (Rothon 1999). Also, a filler size of 30 microns or lower is used with thermoplastics. In polypropylene, the filler provides enhancement in the stiffness at elevated temperatures, high compressive strength and dimensional stability (Maier 1998).

SILICA

Silica or silicon dioxide (SiO_2) is one of the most abundant oxide mineral found in the earth's crust in the form of sand or quartz. It is primarily used in the production of glass for windows, drinking glasses and beverage bottles. Silica is an extensively used cheap filler in composites. They act as an extender as well as functional filler. Quartz, cristobalite and opal are some of the natural silicas used as fillers (Wypych 1993). Quartz has a very compact and perfect structure such that its composition is 100% SiO_2 . Natural silica fillers are further classified as amorphous and crystalline.

Figure 2.16 shows the surface morphology of crystalline silica. Rothon, in his report, lists 5 synthetic silicas: fumed, arc, fused, gel and precipitated silica, out of which gel and precipitated ones are used commonly as additives in small amounts in thermoplastics (Rothon 1999). Literature study showed that addition of 3% silica flour to PP matrix with SEBS-g-MA compatibilizer improved the yield strength and the impact strength of the composite (El-Midany 2011). Chemical inertness and durability of silica expands its application enormously.

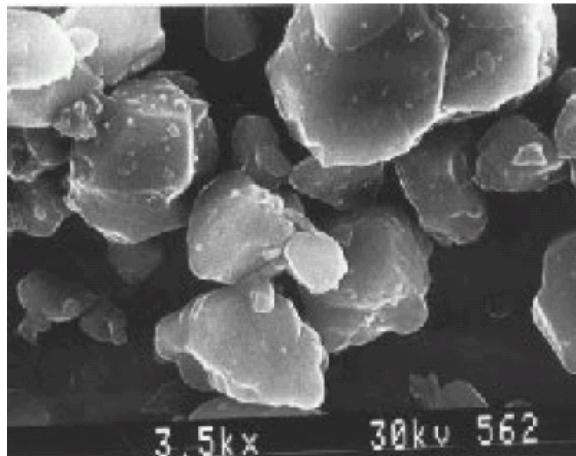


Figure 2.16 Crystalline Silica (Wypych 1993)

2.5 BIOCOMPOSITE COMPOSITION

2.5.1 POLYPROPYLENE MATRIX

ISOTACTIC HOMOPOLYMER POLYPROPYLENE

Polypropylene is a semi crystalline thermoplastic polymer which has both crystalline and amorphous phases. Isotactic PP is the most commercially used PP form due to its inherent properties and end use advantages. It has a high degree of crystallinity because of the arrangement of the molecules in an orderly manner and hence opaque, strong and highly chemical resistant. It is rigid and has better high temperature resistance than its copolymer. Some of the applications of homopolymer PP include automotive interior fabrics, windshield washer tanks, housing for domestic appliances, upholstery fabrics, medical fabrics etc.

HIGH IMPACT COPOLYMER POLYPROPYLENE

The addition of a comonomer (ethylene or 1-butene for example) during polymerization of a homopolymer results in what is called a copolymer. The copolymer composition depends on the nature and amount of comonomer added (Vasile 2003). This insertion of a second monomer into the polymeric system reduces the crystallinity and melting point by introducing irregularities or defects into the molecular chain. The reduction in crystallinity results in an increase in the amorphous content. It is documented that the impact strength of PP copolymer increased upon increasing the content of Pentene-1 comonomer in the matrix

and at low levels, the density and modulus was lower than that of isotactic homopolymer PP (White 2004).

The crystalline fraction has good stiffness and the amorphous part has good impact strength. Impact copolymers are tough and have improved low temperature impact strength due to the presence of an elastomeric phase (the amorphous phase created with addition of comonomer). The copolymer is said to be an elastomer at very high levels of comonomer. The elastomeric phase is uniformly distributed within the polypropylene matrix (Figure 2.17). These impact copolymers are also called hetero-phasic copolymers and they usually contain around 40% of ethylene-propylene rubber (EPR) (Moore 1996).

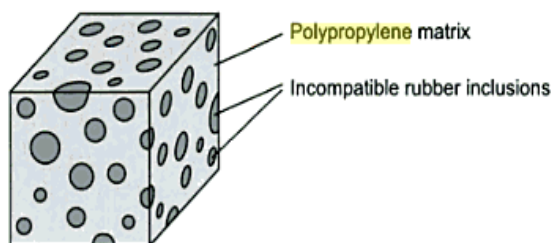


Figure 2.17 Two Phase Structure of Impact Modified Polypropylene (Calhoun 2006)

HOMOPOLYMER-COPOLYMER BLEND POLYPROPYLENE

In the 2002 edition of 'Polymer Blends Handbook' by L.A.Utracki, it is reported that polymer blends constitute 36% of the overall polymer consumption. Polymer blends are the mixtures of two or more species which can be either miscible or immiscible. Most polyolefin blends are prepared by melt mixing or compounding in a single screw or twin screw extruder. Isotactic polypropylene blends with ethylene-propylene copolymer is gaining great importance (Karger-Kocsis 1995B). It is said that the amount of interfacial mixing in a blend influences the morphology and interfacial adhesion, which ultimately affects the physical and mechanical properties of the blend (Vasile 2003). Many studies suggest the incorporation of compatibilizers to improve the interaction between different components in the blend.

The tensile strength and modulus was found to be reducing upon increasing the copolymer rubber content in PP blend (White 2004). Previous studies also indicated an improvement in

impact strength, weather resistance, flame resistance and improved low temperature performance associated with blending (Rosato 2001). A physical blend of PP isotactic homopolymer and PP copolymer is aimed at providing a synergistic improvement in properties.

2.5.2 MINERAL FILLERS

TALC

Talc has a layered structure with chemical formula $\text{Mg}_3\text{Si}_4\text{O}_{10}(\text{OH})_2$, it is a hydrated magnesium sheet silicate. It is composed of a layer of magnesium-oxygen/hydroxyl octahedral sandwiched between 2 layers of silicon-oxygen tetrahedrally bonded together by weak Van Der Waals forces. Due the weak forces combining the layers, they can easily slip apart with little shear force and hence are very soft materials.

Talc is a very soft mineral (Mohr's hardness=1) and it is highly hydrophobic and organophilic in nature. Its particle size typically ranges from 1 μm to 30 μm . When added as filler with thermoplastics (polypropylene or polyvinylchloride), talc increases the stiffness and improves the dimensional stability of the composite. The amount of talc also affects the stiffness of the composite (Karian 1999). Several studies on talc composites based on homopolymer and copolymer PP matrices indicated improved mechanical properties such as tensile strength and modulus and reduced impact strength (Lapcik 2008, Maiti 1992). Due to the property enhancement of talc, they have been widely used in under-the-hood, dashboard, bumper, interior and exterior trim and other automotive parts. They are also used in agriculture and food, ceramics, coatings, paper, personal care and rubbers.

MICA

Mica minerals are sheet silicates (phyllosilicates) with a platy morphology. Muscovite is the most popular and common of all micas and they occur in most geological environments, especially in plutonic igneous rocks. The chemical formula of muscovite mica is $\text{KAl}_2(\text{AlSi}_3\text{O}_{10})(\text{OH})_2$. It is colourless, has a specific gravity of 2.8 g/cm^3 and Mohr's hardness of 2.5-3. The most important property that characterizes muscovite mica is their high aspect ratio, thus making them useful as a filler and reinforcements in polymers. They have good

heat resistance due to which they are used in making windows for high temperature furnaces. They have good insulating properties and are used for circuit boards.

Mica with a high aspect ratio contributes significantly to the increase in flexural modulus (Karian 1999). Jahani, in his work on the effect of mica and talc on mechanical properties of polypropylene composites, reported that there was 25% increase in tensile strength of 30% mica loaded PP composite in the presence of an optimum amount of 3% MAPP coupling agent (Jahani 2011). Another study on mica homopolymer PP composites revealed that surface treated mica had significant effects on Young's modulus of elasticity (Kastner, Nardin et. al. 1988). Improved modulus, heat deflection temperature, acoustic properties, lower warpage and shrinkage make mica highly suitable for automotive applications. 25wt% mica polypropylene copolymer is used in truck with fans that are clutch driven. The fuse block cover where stiffness is a not a critical property, also consists of 12 % mica PP copolymer (Karian 1999).

WOLLASTONITE

Wollastonite is a naturally occurring white or grey mineral mostly present in metamorphosed limestone. It is formed by a combination of calcium oxide CaO and silica SiO₂ consisting of 48.28% CaO and 51.72% SiO₂ and has a chemical formula of CaSiO₃ (Karian 1999). Wollastonite has a repeating, twisted, three silica tetrahedral unit and the chains formed by these tetrahedrals are connected side by side through calcium in octahedral coordination. It grows as a needle shaped crystal due to this chain structure. It has a Mohr's hardness of 4.5-5 because of the high density of the silica chains present in the structure.

Wollastonite is a very inert material, only dissolves in concentrated hydrochloric acid. It has a specific gravity of 2.8-2.9 g/cm³. The alkaline nature of wollastonite makes it a good anti-corrosive agent in paints and coatings. It is widely used as a filler or reinforcement in plastics because it improves the mechanical properties, increases weather resistance and has a very high aspect ratio. It is also used for high temperature applications due to its high melting point (Leong 2004). Other applications of wollastonite include construction, metallurgy and ceramics.

Coarse particles of wollastonite are usually detrimental in polymer composites and an optimization of particle size is required which generally depends on the type of application (Karian 1999). The table 2.9 shows the effect of different aspect ratio wollastonite on PP composite. It is also documented that with the incorporation of wollastonite into PP matrix, there is good balance of stiffness and impact and relatively stiffer composites can be achieved at very low loadings of the filler. Low loadings can contribute to potential weight savings in automotive parts (Karian 1999). It is reported that wollastonite composite is used for automobile applications like spark plugs, interior and exterior door panels, trim parts and under-the-hood parts (Robinson 2006).

Table 2.9 Properties of Wollastonite with different aspect ratios

Material Properties	Neat polypropylene resin	20wt% wollastonite	20wt% wollastonite	20wt% wollastonite
Nominal aspect ratio (L/D)	-	5:1	8:1	19:1
Diameter D ₅₀ (μm)	-	3	15	8
Flexural Modulus	1.00	1.65	1.80	2.25
Gardner impact @ room temperature	1.00	0.73	0.60	0.65

2.5.3 WHEAT STRAW

Wheat straw (WS) is a low cost, agricultural fibrous byproduct. It is obtained after harvesting of wheat. It has a potential to replace the shortage of wood resources as bio-fillers in thermoplastic composites. Approximately 30 million tonnes of wheat straw residue were generated in 2004 in Canada (Kruger, 2007). Wheat straw is used in horse bedding, mushroom composting, as a biofuel substitute to coal, as a binder for clay and concrete in construction and is also a source of fiber for paper making. They are also used for packaging due to their cushioning effect, basketry, crafts and horticulture.

Like any other plant fibre, the chemical composition of wheat straw also comprises of 35-40% cellulose, 45-55% hemicellulose and 15-20% lignin as the major constituents in its cell wall where the cellulose is embedded in an amorphous matrix of hemicelluloses and lignin (Zhang 2011). The composition of wheat straw varies depending on the climate, region of cultivation and age of WS. Table 2.10 shows the varying composition of wheat straw from different sources (Mckean 1997). The cellulose content in wheat straw imparts good mechanical properties and lignin and hemicelluloses contents are responsible for the physical and chemical properties (Sardhashti 2009).

Table 2.10 Composition of WS at Different Location of Cultivation (Mckean, Jacobs 1997)

Composition	Ali <i>et al.</i> [1991] Pakistan	Aronovsky <i>et al.</i> [1948] Illinois	Mohan <i>et al.</i> [1988] India	Utne & Hegbom [1992] Norway	Misra [1987] American	Misra [1987] Denmark
halocellulose	58.5					72.9
α -cellulose	33.7	34.8		29-35	39.9	41.6
hemicelluloses	25.0	27.6	28.9	26-32	28.2	31.3
lignin	16-17	20.1	23.0	16-20	16.7	20.5
ash	7.5-8.5	8.1	9.99	4-9	6.6	3.7
Silica & silicates	4.5-5.5		6.3	3-7		2.0
EtOH-Benzene extr.	5.8	4.5	4.7		3.7	2.9

Extensive study has been carried out in the direction of wheat straw polypropylene composites where the effect of processing temperature, filler size, filler loading, mechanical properties, resistance to water absorption and interaction with the matrix were investigated (Kruger 2007, Digabel 2004). It was reported that the resistance to water absorption can be improved by lowering the processing temperature while, by choosing the appropriate coupling agent, the interfacial interaction or bonding between the hydrophilic fibre and hydrophobic PP matrix can be improved. The loading and aspect ratio of WS highly influenced the mechanical properties. Further, detailed study on hybrid composites based on

wheat straw and clay mineral on PP thermoplastic matrix was conducted by Sardhashti (2009). The effect of mechanical processing, fiber size distribution and coupling agent on the mechanical properties of PP composite were investigated.

The application of wheat straw in PP is relatively new (Reddy 2010). Recently the potential of wheat straw as filler for polypropylene thermoplastics have grown largely towards the automotive industry. In 2010 one exciting application for vehicle interiors was developed by a collaborated team from Ford Motor Co., ASchulman Inc., and University of Waterloo. The Ford Flex 2010 vehicle had its interior storage bins made of 20 wt% WS reinforced PP (Hardy 2010). See Figure 2.18. Like most bio-fillers, the density of WS is also significantly low compared to mineral fillers, hence representing a significant weight savings in automotive parts.



Figure 2.18 WS in Flex 2010

2.5.4 ADDITIVES

Antioxidants

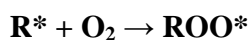
Polymers are susceptible to degradation due to heat, mechanical stress, irradiation etc. which can lead to discoloration, loss of mechanical and electrical properties or deterioration of physical appearance. The presence of oxygen during compounding or processing can cause oxidative degradation of the polymers. This is one of the serious concerns which can affect the end product. Antioxidants aid in preventing such oxidative degradation in polymers. The use of antioxidants can provide better stability to the polymer during processing and also enhance the product's service life.

The oxidation of hydrocarbon polymers occurs through a free radical chain reaction. The mechanism is as follows:

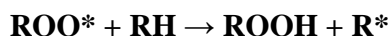
- Breaking of hydrocarbon molecule into 2 radicals,



- These radicals react with oxygen to form a peroxide radical

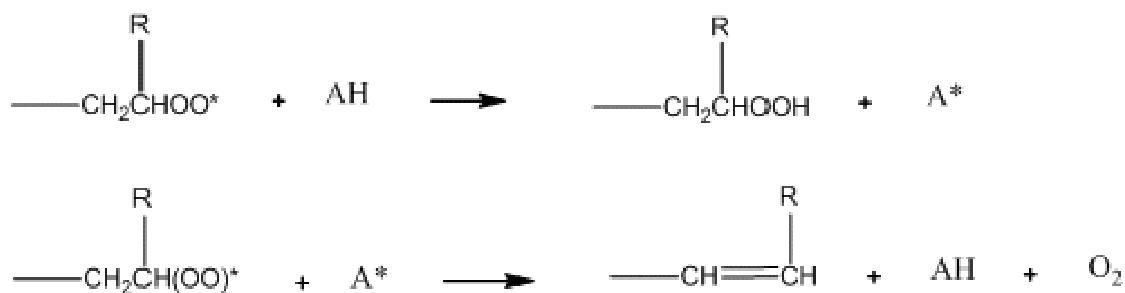


- This peroxide radical now reacts with a hydrocarbon



These reactions continue to form a series of chain reactions.

There are 2 types of antioxidants namely primary or chain breaking antioxidants (called so because these antioxidants break the chain of reactions leading to oxidation) and secondary antioxidants. Primary antioxidant can suppress the oxidation reactions over the product's service life whereas secondary antioxidant prevents the oxidation during the processing cycle. Chain breaking antioxidants (AH) either donate a hydrogen to peroxide radicals or in its oxidized form (A*) accepts a hydrogen from a peroxide radical, thus terminating the series of oxidation reactions.



The most widely used chain breaking antioxidants in plastics are polymer soluble 2,6-di-tert-butyl phenols (figure 2.19) such as butylated hydroxytoluene (BHT).

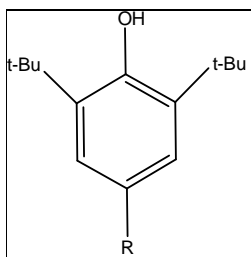


Figure 2.19 Chain Breaking Antioxidant

R = CH₃, BHT

Secondary antioxidants terminate oxidation by preventing the formation of free radicals. These antioxidants react with the hydroperoxide group preventing the decomposition of hydroperoxides into free radicals. For example, phosphites can react with ROOH group to form alcohols and phosphates thus preventing the formation of any free radicals (Pritchard 2005). Some of the sulphur compounds are also used as hydroperoxide decomposers.

The oxidative sensitivity of polypropylene is apparent at room temperature (Zweifel 2001). Two most important antioxidants used with polypropylene are Irganox 1010 and Irgafos 168. Irganox 1010 (3-(3,5-di-tert-butyl-4-hydroxyphenyl)propionate) is a primary hindered phenolic antioxidant and Irgafos 168 (Tris (2,4-di-tert-butylphenyl)phosphite) is a secondary phosphite peroxide decomposer. The chemical structures of the 2 antioxidants are shown in Figure 2.20 and Figure 2.21.

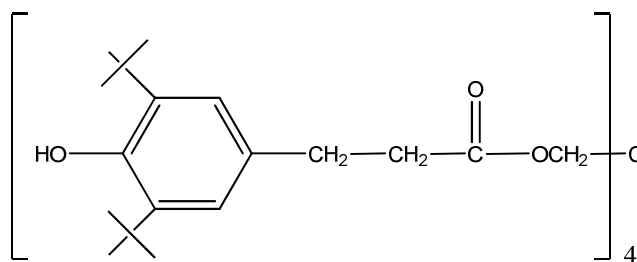


Figure 2.20 Irganox 1010

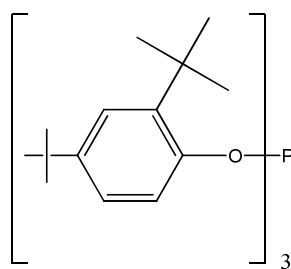


Figure 2.21 Irgafos 168

Coupling Agent

One of the most important factors affecting the final properties of composites is the interfacial bonding interaction between the filler and the polymer. One way of improving the adhesion is by enhancing the wettability of the filler by the polymer. This can be done by two ways:

- Coating the filler with additive having end functional groups – physical bonding
- Covalently bonding the filler and the polymer with the aid of coupling agents – chemical bonding

Common among these two methods is that there are active groups at either end of the additive/coupling agent such that one active end is compatible with the filler and the other end group is compatible with the polymer. The difference being that the physical bonding technique is designed to improve the dispersion of the filler in the matrix whereas chemical bonding improves the adhesion and thus the mechanical properties. In case of physical bonding technique, the surfactants get adsorbed on to the filler surface making it more compatible to the hydrophobic polymers and therefore enhancing dispersion (Pritchard 2005).

Maleic anhydride grafted polypropylene (MAPP) is the most widely used coupling agent for polypropylene. Several studies have showed that MAPP is the most effective compatibilizer for improving the adhesion between filler and PP (Reddy 2010). MAPP has also been proved to be very effective in chemically coupling talc and PP thereby leading to considerable improvement in mechanical performance (Jahani 2010). Y.H.Cui and his coworkers have showed in their work that the optimum amount of compatibilizer/coupling agent used to enhance the adhesion in composite is around 5% (Cui 2010). It has also been reported elsewhere that the improved mechanical properties are due to the esterification (Figure 2.22) of anhydride groups of coupling agent with the hydroxyl groups of cellulose fiber (Zhang 2005).

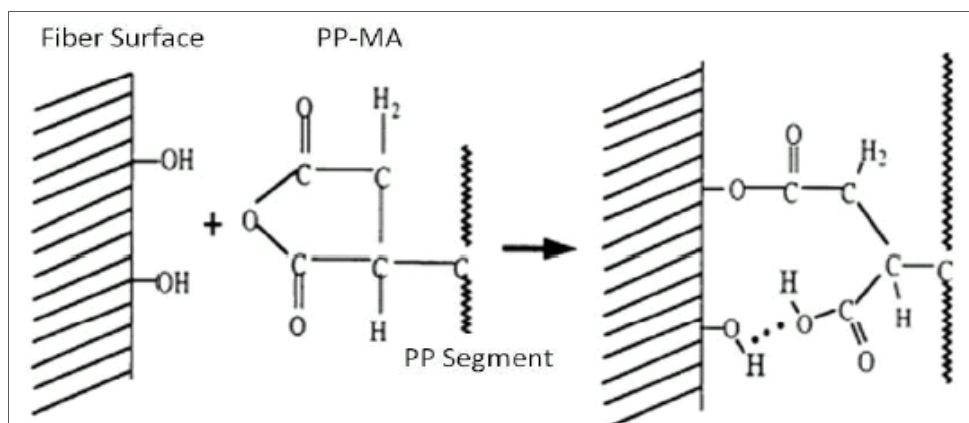


Figure 2.22 Mechanism of MAPP Adhesion with Fiber Surface (Rowell 2007)

2.6 PROPERTIES OF INTEREST

2.6.1 MECHANICAL PROPERTIES

All materials undergo some amount of deformation when subjected to a load. These deformations are the principal aspects which assess the mechanical behaviour in polymers. The mechanical performance of polymers and polymer composites are greatly influenced by the processing technique, processing conditions and various fillers or additives used in the system. The properties are also affected by factors like crosslinking, branching, and crystallinity.

Several studies have reported that type of filler, filler size, filler content and type of coupling agent have significant effect on the properties of composites. It has been documented that the ultimate properties of composites depend on the extent of bonding between the two phases, surface area of the filler and the extent of packing of the filler particles (Seymour 1990). Kocsis J. K. have reported in his work that the mechanical properties of PP composites consisting of non treated fillers highly depend on the particle characteristics. The fibre aspect ratio, alignment and packing arrangement in the matrix also influence the mechanical behaviour to a large extent (Joseph, Varghese et. al. 1996). For any kind of applications, these composites are required to meet certain property standards.

TENSILE STRENGTH AND MODULUS

When a polymer is subjected to a load, it exhibits an elastic behaviour followed by a visco-elastic behavior. Load and deformation are representations of stress and strain, stress is the ratio of force or load acting per unit area of the specimen. Strain is the amount of deformation/elongation per unit length of the specimen. When a force is applied, the material undergoes elastic deformation initially and so it can regain its shape once the force is released. At this region, the stress is directly proportional to the strain. At a certain point of stress, the material loses its elasticity and tends to deform permanently thereafter. The stress until which it can resist this deformation is called the yield stress or yield strength. The maximum load per unit cross sectional area, the material can withstand before breaking is the tensile strength of the material. Young's modulus or modulus of elasticity is the ratio of stress and strain at the elastic region.

$$E = \frac{\sigma}{\varepsilon}$$

Where, E is modulus of elasticity, σ is the force acting per unit area of the material and ε is strain. Modulus is a measure of stiffness of a material. In general, addition of fillers increases the modulus and tensile strength of the composite and decreases the elongation at break. The tensile strength and young's modulus highly depend on optimum filler loading, good dispersion of filler in matrix and strong interaction of filler and matrix.

FLEXURAL STRENGTH AND MODULUS

The flexural test is carried out using a three or four point bending technique. In the three point procedure, the specimen is placed on 2 supports at the end and force is exerted in the center. Force acts perpendicular to the axis of the specimen. The top surface of the specimen undergoes compression and the bottom surface experiences tension. Unlike in case of tensile property, flexural stress is measured using specimen thickness, bending moment and the moment of inertia of the cross-section (Callister 2001). The fracture occurs at the surface of tension and the stress at this point is known as the flexural strength. For a rectangular specimen, according to ASTM standard 790-10, the flexural properties are obtained using the formulas:

$$\text{Flexural stress or Flexural strength, } \sigma = \frac{3FL}{2bd^2}$$

$$\text{Flexural strain, } \epsilon_f = \frac{6Dd}{L^2}$$

$$\text{Modulus of elasticity, } E = \frac{\text{flexural stress}}{\text{flexural strain}}, \text{ within elastic limit}$$

where, F is the applied load, L, b and d are the specimen length, width and thickness respectively. D is the maximum deflection at the centre. The flexural strength is generally higher than tensile strength due to the fact that during flexural bending, the specimen is subjected to both compression and tension. So there is a synergy of compressive strength and tensile strength.

IZOD IMPACT STRENGTH

Impact tests measure the energy to break a specimen. Impact strength is the amount of energy a material absorbs during impact before it fractures. The area under the stress strain curve implicates the impact strength of the material, thus impact strength is related to the tensile strength and elongation. The procedure for a notched impact mechanical test is described in the standard ASTM 256-10. The impact strength for a notched specimen is less than that of an un-notched specimen and this is due to the fact that notches act as stress concentration points. Therefore the deformation is experienced mostly around the neighborhood of the

notch. Also the energy absorbed during impact is primarily the energy to propagate the crack. The presence of a crack, scratches or a notch has great influence on the impact strength of the material (Nielson 1974).

2.6.2 DIFFERENTIAL SCANNING CALORIMETRY

Differential scanning calorimetry is an important tool to study the thermal behaviour of a polymer mainly glass transition temperature (T_g), melting, percentage crystallinity and phase changes. This instrument is designed to analyze the different transitions undergone by a polymer or a composite when it is subjected to heating and measures the amount of heat absorbed or released during heating and cooling cycles. It contains two pans, a reference pan which is empty and another pan which contains polymer sample. Both the pans are heated at the same rate using a heating device. The presence of material/polymer in the sample pan indicates that it will take more heat to heat the material and to keep the temperature of the pan increasing at the same rate as the reference pan.

Glass transition, T_g , is associated with the amorphous phase of the polymer. At T_g , the material undergoes a transition from its brittle state to a rubbery state. There is more heat flow and the heat capacity of the polymer increases. It is an endothermic transition. The transition affects the hardness, volume, young's modulus and elongation at break.

The mechanical properties of polypropylene are strongly dependent on its crystallinity. An exothermic transition releases heat during crystallization and the chains have enough energy to arrange in a regular manner. When the polymer is heated further, the crystals fall apart and start to melt. It is an endothermic reaction with an increase in heat flow. At melting point, the polymer undergoes a transition from solid to liquid state. Higher the crystallinity, higher will be the melting point. Crystallization and melting points represent a first order transition and T_g represents a second order thermodynamic transition (Güttler 2009). Percentage crystallinity can also be found using DSC.

2.6.3 SCANNING ELECTRON MICROSCOPY

Scanning electron microscopy is a technique employed to study the morphology of a material. The internal structure, distribution or dispersion of fillers in polymer matrix, and interface between filler and matrix can be clearly studied using this technique. Scanning electron microscope is a high resolution microscope consisting of a beam of electrons to probe the sample surface. Electron microscopes are preferred over light microscopes due to the shorter wavelengths of electrons and the ability to focus very deeply.

SEM is also used to study the surface of fractured surfaces, particle shapes and sizes. The sample preparation for SEM is relatively easy. The surface is sputter coated with gold or carbon up to a thickness of 10 nm to make it electrically conductive. Gold is normally preferred for irregular surfaces. As the electron beam hits the specimen surface, the electrons interact with atoms on the surface and also penetrate deep into the sample. Secondary electrons get elastically scattered on the surface, back scattered electrons go a little deeper and the X rays penetrate deep into the sample. Secondary electrons are those which have enough kinetic energy to be knocked off into free space. The electrons close to the surface of the sample having low kinetic energy can escape from the sample. Secondary electrons are collected by an Everhart-Thornley (ET) detector and gives information about the topography of the sample. When the incident electrons pass near the atom's potential, they change their direction or velocity due to electrostatic interaction and some of these electrons are redirected back to the sample surface which then help in imaging. Backscattered electrons are usually collected using a solid state detector and they give information about atomic number of atoms in the sample. X rays emitted from the sample gives information about the composition or the different elements present in the sample.

2.6.4 WATER ABSORPTION

Water uptake of composites containing hydrophilic fillers limits its use in certain applications which require exposure to moisture or water. Natural plant fibres have an inherent tendency to absorb moisture due to the hydroxyl group present in their structure. Incorporation of these hydrophilic fibres into hydrophobic matrix (Rothon 1999) results in reduced compatibility

between the two phases, leading to weak interfacial bonding which ultimately affects the mechanical properties of composites. Arbelaiz and coworkers reported that water absorption is high in the cellulose and hemicellulose content of the fiber because they contain larger number of hydroxyl groups (Arbelaiz 2005). Water absorption also results in fiber swelling thereby causing change in the dimensions of the composite parts. Reports indicate that it is possible to reduce the amount of moisture absorbed by using compatibilizers or by acetylation of hydroxyl groups present in the fiber (Rana 1998, Rowell 1986).

Water absorption is measured using immersion technique according to the specifications mentioned in ASTM standard, D570-98. According to the technique, the specimens are immersed in water for a specified time and weights of dried specimens are noted at regular intervals of time. The percentage increase in weight will estimate the affinity of composites towards moisture.

3 MATERIALS AND METHODS

3.1 MATERIALS

The biocomposite mixture consisted of the polymer as base resin, fillers/fibres as the additives, antioxidants and coupling agents.

Three different grades of polymers used as base resins were:

1. Isotactic homopolymer Polypropylene (hPP), grade D180M, manufactured and supplied by Sunoco chemicals, Inc., Philadelphia, (see Appendix C for specification sheet). (Braskem America)
2. High Impact copolymer Polypropylene (icPP), grade TI6200N, manufactured and supplied by Sunoco chemicals, Inc., Philadelphia, (see Appendix C for specification sheet) (Braskem America)
3. Blend of homopolymer and copolymer Polypropylene (bPP), a proprietary blend developed and supplied by A.Schulman Inc., Akron, OH.

The melt flow index of the above base resins were informed by the suppliers as 18 g/10min, 18 g/10min and 30 g/10 min respectively. The polymers obtained in the form of pellets were ground to powder in a blender for better mixing with the fibres/ fillers.

The fibers/fillers used were:

1. Wheat Straw (two grades: medium and fine) – manufactured and supplied by Omtex Inc, Chatham, ON.
2. Talc (BT 2207) – supplied by A.Schulman Inc., Akron, OH.
3. Mica (CD 2200) – manufactured by Georgia Industrial Minerals, Inc. (see Appendix C for specification sheet) and supplied by A.Schulman Inc., Akron, OH.
4. Wollastonite (Nyglos 8) – manufactured by NYCO, USA (see Appendix C for specification sheet) and supplied by A.Schulman Inc., Akron, OH.

Irganox 1010 and Irgafos 168 manufactured by CIBA Inc. were used as antioxidants. Maleic anhydride grafted polypropylene (grade MD-353D) from DuPont was used as coupling agent.

3.2 PROCESSING METHODS

3.2.1 COMPOUNDING VIA EXTRUSION

In the first stage of the project, wheat straw fibers and the mineral fillers were added individually to the base resins at 20 wt%, 30 wt% and 40 wt% each with the objective of understanding the effects of the type and amount of matrix and dispersed phase. In the second stage, the dispersed phase consisted of wheat straw fiber and inorganic filler which were mixed together at a total level of 30 wt% in varying ratios of a) 10 wt% and 20 wt%, b) 15 wt% and 15 wt%, and c) 20 wt% and 10 wt% of straw fiber and inorganic filler respectively.

The composite mixture (200g) was initially hand blended to make it homogeneous and then fed into a Haake Minilab Micro-compounder, a co-rotating twin screw extruder (Thermo Scientific, Waltham, MA) where the operating conditions were set to 190°C and 40 rpm. The mixture underwent continuous melting and mixing while moving in between the screws. The extrudate which exited through the flush orifice were collected, cooled and pelletized (without contact with water). The formulations for compounding are shown in Table 4.1, 5.2 and 6.1. A typical twin screw extruder is shown in figure 3.1.



Figure 3.1 Haake Minilab Microcompounder (left) and conical screws (right) (Sardhashti 2009).

3.2.2 INJECTION MOLDING

The pellets formulated with polypropylene, straw fiber and inorganic fillers were injection moulded using a Ray Ran Laboratory Injection Moulding machine (Ray Ran Test Equipment Ltd., UK) to obtain bars according the dimensions set in the ASTM standards. The standard dimensions are shown in Table 3.1.

In this moulding technique, the pellets were fed into the barrel of the injection moulding machine where the temperature was set to 190°C. Once the pellets melted inside, pressure of 100 psi was applied to pneumatically move the ram down thereby pushing the material through the nozzle to flow to the mould platen. The mould tool temperature was set to 50°C and the molten composite material was allowed to flow for 15 sec before releasing the pressure. Then the bars were removed from the mould tool and inspected for any defects. These test bars were then placed in a Hewlett Packard 5890A GC oven for annealing to remove any thermal history occurred during extrusion and inection moulding. The temperature inside this oven increased from initial temperature 25°C at a rate of 10°C per minute till a final temperature of 150°C \pm 1°C was reached. It was left there for 10 min and then cooled to room temperature.

3.3 CHARACTERIZATION METHODS

3.3.1 MORPHOLOGY

The morphology of pure wheat straw fibres, mineral fillers (talc, mica and wollastonite) and polypropylene composites were observed using a scanning electron microscope LEO SEM consisting of a Field Emission Gemini Column. Pieces of the thermoplastic composites samples used for impact strength measurement were cut using a knife from the fractured surfaces and fixed to an aluminum stub with a double sided carbon adhesive tape such that the fractured surfaces were facing upward towards the electron source of SEM. Prior to scanning, the samples were sputter coated with gold to a thickness of approximately 10 nm to make the surface electrically conductive.

3.3.2 PARTICLE SIZE ANALYSIS

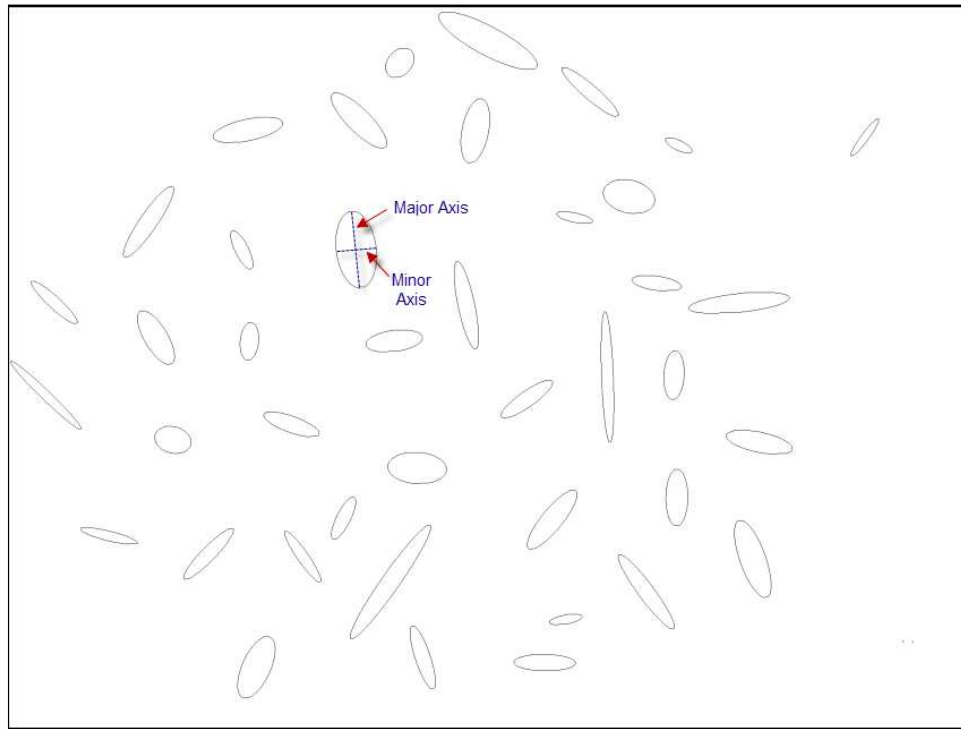


Figure 3.2 Best Fitting Ellipses for fWS Particles

The particle size and the aspect ratio of the straw fibers were measured using optical microscopy. The stereomicroscope Leica MZ6 (Type DFG 290, Leica Microsystems Ltd.) was used for image generation and acquisition. The wheat straw particles were placed on the surface of a glass slide such that each particle did not touch each other. The images of the particles were taken using a digital camera with the stereomicroscope at a magnification of 63X. The images taken were then analyzed using an image processing software program called ImageJ. The number of particles in each image was also counted using the software. Approximately 100-150 particles of fine and medium WS were measured. This program provides the dimensions of the particle by drawing the best fitting ellipse around the particle. From this ellipse, the major and minor axis is drawn to obtain the length and width of the particle being measured. The aspect ratio is calculated as the ratio of length and width. See Figure 3.2.

3.3.3 DIFFERENTIAL SCANNING CALORIMETRY (DSC)

The melting point, crystallization peaks, and enthalpy of phase transition (melting) were determined using Q 2000 DSC equipment. Calibration was done according to the Tzero TM method. An exact amount of sample in the range of 5-10 mg was taken into the T-zero pans and sealed with a T-zero hermetic lids using a T-zero press. The equipment has an automatic sample loading device (up to 16 samples), although each sample was analyzed individually. The analysis was carried out in 3 cycles. In the first cycle, the samples were heated from 35° C room temperature to 220°C at a rate of 10°C/min and remained at 220°C for 3 minutes. This was done to remove the thermal history of the samples. In the second cycle, the samples were cooled from 220°C to 50°C again at 10°C/min and at 50°C for 3 minutes. In cycle 3, the samples were heated further from 50°C to 220°C at the same rate. Cycle 2 and 3 were used to analyse the samples for their thermal properties. The data obtained were plotted using the TA Universal Analysis software. % crystallinity was calculated using the formula:

$$\% = \frac{\Delta H}{\Delta H^\circ (1 - wt\% \text{ filler})} \times 100$$

3.3.4 MELT FLOW INDEX (MFI)

Flow properties of the three different grades of polypropylene were measured using a Dynisco D4001DE MFI tester at a temperature of 230°C and a load of 2.16 kg according to the ASTM standards ASTM 1238-A. Each time approximately 5g of the resin was placed inside the heated chamber and left to melt for 360 seconds. Once melted, the molten material was pushed using the load (placed above the tester) down through an 8 mm die and 4-5 sample cuts were made at regular intervals of 10 sec. The weight of each sample cut is reported in g/10 min.

3.3.5 WATER ABSORPTION

The amount of water absorbed by the sample was measured by immersion technique, according to the ASTM standard D570-98(Reapproved 2010). Three injection molded bars were initially conditioned by placing inside an oven at 108°C for approximately 1 hour, after which they were placed in a desiccator to cool down. The conditioned weight was noted as 0 hour reading, using a

Mettler Toledo analytical balance (AB 304-S), before immersing the bars in deionised water. The measurements were done at regular time intervals of 0hr, 6hrs, 12 hrs, 24 hrs(for 5 days), once in 3 days, 4 days, 5 days, once a week and so on until there was no change in the weight further (saturation). The amount of water absorbed was measured using the formula given in ASTM D570-98:

$$\text{Increase in weight, (wt \%)} = \frac{\text{wet weight} - \text{conditioned weight}}{\text{conditioned weight}} \times 100$$

3.3.6 DENSITY

The injection molded bars were cut into 2 halves to make small length specimens for density measurements. They were conditioned at $23 \pm 2^\circ \text{C}$ and $50 \pm 5\%$ relative humidity for 40 hours according to the ASTM standard D 792-08. The test was carried out in ethanol since the composites made of wheat straw were lighter than water and so had a tendency to float in water. Ethanol was used for all the other composites as well to maintain uniformity. Weights were measured using a Mettler Toledo analytical balance. The density of ethanol was measured using a pycnometer.

The specific gravity and density of the composite was calculated using the formula:

$$\text{Sp gr } 23/23^\circ\text{C} = \frac{a}{a-b}$$

$$D^{23^\circ\text{C}}, \text{ kg/m}^3 = \text{Sp gr } 23/23^\circ\text{C} \times (\text{density of ethanol})$$

Where,

a = apparent mass of specimen, without wire or sinker, in air,

b = apparent mass of specimen completely immersed and of the wire partially immersed in liquid.

3.3.7 MOISTURE CONTENT

The straw fibres and mineral fillers were tested for the amount of moisture present, prior to compounding them, using a MB 45 Metler Toledo Moisture Analyser (Ohaus Corporation,

Pinebrook, NJ, USA) . The samples were uniformly spread on an aluminum pan and placed on the analyser where it was heated to 110°C until all the moisture was absorbed. The results were recorded at regular intervals in terms of percentage of moisture evaporated from the sample. WinWedge software was used to record the data.

3.3.8 MECHANICAL PROPERTIES

The sample specimens were conditioned at a temperature of (23±2) °C and relative humidity of (50±10) % for 40 hours prior to testing and the same conditions were maintained during testing as well. These parameters were set according to the procedure A of ASTM standard D618-08.

TENSILE PROPERTIES

The preconditioned injection molded composite bars were tested for their tensile properties using a Q Series Mechanical Test Machine (Test Resources Inc., Shakopee, MN, USA). In this testing technique, the dog bone shaped bar was placed between two grips and the rectangular portion of the bar, outside the grips was subjected to stretching. The distance between the upper and lower grips was set to 22±0.05 mm after placing the sample and the grips tightened to prevent the specimen from slipping. Testing was done according to the standard ASTM D1708-10. Force was applied to pull the specimens at a rate of 1.3 mm/min and a stress strain graph was plotted from the values obtained. The measurement for strain was obtained by measuring the displacement of the crossheads without the use of an extensimeter or strain gauge. Therefore, minor slippage of the sample specimen may contribute to experimental uncertainty during the calculation of strain.

The tensile strength, yield strength, percentage elongation at break and modulus of elasticity were calculated using the given formulas:

- Tensile strength $= \frac{\text{maximum load}}{\text{cross-sectional area}} = \frac{\text{maximum Force}}{\text{unit cross-sectional area}}$
- Yield strength $= \text{Tensile stress at yield}$
- % elongation at break $= \left(\frac{\text{final gage length} - \text{original gage length}}{\text{original gage length}} \right) * 100$

$$= \left(\frac{\text{position}}{\text{original length}} \right) * 100$$

- Elastic modulus $= \frac{\text{stress}}{\text{strain}} = \frac{\text{force/cross-sectional area}}{\text{change in length/original length}}$

FLEXURAL PROPERTIES

Three point bending technique was used to determine the flexural strength and modulus of the composite material, as per the ASTM standard D790-10. The rectangular bar was placed on 2 supports and loaded by means of a loading nose in the centre. The load acting at the centre of the bar continued until the outer surface ruptured or until 5% strain was reached. Flexural tests were also carried out using the Q series Mechanical Test Machine. The following equations were used to calculate the rate of crosshead motion, flexural strength and modulus of the material:

- Rate of crosshead motion, $R = \frac{ZL^2}{6d}$
- Flexural stress, $\sigma_f = \frac{3PL}{2bd^2}$
- Flexural strain, $\epsilon_f = \frac{6Dd}{L^2}$
- Modulus of elasticity, $E_B = \frac{\text{flexural stress}}{\text{flexural strain}}$, within elastic limit

Where,

L = support span (mm), d = depth of bar (mm), Z = rate of straining outer surface (mm/mm/min), P = load at a given point on the curve (N), b = width of the bar (mm) and D = maximum deflection at the centre (mm). See Table 3.1.

IMPACT STRENGTH

The impact strength of the composite materials was measured according to the ASTM standard 256-10 Test Method A. The specimens were prepared by injection molding. The specimens were notched at an angle of $45 \pm 1^\circ$ and a depth of 2.5 mm using a milled notch cutter prior to testing under the preset temperature and humidity conditions. The notch creates stress concentration on the specimen increasing the chance of a brittle failure. After sampling, the specimen was

mounted vertically on a Monitor Impact Tester (Testing Machines Inc (TMI), New Castle, DE) and hit by a swinging pendulum type hammer (Izod Hammer 0-1 X 0.01 FT Lbs, TMI 43-0A-03) at 90°. The results were recorded in Joules/meter. Six replicate tests were carried out for each sample and their averages are reported.

Table 3.1 Specimen Dimensions According to ASTM Standards

	LENGTH (mm)	WIDTH (mm)	THICKNESS (mm)
TENSILE TESTING	22±0.05	5±0.25	1.5±0.3
FLEXURAL TESTING	31.8±0.2	12.7±0.2	3.2±0.4
IMPACT TESTING	63.5±0.2	12.7±0.2	3.2±0.4
WATER ABSORPTION	63.5±0.2	12.7±0.2	3.2±0.4

4 RESULTS AND DISCUSSIONS: POLYPROPYLENE RESINS

4.1 FORMULATIONS

Three different polypropylene matrix namely homopolymer (hPP), impact copolymer (icPP) and homopolymer-copolymer blend PP (bPP) were used in this study to analyse the properties of composites. Table 4.1 represents the formulations for the three grades of polypropylene used with 0.5 wt% of antioxidants (Irganox 1010 and Irgafos 168). For the pure polymer formulations, no coupling agent or fillers were added.

Table 4.1 Formulations for Pure Polypropylene Resins

Polymer	Expt#	Polymer (%)	Filler/fibre (%)	Antioxidant (%)	Coupling agent (%)
hPP	I	99.5	-	0.5	-
icPP	II	99.5	-	0.5	-
bPP	III	99.5	-	0.5	-

4.2 PROPERTIES

4.2.1 DIFFERENTIAL SCANNING CALORIMETRY

Differential Scanning Calorimetry (DSC) analysis was conducted to study the thermal behaviour of resins. Melting temperature (T_{m2}), crystallization temperature (T_c) and % crystallinity are noted for each of the resins used in this study. The % amount of crystallinity in pure polymers was calculated using the following equation,

$$\text{Crystallinity (\%)} = \frac{\Delta H}{\Delta H^\circ (\text{wt\% resin})} \times 100$$

where, ΔH is the heat of enthalpy required to melt the resin and ΔH° is the heat of fusion of a 100% crystalline polypropylene (209 J/g). The results obtained from DSC measurements are summarized in Table 4.2. It is observed that generally, the addition of antioxidants did not show

any considerable effect on the melting temperature of the resins. Though not significant, it is interesting to note that both the melting point and crystallization temperature for homopolymer PP increased by around 2°C in the presence of irganox 1010 and irgafos 168. The impact copolymer PP exhibits a melting point of 166°C higher than both homopolymer and blend. This increase in melting temperature can be associated with the presence of a comonomer in the copolymer matrix.

Table 4.2 Results from DSC Analysis

Polymer	T _{m1} (°C)	T _{m2} (°C)	T _c (°C)	T _c ⁰ (°C)	ΔH _{m1} (J/g)	ΔH _{m2} (J/g)	ΔH _c (J/g)	%C _{m1}	%C _{m2}	%C _c
hPP	167.43	159.54	111.08	115.86	158.4	107.6	95.21	75.79	51.48	45.55
hPP+AO	167.28	162.05	113.66	117.75	105.8	106.5	92.98	50.62	50.96	44.49
icPP	166.9	165.85	133.48	136.14	91.54	98.62	75.19	43.8	47.19	35.98
icPP+AO	166.8	166.92	133.23	136.32	89.84	93.87	78.54	42.99	44.91	37.58
bPP	163.05	162.56	119.66	122.69	81.8	78.96	95.36	39.14	37.78	45.63
bPP+AO	166.53	163	120.13	123.52	103.2	102.8	95.28	49.38	49.19	45.59

The crystallization temperature (T_c) remained unaffected with the addition of antioxidants for all the resins. The crystallization peak for copolymer was higher than homopolymer and PP blend (bPP). As expected, the % crystallinity at melting (%C_{m2}) for homopolymer with and without antioxidants was significantly higher than the other two resins, because of a high degree of isotacticity in its structure. However, the % crystallinity of copolymer and blend were largely influenced by the presence of antioxidants. PP blend with antioxidants, showed a 28.9% increase in percentage crystallinity at melting whereas the % crystallinity of copolymer decreased by 4.5%. It is also interesting to note that PP blend exhibited similar value for % crystallinity at crystallization as did the homopolymer. Both polymers had significantly higher amount of crystallinity than icPP. The plots for DSC curves are available in Appendix A.

4.2.2 MELT FLOW INDEX

Table 4.3 Melt Flow Index for PP Resins

Polymer resins	MFI(g/10min)
hPP	17.72
icPP	16.39
bPP	27.41

The flow property of a material largely depends on temperature and shear rate, and influences processing. Injection moulding involves high shear rate and extrusion involves medium to high shear rate and therefore, it is important to analyse the flow property of polypropylene prior to processing. It is reported that the presence of a comonomer can affect the rheology of the polymer and also, high MFI grades of polypropylene are suitable for injection moulding (Maier 1998). The melt flow rates for pure polypropylene resins are shown in Table 4.3. It is observed that the MFI value for PP blend is significantly higher than hPP and icPP. The flow rates measured for copolymer and homopolymer are close to the values obtained from the supplier.

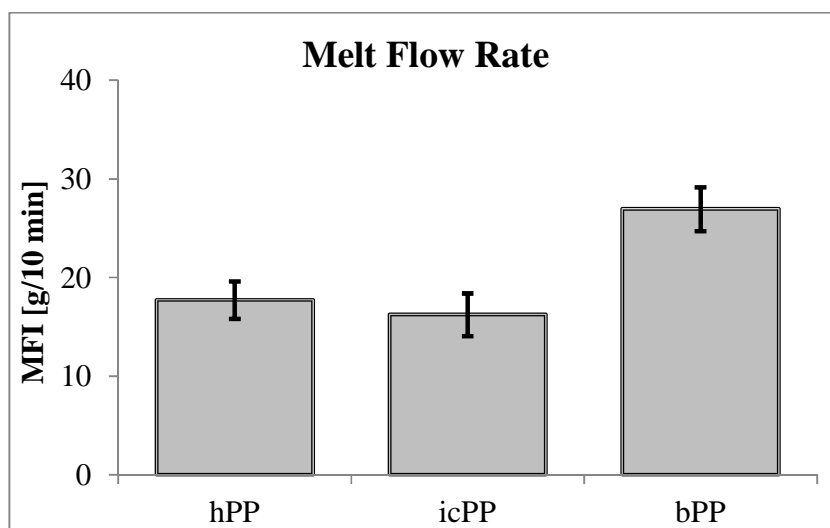


Figure 4.1 Plot showing MFI Values for pure Resins

4.2.3 WATER ABSORPTION

The water absorption plots for homopolymer, copolymer and blend are represented in Figure 4.2. It can be observed that icPP and bPP absorb a significant amount of water in comparison to the homopolymer. The copolymer PP gained a weight of 0.35% without any saturation even after 40 weeks. PP blend reached saturation at 22 weeks with an increase in weight of 0.2% after 40 weeks of exposure. However, after 13 weeks of saturation, the blend appears to have gained slight weight. In contrast, homopolymer absorbed the least amount of water and reached saturation at an early time period, and the increase in weight is observed to be decreasing to 0 after 40 weeks. The water absorption characteristic of homopolymer seems to be insignificant when related to the property of composite specimens whereas the water absorption results for copolymer and blend can be significantly compared with those of composites.

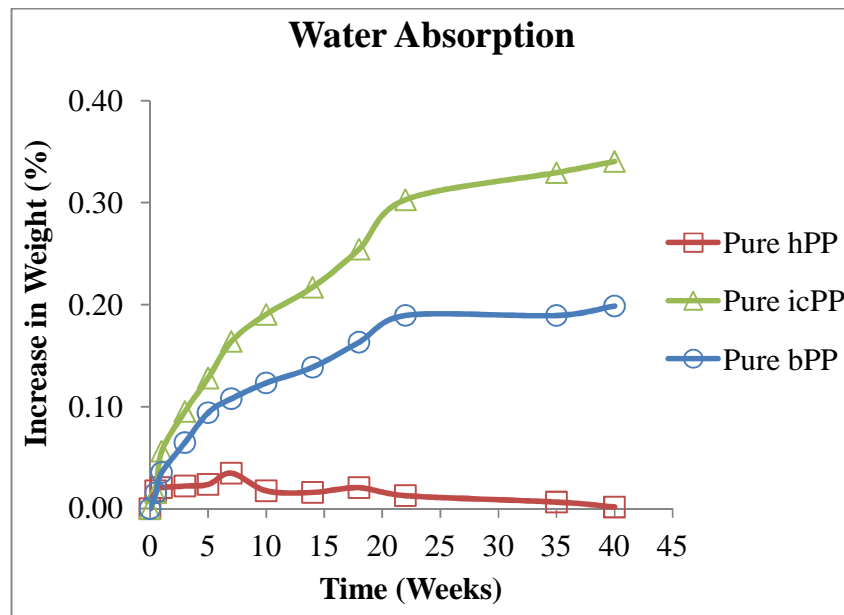


Figure 4.2 Water Absorption plots for hPP, icPP and bPP Resins

5 RESULTS AND DISCUSSIONS: POLYPROPYLENE-FILLER COMPOSITES

5.1 CHARACTERIZATION OF WHEAT STRAW

5.1.1 PARTICLE SIZE ANALYSIS

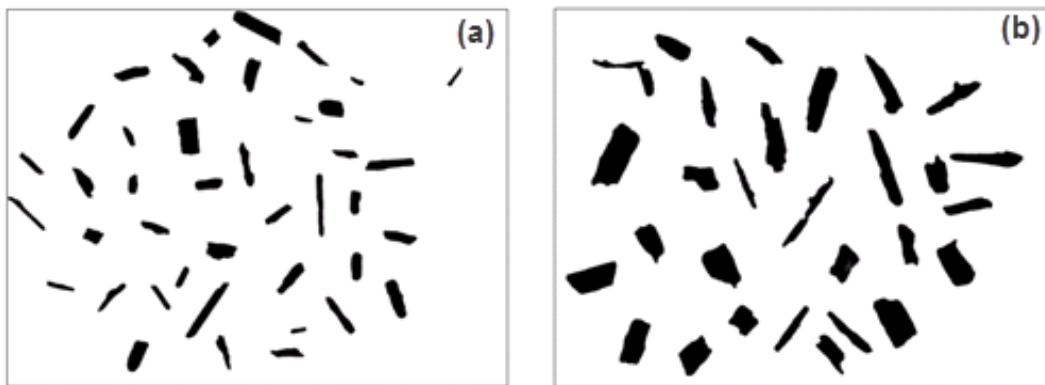


Figure 5.1 Optical Microscope Image of (a) fine WS and (b) medium WS

The stability, chemical reactivity, flow ability and strength of many materials are affected by the size and characteristics of the particles within them. Particle size analysis was performed on fine (fWS) and medium wheat straw (mWS) batches as obtained from Omtec Inc., Chatham, ON, to measure the average length, width and aspect ratio of the particles. Samples were picked at random from both the batches and around 100-150 particles (Figure 5.1) were analysed while allowing 3-4 replications. Image processing software program called ImageJ was used for the analysis. The results obtained are shown in Figures 5.2 to 5.4.

It was found from particle size analysis that the fine wheat straw particles had a length ranging from 0.1 to 1.2 mm with more than 30% particles having length between 0.2 and 0.4 mm (Figure 5.2). The average length of fWS particles was found to be 0.35 mm. Analysis on medium WS particles revealed that more than 40% particles had length between 0.8 and 1.2 mm. The overall mWS sample analyzed had length ranging from 0.4 to 2.4 mm. Moreover, 29% of mWS particles had length between 1.2 and 1.6. The average length of mWS particles was 1.25 mm. It is

interesting to observe that the value representing peak of the distribution curve for mWS also corresponds to the shortest fWS fibres (or the tail of the distribution curve for fWS).

There is huge variation in the fiber width results obtained for fine and medium wheat straw particles. While, the width of maximum number (37%) of fWS particles was found to be lying between 0.04 mm and 0.08 mm with a narrow distribution, mWS particles showed a broader distribution curve with 18% (peak) particles having width ranging from 0.28 to 0.32 mm (Figure 5.3). The fWS particles had width as low as 0.0028 mm and as high as 0.24 mm. Medium WS sample analyzed had lowest width of approximately 0.16 mm and highest width of 0.80 mm. The average width of mWS was 0.38 mm and that of fWS particles was 0.08 mm.

Figure 5.4 represents the aspect ratio plot for fWS and mWS. It is interesting to note that the maximum number of particles for both fWS and mWS had an aspect ratio between 3.0 and 5.0. The samples analyzed for fWS contained aspect ratio ranging from 1.0 to 15.0 whereas mWS samples contained aspect ratio limited between 1.0 and 12.0. Around 31% of fWS and 40% of mWS particles had an aspect ratio of 1.0-3.0. The average aspect ratio for fWS was found to be 4.5 and a lower average aspect ratio of 3.7 was obtained for mWS sample.

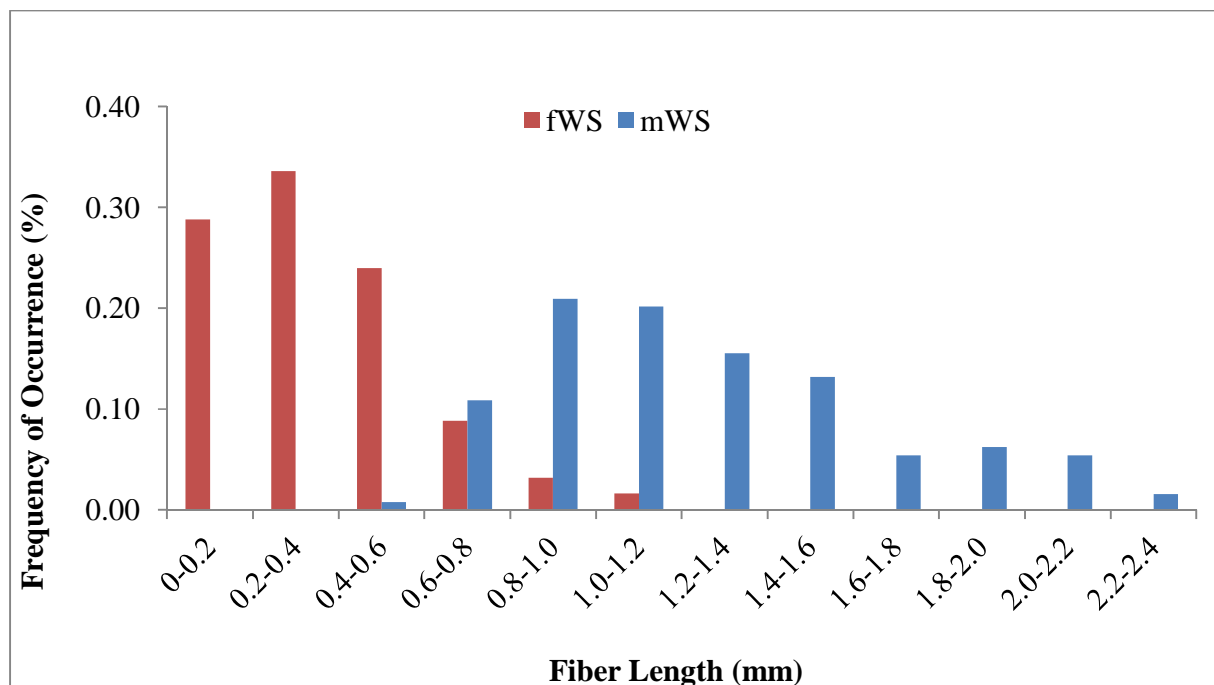


Figure 5.2 Plot Showing Length Distributions of Fine and Medium WS Particles

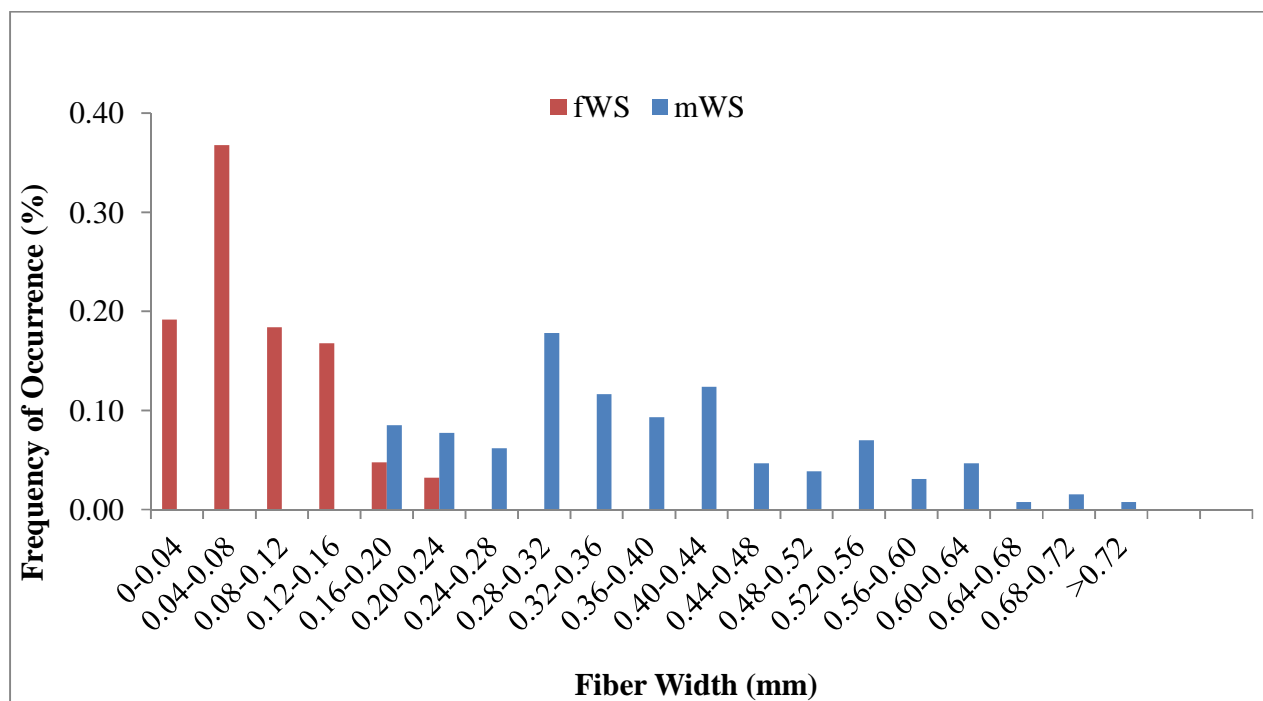


Figure 5.3 Plot Showing Width Distributions of Fine and Medium WS Particles

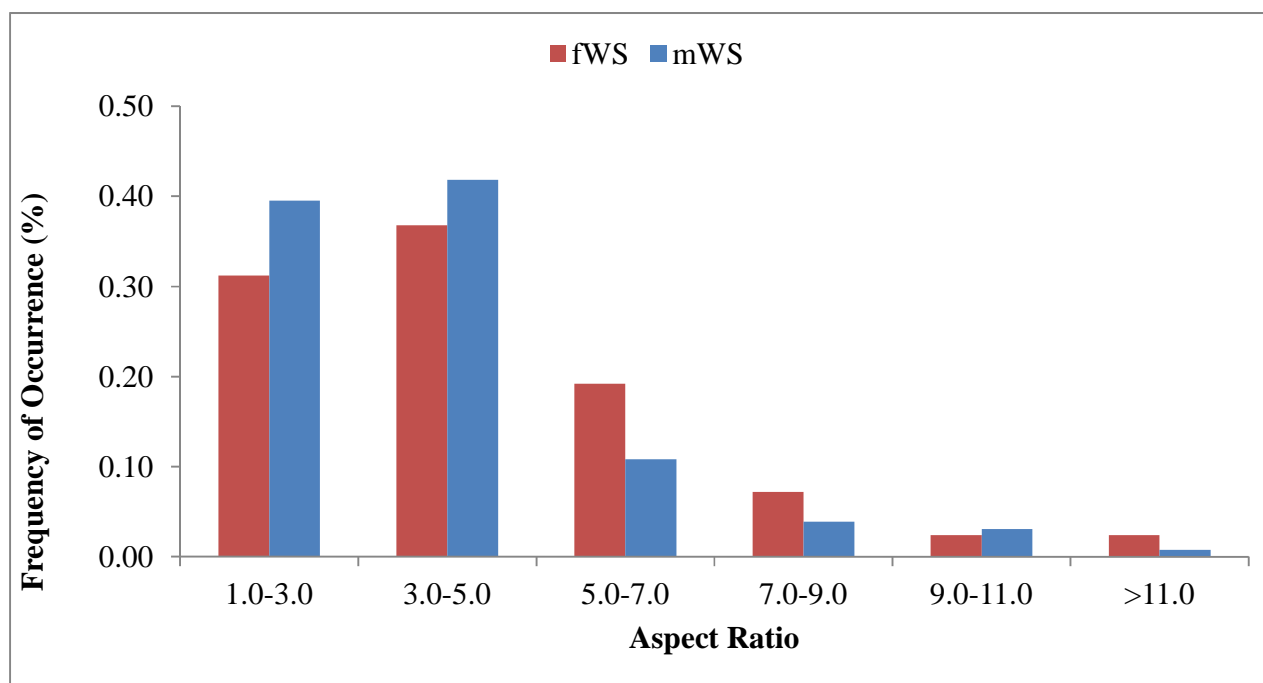


Figure 5.4 Plot Showing Aspect Ratio of Fine and Medium WS Particles

5.1.2 MOISTURE CONTENT ANALYSIS

Moisture content analysis was performed to quantify the water content in the wheat straw samples prior to compounding. Due to its inherent hydrophilic characteristics, wheat straw tends to absorb moisture as soon as it is exposed to atmosphere. Therefore it is important to know the amount of moisture present in the samples, although the present work did not study the effect of initial moisture of WS on the mechanical properties of the composite. The moisture content in minerals fillers was also examined and the percentage values are tabulated in Table 5.1.

Table 5.1 Moisture Content Results for Fillers

Filler	Moisture Content (wt% moisture)
Fine wheat straw	7.70
Medium wheat straw	7.24
Talc	0.60
Mica	1.13
Wollastonite	0.09

5.2 FORMULATIONS AND PROPERTIES: POLYPROPYLENE-FILLER COMPOSITES

The formulations were prepared using three grades of polypropylene, two grades of wheat straw and three types of mineral fillers. The results of the mechanical properties are presented in Table 5.2. The detailed presentation and discussions are presented in the following sections. The loadings of the dispersed phase were 20 (low), 30 (medium) and 40 (high) wt%.

Table 5.2 Formulations and Properties Chart for Single Filler PP Composites

Antioxidant (AO) – Irganox 1010, Irgafos 168 – 0.25 wt% each Coupling agent (CA) – Fusabond MD 3532 – Maleic anhydride grafted Polypropylene – 2 wt%									
Sample name	Mineral filler (wt %)	Biobased fiber (wt %)	Flexural Modulus (GPa)	Flexural Strength(MPa)	Tensile Modulus (MPa)	Tensile Strength (MPa)	Impact Strength (J/m)	Density (kg/m ³)	Specific Flexural Modulus (Mpa.m ³ /kg)
hPP	-	-	1.24(.11)	50.0(3.1)	241(33)	38.7(0.9)	21.6(2.3)	925(0.9)	1.34
icPP	-	-	1.10(.08)	33.0(1.2)	204(80)	23.7(1.2)	166.3(19.2)	910(2.9)	1.21
bPP	-	-	1.19(.03)	49.8(0.9)	228(48)	34.7(0.5)	65.0(6.4)	921(5.8)	1.30
hPP-fWS	-	20	1.73(.14)	56.7(2.4)	276(61)	34.1(4.0)	22.1(1.9)	990(4.7)	1.74
	-	30	1.94(0.4)	51.2(9.6)	269(38)	30.6(2.7)	23.9(1.7)	1036(17.2)	1.88
	-	40	2.33(.26)	59.2(1.2)	284(30)	29.9(2.9)	23.0(1.7)	1057(22.7)	2.20
icPP-fWS	-	20	1.52(.06)	39.2(0.3)	223(32)	26.8(0.5)	56.0(1.7)	979(2.9)	1.55
	-	30	1.75(.09)	42.6(0.4)	224(39)	27.5(1.3)	47.1(3.3)	1016(3.2)	1.72

	-	40	2.15(.06)	44.2(1.3)	239(27)	27.7(1.8)	38.4(1.1)	1061(3.9)	2.02
bPP-fWS	-	20	1.66(.07)	51.2(1.0)	257(35)	32.4(2.4)	27.0(0.9)	990(4.3)	1.68
	-	30	2.06(.05)	52.6(1.7)	280(36)	32.5(2.2)	26.0(1.1)	1024(6.0)	2.01
	-	40	2.39(.07)	53.3(1.5)	288(20)	29.3(1.8)	25.7(0.7)	1075(3.9)	2.23
hPP-mWS	-	20	1.82(0.1)	57.1(1.0)	281(31)	37.9(1.7)	22.0(1.5)	992(5.1)	1.84
	-	30	2.30(.16)	59.9(0.2)	288(26)	35.1(3.5)	25.1(1.1)	1023(7.1)	2.25
	-	40	2.64(.09)	60.9(1.5)	306(33)	32.1(4.6)	25.9(1.4)	1067(6.8)	2.47
icPP-mWS	-	20	1.37(.07)	37.3(1.0)	238(42)	27.1(0.4)	66.6(6.5)	979(5.8)	1.40
	-	30	1.72(.03)	41.0(0.9)	241(21)	27.5(1.6)	49.9(2.3)	1019(6.2)	1.69
	-	40	1.97(.02)	42.8(1.0)	256(31)	28.1(1.1)	49.6(1.3)	1063(6.3)	1.85
bPP-mWS	-	20	1.65(.03)	49.7(1.4)	220(51)	31.6(5.4)	31.4(1.4)	989(6.9)	1.67
	-	30	2.03(.07)	53.0(2.0)	212(23)	25.0(4.6)	31.2(1.9)	1013(10.4)	2.01
	-	40	2.37(.09)	55.4(1.1)	297(38)	32.7(5.0)	28.9(1.2)	1071(7.1)	2.21
hPP-Talc	20	-	2.03(.16)	62.4(2.0)	366(69)	40.2(0.3)	27.5(1.5)	1058(7.6)	1.92
	30	-	2.36(.11)	62.7(2.8)	275(40)	38.8(0.8)	24.5(1.3)	1101(78)	2.15
	40	-	2.55(.12)	61.6(1.1)	274(36)	38.7(0.8)	28.5(2.3)	1258(2.8)	2.03
icPP-Talc	20	-	1.45(.07)	35.4(0.9)	281(76)	25.0(0.4)	54.1(4.0)	1073(26)	1.35
	30	-	1.48(.04)	35.2(0.8)	280(44)	25.5(0.4)	46.3(3.0)	1134(7.9)	1.31
	40	-	1.77(.12)	37.0(0.4)	277(35)	27.2(0.4)	38.4(2.7)	1270(52)	1.39
bPP-Talc	20	-	1.65(0.1)	49.0(2.2)	261(63)	32.1(2.2)	37.6(4.5)	1065(1.7)	1.55
	30	-	1.74(0.2)	48.4(1.1)	263(59)	31.7(2.4)	29.1(1.6)	1149(4.2)	1.51
	40	-	2.22(.04)	51.1(1.3)	295(55)	33.0(1.1)	28.0(1.5)	1258(1.3)	1.77
hPP-mica	20	-	2.01(.08)	55.7(1.4)	271(47)	38.7(0.2)	26.6(1.9)	1062(4.6)	1.90
	30	-	2.45(.08)	56.0(0.9)	266(25)	36.8(1.0)	26.6(1.1)	1143(2.8)	2.14
	40	-	3.17(.05)	56.1(1.0)	287(36)	30.5(3.6)	22.2(4.8)	1248(2.7)	2.54

icPP-mica	20	-	1.47(.06)	34.3(0.5)	243(49)	24.8(0.6)	58.7(6.3)	1051(4.4)	1.40
	30	-	1.83(.06)	36.2(0.8)	256(36)	25.4(0.2)	40.8(2.9)	1137(7.5)	1.61
	40	-	2.03(0.3)	35.5(5.3)	238(37)	26.4(0.7)	30.1(2.1)	1216(25.8)	1.67
bPP-mica	20	-	1.75(0.1)	50.6(1.2)	227(52)	32.8(0.9)	34.4(5.7)	1057(4.5)	1.66
	30	-	2.07(.08)	50.1(1.0)	263(62)	32.5(1.4)	34.9(15.8)	1147(2.7)	1.81
	40	-	2.76(0.1)	51.4(0.8)	256(33)	29.4(2.8)	27.2(1.6)	1238(11.5)	2.23
hPP-Wnite	20	-	2.50(.08)	65.1(1.7)	262(38)	42.5(0.6)	24.1(2.1)	1068(3.5)	2.34
	30	-	3.17(.09)	72.5(0.8)	353(43)	43.4(2.8)	27.6(1.9)	1169(8.8)	2.71
	40	-	3.92(0.2)	77.1(1.3)	325(49)	42.7(3.8)	30.5(2.2)	1279(8.1)	3.07
icPP-Wnite	20	-	1.81(0.1)	40.7(1.8)	239(37)	28.3(0.8)	65.3(4.0)	1069(3.9)	1.70
	30	-	2.27(0.1)	46.0(0.8)	249(35)	31.8(0.7)	58.7(1.5)	1149(3.3)	1.98
	40	-	2.80(.08)	50.9(1.2)	297(49)	34.1(1.0)	58.3(2.3)	1252(7.6)	2.24
bPP-wnite	20	-	2.17(0.1)	56.3(1.4)	225(46)	36.2(0.6)	31.7(2.4)	1063(10.0)	2.04
	30	-	2.50(0.1)	57.9(2.1)	287(53)	35.8(1.4)	33.6(1.4)	1159(1.6)	2.15
	40	-	3.07(0.2)	62.1(2.8)	294(57)	34.8(3.5)	34.4(0.9)	1272(6.6)	2.42

5.2.1 FLEXURAL STRENGTH

The effect of wheat straw and minerals on the flexural strength of polypropylene composites was studied and is represented in Figure 5.5. At medium and high loading percentages (30 and 40 wt%), addition of wollastonite significantly improved the flexural strength of homopolymer polypropylene composites. At low percentage loading (20 wt%) the effect of talc and wollastonite did not seem to be considerably different although both increased the flexural strength of hPP. The addition of fine WS, medium WS and mica did show an increase in the flexural strength of hPP. mWS and fWS enhanced the strength of hPP from 50 MPa to around 60Mpa at 40% loading whereas no improvement in strength was observed by increasing the mica

content from 20 to 40 wt%. The flexural strength of mica filled homopolymer PP composite was much lower than the strength of talc-hPP composite.

The effect of the fillers on impact copolymer polypropylene is shown in the Figure 5.5 (b). Addition of talc and mica to icPP did not have any significant effect since the flexural strength values were similar to the result shown by the pure copolymer resin. Same observation has been maintained at all filler levels too. Fine WS, medium wheat straw and wollastonite showed a similar trend of increasing flexural strength with increasing percentage loadings. However the performance of wollastonite was much more significant as is the case with homopolymer polypropylene. The effect of fWS is slightly higher than that of mWS, though not so evident, because of the fact that smaller fibers have larger surface area than longer fibres and thus better wetting of the fiber with the matrix is possible (Cui 2010). This characteristic would have enabled strong interfacial interaction in fWS-icPP composite.

The highest flexural strength for wollastonite filled icPP composites is attributed to the high aspect ratio of the filler and good interfacial adhesion between the matrix and the filler. It has also been indicated that maleic anhydride grafted PP enhances the interfacial bonding between the matrix and wollastonite (Chen 2008).

The homo-co blend PP (bPP) showed higher flexural strength than the homopolymer or copolymer PP alone. The performance of talc and mica appeared to be lowering from 20 to 30wt% and increased by 1-2 MPa at 40 wt% loading (Figure 5.5 (c)). The effect produced by fine wheat straw and medium straw was not significantly different at the three filler loading percentages. The flexural strength of fWS, mWS and wollastonite increased from 20 to 40 wt%. Wollastonite improved the flexural strength of homopolymer, copolymer and blend PP significantly.

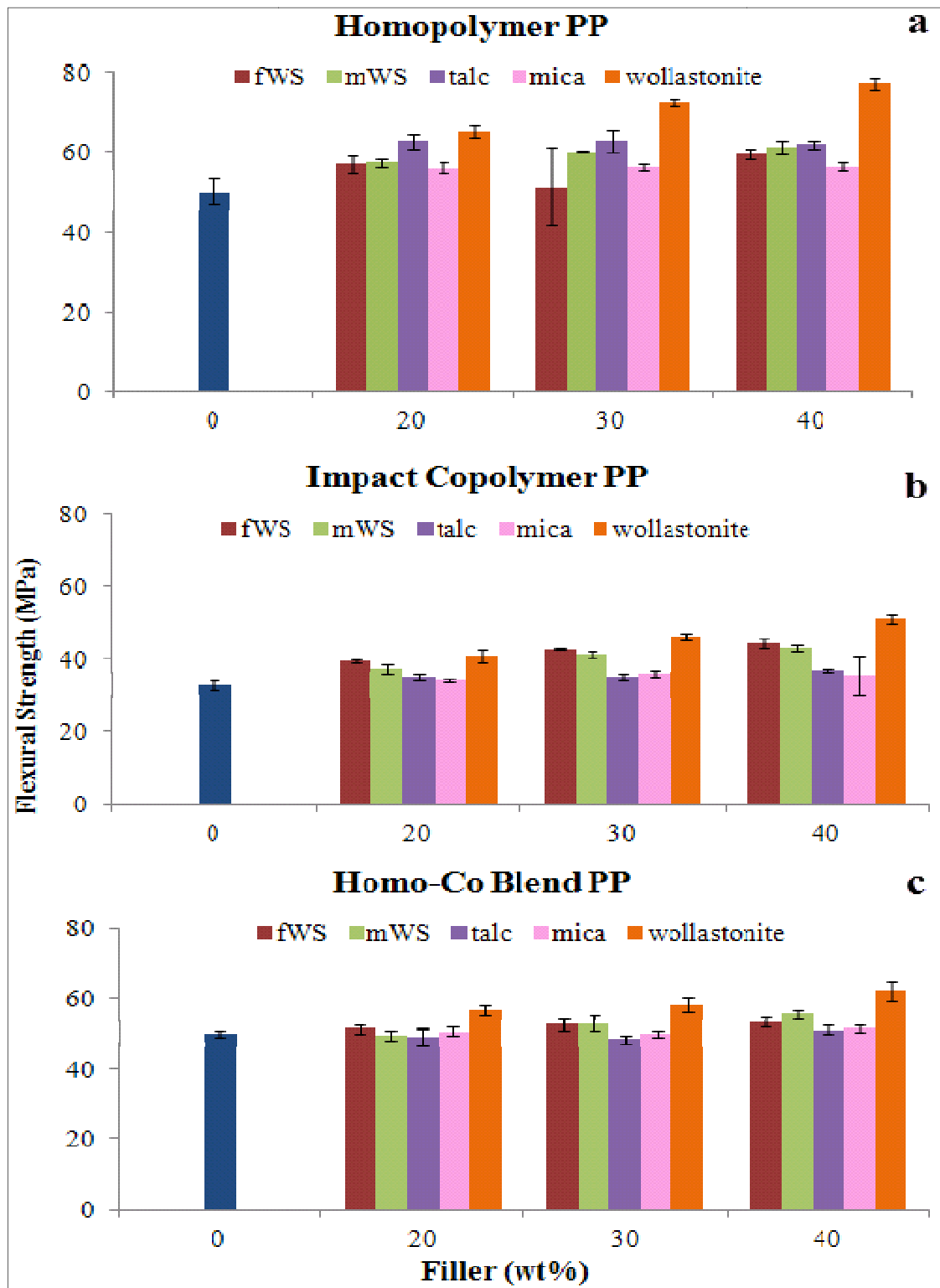


Figure 5.5 Flexural Strength of Single Filler (a) hPP, (b) icPP and (c) bPP Composites

5.2.2 FLEXURAL MODULUS

The flexural modulus of hPP composites increased considerably upon increasing the filler content. At all loading levels, the effect of wollastonite was very prominent. At 20 and 30 wt%, both mica and talc showed similar effects on the flexural modulus of hPP. The effect of mWS was observed to be higher than that of fWS. At 40 wt% however, mica showed a significant improvement whereas the modulus values for talc, fWS and mWS all fell within the same range. Wollastonite exhibited a tremendous improvement in modulus by more than 100% at the lowest loading level 20 wt%.

Figure 5.6 (b) shows that the flexural modulus of copolymer PP composites improved upon increasing the content of fillers in its matrix. All the fillers showed an increasing trend in the flex modulus. It is well known that addition of rigid particles improves the stiffness of polymeric matrices (Leong 2004). The enhancement in the property with addition of talc or mica is also attributed to the high aspect ratio of the platy sheet like structures. Mica exhibits better modulus than talc and this is due to the fact that mica has larger flake size and higher aspect ratio. Thus mica is likely to exhibit higher stiffness than talc (Jahani 2011, Maritomi 2010). The effect of wollastonite on the matrix is superior to the effects produced by other fillers at all percentage levels.

PP blend of homopolymer and copolymer showed a flexural modulus of 1192.5 MPa. With the addition of fWS, mWS and talc at 20% loading, a 39% increase in flexural modulus was observed. Mica and wollastonite further enhanced the modulus of the composite. At 30% filler content, fWS, mWS and mica significantly improved the modulus by 72%, 70% and 74% respectively. Wollastonite showed more than 100% increase in modulus at 30 wt% loading. The enhancement in modulus with talc was not significantly high. The increase in modulus was again observed at 40 wt% filler content with mica and wollastonite showing the maximum effect. Relatively, the maximum enhancement in modulus was observed with the addition of wollastonite among all filler types.

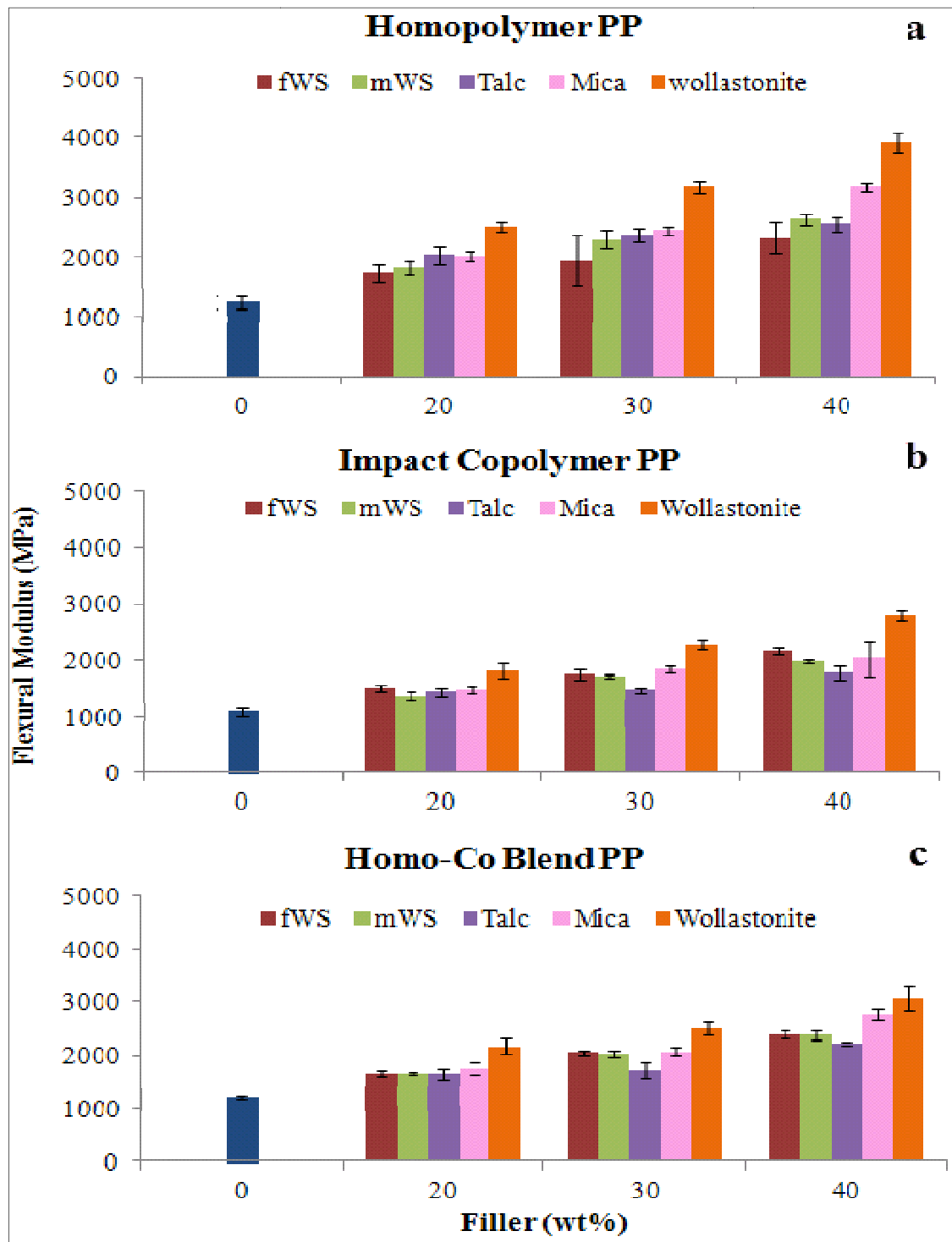


Figure 5.6 Flexural Modulus of Single Filler (a) hPP, (b) icPP and (c) bPP Composites

5.2.3 TENSILE STRENGTH

The tensile strength of talc and wollastonite filled hPP composites increased slightly at 20 wt% loading and remained almost the same at higher loading levels. At 20 wt% both mWS and mica showed similar results as that of pure homopolymer and at higher loadings the tensile strength greatly reduced. Wollastonite showed better results than all the other organic and inorganic fillers used in this study. The tensile strength of fWS-hPP composite reduced to around 34 MPa and also seemed to exhibit a decreasing trend upon adding fine WS.

The tensile strength of fWS, mWS and wollastonite filled icPP composites is much higher than that of the pure matrix and the obtained results for WS are in accordance with the datas provided in the literature (Mengeloglu 2008). Wollastonite has a needle shaped structure, a fiber like appearance very similar to that of wheat straw particles. This could be one of the possible reasons why wollastonite and wheat straw behave alike in certain cases. Addition of talc or mica to impact copolymer polypropylene (icPP), however, did not prove to be effective at any filler level. This is unexpected since it is documented that addition of talc improves the tensile strength of the composite (Eroglu 2007, Lapcik 2008, Leong 2004). The elastomer present in the copolymer matrix would have possibly encapsulated the filler materials (having a sheet like structure) resulting in poor distribution of the particles in the matrix and also failing to expose the effect of talc or mica onto the matrix. The same phenomena happens at higher levels too but since there is a higher content of talc or mica, the tensile strength either remains the same (at 30 wt%) or increases slightly at 40 wt%.

From the tensile tests carried out for the PP blend (bPP) composites it was observed that the tensile strength decreased with the addition of fillers. Wollastonite was an exception at 20 wt% content. A 4% increase in tensile strength was observed at 20wt% wollastonite loading; further increasing the amount of wollastonite to higher percentages decreased the tensile strength to 34.8 MPa. From Figure 5.7 (c) the tensile strength of the composite seemed to be independent of the filler content.

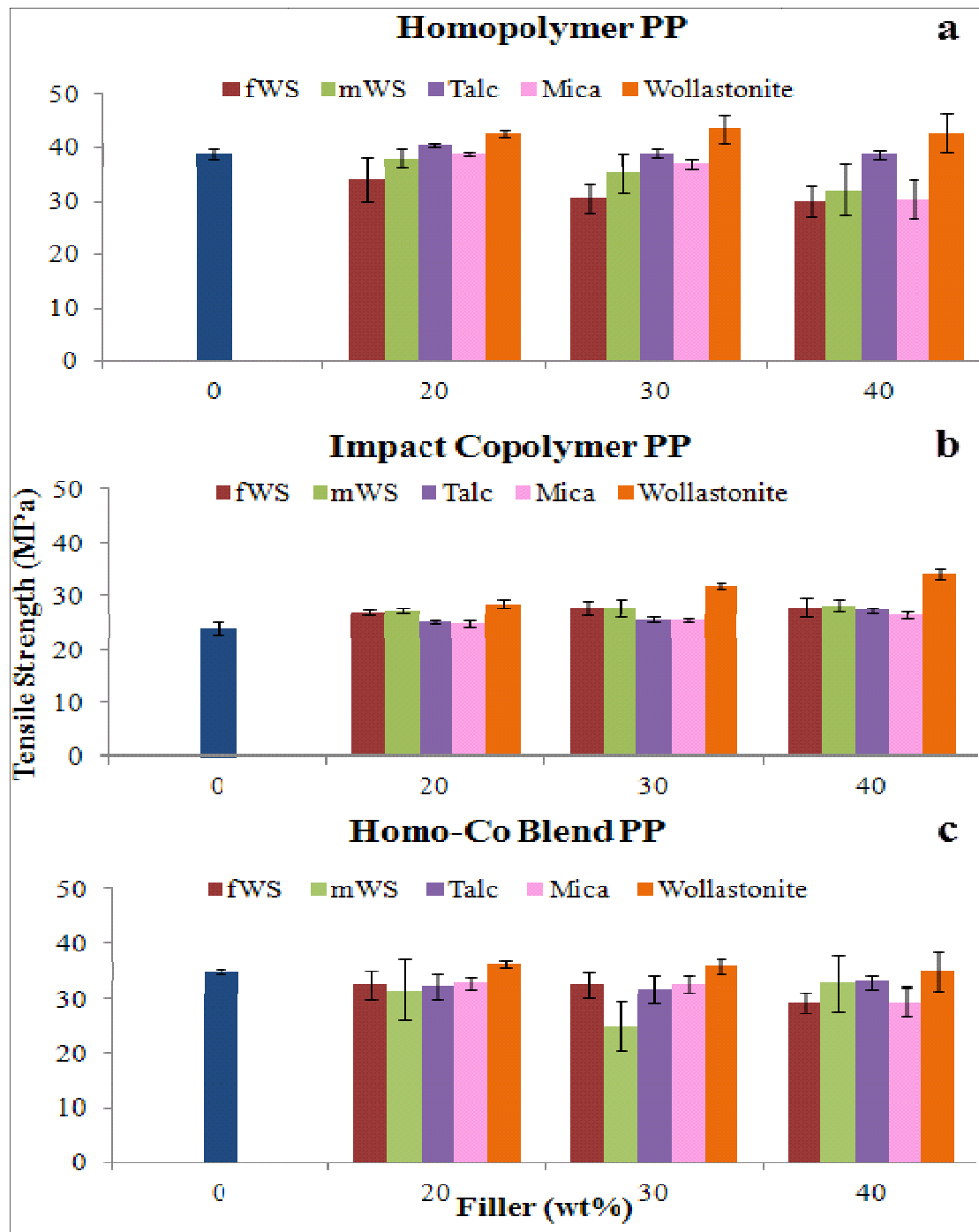


Figure 5.7 Tensile Strength of Single Filler (a) hPP, (b) icPP and (c) bPP Composites

5.2.4 TENSILE MODULUS

The tensile modulus of isotactic homopolymer PP increased significantly with addition of talc to its matrix system at the lowest concentration of 20 wt%. This increase is attributed to the fact that the talc particles impose restrictions on the mobility of the hPP molecules and thus contributed to increasing the rigidity of hPP. However the modulus decreased upon further increasing the content of talc from 20 to 40 wt %. This reduction could be the result of formation of talc agglomerates at higher concentration. Unlike talc, all the other four fillers improved the tensile modulus from 20 to 40 wt% though the magnitude of increase is very small. At 30 percent loading, mica and fWS reduced the modulus of hPP which is not very significantly low whereas wollastonite improved the modulus greatly.

Tensile modulus of talc-icPP composites did not show any difference upon increasing the content of talc in the copolymer matrix. However previous literature study indicates a linear increase in the tensile modulus of talc filled copolymer composite (Leong 2004). This decreased modulus could be the result of a poor interfacial adhesion between talc and the matrix. Modulus of mica-filled composite was much lower than that of talc composite. At 30 wt% however mica showed a slight improvement in the modulus with a value of 256 MPa. A significant improvement in modulus is observed only in case of wollastonite filled icPP composites. Fine WS and medium WS also improved the tensile modulus at all filler loading levels but the difference in values is not very high. Literature shows that there is no significant effect of polymer type on the tensile modulus of the composite, therefore the increase in tensile modulus, in general, is due to the presence of coupling agent which enhances adhesion between matrix and filler (Megeloglu 2008).

The tensile modulus of PP blend increased with increasing filler content. At 20 wt% loading, the effect of mica, wollastonite and mWS was similar and the modulus values were lower than the pure blend. Talc and fWS exhibited higher modulus. At 30 wt% and 40 wt% respectively, addition of mWS and mica was detrimental to the blend. The other fillers showed similar trend of higher modulus at 30 and 40 wt% input (Figure 7.8 (c)).

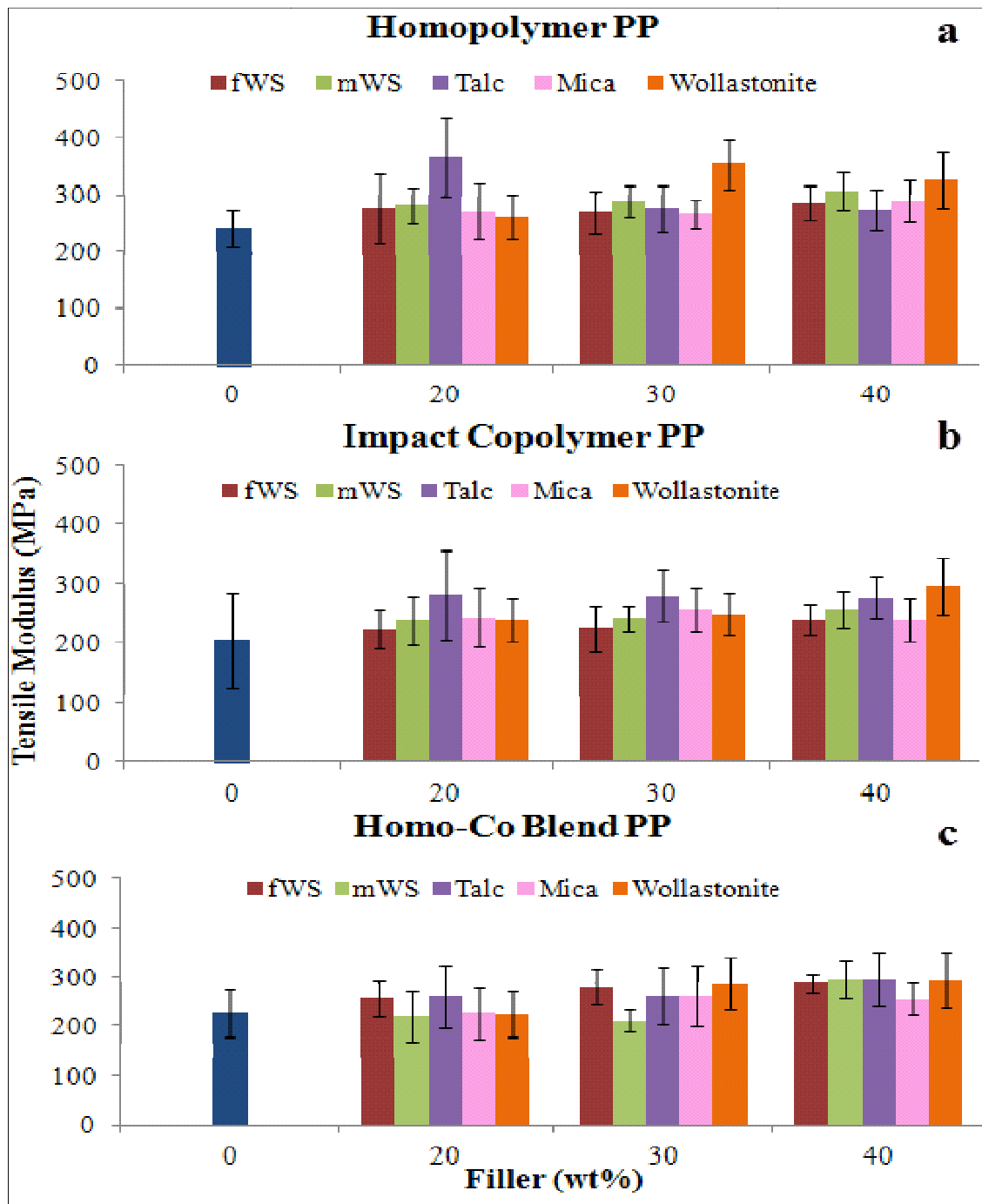


Figure 5.8 Tensile Modulus of Single Filler (a) hPP, (b) icPP and (c) bPP Composites

5.2.5 IMPACT STRENGTH

The impact strength of homopolymer polypropylene decreased upon adding the fillers (Figure 5.9). It was observed that as the amount of wollastonite increased from 20 wt% to 40 wt%, the impact strength of the hPP composite increased from 24.1 J/m at 20 wt% to 30.5 J/m at 40 wt%. Almost all the fillers showed a similar trend of increasing impact strength. It was interesting to note that wollastonite filled composite at the highest loading level had impact strength very close to that of the pure resin. It was also observed that talc performed better than mica and this is very much in accordance with the literature studies which state that talc is more efficient in maintaining impact strength whereas mica is more efficient in maintaining stiffness (Jahani 2011, Maritomi 2010).

The impact strength of impact copolymer PP decreased significantly with the incorporation of filler into the matrix. According to literature, fillers like talc and mica suppresses the mobility (deformability) or flexibility of the polymeric chain (Maiti 1992). The impact strength also decreased with increasing filler content. The results obtained at low filler content are higher than those obtained at higher contents. This could be related to the fact that as the concentration of fillers increases they tend to form agglomerates in the matrix (Eroglu 2007), resulting in non-homogeneous distribution of the filler, thus failing to transfer stress during an impact. The addition of filler counteracts the effect of elastomer/comonomer in the copolymer matrix. At 20 and 40 wt% loading, the effect of medium WS and wollastonite on the impact strength of the composite is higher than the other fillers. At 30wt%, only wollastonite shows a high value for impact strength and all the other fillers have similar low effect on the notched impact toughness.

As is the case with homopolymer PP and copolymer PP, the impact strength of the PP blend (bPP) also decreased drastically upon adding rigid fillers. With all fillers except wollastonite, the strength decreased with increasing content as well. However, at 20 wt% talc exhibited higher impact strength of 37.6 J/m whereas at 40wt% wollastonite exhibited higher impact strength of 34.4 MPa. At 30 and 40 wt%, the effect of filler type was negligible. Overall, the incorporation of filler to the copolymer and PP blend matrix proved to be detrimental. Though fillers reduced the impact strength of homopolymer PP, it was not a large change.

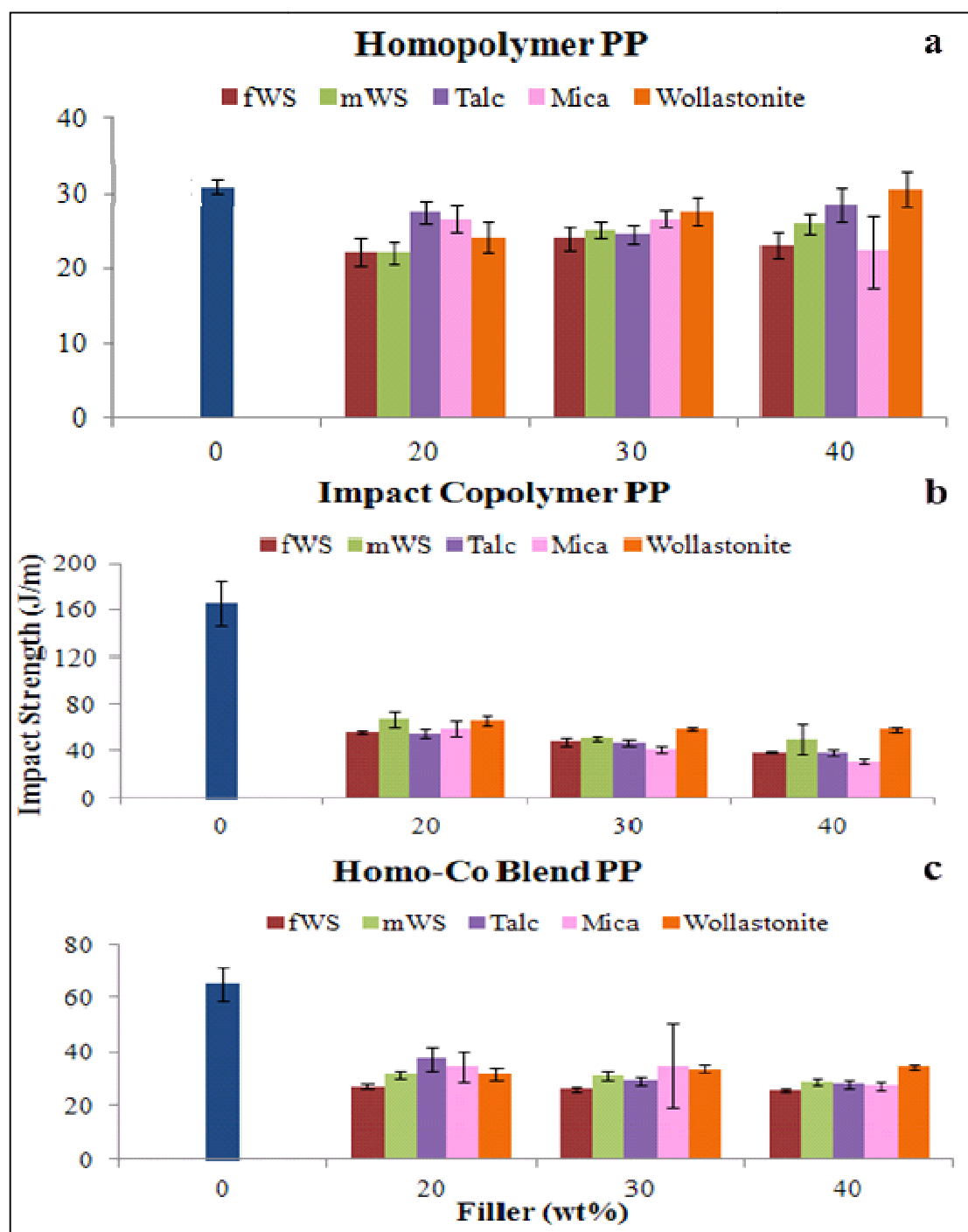


Figure 5.9 Impact Strength of Single Filler (a) hPP, (b) icPP and (c) bPP Composites

5.2.6 SPECIFIC FLEXURAL MODULUS

The specific flexural modulus (SFM) relates the flexural modulus with density of the composite. The density values for all composites and pure resins are shown in Table 5.2. Mineral fillers have higher densities than bio-fibres. As expected, the density of composites was greatly influenced by the type of filler and filler loading. The relative results of specific flexural modulus are represented in Figure 5.10.

For homopolymer composites, the specific flexural modulus increased with increasing filler loading. Increase in the property is quite significant with fWS, mWS, mica and wollastonite. Though the flexural modulus of talc hPP composites increased significantly from 20 to 40 wt%, SFM did not show any such trend. Mica and mWS exhibited almost the same behaviour at all the filler contents. Comparing mWS and wollastonite, the high SFM showcased by wollastonite at 20% loading was achieved by mWS only at 40 wt% loading, which indicates a potential for weight savings with the use of wollastonite.

The specific flexural modulus of talc icPP composites was higher than pure copolymer but relatively lower than other fillers at all filler percentages. Again wollastonite had a superior effect on the SFM of the composite. The effect produced by wollastonite at 20wt% is similar to the effect of fWS at 30wt% and the effect of wollastonite at 30wt% is similar to the effect of fWS at 40wt%. It can be inferred from this that higher loadings of WS is required to achieve the properties achieved by wollastonite at lower percentage and thus wollastonite can replace WS where low loadings with improved properties are preferred.

With homo-co blend PP also, the specific flexural modulus increased with increasing filler. The addition of talc did show an improvement from 20 to 40 wt%, unlike in homopolymer and copolymer. The behaviour of fWS, mWS and mica was observed to be same at 20 and 40 wt% loadings. The effect of wollastonite in PP blend with respect to the SFM did not change at 30 wt% loading but showed an increase at 40wt%. Mica, mWS and fWS increased the specific flexural modulus by 72% at 40 wt% loading whereas wollastonite improved the property by 86%. The improvement exhibited by talc on PP blend was only 36.2 %.

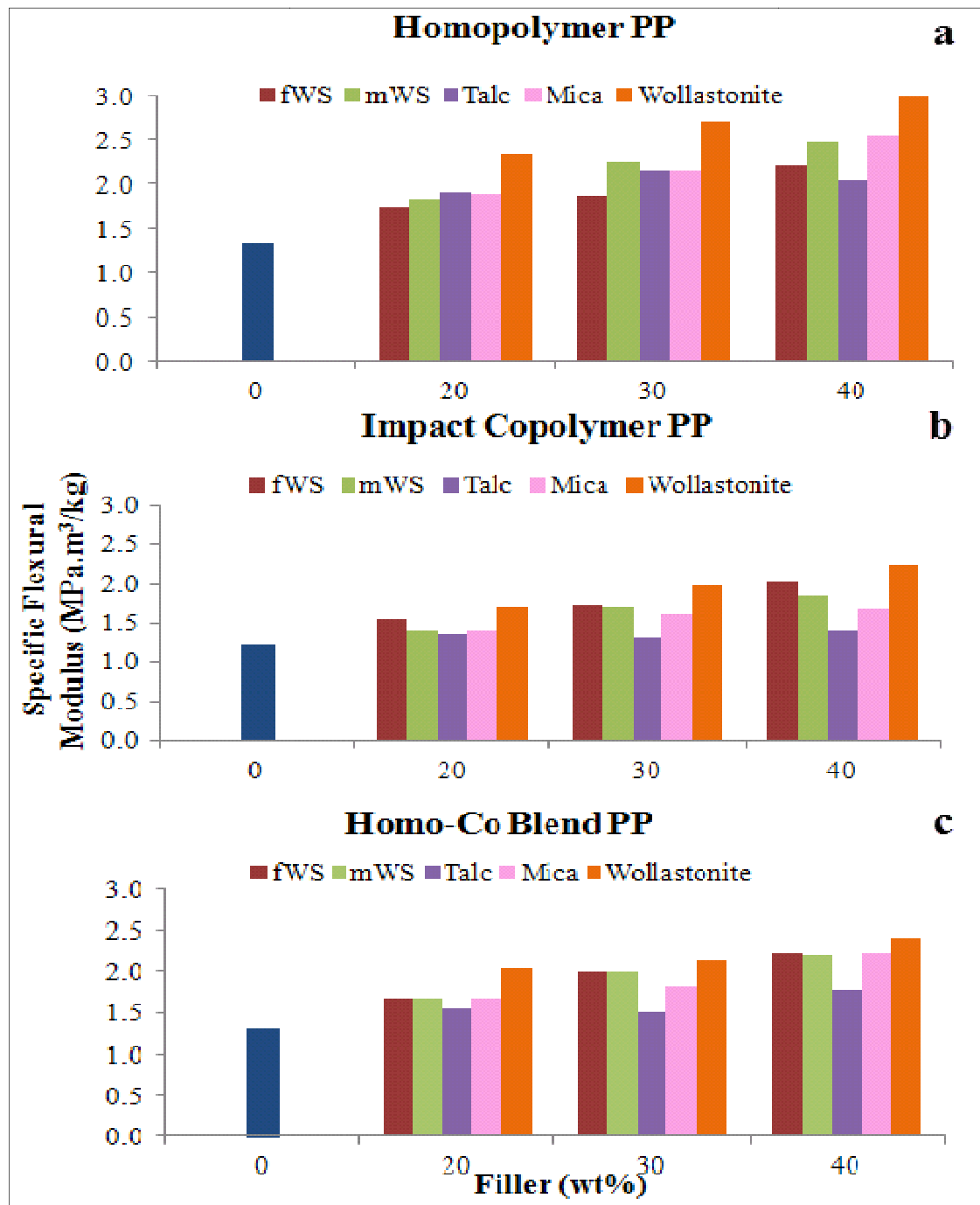


Figure 5.10 Specific Flexural Modulus of Single Filler (a) hPP, (b) icPP and (c) bPP Composites

5.2.7 SEM

The interaction between filler and matrix has great influence on the mechanical properties of the composite. A composite with a better filler/matrix interface can result in good overall performance. In this study, SEM analysis was conducted to investigate the interaction of fine WS and medium WS at 30 wt% loading with homopolymer, copolymer and polypropylene blend. The interface interactions in hybrid composites made of 15/15 wt% of mineral/WS were also investigated. Impact fractured surfaces of the composites were probed for distribution and interaction of fillers. All the composites contained MAPP coupling agent.

Figures 5.11, 5.12 and 5.13 represent the fractured surface of 30 wt% filled fWS-hPP, fWS-icPP and fWS-bPP composites. It can be clearly observed from Figure 5.11 that fWS is strongly bonded to the homopolymer matrix without letting itself to be pulled out during impact which indicates a good interfacial interaction between the filler and the matrix. The strong interface between the hydrophilic fiber and hydrophobic resin can be associated with the presence of coupling agent as supported by other literature studies (Mengeloglu 2008, Güttler 2009). In Figure 5.12, wide gap in the interface between fWS and icPP is an indication of poor interaction or bonding. It can be clearly seen in Figure 5.13 that the fWS fibers are cut out from the surface of the PP blend matrix, which demonstrates the strong bonding of fWS with bPP matrix. These SEM investigations support some of the earlier discussions on mechanical properties of fWS based composites (Section 5.2.1). The better mechanical performance of fWS-homopolymer composite at 30wt% loading against that of fWS-copolymer composite at the same composition can be favorably associated with the observation made from SEM analysis.

Figures 5.14 and 5.15 represent the fractured surfaces of 30 wt% mWS filled icPP and bPP composites. The SEM image for mWS-hPP composite is shown in Appendix B. The icPP matrix filled with mWS also show poor interaction of the filler with the matrix due to the presence of visible gap in the interface. This poor interaction with copolymer can be thought to be associated with the type and amount of coupling agent used. These parameters (consistently used at same composition for all formulations) may not be the optimum for a copolymer bio-fiber composite. It can be concluded from SEM analysis that mWS based hPP composite performs better than the copolymer or PP blend which also supports the previous discussions on superior mechanical

performance for mWS hPP composite at 30wt% loading. Figure 5.15 shows fiber pull out from the surface of mWS-bPP composite which again is an indication of poor bonding with the blend.

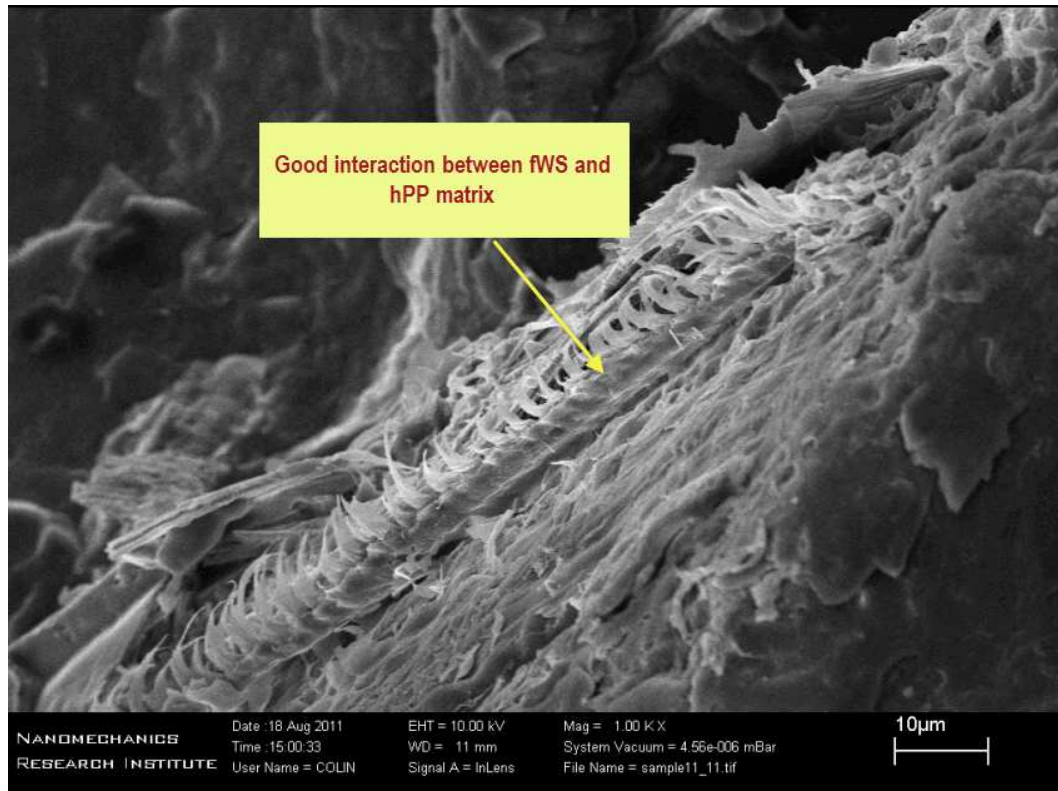


Figure 5.11 SEM of 30 wt% fWS-hPP composite (1000X)

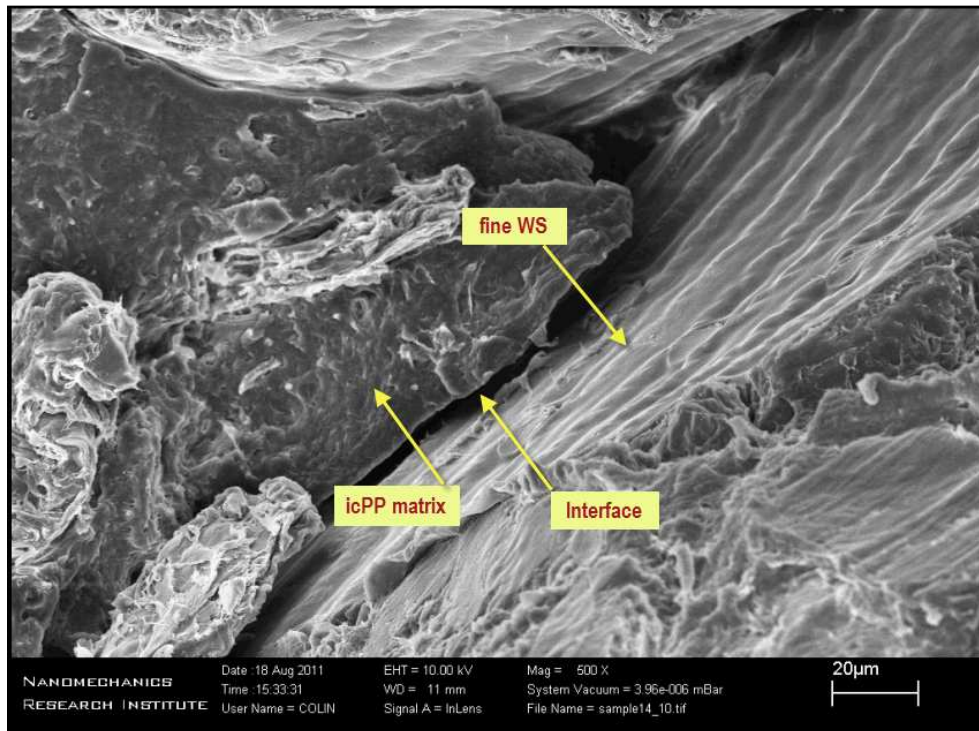


Figure 5.12 SEM of 30 wt% fWS-icPP composite (500X)

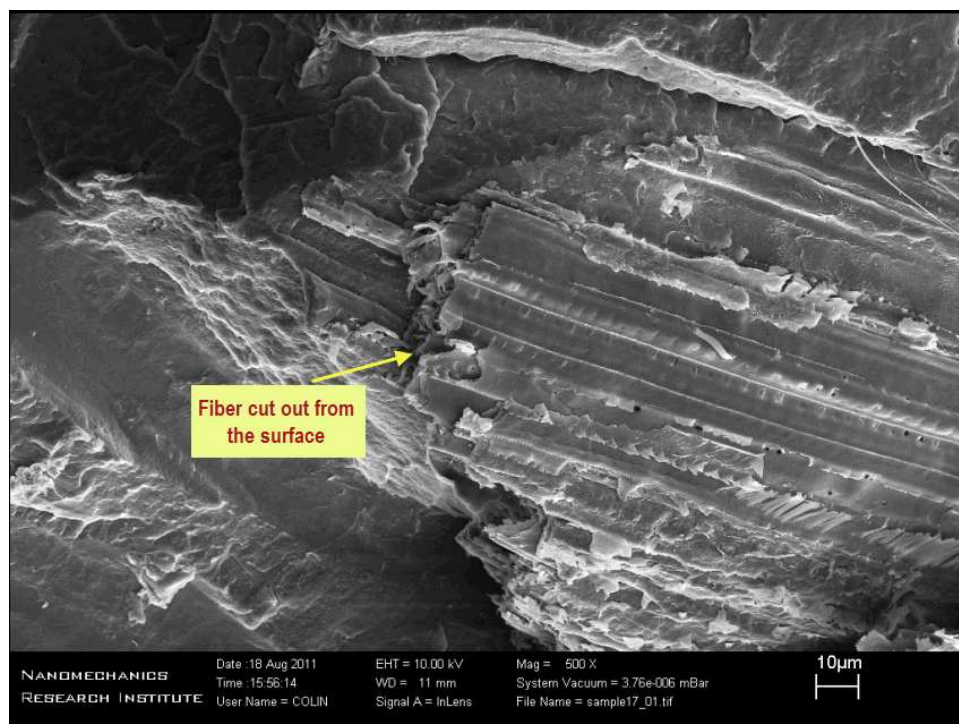


Figure 5.13 SEM of 30 wt% fWS-bPP composite (500X)

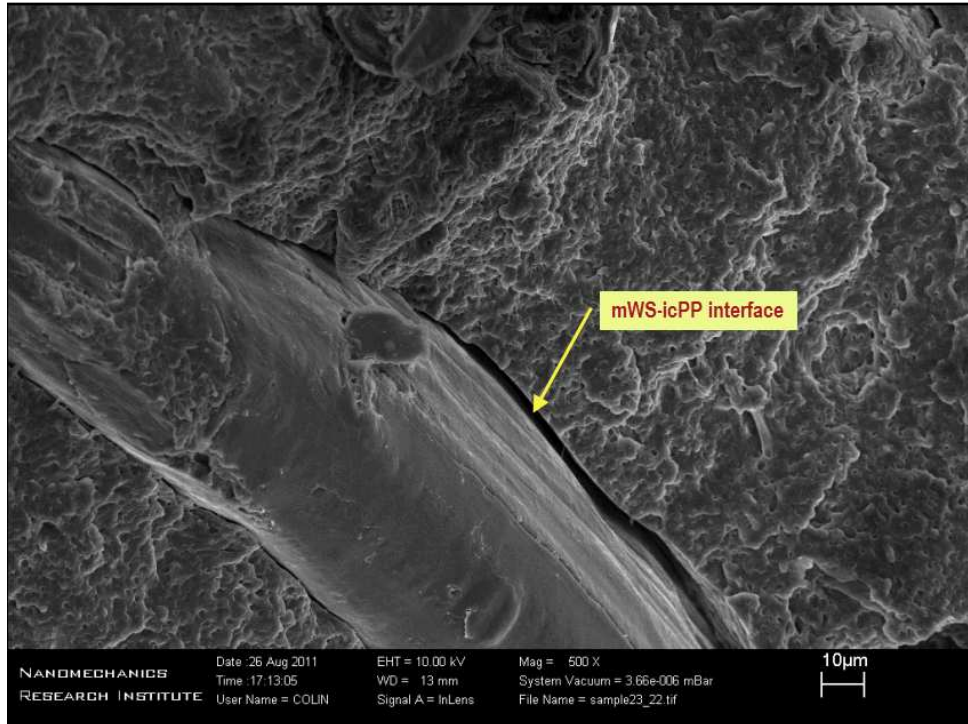


Figure 5.14 SEM of 30 wt% mWS-icPP composite (500X)

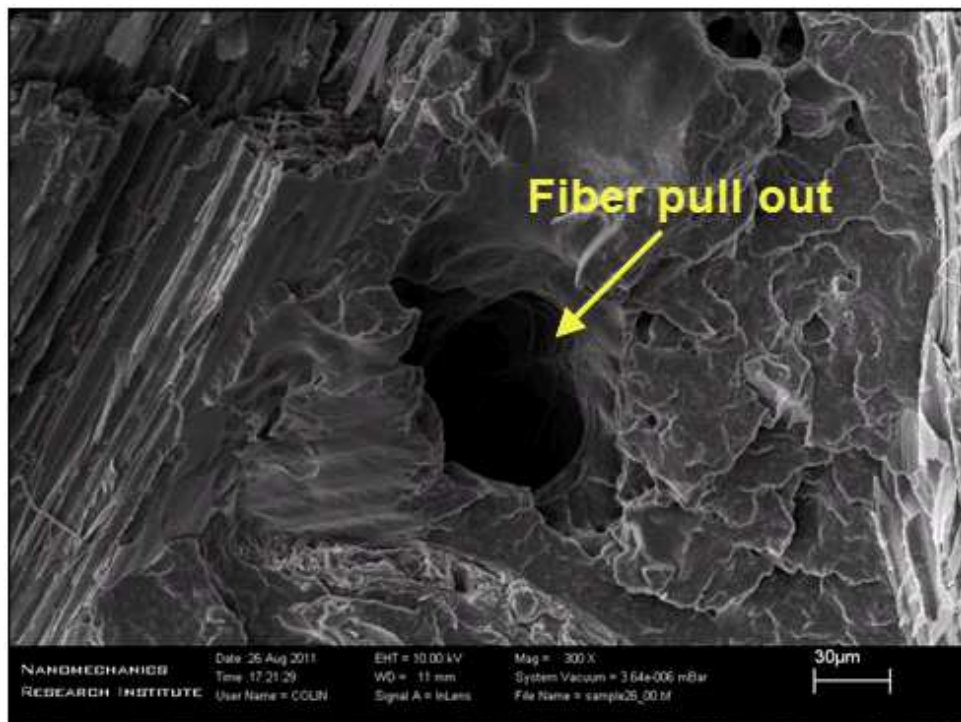


Figure 5.15 SEM of 30 wt% mWS-bPP Composite (300X)

5.2.8 WATER ABSORPTION

The water absorption plots for wheat straw filled composites are presented in Figure 5.16. The effect of absorption of water was studied by varying the type of WS (fine WS and medium WS) and content of WS (0 to 40 wt %) in homopolymer, copolymer and the blend, keeping other parameters (antioxidant and coupling agent concentration) constant during composite preparation.

An increase in composite weight was observed upon increasing the amount of wheat straw in all the composites. It was found that at the pure polymer at 0 wt% fWS did not absorb any significant amount of water even after 40 weeks of exposure, typical of any hydrophobic polymer. At 20 wt% loading of fWS, there was a weight gain of 4.2% after 40 weeks, which can be associated with the water absorption characteristics of WS. Upon increasing the percentage loading to 30 and 40 wt%, the composite gained a weight of 6.4% and 9.4% respectively. However, the sample having 40 wt% fine WS appeared to have saturated after 10 weeks. The same trend was observed for samples containing higher amounts of medium WS as well. The hPP composite having 20 wt% mWS gained around 3.7% weight, a little less than fWS. At 30wt% loading, the percentage gain in weight of 8.2% was significantly higher than that of fWS. The composite with 40 wt% mWS with 10.3% weight gain also saturated after 10 weeks.

The impact copolymer PP composites also showed the same pattern of increasing water absorption with increasing filler content. The filler type did not show any effect at 20 and 30 wt% filler. Both fWS and mWS gained a weight of 3.9% at 20 wt% loading and 8.5% at 30 wt% loading. At 40 wt% fWS and mWS loading, the composite samples gained 15% and 14.1% respectively. No saturation was observed in any of the icPP composites after 40 weeks of exposure.

It was observed that bPP composites with 40wt% fWS reached saturation after 10 weeks and the sample with 40wt% mWS saturated after 13 weeks. The higher the concentration of WS in bPP, the higher was the percentage gain in weight. At 30wt%, the % gain in weight was similar for fWS and mWS, like in impact copolymer composite, whereas at 20wt% the fWS composite gained slightly higher weight than mWS. Composites with 20 and 30 wt% loading continued to gain weight even after 40 weeks with an increase of 5% and 8.7% for fWS and 4.3% and 9.3% for mWS respectively.

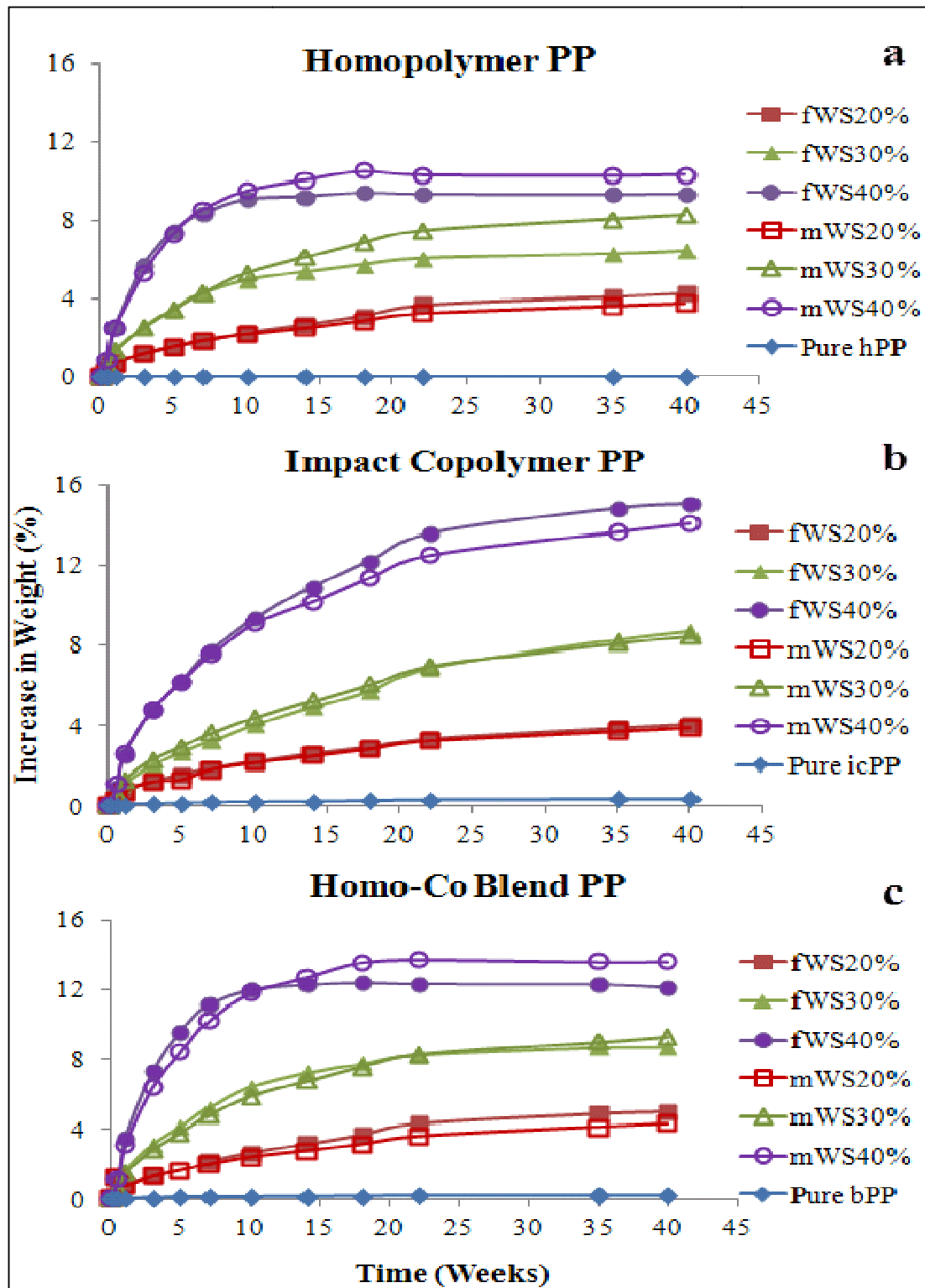


Figure 5.16 Water Absorption Plot for WS filled (a) hPP, (b) icPP and (c) bPP Composites

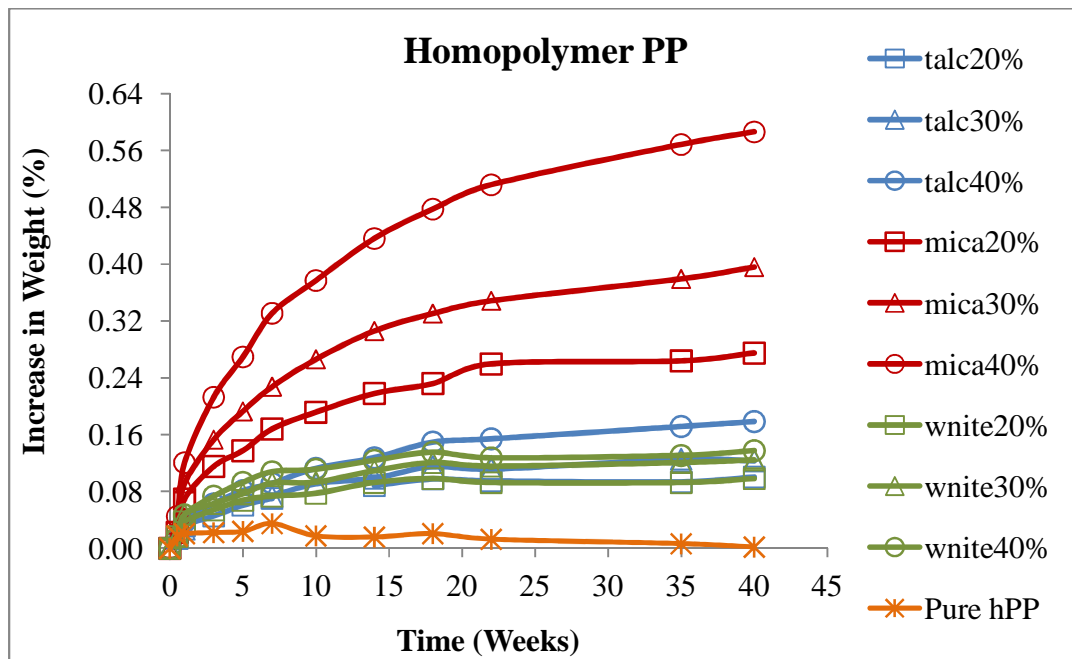


Figure 5.17 Water Absorption Plot for Mineral filled hPP Composites

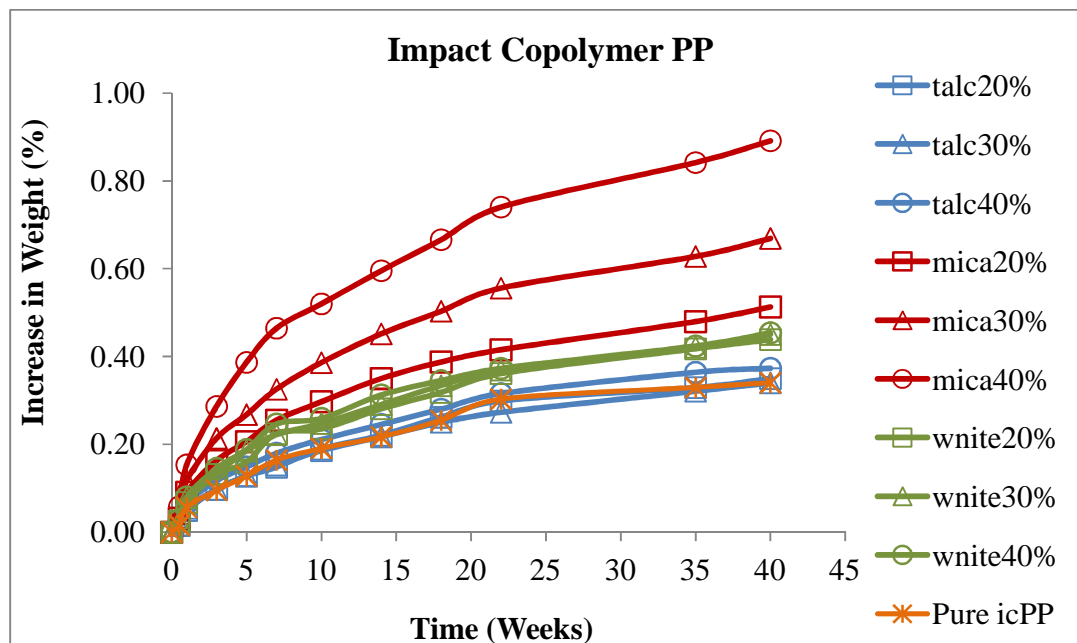


Figure 5.18 Water Absorption Plot for Mineral filled icPP Composites

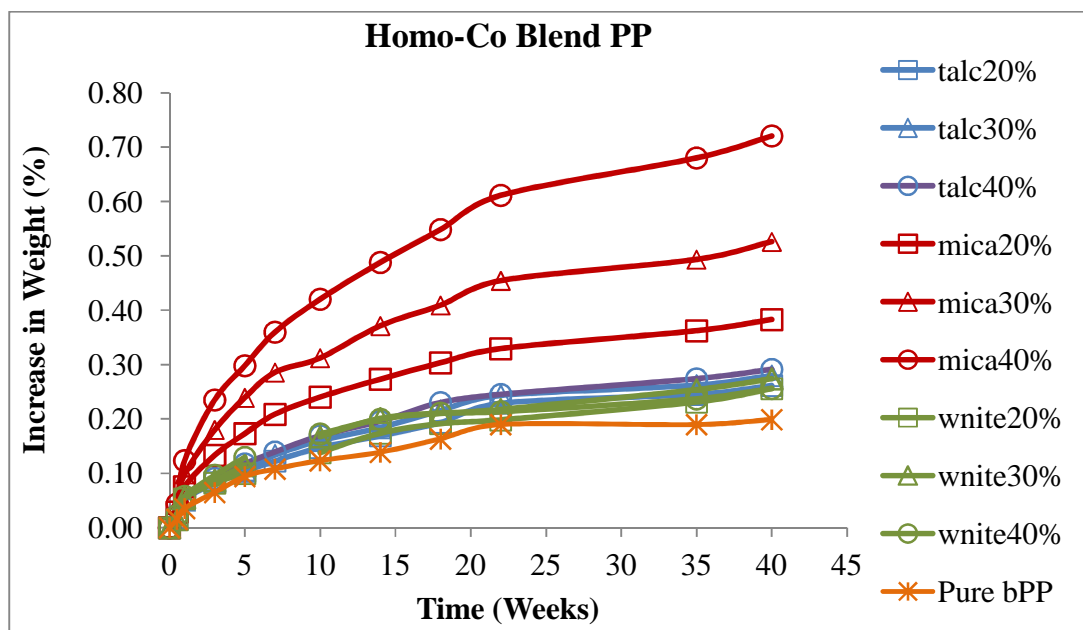


Figure 5.19 Water Absorption Plot for Mineral filled bPP Composites

The water absorption characteristic of talc, mica and wollastonite filled hPP, icPP and bPP composites are represented in Figure 5.17, 5.18 and 5.19. An increase in composite weight can be observed with the addition of mineral fillers and with increasing loading of the fillers in pure resin. However this increase is significantly lower than WS based composites. At 20, 30 and 40 wt% loading, talc hPP composite gained a weight of 0.1%, 0.12% and 0.18% respectively after 40 weeks of immersion in water. Such behaviour can be associated with the hydrophobicity of minerals in general. Wollastonite also exhibited similar characteristic as talc when exposed to water except at 40 wt% loading where there is only 0.14% gain in weight. Also, talc and wollastonite composites saturated at 22 weeks of exposure. The behaviour of mica was completely different from the other minerals. From Figure 5.17 it is clearly observed that mica filled homopolymer at 20, 30 and 40% loadings absorbed more water than talc and wollastonite composites. Mica at 20 wt% experienced a weight gain of 0.3% which is higher than talc composite at 40wt% but reached saturation at 22 weeks, like talc and wollastonite. Mica hPP composites at 30 and 40 wt% do not show any indication of saturation even after 40 weeks of exposure as seen in the figure. The percentage gain in weight for 40wt% mica composite is maximum at 0.6%.

The incorporation of talc at 20 wt% to the copolymer matrix did not show any effect on water absorption property of the composite. It is observed from Figure 5.18 that the water absorption characteristic of copolymer composite did not depend on talc or talc loadings, whereas a significant increase in weight is observed with mica and a little lower effect with wollastonite. Neither the composite specimens nor the pure resin reached saturation even after immersion for 40 weeks. It is interesting to note that wollastonite at all loadings behaved in the same manner which indicate that the water absorption characteristic of wollastonite filled copolymer composite is independent of the wollastonite content in the matrix. After exposure for 40 weeks, wollastonite composite showed a 0.5 % gain in weight in comparison to icPP. The trend for mica with copolymer is similar to the trend observed with homopolymer. At 30 and 40 wt% fill, mica-icPP composite showed a weight gain of 0.7 and 0.9 % respectively. It is also important to note that copolymer composites exhibited higher weight gain than homopolymer composites.

Homopolymer-copolymer blend PP composites showed similar trend as copolymer composites. It can be observed that the blend without any filler, saturated at 22 weeks of exposure to water (Figure 5.19). The filled composites did not show any such behaviour of saturation. Talc and wollastonite showed a similar increase in weight of 0.3% after 40 weeks. No significant change in water absorption behaviour is noted for the two minerals but it is important to mention that there is 0.3% increase in weight gain compared to pure blend after 40 weeks. Like homopolymer and copolymer, the blend showed maximum absorption of water with the presence of mica. Mica at 20wt% loading increased the weight of the composite by 0.4%. Higher percentages of mica showed a weight gain of 0.53% and 0.72% without any sign of saturation.

6 RESULTS AND DISCUSSIONS: POLYPROPYLENE HYBRID COMPOSITES

6.1 FORMULATIONS AND PROPERTIES

Several tests were carried out to analyze the behaviour of composites when two fillers, organic and mineral fillers, were combined together in the matrix to produce hybrid composites. The total concentration of fillers was maintained at 30 wt% and the properties were tested by varying the composition of mineral and organic fillers at 10/20, 15/15 and 20/10 weight percentages.

Table 6.1 Formulations and Properties Chart for Hybrid PP Composites

Sample name	Mineral filler (wt %)	Biobased fiber (wt %)	Flexural Modulus(GPa)	Flexural Strength(MPa)	Tensile Modulus (MPa)	Tensile Strength (MPa)	Impact Strength (J/m)	Density (kg/m ³)	Specific Flexural Modulus (MPa.m ³ /kg)
hPP-Talc-fWS	10	20	2.17(.09)	58.1(0.9)	272(29)	30.2(2.0)	22.2(1.1)	1056(14.3)	2.06
	15	15	2.16(0.1)	55.6(0.8)	278(37)	33.2(3.5)	23.6(2.4)	1095(3.3)	1.97
	20	10	2.14(0.1)	56.2(1.5)	278(24)	34.3(2.6)	21.6(1.1)	1109(2.9)	1.93
icPP-Talc-fWS	10	20	1.52(.04)	37.6(0.6)	259(24)	25.7(1.1)	45.2(2.7)	1049(6.1)	1.45
	15	15	1.58(.02)	36.9(0.5)	237(31)	26.3(0.6)	45.2(3.3)	1079(3.4)	1.47
	20	10	1.47(.06)	34.8(0.8)	248(30)	25.0(0.6)	48.0(3.0)	1100(2.7)	1.34
bPP-Talc-fWS	10	20	1.72(.08)	48.1(1.2)	265(33)	30.4(2.4)	22.3(0.7)	1064(4.5)	1.61
	15	15	1.74(.08)	49.8(0.8)	250(37)	28.1(2.2)	26.4(1.3)	1083(5.0)	1.61
	20	10	1.89(.06)	49.9(0.9)	260(36)	30.9(1.1)	25.4(1.3)	1116(7.6)	1.69
hPP-mica-fWS	10	20	1.98(0.3)	57.6(2.7)	276(41)	28.7(2.5)	21.3(1.0)	1076(6.7)	1.84
	15	15	2.02(0.2)	56.7(0.9)	275(45)	31.4(2.1)	21.9(1.4)	1091(3.2)	1.85
	20	10	2.29(.05)	56.1(1.5)	287(50)	30.2(2.1)	22.8(0.5)	1099(11.1)	2.08
icPP-mica-	10	20	1.51(.03)	36.8(0.3)	243(37)	25.5(0.8)	47.7(1.9)	1040(6.2)	1.46

fWS	15	15	1.70(.03)	36.2(0.6)	267(10)	26.1(0.2)	42.8(3.1)	1074(4.2)	1.58
	20	10	1.60(0.1)	36.1(1.9)	256(40)	26.0(0.5)	45.2(3.1)	1089(5.6)	1.47
bPP-mica-fWS	10	20	1.91(.12)	49.4(2.1)	262(36)	28.0(2.5)	26.3(1.4)	1061(10.5)	1.80
	15	15	2.46(.07)	54.3(0.8)	271(32)	29.2(2.3)	25.4(0.7)	1085(4.7)	2.26
	20	10	2.12(.36)	49.3(4.5)	302(52)	29.9(3.6)	25.4(0.7)	1078(10.2)	1.96
hPP-Wnite-fWS	10	20	2.37(.09)	58.2(1.8)	307(56)	35.8(2.6)	23.6(0.8)	1075(3.4)	2.21
	15	15	2.24(0.1)	59.0(1.3)	325(29)	36.8(2.9)	23.8(2.2)	1087(3.0)	2.06
	20	10	2.51(0.2)	63.1(3.4)	327(56)	38.8(3.3)	25.4(1.7)	1109(3.7)	2.26
icPP-Wnite-fWS	10	20	1.81(.08)	39.6(1.7)	265(30)	25.8(0.9)	50.9(1.6)	1050(7.3)	1.73
	15	15	1.72(.04)	38.3(0.6)	221(28)	27.0(0.5)	47.8(2.8)	1075(6.2)	1.61
	20	10	1.89(.08)	40.1(2.0)	233(36)	27.8(0.5)	55.8(2.7)	1103(2.6)	1.72
bPP-Wnite-fWS	10	20	2.07(.05)	51.2(1.4)	281(39)	30.5(1.9)	27.3(0.9)	1071(2.5)	1.93
	15	15	2.11(.05)	50.7(0.5)	278(43)	31.7(4.1)	28.6(2.0)	1096(3.0)	1.92
	20	10	2.19(.07)	53.8(2.3)	284(52)	33.3(2.3)	28.8(1.7)	1111(7.1)	1.97
hPP-Talc-mWS	10	20	2.08(.06)	56.6(1.5)	285(46)	30.4(3.9)	24.3(1.2)	1068(3.5)	1.95
	15	15	2.03(.08)	54.7(1.2)	273(56)	32.7(4.2)	23.2(1.8)	1095(11)	1.85
	20	10	2.02(.14)	56.4(1.7)	301(31)	33.8(1.9)	25.1(1.2)	1096(11)	1.84
icPP-Talc-mWS	10	20	1.60(.04)	37.1(0.8)	263(33)	25.1(1.4)	49.1(2.1)	1062(6.6)	1.51
	15	15	1.57(.04)	36.0(0.4)	260(40)	24.5(1.6)	49.4(2.4)	1071(5.4)	1.47
	20	10	1.53(.05)	35.5(1.3)	256(37)	24.2(0.5)	47.3(2.6)	1095(5.3)	1.40
bPP-Talc-mWS	10	20	1.77(0.1)	48.9(1.0)	267(45)	25.9(2.5)	28.9(1.2)	1069(4.1)	1.66
	15	15	1.83(.06)	50.0(0.6)	275(43)	29.5(2.4)	28.0(1.5)	1087(3.9)	1.68
	20	10	1.85(.04)	49.6(0.8)	302(13)	30.0(1.8)	27.7(1.5)	1110(2.8)	1.67
hPP-mica-mWS	10	20	2.28(0.1)	56.0(0.9)	307(56)	35.8(2.6)	26.5(0.7)	1038(16.7)	2.19
	15	15	2.31(.05)	54.8(1.1)	311(43)	32.3(3.5)	23.1(1.5)	1080(1.8)	2.13
	20	10	2.33(.07)	52.7(1.7)	286(50)	30.2(2.1)	23.4(2.0)	1095(2.9)	2.13
icPP-mica-mWS	10	20	1.64(.08)	35.4(1.5)	254(52)	25.0(1.4)	42.2(2.8)	1056(4.7)	1.56
	15	15	1.62(.07)	35.6(0.8)	270(35)	27.0(0.4)	40.4(3.2)	1061(17.1)	1.52
	20	10	1.64(0.1)	34.1(0.8)	280(40)	25.6(0.8)	42.5(3.2)	1075(12.0)	1.53

bPP-mica- mWS	10	20	1.93(.08)	48.9(1.7)	273(49)	29.0(4.2)	26.5(1.0)	1057(7.8)	1.83
	15	15	1.99(.08)	47.9(1.0)	291(47)	31.0(1.4)	25.6(1.3)	1080(14.0)	1.84
	20	10	2.07(.16)	47.4(1.6)	287(33)	29.9(2.4)	22.7(1.6)	1100(4.5)	1.88
hPP- Wnite- mWS	10	20	2.33(0.1)	59.2(1.7)	279(30)	31.6(2.8)	25.0(2.1)	1069(3.8)	2.18
	15	15	2.55(.05)	62.9(1.7)	299(31)	34.0(2.6)	25.7(0.9)	1100(8.8)	2.32
	20	10	2.63(.08)	64.1(1.8)	326(17)	38.2(2.5)	26.2(0.3)	1104(10.5)	2.38
icPP- Wnite- mWS	10	20	1.66(.09)	37.0(1.4)	250(43)	26.9(0.8)	61.7(4.0)	1048(3.5)	1.58
	15	15	1.76(.09)	37.2(1.0)	231(39)	27.4(0.8)	60.6(1.8)	1070(6.6)	1.64
	20	10	1.78(0.1)	36.7(2.2)	260(37)	27.5(1.0)	62.8(3.0)	1100(3.5)	1.62
bPP- Wnite- mWS	10	20	2.10(.02)	51.6(1.9)	266(35)	30.3(3.6)	29.1(1.6)	1057(5.5)	1.99
	15	15	2.16(.05)	52.9(1.5)	261(39)	30.1(3.5)	30.9(1.7)	1091(4.3)	1.98
	20	10	2.40(.11)	54.3(2.9)	274(38)	31.5(4.4)	31.6(2.4)	1114(3.0)	2.15

6.1.1 FLEXURAL STRENGTH

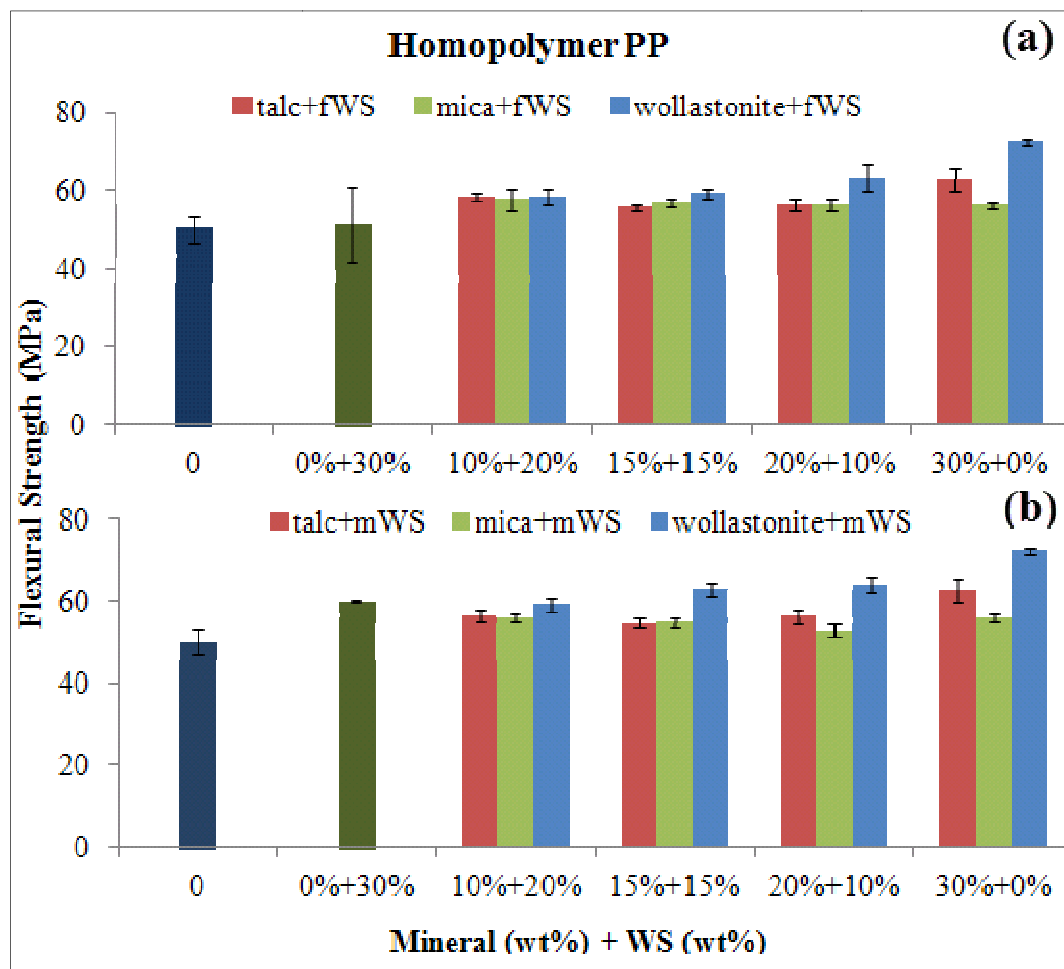


Figure 6.1 Flexural Strength of (a) Mineral/fWS (b) Mineral/mWS hPP Composites

The combined effects of mineral filler and agro-based filler on PP hybrid composites were investigated. Figure 6.1 (a) shows the flexural strength results obtained on combining a mineral filler and fine WS into the homopolymer matrix. It is clearly seen that at 30 wt% single filler loading, all mineral fillers behaved very well compared to the effects shown by fWS. When this result is weighed against the result obtained for hybrid composite, it is found that, the hybrid talc-fWS, mica-fWS and wollastonite-fWS hPP composites have greater flexural strength than pure fWS composite and lower strength than pure mineral composites. The hybrid property of wollastonite and fWS composites at 20 wt% and 10 wt% loading respectively did show a significant improvement in comparison with other combinations. There is synergy effect

observed for hybrid composites when comparing the values with pure fWS. But mixing the straw filler with a mineral did not prove to be effective to the mineral-hPP composite.

From previous results obtained for pure hPP composites, it is inferred that fWS composites have lower flexural strength than mineral based composites at 30 wt%. So the replacement of fWS with mineral fillers in the total 30 wt% filler content is expected to improve the strength as is clearly shown in the Figure 6.1(a). The flexural strength of hybrid homopolymer composites is significantly higher than the pure homopolymer.

Similar effect of increasing flexural strength, compared to pure hPP composite, was observed in case of mineral filler-medium WS filled homopolymer as well. See Figure 6.1(b). The more mineral content in the hybrid composite, higher is the flexural strength of the wollastonite-mWS hybrid hPP composite. Synergy is observed only in case of 15/15 and 20/10 wollastonite/mWS combination with respect to the mWS hPP composite. The fibre like needle shaped morphology of wollastonite could be the contributing factor for increasing flexural strength. In case of other blends, the flexural strength was lower than that of pure hPP composites.

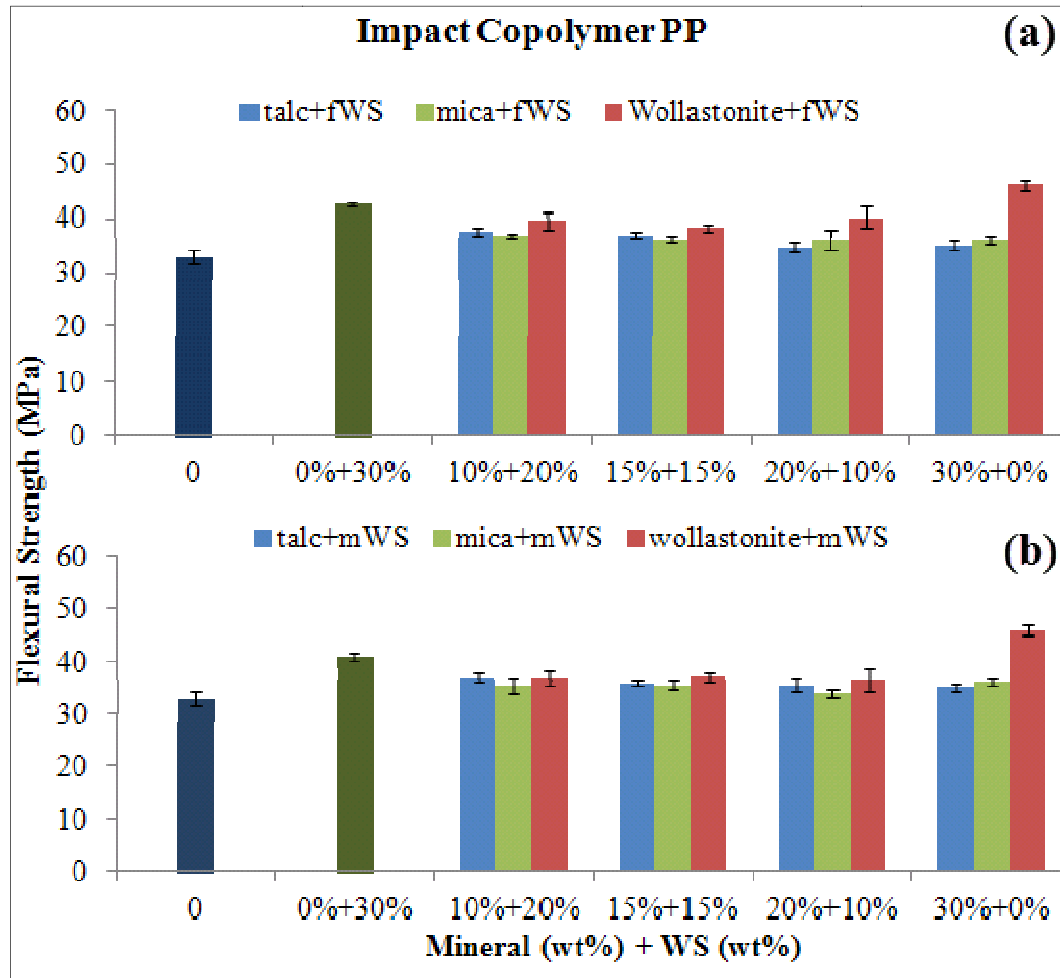


Figure 6.2 Flexural Strength of (a) Mineral/fWS (b) Mineral/mWS icPP Composites

The flexural strength results obtained for hybrid mineral-bio-fiber icPP composites are reported in Figure 6.2(a) and 6.2 (b). At 30 wt% loading of individual fillers, fine and medium WS improves the flexural strength of impact copolymer PP in comparison with talc or mica. The influence of wollastonite is however much greater than both grades of wheat straw. There is a reduction in the flexural strength on mixing two fillers into icPP matrix. Mixing of talc, mica and wollastonite, to fWS in the composite, showed a slight increase in the strength compared to the effects shown by pure talc and pure mica composites. Changing the composition of mineral fillers or the organic fibres in the hybrid composite did not have much effect on flexural property. There was a slight increase in strength upon changing the content of wollastonite and fWS which is smaller than pure fWS icPP composite.

Higher flexural strength of fWS and mWS icPP composites at 30 wt% loading indicates that addition of WS into the mineral based composites (except wollastonite) only increases the flexural strength. It was also observed that the hybrid properties were higher than that of pure impact copolymer.

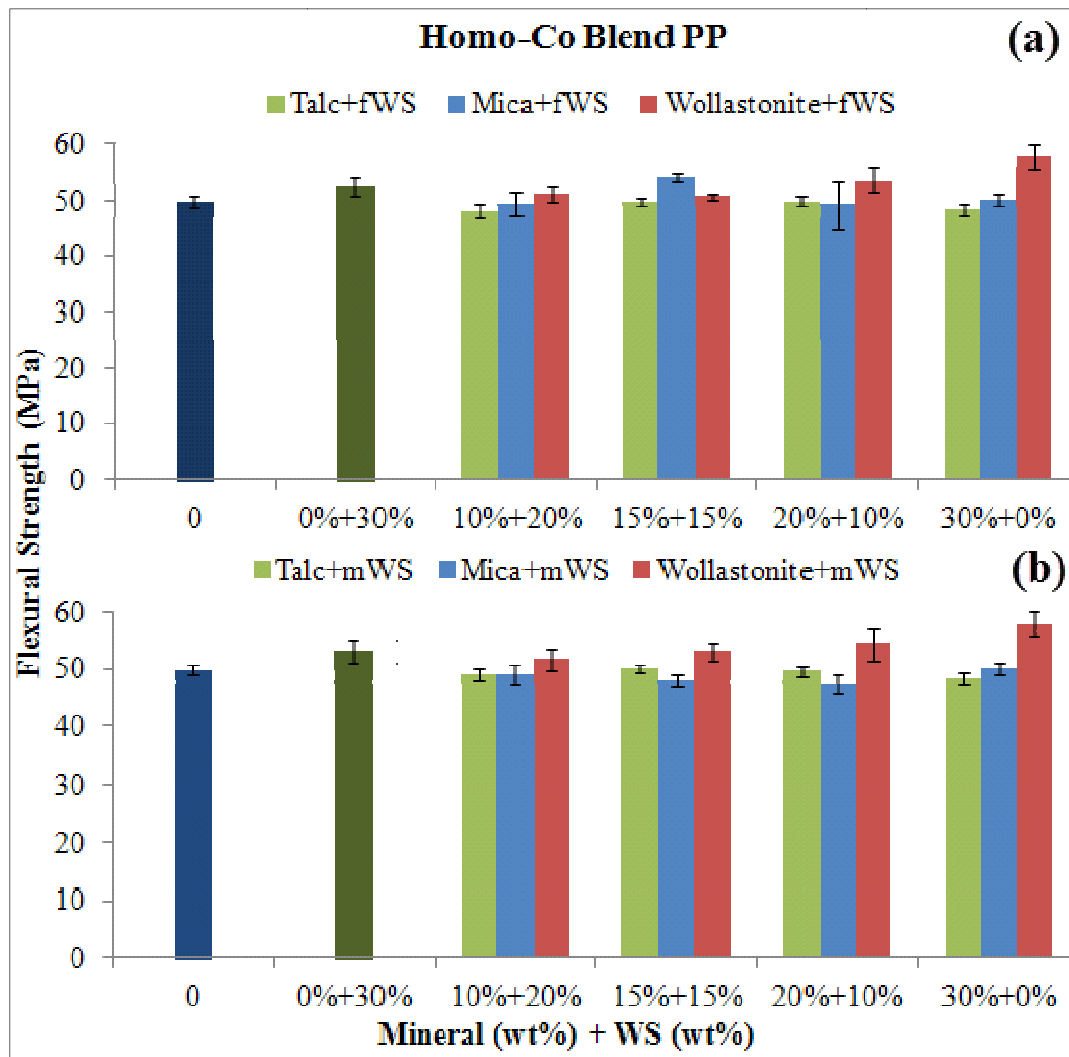


Figure 6.3 Flexural Strength of (a) Mineral/fWS (b) Mineral/mWS bPP Composites

The order of increasing flexural strength for individual filler bPP (single filler bPP composite) at 30 wt% loading was observed to be talc, mica, fWS and wollastonite. The latter seemed to behave very well almost with all grades of PP as well as at different compositions. At 10/20 and 20/10 loading of mineral/fiber fillers, the highest flexural strength was obtained for wollastonite-

fWS bPP composite. A slightly different observation was seen for mica-fWS composite at 15/15 loading (Figure 6.3 (a)). They exhibited higher strength than the other two compositions at 15/15. Incorporation of mica at 15 wt% and wollastonite at 20 wt% improved the flexural strength of fWS-bPP composite, whereas these results were much lower than that of pure wollastonite based composite. Similarly addition of fWS at 15 wt% enhanced the strength of mica composite.

The results obtained with incorporation of medium WS and minerals together into bPP matrix are very similar to that of fWS-mineral hybrid composites. The flexural strength of wollastonite/mWS composite at 20/10 wt% loading is higher than pure mWS and lower than pure wollastonite based composite. The order of increasing strength at 15/15 and 20/10 wt% loading is mica/mWS, talc/mWS and wollastonite/mWS. Addition of mWS to talc or mica do not improve the strength of pure talc or mica based bPP. Here too only wollastonite shows enhancement with respect to the strength of pure mWS-bPP composite.

6.1.2 FLEXURAL MODULUS

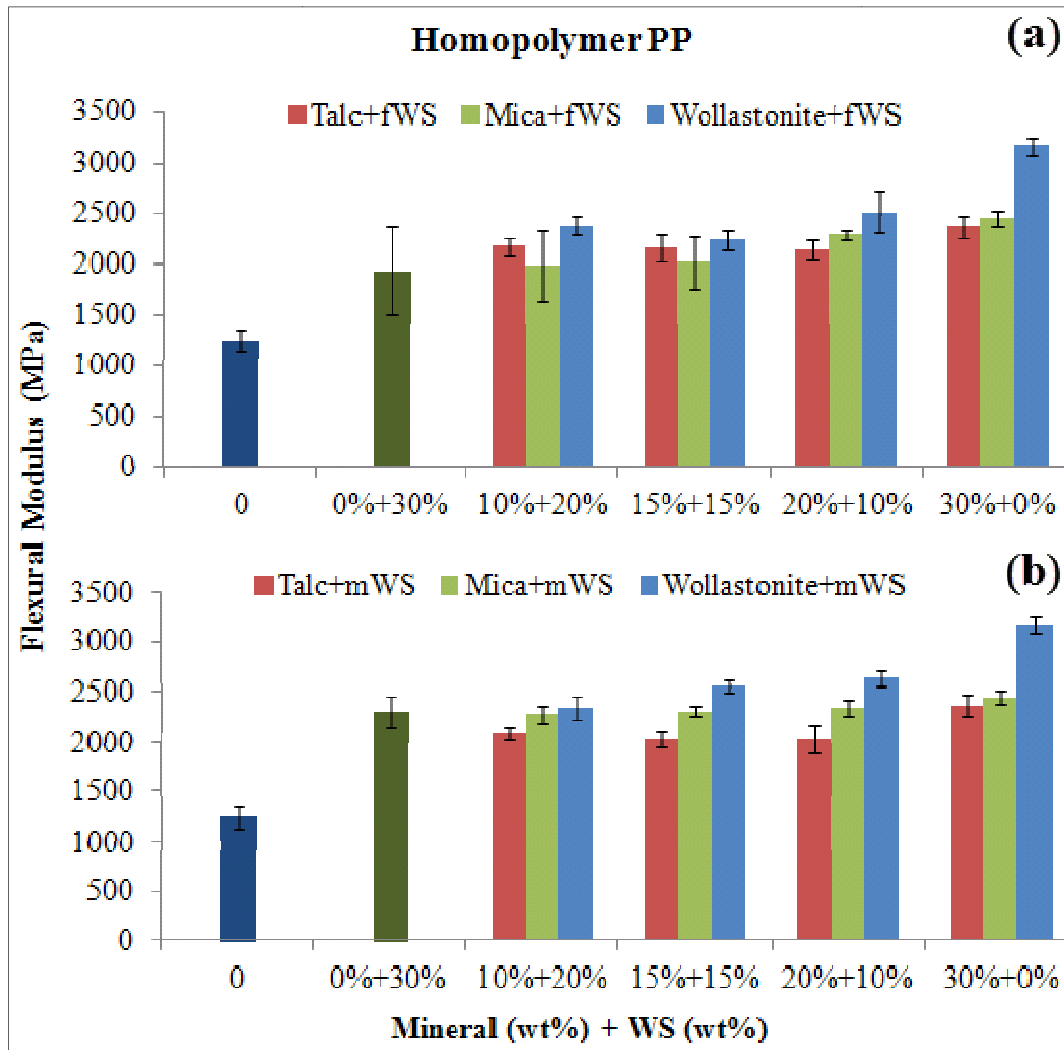


Figure 6.4 Flexural Modulus of (a) Mineral/fWS (b) Mineral/mWS hPP Composites

The addition of two types of fillers in the homopolymer matrix was quite challenging with respect to flexural modulus of 30 wt% fWS composite. The latter had a modulus of around 1.9GPa whereas the lowest stiffness value for the hybrid composites itself is 2GPa for mica/fWS filled at 10/20 wt %, although there are experimental errors as shown in Figure 6.4(a). As the percentage of mineral fillers was increased from 10 wt% to 20 wt% and the amount of fWS was decreased from 20 wt% to 10 wt% in each composition, a significant increase in stiffness was observed. For each hybrid mixture, wollastonite/mWS showed higher stiffness than mica and

talc filled mWS composite. Results obtained for hybrid composites were lower than that of pure mineral filled hPP composites, but certainly higher than 1.4 GPa, flexural modulus of pure resin.

Homopolymer hybrid composites comprising of mineral fillers and medium WS showed different characteristics. Talc/mWS and mica/mWS hybrids had lower stiffness than individual mWS, talc or mica hPP composites. The modulus of wollastonite and mWS hybrid variety at 15/15 and 20/10 wt% loadings was considerably greater than that of individual mWS composite, but significantly lower than that of pure wollastonite filled homopolymer matrix. As in all cases, the hybrid property was higher than that of pure matrix.

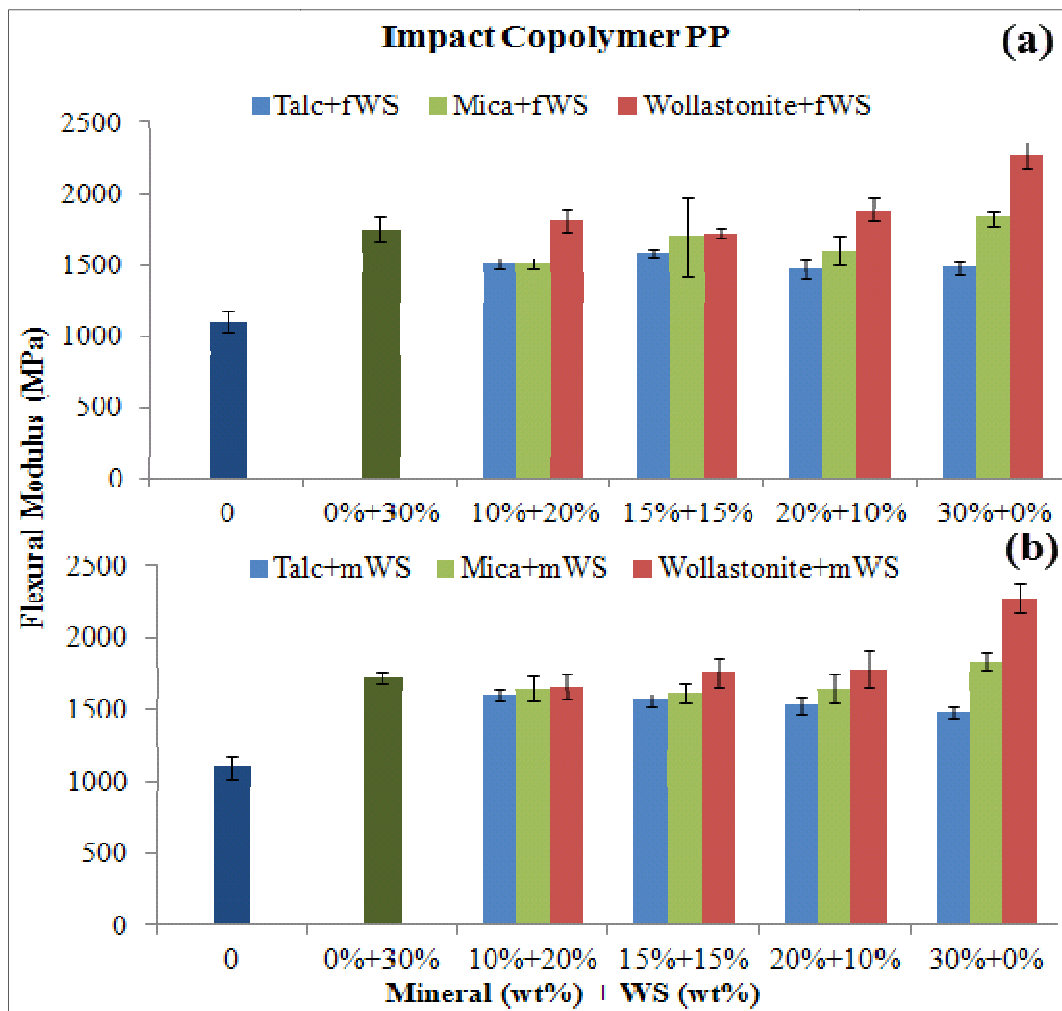


Figure 6.5 Flexural Modulus of (a) Mineral/fWS (b) Mineral/mWS icPP Composites

The flexural modulus of impact copolymer hybrid PP composites was comparable with those results obtained for homopolymer mineral/medium WS hybrids. At 10/20 and 20/10 loadings wollastonite/fWS combination showed significantly higher stiffness than the other hybrid varieties. This observation indicates that there is small amount of synergy effect for wollastonite and fine WS compared to pure fWS composite. The effect of mica/fWS and wollastonite/fWS at 15/15 wt% loading were not different but high. Again, the hybrid composites had higher modulus than pure matrix.

When comparing the results obtained for pure medium WS and mineral composites at 30wt% loading, it is clearly seen that the stiffness of hybrid composite made of talc/mWS increased at a slow rate from 20 wt% to 10 wt% loading (Figure 6.5(b)). Before hybridization, talc based icPP had a modulus of around 1.48 GPa whereas after incorporation of both talc and mWS into the matrix the stiffness rose to 1.6 GPa which indicates synergy. This was not observed in case of mica or wollastonite hybrids with mWS. Wollastonite/mWS hybrid also showed a slight increase in stiffness of 1.78 GPa compared to the modulus of mWS icPP composite, 1.71 GPa.

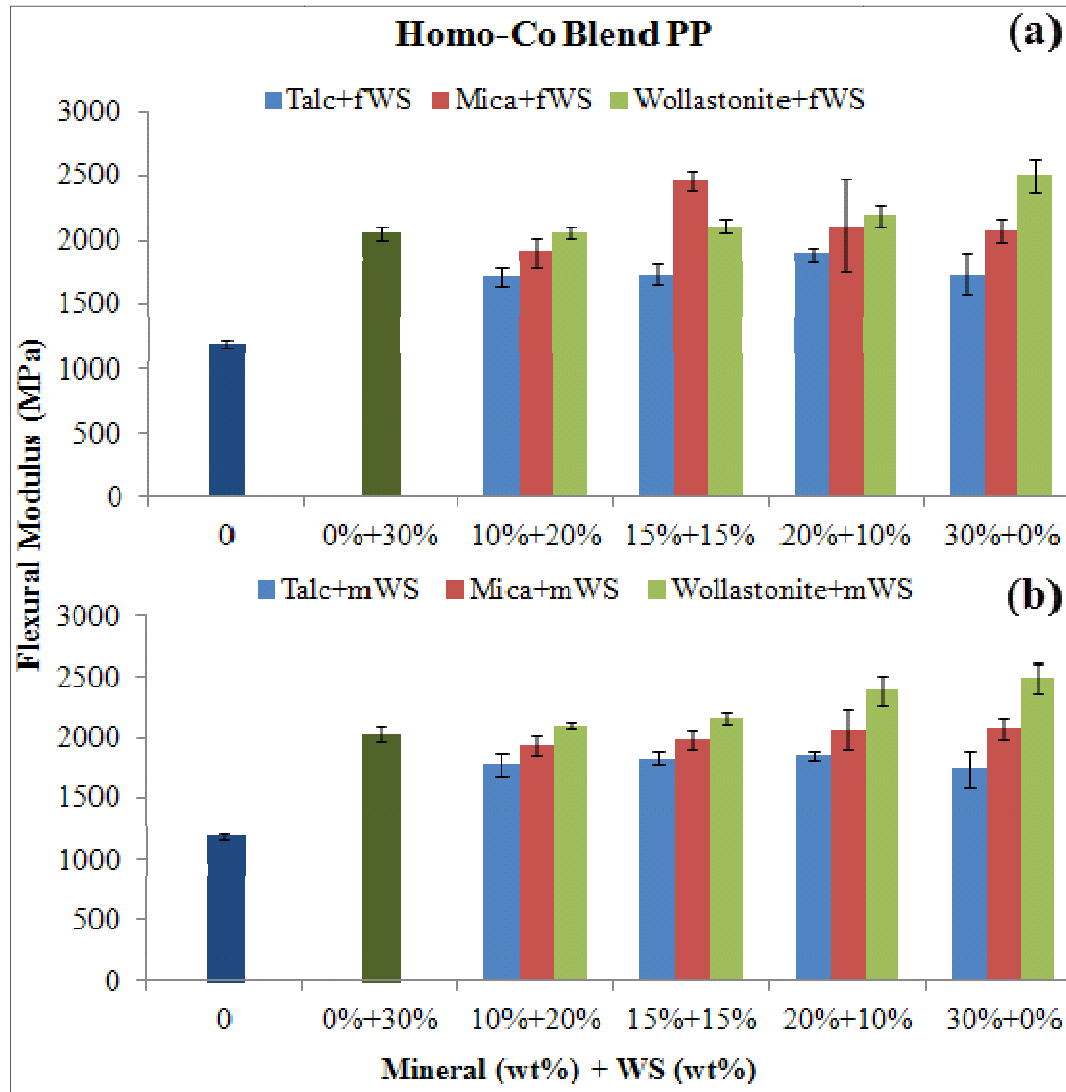


Figure 6.6 Flexural Modulus of (a) Mineral/fWS (b) Mineral/mWS bPP Composites

Addition of mica and fWS at 15/15 wt% to polypropylene blend did produce an unusual increase in stiffness of 2.45 GPa which appeared to be very close to the modulus value of 2.49 GPa for wollastonite composite. It can be inferred from Figure 6.6(a) that at 10/20 and 20/10 wt% loadings wollastonite/fWS mixture had the highest flexural modulus whereas at 15/15 wt% loading mica/mWS improved the stiffness of PP blend significantly. Wollastonite/mWS had similar modulus as pure mWS with a slight increase at 20/10 wt% loadings which again indicates synergy.

The hybrid composites had a higher stiffness compared to the pure blend polymer. Combination of wollastonite and medium WS showed synergy upon increasing the content of wollastonite from 10 wt% to 20 wt%. This combined effect was observed at 20/10 wt% loading of mica/mWS as well. The stiffness effect shown by talc/mWS cannot be avoided because there is indeed a minor increase upon varying the percentage of mWS from 10 to 20 wt%.

6.1.3 TENSILE STRENGTH

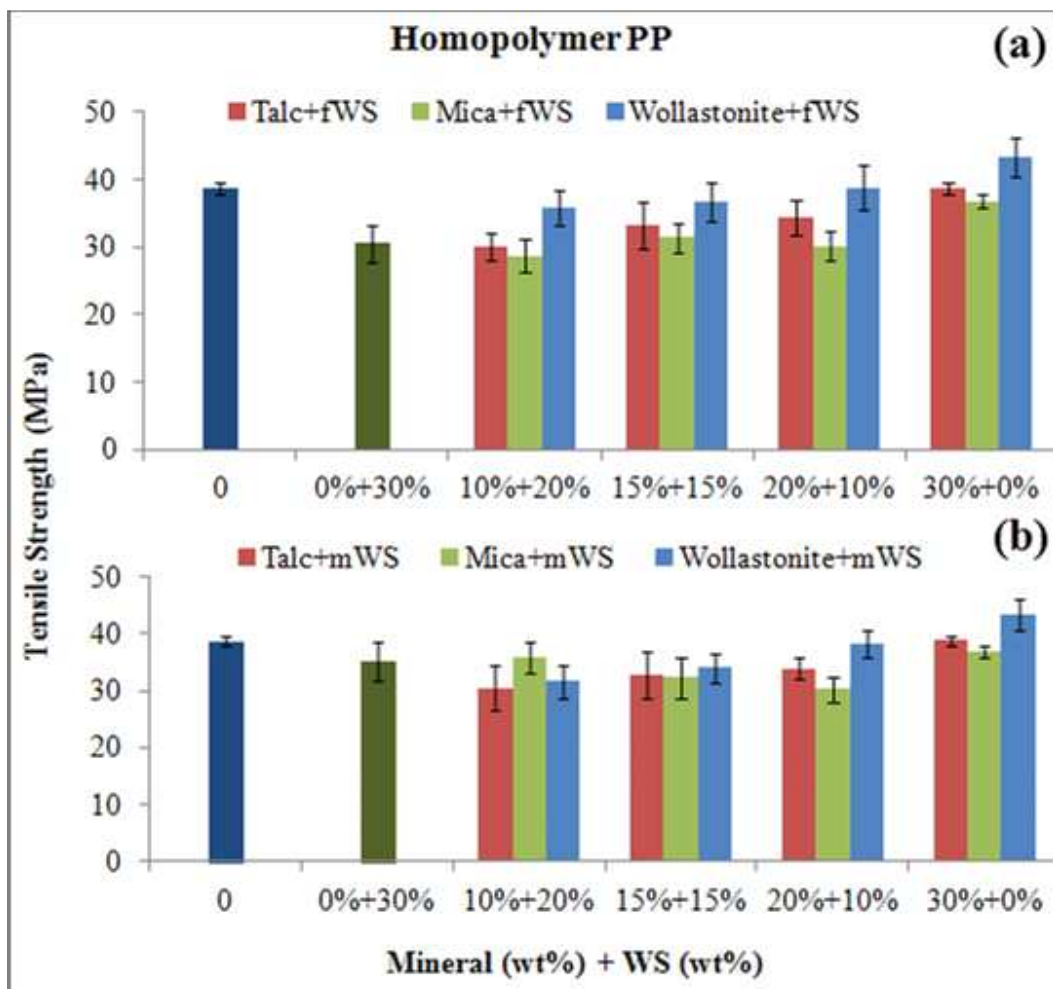


Figure 6.7 Tensile Strength of (a) Mineral/fWS (b) Mineral/mWS hPP Composites

Figure 6.7 (a) and (b) shows the tensile strength of hybrid composites of WS and minerals at 10/20, 15/15 and 20/10 wt% loadings in comparison with the effect of individual fillers at 30 wt% on the homopolymer composite. Homopolymer filled with fWS/talc and fWS/wollastonite show increasing tensile strength when evaluated against 30 wt% fWS-hPP composite. The positive effect of hybridization also increases with the increasing fraction (10 to 20 wt %) of the mineral fillers (talc and wollastonite). The hybrid effects of mica and fWS were not evident at any filler ratios. When comparing these hybrid results with 30wt% mineral loading on hPP, the effect is low. The tensile strength is observed to be decreasing (from right to left of Figure 6.7(a)) for all mineral/biofiber filled hybrid hPP. This plot suggests that at any loading level, replacement of fraction of fWS with mineral filler is advantageous to the homopolymer composite property but not vice versa.

At 10/20 ratio of mica/mWS loading, the homopolymer shows a tensile strength of 35.8 MPa, very close to the strength of pure mWS filled composite (35.1 MPa). As the percentage of mica in the hybrid composition is varied from 10 to 20 wt%, the tensile strength decreases. Talc/mWS and wollastonite/mWS hybrids show poor property with respect to mWS. But unlike mica, as the loading levels of these minerals are increased from 10 to 20 wt%, slight increase in tensile strength can be noticed. Wollastonite/mWS hybrid variety at 20/10 ratio exhibits higher strength than pure mWS. Overall the tensile strength of hybrid composites is lower than the pure mWS and pure mineral hPP composites. There is no synergy observed with hybridization. The tensile strength for both fWS and mWS mineral hybrids were lower than the pure homopolymer.

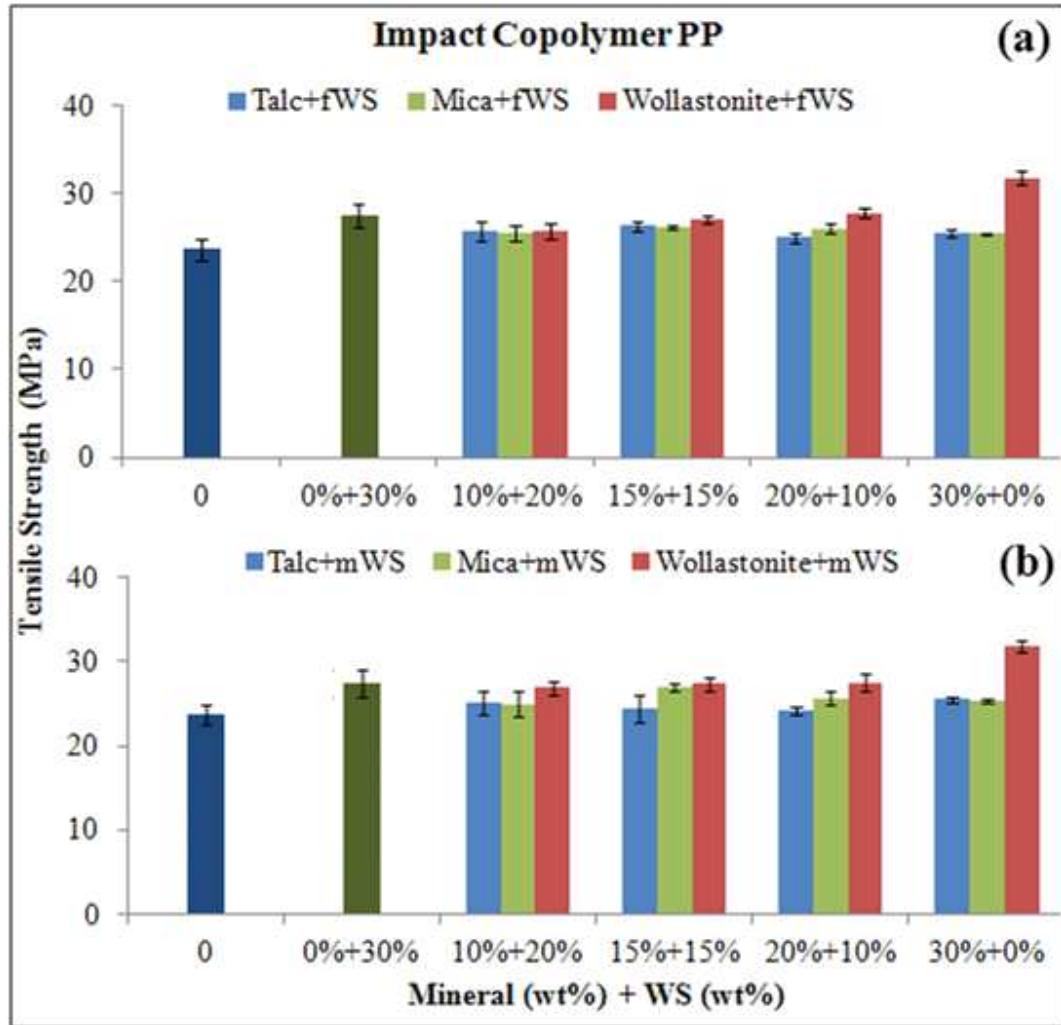


Figure 6.8 Tensile Strength of (a) Mineral/fWS (b) Mineral/mWS icPP Composites

Impact copolymer PP fWS-mineral hybrid composites also follow the same trend as that of hPP mWS-mineral hybrids. The tensile strength decreases upon hybridizing, compared to the strength of 30wt% fWS and wollastonite icPP composites (Figure 6.8(a)). At 10/20 and 15/15 wt% loadings, hybrids exhibit the same tensile strength independent of filler type whereas at 20/10 ratio of fWS/mineral icPP composite, the strength increases with varying mineral type (talc → mica → wollastonite). The tensile strength of talc/fWS and mica/fWS at all hybrid loadings are similar to the effect of the minerals at 30wt% individual loading, but wollastonite/fWS hybrid showed poor property. However, the hybrid composites had higher strength than pure icPP.

It is interesting to note that the behaviour of wollastonite with medium WS is same irrespective of the change in hybrid percentages but significantly lower than pure wollastonite icPP composite. The tensile strength of talc and mica is however fluctuating. At 10/20 wt%, strength of talc/mWS and mica/mWS is lower than pure mWS but effectively same as that of pure talc and mica composites at 30wt%. At 15/15 wt%, mica/mWS provides higher strength compared to pure mica composite. At 20/10 wt% composition, the tensile strength of hybrids increases in the order of talc/mWS, mica/mWS, wollastonite/mWS. All the hybrid composites had strength higher than the pure resin.

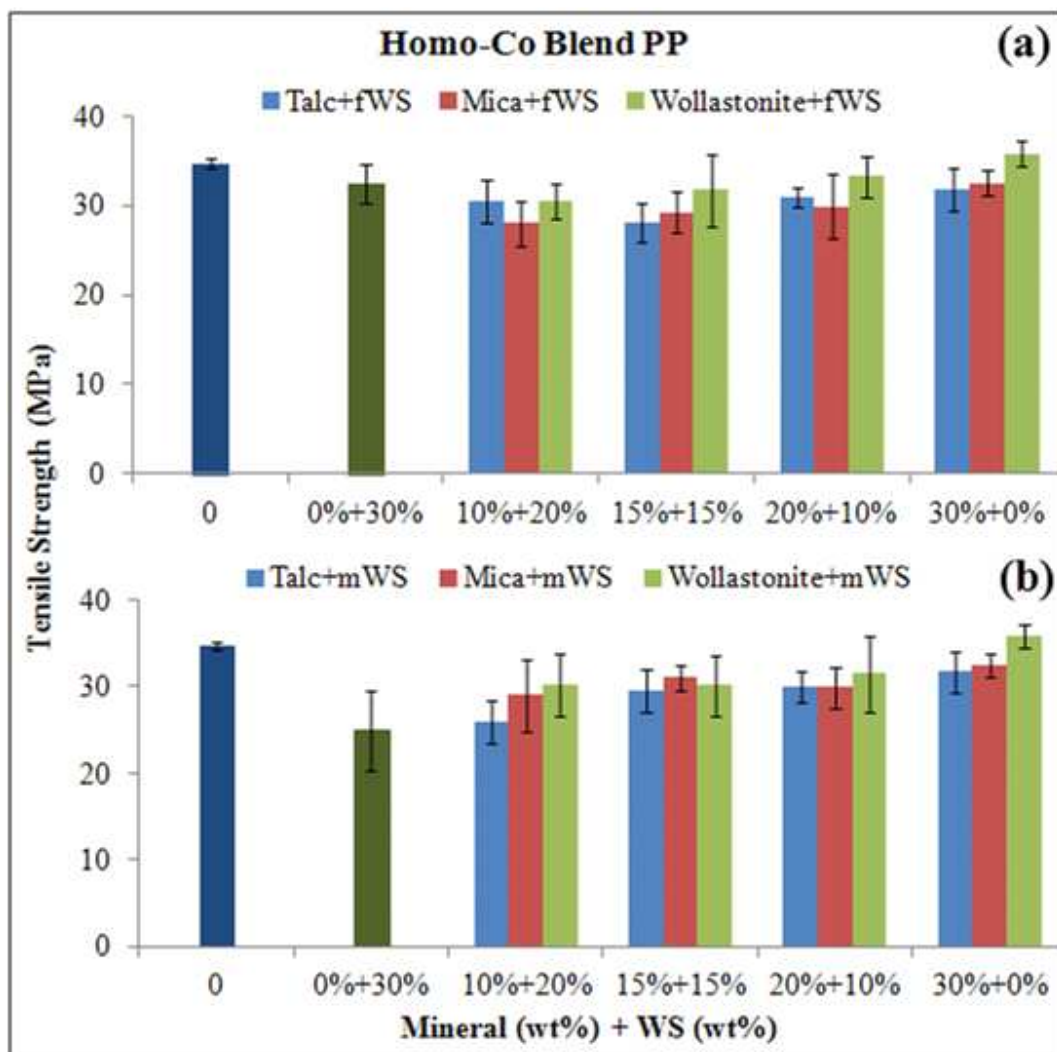


Figure 6.9 Tensile Strength of (a) Mineral/fWS (b) Mineral/mWS bPP Composites

The tensile strength for bPP hybrid composites, as shown in Figure 6.9(a), is lower than the pure fWS and pure mineral filled bPP composite. There is no property enhancement with hybridization. Among hybrid composites, the tensile strength increases with increasing mineral content in the hybrid composition. Mica/mWS shows lowest tensile strength at all percentage loadings. The overall strength of polypropylene blend is higher than those of hybrid composites.

The results obtained for hybridization with mWS are way different from the fWS hybridized composites. The tensile strength of bPP is significantly improved with the incorporation of hybrid fillers. A significant amount of synergy is observed between minerals and mWS with respect to the tensile strength of 30wt% mWS bPP composite. When considering the tensile strength of mineral filled composite, hybrids have low strength like in all the cases observed before. Here too, the replacement of a fraction of 30wt% mWS with 10, 15 or 20 wt% mineral filler positively influences the property of hybrid bPP composite. But the tensile strength of hybrids is much lower than pure blend.

6.1.4 TENSILE MODULUS

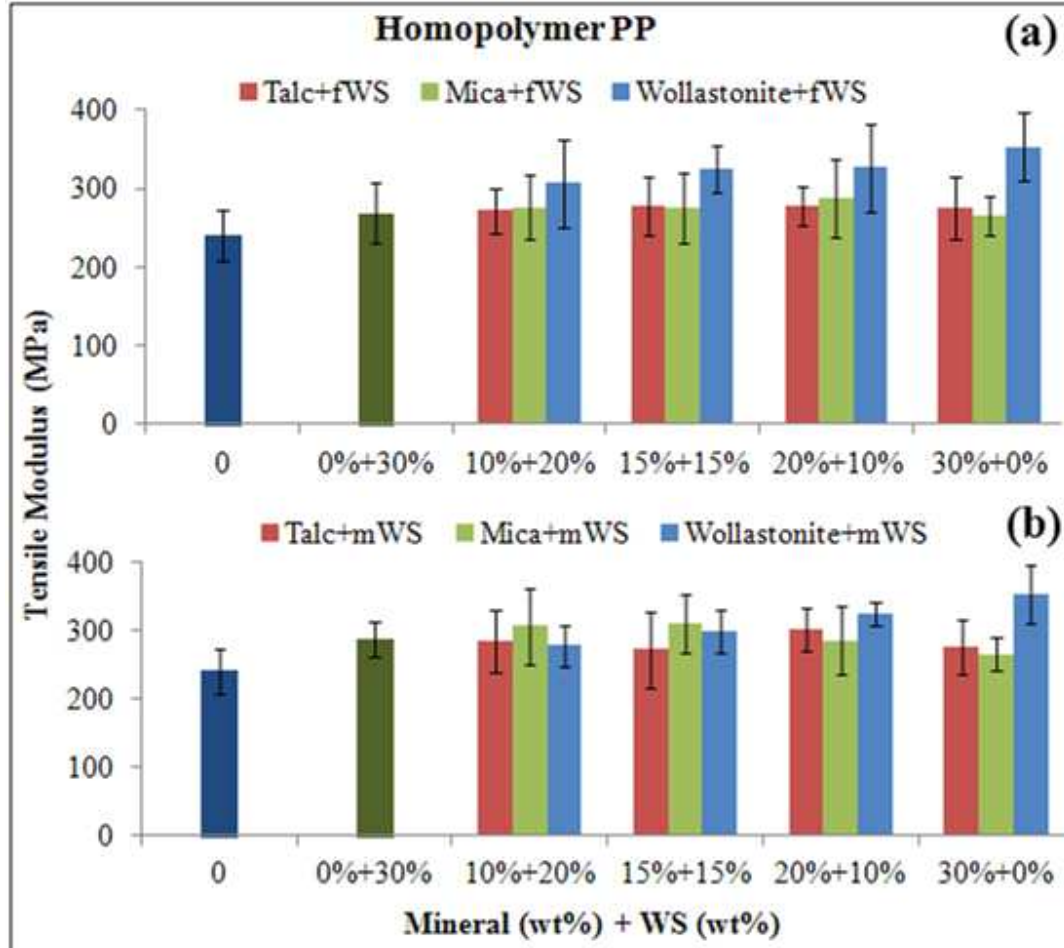


Figure 6.10 Tensile Modulus of (a) Mineral/fWS (b) Mineral/mWS hPP Composites

Talc-fWS and mica-fWS hybrid composites have tensile modulus very similar to that of pure fWS and pure talc or mica composites. Wollastonite-fWS hybrid combination increases the modulus of the composite by 14% at 10/20 wt% loadings. The increase at higher percentages of wollastonite is minimal. The incorporation of low modulus fine WS from 10 to 20 wt% (Figure 6.10(a) right to left) only decreases the modulus of wollastonite/fWS hybrid composite in comparison with the modulus of pure wollastonite hPP composite. Therefore there is synergy observed in case of wollastonite/fWS hybrids but not with any other combinations. In general, the tensile modulus of hybrid composites is higher than pure matrix hPP.

The replacement of fWS with mWS in the hybrid composites did not give any significant results either. The behaviour of mica/mWS is more prominent at 10/20 and 15/15 concentrations with respect to pure mWS and pure talc or mica composites, whereas wollastonite /mWS showed their effect at 20/10 wt% loading. However this increase in modulus is not higher than pure 30 wt% wollastonite hPP composite but it is definitely larger than the modulus of pure homopolymer.

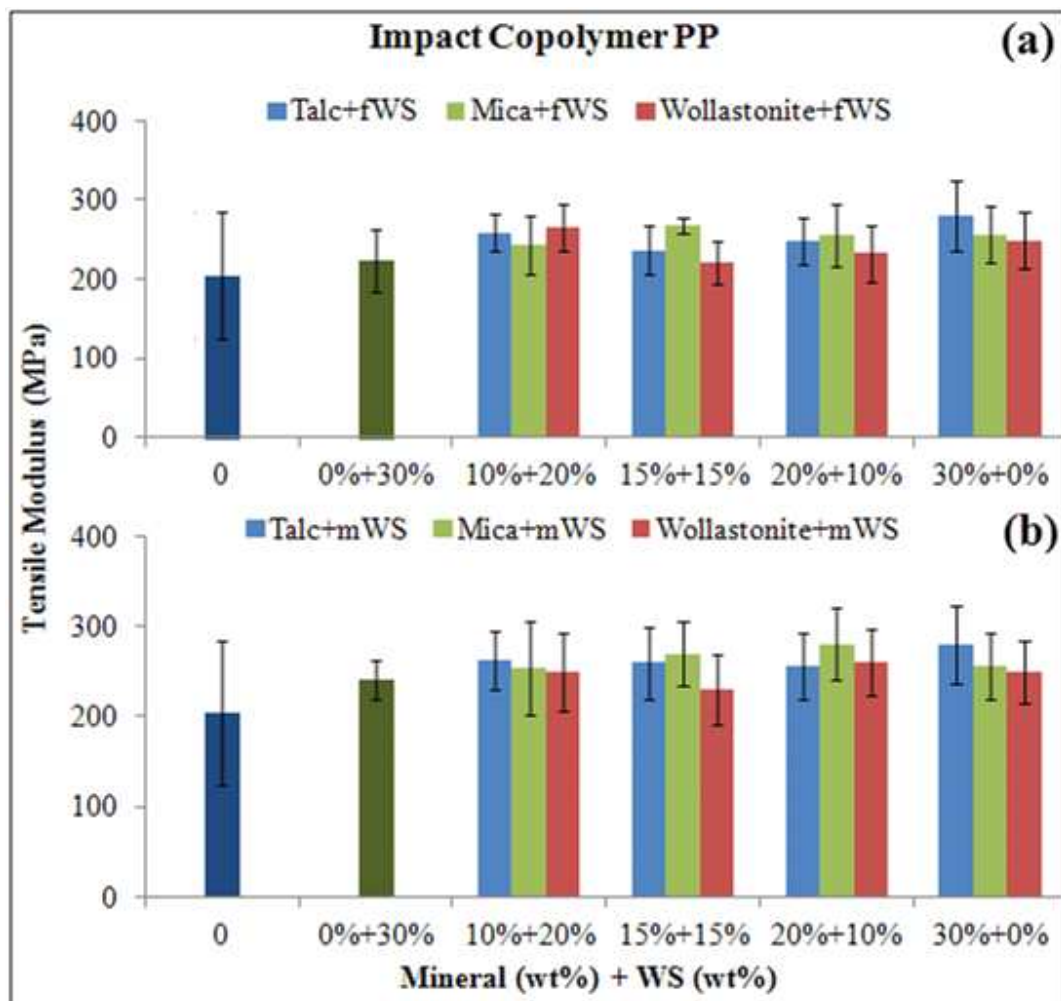


Figure 6.11 Tensile Modulus of (a) Mineral/fWS (b) Mineral/mWS icPP Composites

The modulus of elasticity of impact copolymer PP is increased with hybridization. When comparing the results obtained for icPP hybrid composites with the modulus at 30 wt% pure fWS and mineral composites, it is found that tensile modulus increases at 10/20 wt% and then

decreases further at 15/15 and 20/10 wt% loadings. For mica/fWS alone, the tensile modulus is high at 15/15 wt% loading ratios. The overall property of the hybrids is certainly higher than the modulus of fWS but lower than the modulus of mineral composites. Therefore the addition of fWS to minerals seems advantageous to fWS composites but addition of mineral to fWS seems detrimental to mineral composites.

Same trend is observed for mineral/mWS hybrid icPP composites as well. All the hybrids at all the loading ratios have higher modulus than pure medium WS. Mica/mWS have slightly higher Young's modulus than pure mica icPP composite whereas the modulus of talc/mWS and wollastonite/mWS combinations is not affected much. It is also observed that hybridization significantly improved the tensile modulus of pure copolymer.

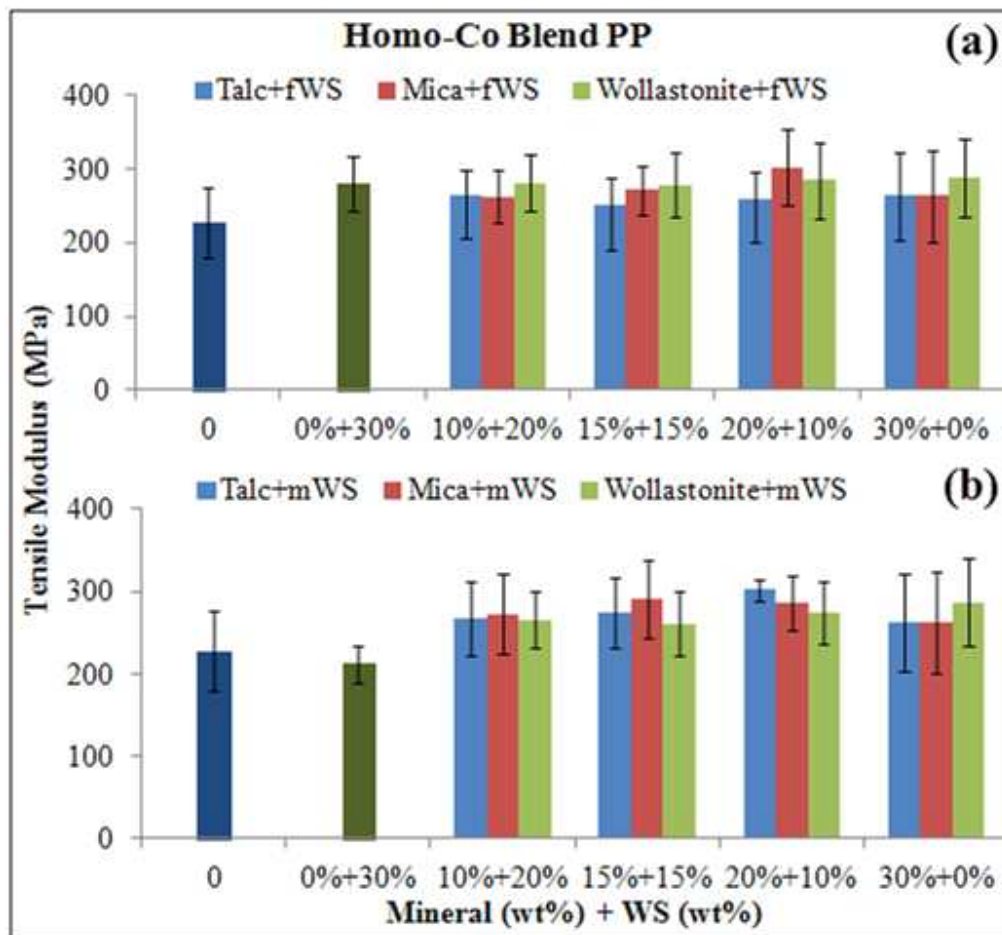


Figure 6.12 Tensile Modulus of (a) Mineral/fWS (b) Mineral/mWS bPP Composites

Tensile modulus of polypropylene blend increased with the addition of 30wt% individual fillers. Further increase in modulus is not achieved by hybridization at varying filler contents. However, mica/fWS combination at 20/10 wt% did show a slight increase in modulus with respect to pure fWS and pure mica bPP composite. A synergistic effect is produced in the case of combining mica and fWS in polypropylene homo-co blend. The other filler combinations did not show any successful results.

The results obtained for mWS hybridized mineral composites are interesting due to the fact that a huge improvement in property is observed in comparison to pure mWS composite. The modulus of hybrid composites significantly increased at 10/20, 15/15 and 20/10 wt% loading concentrations. With respect to mWS-bPP composite, there is 26% increase in modulus of hybrid composite at 10/20 wt% loading. At 15/15 wt%, mica/mWS shows a modulus increment of 37% and at 20/10 wt% talc/mWS produces an enhancement of 42%. An increase of 9% modulus for mica/mWS hybrid and 15% modulus for talc/mWS hybrid at 20/10 wt% loading levels compared to pure mica and talc composites are also reported.

6.1.5 IMPACT STRENGTH

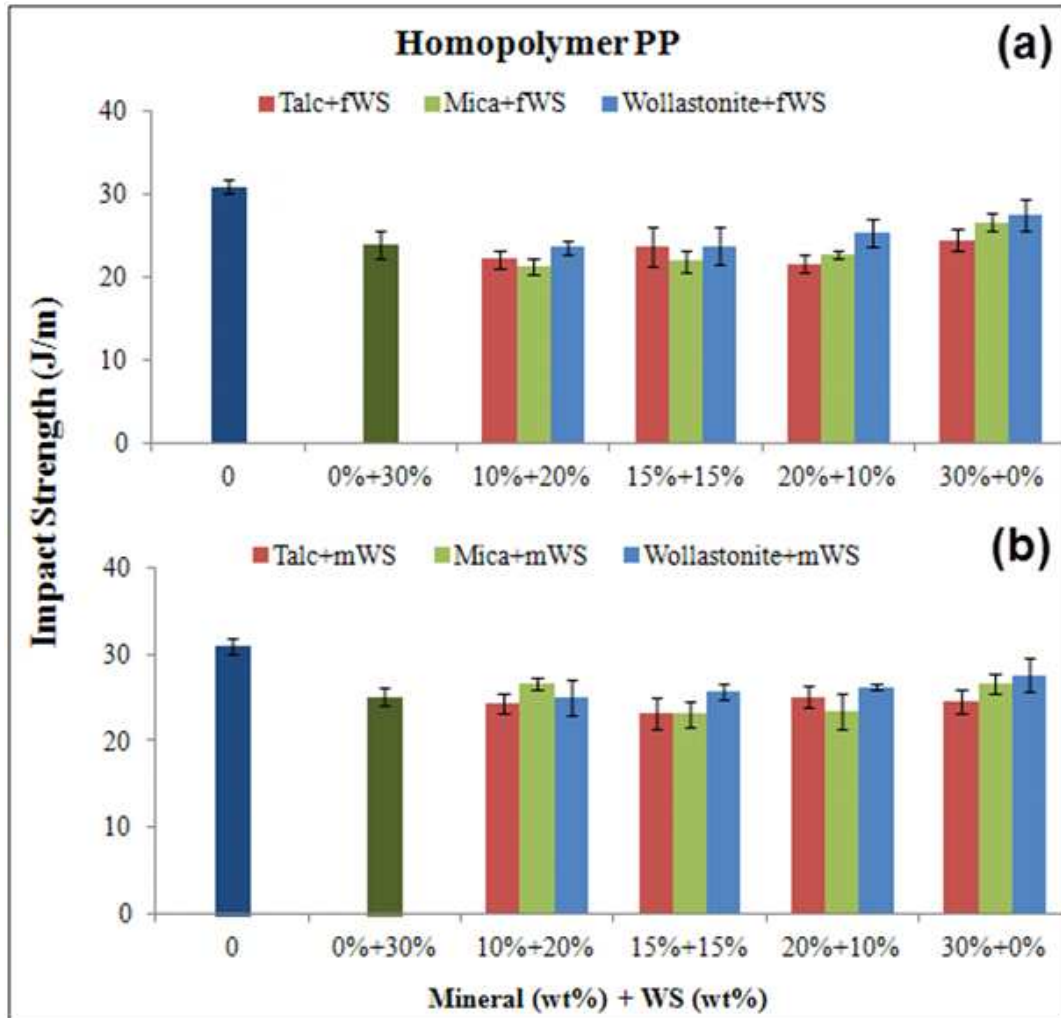


Figure 6.13 Impact Strength of (a) Mineral/fWS (b) Mineral/mWS hPP Composites

Figure 6.13(a) and (b) represents the impact strength property of homopolymer PP composites made of mineral filler/fWS and mineral filler/mWS hybrids respectively. It is observed that the impact strength of hybrid composites is significantly lower than the pure homopolymer. With respect to fine WS and medium WS, the composites did not achieve any property improvement by hybridization. Behaviour of wollastonite/fWS is considerable at 20/10 wt% loadings, with a 6.3% increase in impact strength. When comparing the hybrid properties with the impact strength of pure mineral homopolymer composite, it is observed that hybridization with fWS or

mWS lowered the impact strength or in some cases it showcased similar behaviour. There was no synergistic effect with any of the mineral/fWS or mineral/mWS homopolymer PP composites.

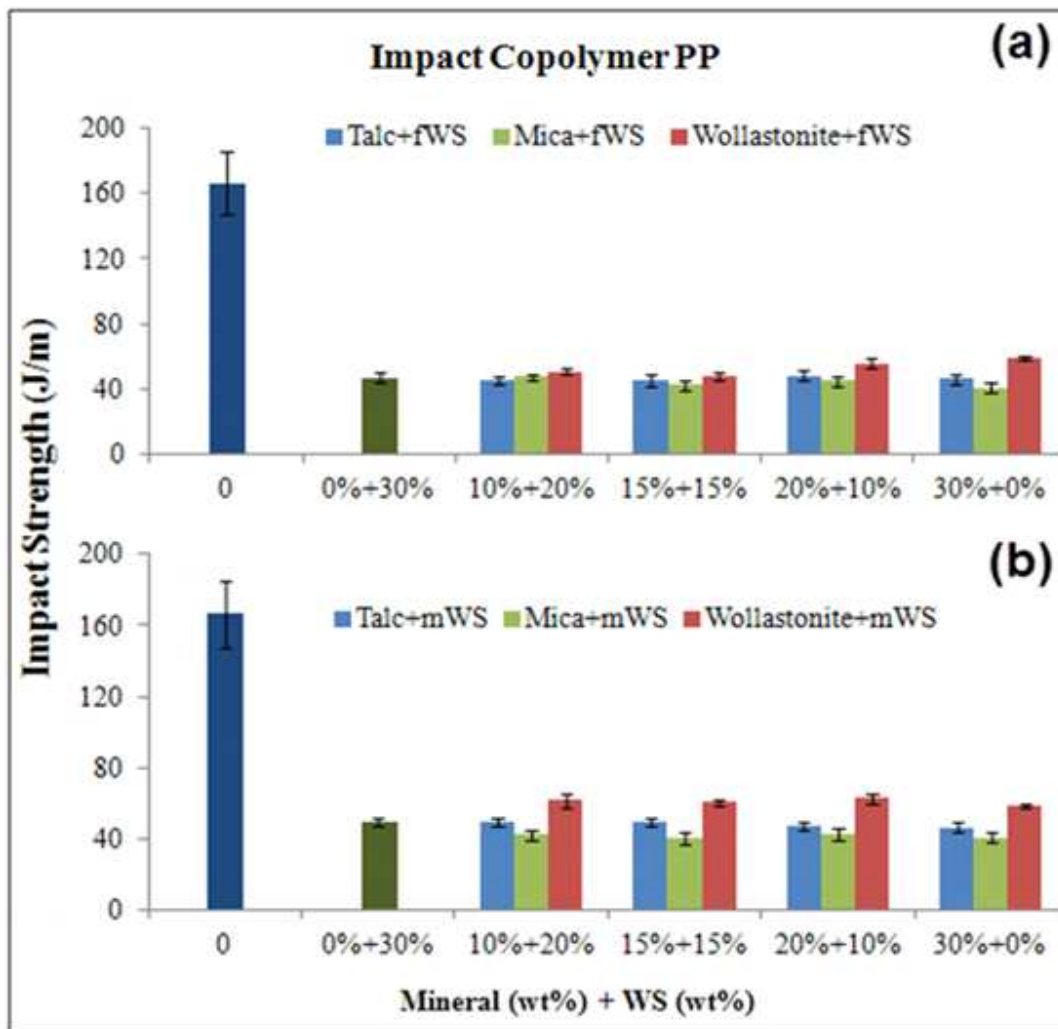


Figure 6.14 Impact Strength of (a) Mineral/fWS (b) Mineral/mWS icPP Composites

There is a tremendous decrease in impact strength with the incorporation of single fillers and hybrid fillers in impact copolymer PP matrix. The presence of varying percentages of talc/mica/wollastonite and fWS did not affect the property of the composite (figure 6.14(a)). It is also interesting to note that hybridization did not reduce the impact strength. At 20/10 loading of wollastonite/fWS to the copolymer, the impact strength showed an increase of 18.5% compared to pure fWS composite at 30wt%. Figure 6.14(b) shows the impact strength of mineral-mWS

filled icPP composite. It can be observed that the mixture of mica and mWS decreased the impact property when compared to the impact strength of mWS at 30 wt% whereas talc/mWS hybrid combination behaved similar to pure mWS and mineral icPP composites. A significant improvement of 24% is observed in case of wollastonite-mWS filled composite (against mWS composite) at all varying filler ratios. The improvement with respect to pure wollastonite composite is not very significant.

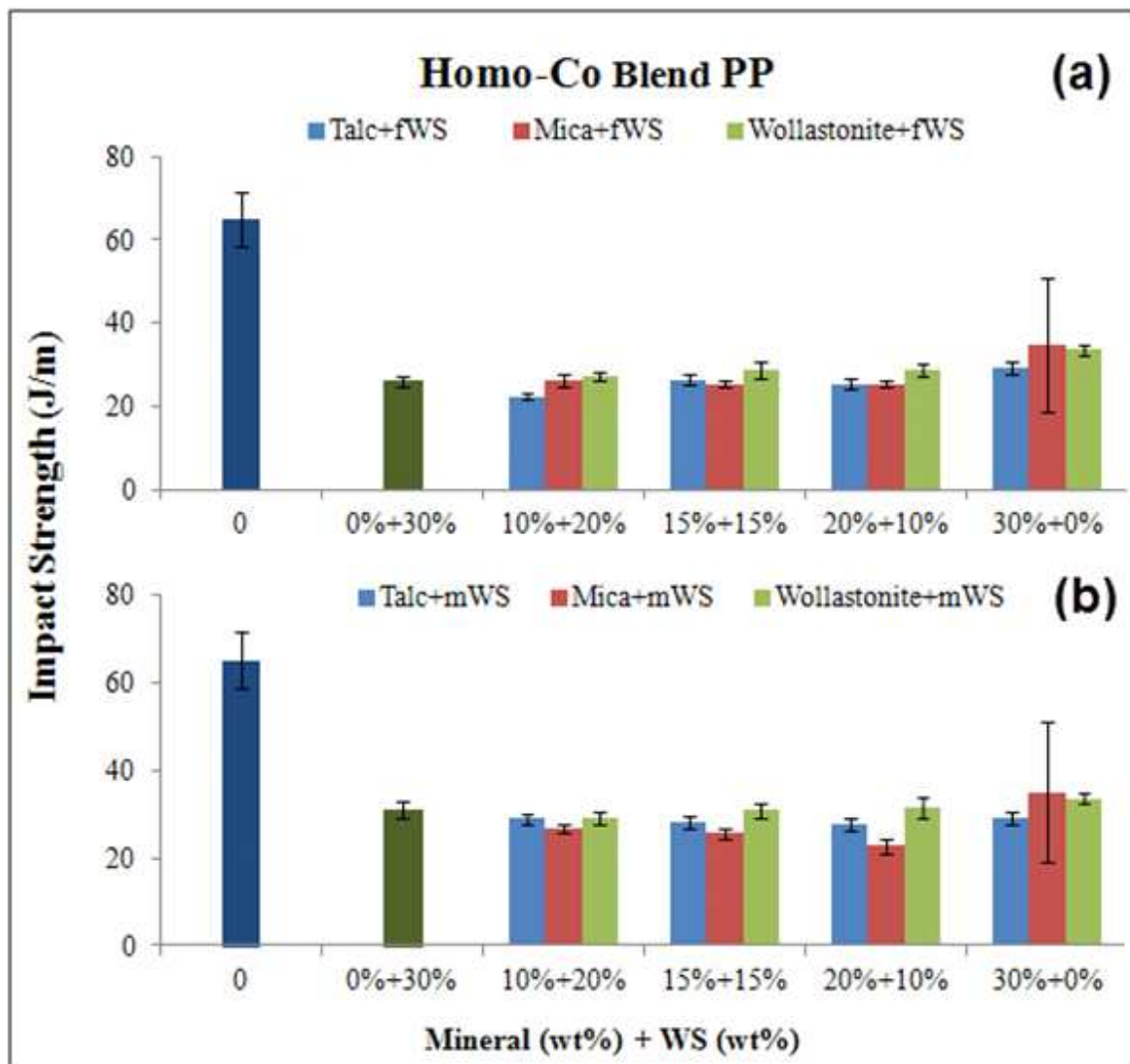


Figure 6.15 Impact Strength of (a) Mineral/fWS (b) Mineral/mWS bPP Composites

Impact strength of homo-co blend PP significantly lowered with the addition of hybrid fillers. Figure 6.15(a) and (b) represents the impact strength of bPP composite with varying percentages of hybrid fillers. It can be observed from figure (a) that all the hybrid combinations had lower

impact strength than pure mineral based bPP composites. Compared to pure fWS composite at 30wt% loading, the increase in impact strength for mica or wollastonite fWS hybrids at 10/20 wt% loadings is not significantly high. Wollastonite/fWS variety at 15/15 and 20/10 wt% loadings showed a 10.8% increase in impact strength. From figure (b) it is clear that the bPP hybrid composites containing mineral filler and medium WS also did not show any synergy effect. The composites had lower impact strength than pure mWS and mineral filled bPP (blend PP). The strength of talc/mWS and mica/mWS decreased with increasing content of talc and mica respectively in the bPP matrix. Wollastonite/mWS showed an increasing trend, and at 20/10 combination, the composite gained more strength than pure mWS composite but not very significant.

6.1.6 SPECIFIC FLEXURAL MODULUS

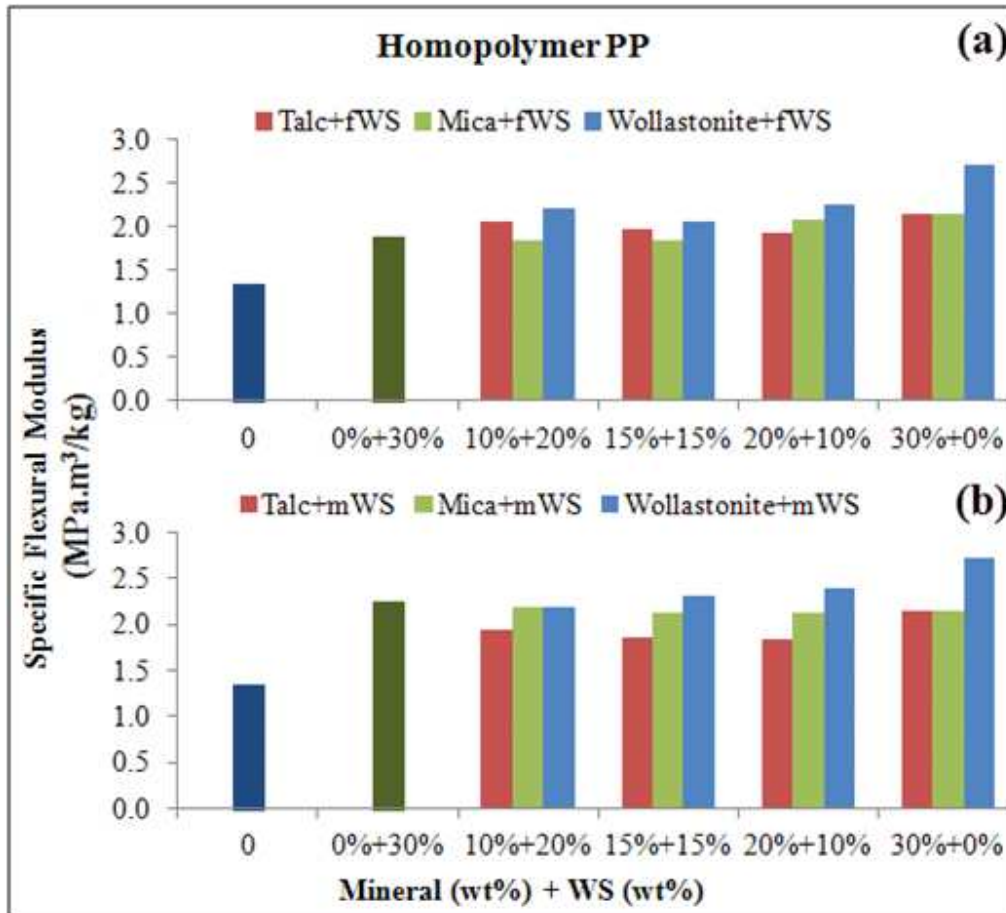


Figure 6.16 Specific Flexural Modulus of (a) Mineral/fWS (b) Mineral/mWS hPP Composites

Specific flexural modulus of homopolymer, copolymer and blend polypropylene hybrid composites was investigated and the results obtained are presented in the Figure 6.16. It can be observed that the specific property improved significantly upon addition of single and multiple fillers. At 10/20 wt% loadings, talc/fWS and wollastonite/fWS showed an increment in specific flexural modulus of hPP composite by 9.6% and 17.6% respectively (Figure 6.16 (a)). At 15/15 and 20/10 wt% loadings the improvement shown by talc/fWS is not significant. At 20/10 wt% loadings the property increased in the order of talc/fWS, mica/fWS and wollastonite/fWS with the latter showing an increment of 20%. The specific flexural modulus of pure mineral hPP composites is higher than the hybrids. Figure (b) represents the specific flexural modulus of

mineral/mWS hPP composites. The multiple filler composites did not show any synergy effect in comparison with pure mWS or pure mineral hPP composite. Incorporation of talc and mWS at varying filler percentages seem to be detrimental to the property. A small increase in modulus with respect to pure mWS is observed with wollastonite/mWS at 15/15 and 20/10 wt% loadings. The combination of mica and mWS did not reduce the specific flexural modulus of mica hPP composite.

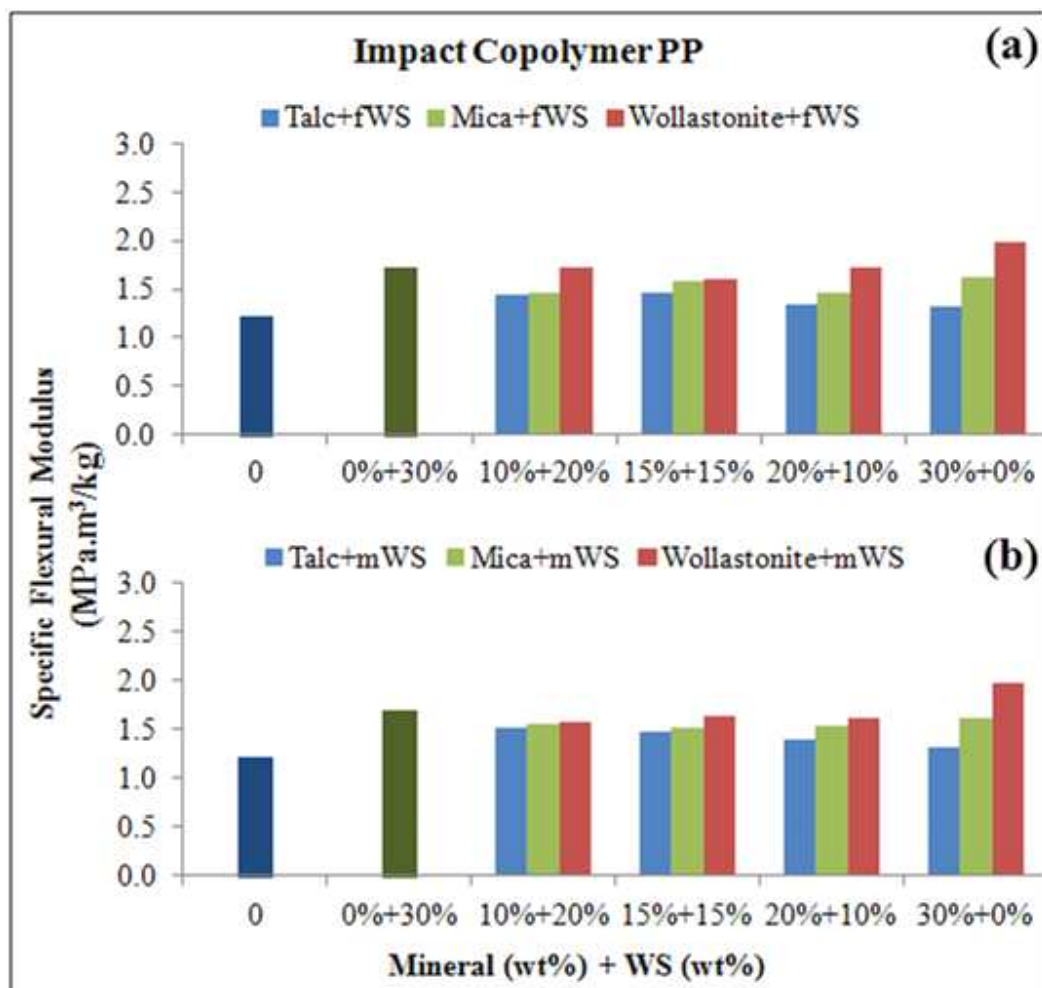


Figure 6.17 Specific Flexural Modulus of (a) Mineral/fWS (b) Mineral/mWS icPP Composites

The differences in specific flexural modulus values for single filler and hybrid filler composites are lower with impact copolymer than that of homopolymer. The specific property of icPP hybrid composites is shown in Figure 6.17(a) and (b). All three combinations of fillers at three

different percentage loadings decreased the specific flexural modulus of the icPP fWS and icPP mineral composites. There is no synergistic effect observed with any of the multiple fillers. Although hybrid fillers improved the specific flexural modulus of pure copolymer, it did not have a positive effect on the composite. Same trend is observed with mineral/mWS combinations as well (Figure 6.17(b)). Hybridization decreased the property of single filler icPP composites except for talc/mWS hybrids. It can be noted that the specific modulus of talc/mWS increased with decreasing loading of talc and increasing content of mWS. At 10/20 wt% the hybrid combination showed an increment of 15.3% compared to pure talc icPP composite.

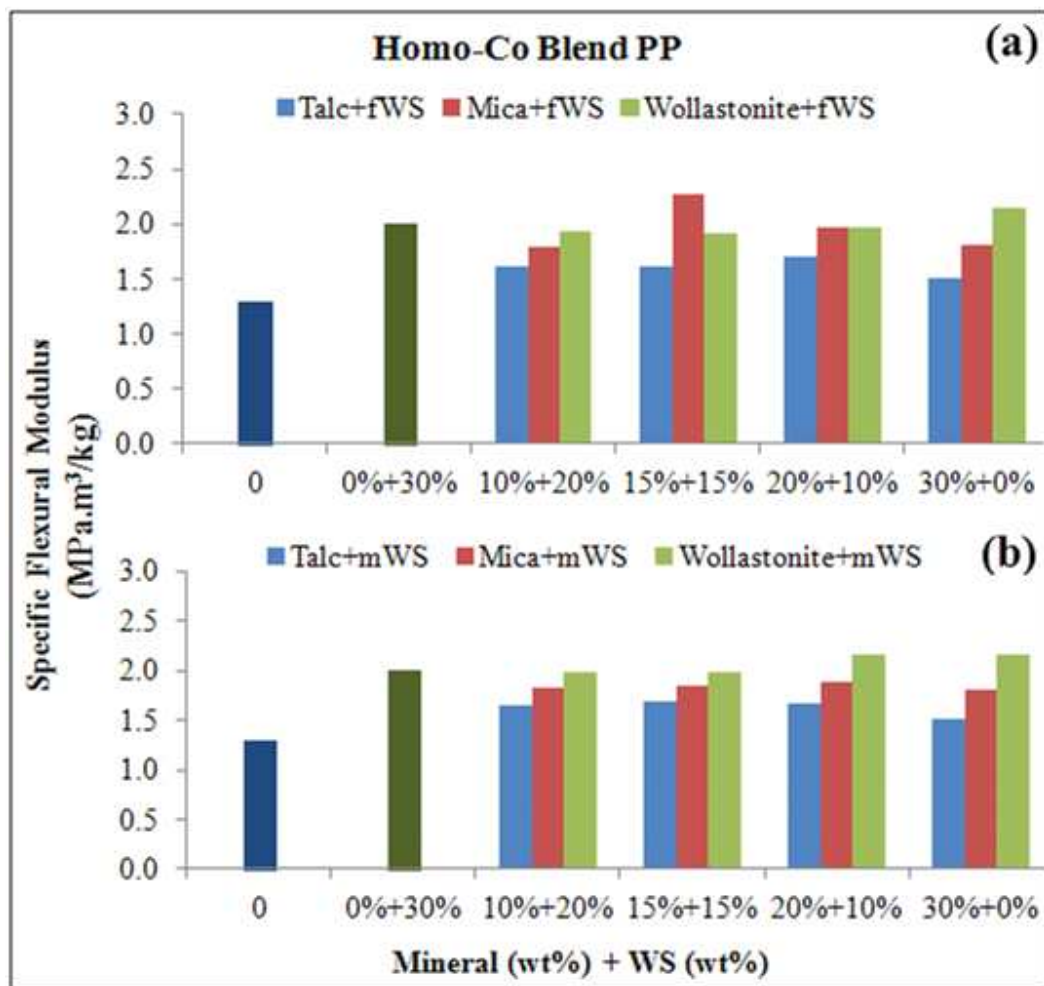


Figure 6.18 Specific Flexural Modulus of (a) Mineral/fWS (b) Mineral/mWS bPP Composites

The hybrid bPP composites and single filler bPP composites showed higher specific flexural modulus than pure bPP itself. It can be observed from Figure 6.18(a) that at 30 wt% loading, fWS, talc, mica and wollastonite bPP composites exhibited a modulus value of 2.01, 1.51, 1.81 and 2.15 MPa.m³/kg respectively. When comparing these results to the hybrid composites, it is interesting to note that talc/fWS composites at all three hybrid compositions and mica/fWS at 15/15 and 20/10 wt% loadings have higher specific flexural modulus than pure talc or mica bPP (blend PP) composite but lower specific property than pure fWS bPP composite. Mica/fWS at 15/15 wt%, showed a significantly high specific modulus value of 2.26 MPa.m³/kg, which is nearly 5.12% increase over pure wollastonite composite. At 20/10 wt% loading level mica/fWS and wollastonite/fWS samples showed a similar behaviour. The specific flexural modulus of pure talc and mica bPP composites increased with hybridization with medium WS (Figure 6.18(b)). The property increased with increasing percentage of talc or mica in the hybrid composition. It is an interesting observation that at 30 wt% total loading, both mWS and fWS has a specific flexural modulus of 2.01 MPa.m³/kg. Therefore, the hybrid composites of mineral/mWS are compared to the same standard values as that of mineral/fWS bPP composites. At all three percentage loadings of 10/20, 15/15 and 20/10 wt%, the specific flexural modulus increases in the order of talc/mWS, mica/mWS, wollastonite/mWS. At 20/10 wt% wollastonite/mWS showed a similar behaviour as exhibited by pure wollastonite composite. The hybrids except wollastonite/mWS at 20/10 wt% had lower specific modulus than pure mWS bPP composite.

6.1.7 SEM

The morphology of hybrid composites containing 15wt% of mineral filler and 15 wt% of WS fibers in homopolymer, copolymer and blend PP was investigated. All formulations contained 2 wt% MAPP coupling agent. Figure 6.19 to 6.25 represents the morphology of fWS-mineral composites for hPP, icPP and bPP. Figures 6.26 to 6.29 represent the morphology of mWS-mineral composites for hPP, icPP and bPP. Some of the results are shown in Appendix B. Figure 6(a) shows the interaction of talc and fWS with homopolymer at 1000X magnification. It can be observed that there is a homogeneous distribution of the filler particles throughout the matrix. It appears like talc has engrossed the fine WS fibres and the fibres are barely visible. The analysis

also show the orientation of flow for the composite. SEM analysis on mica-fWS-hPP composite indicates that the interface interaction is not very strong because of which there is a gap developed between the fillers and the matrix during impact. In the earlier discussions on morphology of fWS homopolymer composite it was observed that the filler and the matrix had good interfacial bonding. In Figure 6.20, mica appears to be detrimental to the hybrid composite in maintaining the bonding. The same type of reduced interaction can be observed for mica-fWS-icPP composite as well (Figure 6.22). However the gap observed for the hybrid is significantly smaller than the gap shown in Figure 5(b) for fWS-icPP composite which indicate that the interaction between the hybrid and icPP matrix is improved. SEM analysis of fWS-talc icPP is shown in Figure 6.21. It is interesting to observe that the copolymer undergoes a visco-elastic deformation prior to fracture. The interface between the polymer and the fibre seems to be intact with less or negligible separation. SEM with 500X magnification for wollastonite/fWS icPP composite at 15/15 wt% loading is significantly small to view the presence or behaviour of wollastonite (with a particle size of 8 μm) in the hybrid composite system. However it can clearly noted in Figure 6.23 that there is a small gap between the matrix and fWS fibres which indicate a reduced interaction between each other. Figures 6.24, 6.25 and 6.29 represent the SEM images for talc/fWS, mica/fWS and talc/mWS bPP composites. The analysis on all three hybrid composites showed that the fracture occurred across the particle or fibre (or along the transverse axis of the fibre) without affecting the fibre-matrix interface. In Figure 6.25 the cross section of fWS in mica/fWS bPP composite surface can be clearly identified and shows that there is a strong bonding between the filler and the matrix. SEM analysis on talc/mWS hPP and icPP composites at 15/15 wt% loadings indicates strong bonding between fillers and the matrix (Figures 6.26 and 6.27). A uniform distribution of the fillers, talc and mWS on the icPP matrix can be clearly identified at 500X magnification. Figure 6.27 shows that the addition of coupling agent really improved the bonding between fibres and the matrix. Another observation that can be made is that the fibre appears to be uniformly coated with the mineral particles in the composite system. A coated fibre can be seen popping out of the surface without being pulled out during impact.

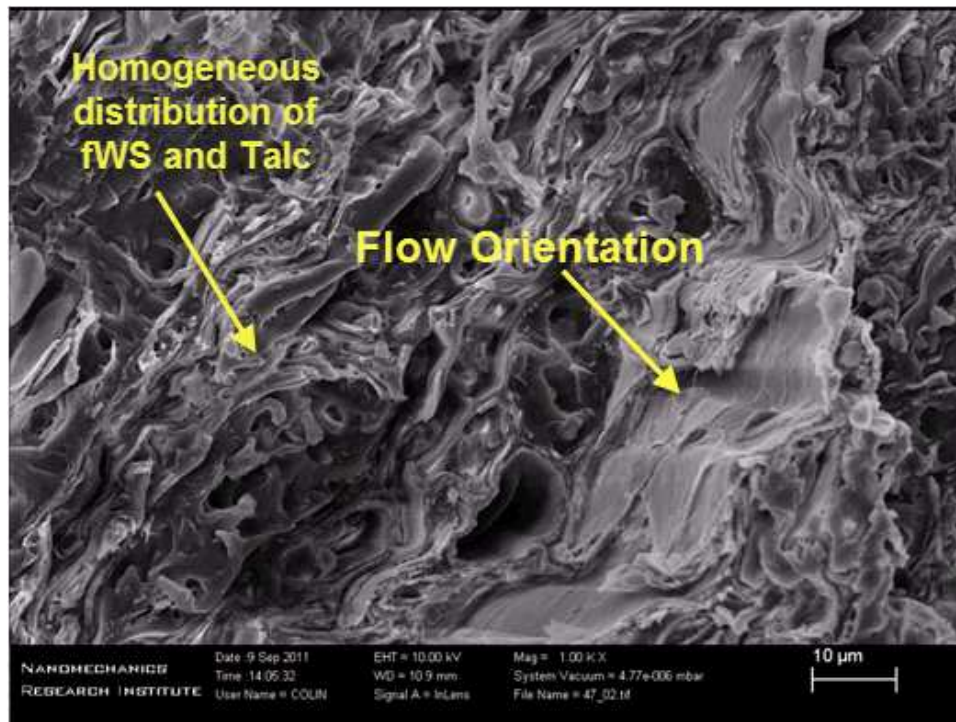


Figure 6.19 SEM of 15% talc-15%fWS-hPP Composite (1000X)

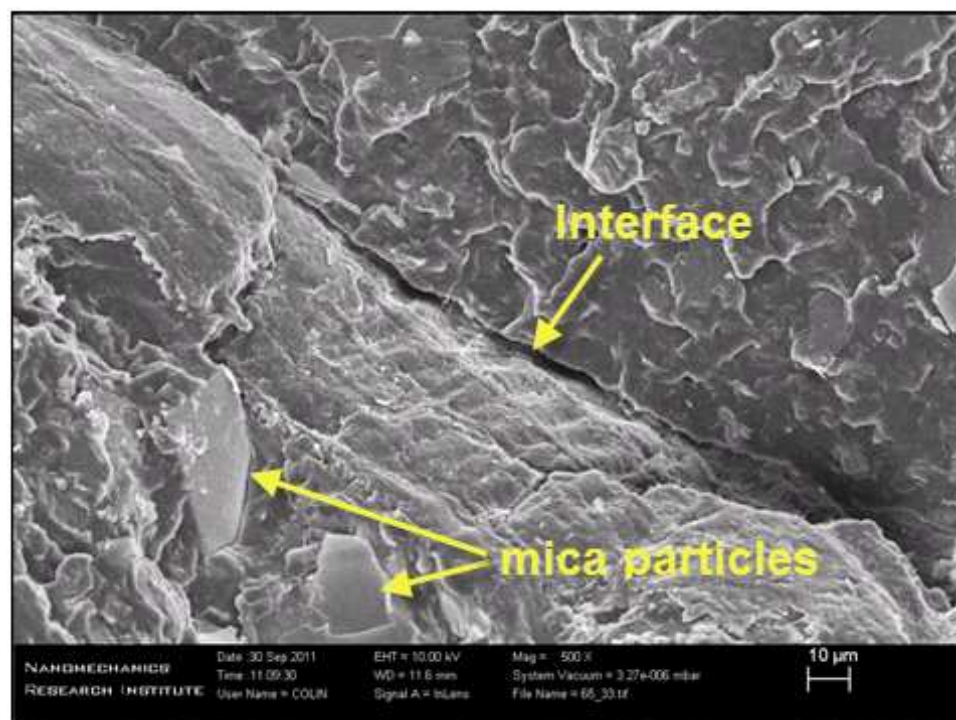


Figure 6.20 SEM of 15% mica-15%fWS-hPP Composite (500X)

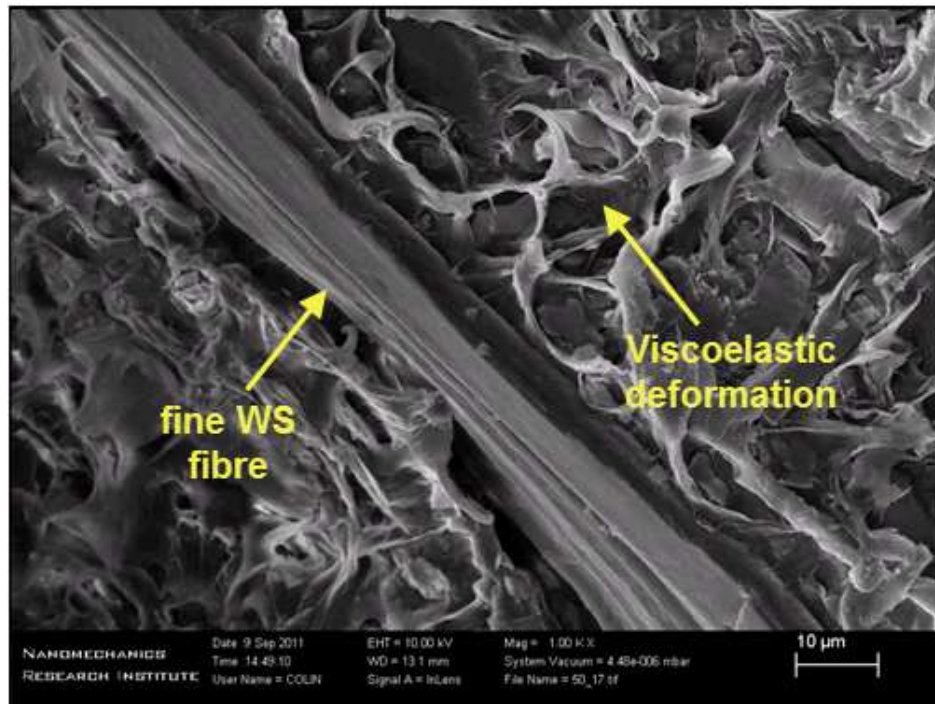


Figure 6.21 SEM of 15% talc-15%fWS-icPP Composite (1000X)

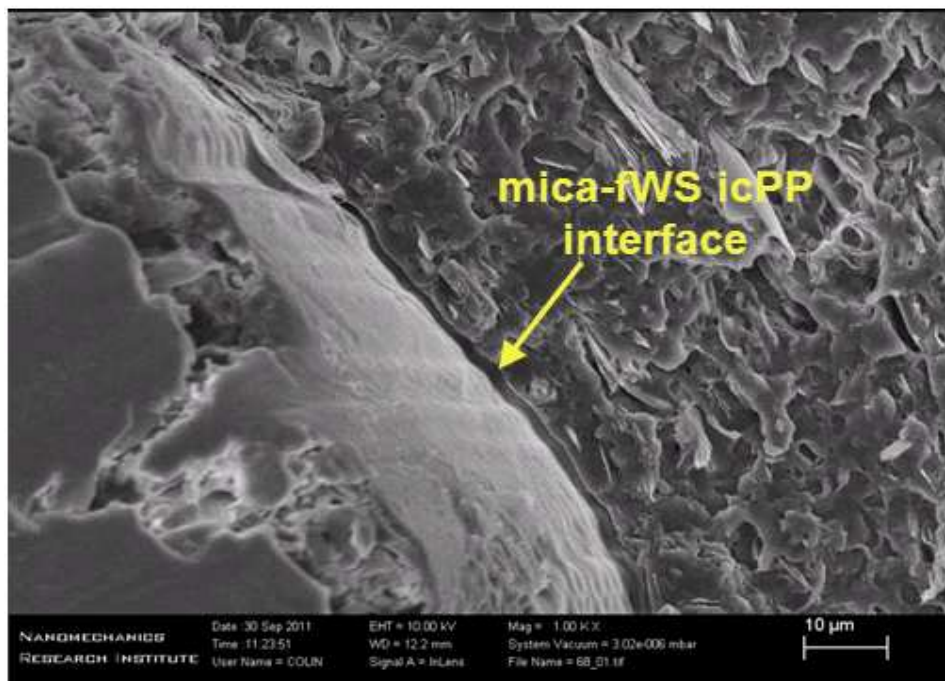


Figure 6.22 SEM of 15% mica-15%fWS-icPP Composite (500X)

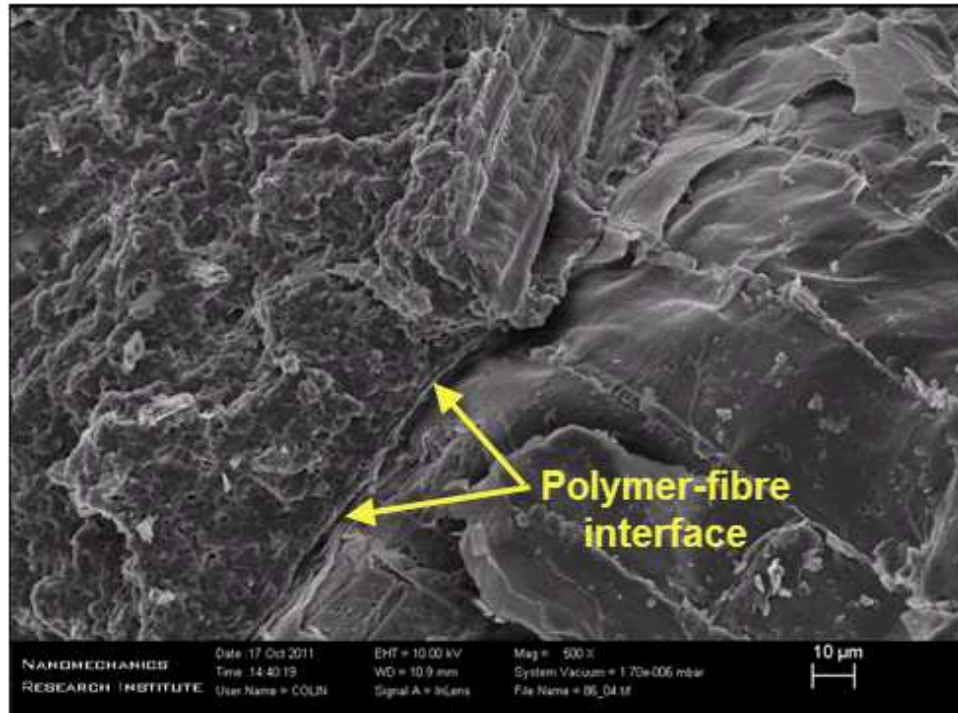


Figure 6.23 SEM of 15% wollastonite-15%fWS-icPP Composite (500X)

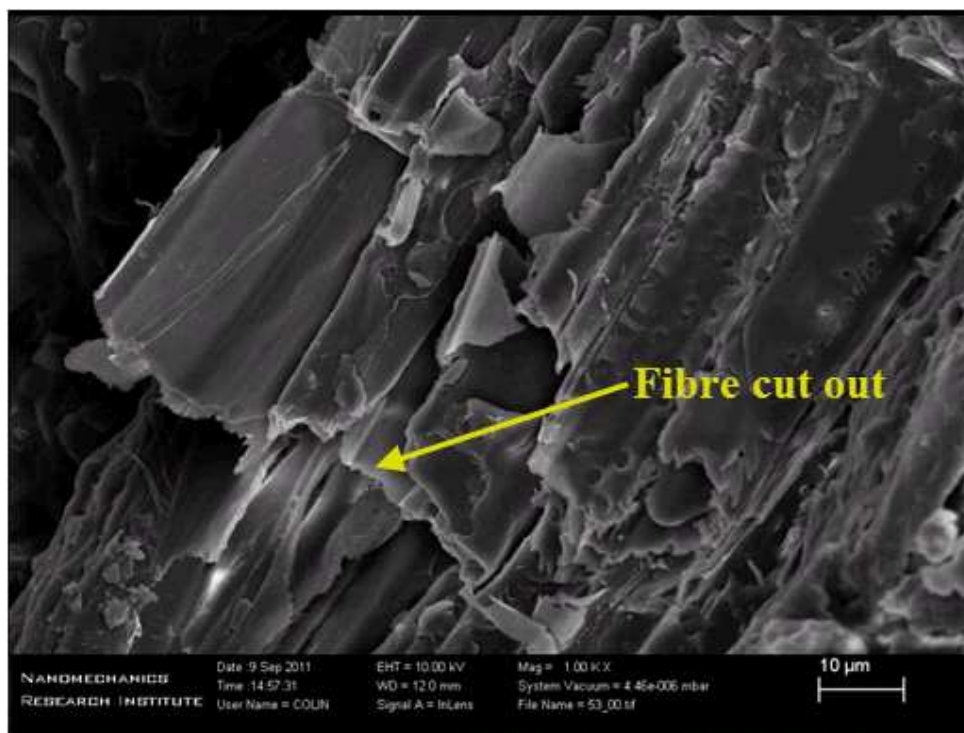


Figure 6.24 SEM of 15% talc-15%fWS-bPP Composite (1000X)

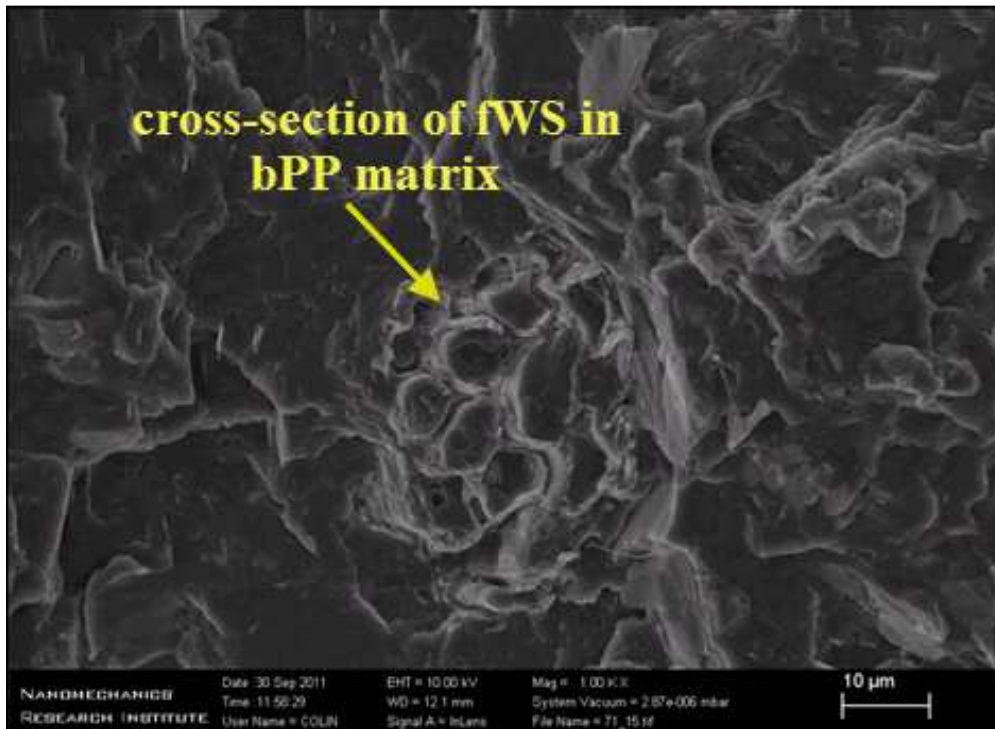


Figure 6.25 SEM of 15% mica-15%fWS-bPP Composite (1000X)

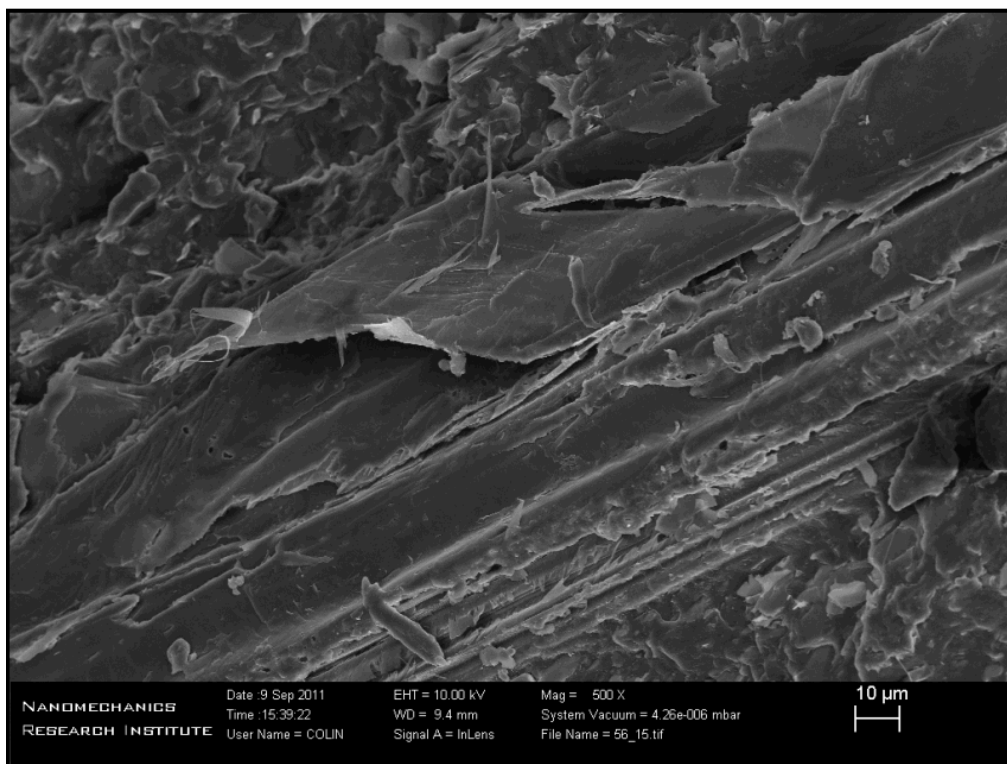


Figure 6.26 SEM of 15% talc-15% mWS-hPP Composite (500X)

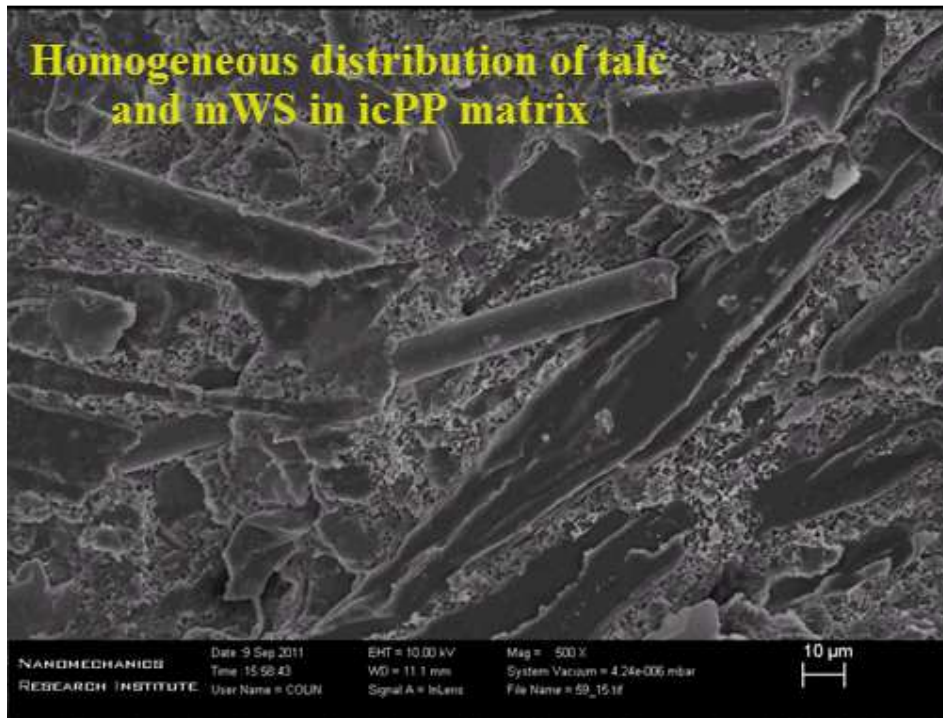


Figure 6.27 SEM of 15% talc-15% mWS-icPP Composite (500X)

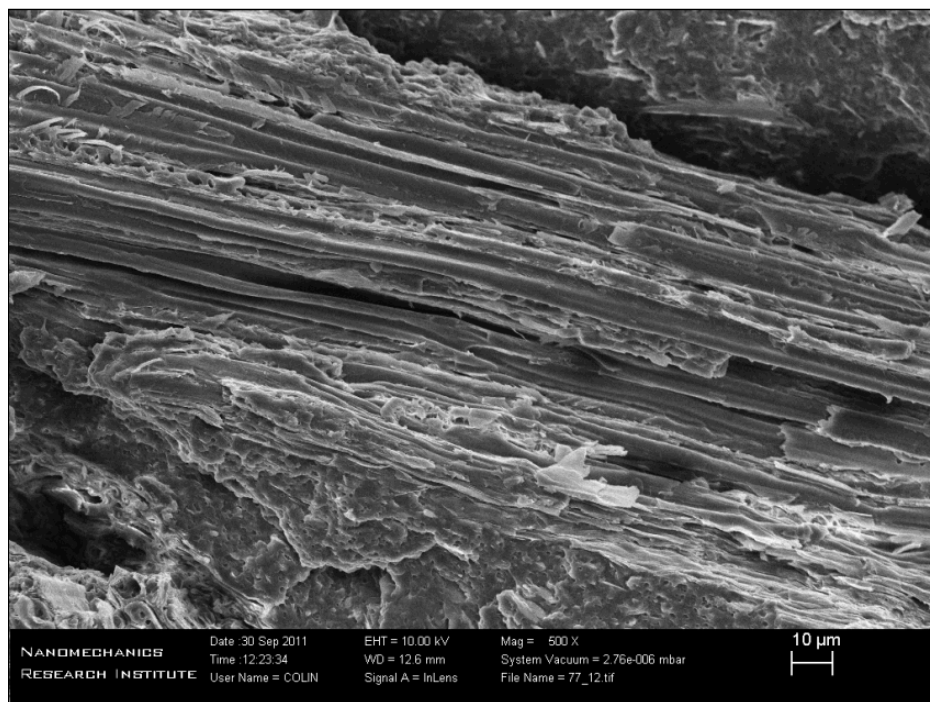


Figure 6.28 SEM of 15% mica-15% mWS-icPP Composite (500X)

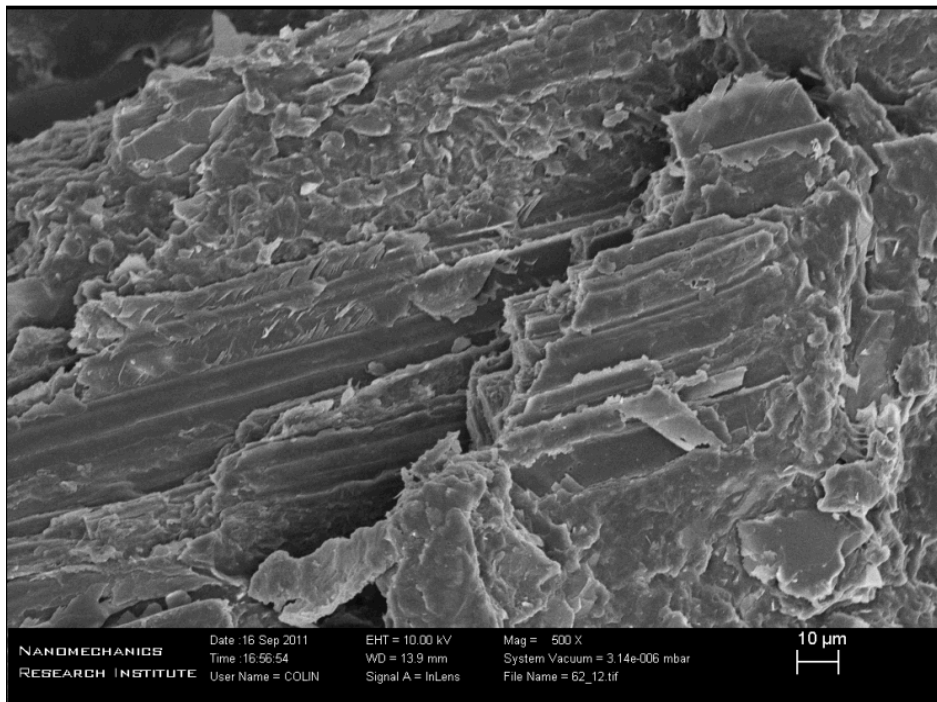


Figure 6.29 SEM of 15% talc-15% mWS-bPP Composite (500X)

6.1.8 WATER ABSORPTION

Water absorption plots for hybrid composites containing minerals and bio-fibers in homopolymer, copolymer and blend are represented in Figures 6.30 to 6.35. The test was conducted by keeping the total concentration of two fillers at 30 wt% while varying the content of each filler at 10/20, 15/15 and 20/10 wt%. The amount of antioxidant and coupling agent were kept constant. The evaluation of water absorption was limited to 35 weeks of exposure period due to time limitation to complete this document.

All hybrid composites absorbed more water than the pure resins as well as composites containing pure minerals. This observation is expected since the hybrid composites contain biofibres which are inherently hydrophilic in nature. It is also interesting to find that the rate of water absorption increased with increasing amounts of wheat straw (fine and medium) in all the composites.

Figure 6.30 represents the weight gain in homopolymer hybrid composites made talc/fWS, mica/fWS and wollastonite/fWS. The hPP with 10/20 wt% of talc/fWS gained a weight of 3.9%, three times that of 20/10 wt% talc/fWS composite after 35 weeks of exposure in water. It is

observed that the composites reached saturation at about 31 weeks. The percentage gain in weight is however significantly lower than pure fWS hPP composite at 30 wt% loading. Composites containing 20/10 and 10/20 wt% of mica/fWS also saturated in 31 weeks with a weight gain of 1.15% and 3.55% respectively at the end of 35 weeks. The hybrid composite with 20 wt% mica showed a water absorption value closer to the value for pure mica hPP composite at a content of 30 wt%. Wollastonite/fWS hPP composites did not saturate even after exposure for 35 weeks. It is interesting to note that the difference in weight gain for 20/10 and 15/15 loadings of wollastonite/fWS is smaller and that of 15/15 and 10/20 loadings is larger when compared to the mica or talc fWS hPP composites. Similar trend is observed with talc/mWS hPP composites as well (Figure 6.31). Here, the differences in weight gain between the three ratios of fillers are consistently same and smaller. The results indicate that hybridization did have a positive effect on water absorption property, due to the hybrid composites having relatively lower weight gain than pure mWS composite. Mica/mWS composites at 20/10 wt%, exhibited lower weight gain than talc/mWS composites at the same composition. With decreasing mica content and increasing mWS content, the composites gained more weight and at a higher rate than talc/mWS hPP composites. There is no sign of saturation for any of the combinations. The water absorption behaviour of wollastonite/mWS composites is observed to be closely related to that of talc/mWS composites. The composites gained 1.3%, 2.5% and 3.9% weight at 20/10, 15/15 and 10/20 wt% loadings of wollastonite/mWS respectively.

The differences in the percentage increase in weight for copolymer hybrid composites are smaller than the homopolymer hybrids (Figure 6.32). Like the homopolymer, the copolymer talc/fWS composites appear to have reached saturation at 31 weeks. The composite with 20/10 talc/fWS gained a weight of 1.4% with a gradual increase at higher loadings of fWS. Hybrid combination of talc and fWS at 10/20 wt% showed an increase in weight of 3.2% which is more than 150% lower than the weight gain exhibited by pure 30 wt% fWS copolymer composite. Mica and wollastonite mWS composites also displayed similar water absorption characteristics at varying percentages of the fillers. The mineral fWS impact copolymer did not show any significant variation in the property with varying mineral type. Figure 6.33 shows that talc/mWS icPP composite at 20/10 wt% gained a weight of 1.9%, three times lower than that of 10/20 wt% combination fillers, with small difference in weight gain between 20/10 and 10/20 wt% loadings.

In case of mica/mWS composites, the difference is quite larger. Wollastonite mWS composites also did not show any indication of saturation after immersing them in water for 35 weeks.

Like homopolymer and copolymer, blend also reached saturation in 31 weeks for the same filler combination of talc and fWS. Talc/fWS PP blend at 10/20 wt% showed a higher increase in weight of 4.4% in 35 weeks, compared to hPP and icPP hybrids. Also, the difference in weight gain for hybrid composites and pure fWS or mWS bPP composites are significantly larger. It can be observed that wollastonite/fWS bPP composite at 10/20 wt% loading has a weight gain of 6% higher than all the other filler combinations. The behaviour of talc/mWS bPP composites appear to be similar to that of wollastonite/fWS hPP composites with percentage weight gain of 1.7, 2.4 and 4.5% for 20/10, 15/15 and 10/20 wt% loadings respectively. The differences in weight gain for wollastonite/mWS bPP composites at varying percentages are smaller than that for mica/mWS bPP hybrid variety (Figure 6.35).

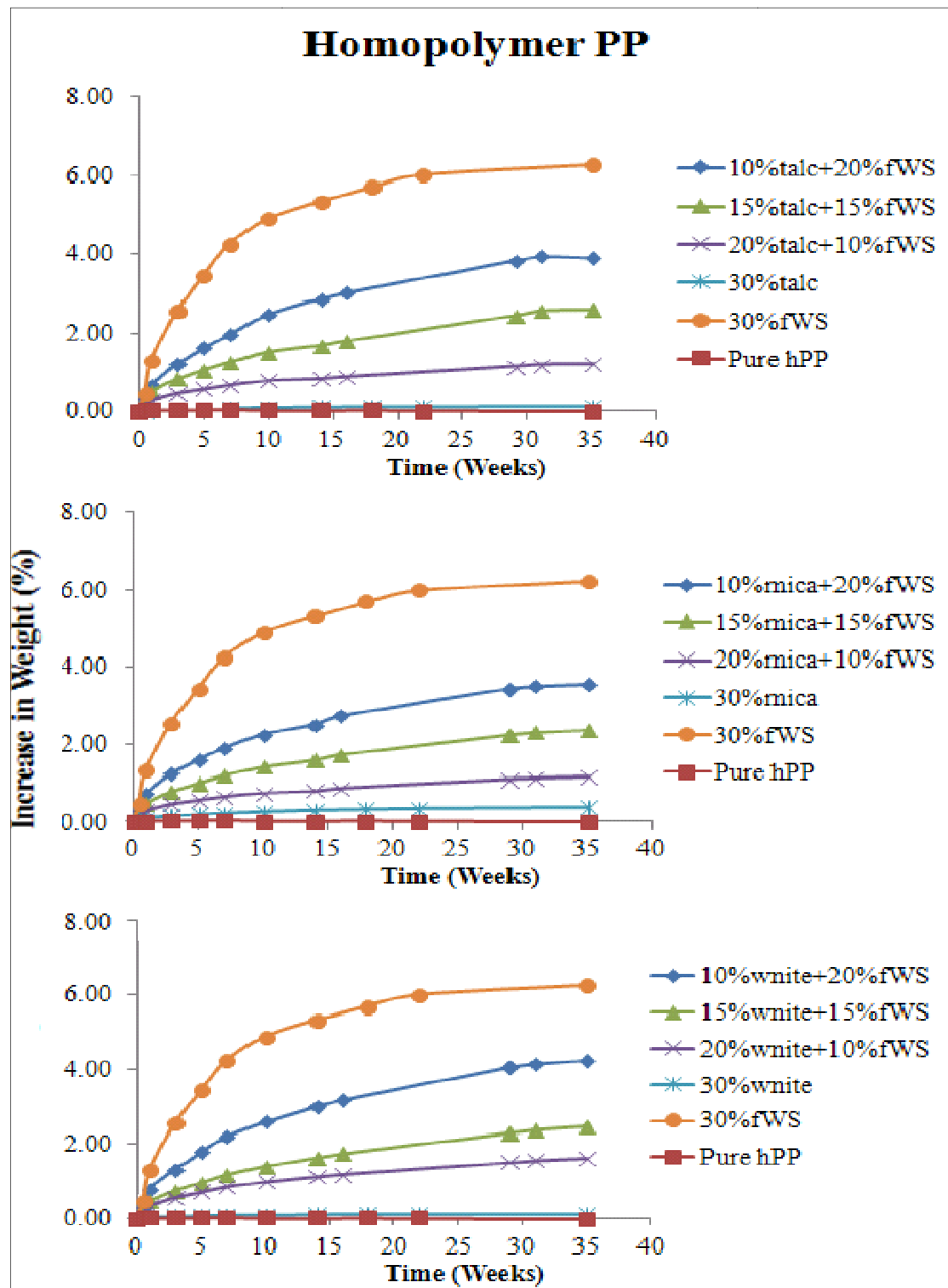


Figure 6.30 Water Absorption Plots for Mineral/fWS hPP Composites

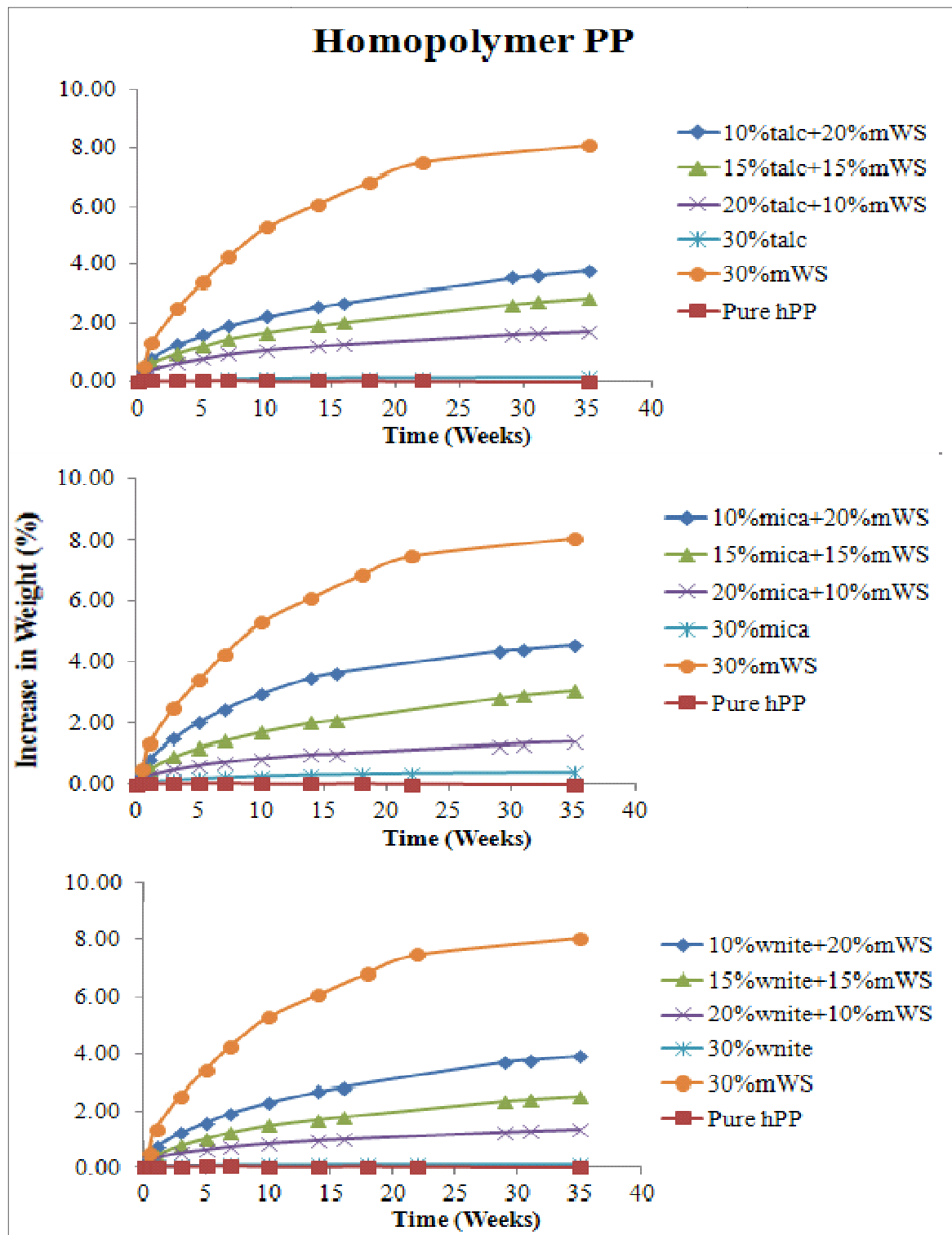


Figure 6.31 Water Absorption Plots for Mineral/mWS hPP Composites

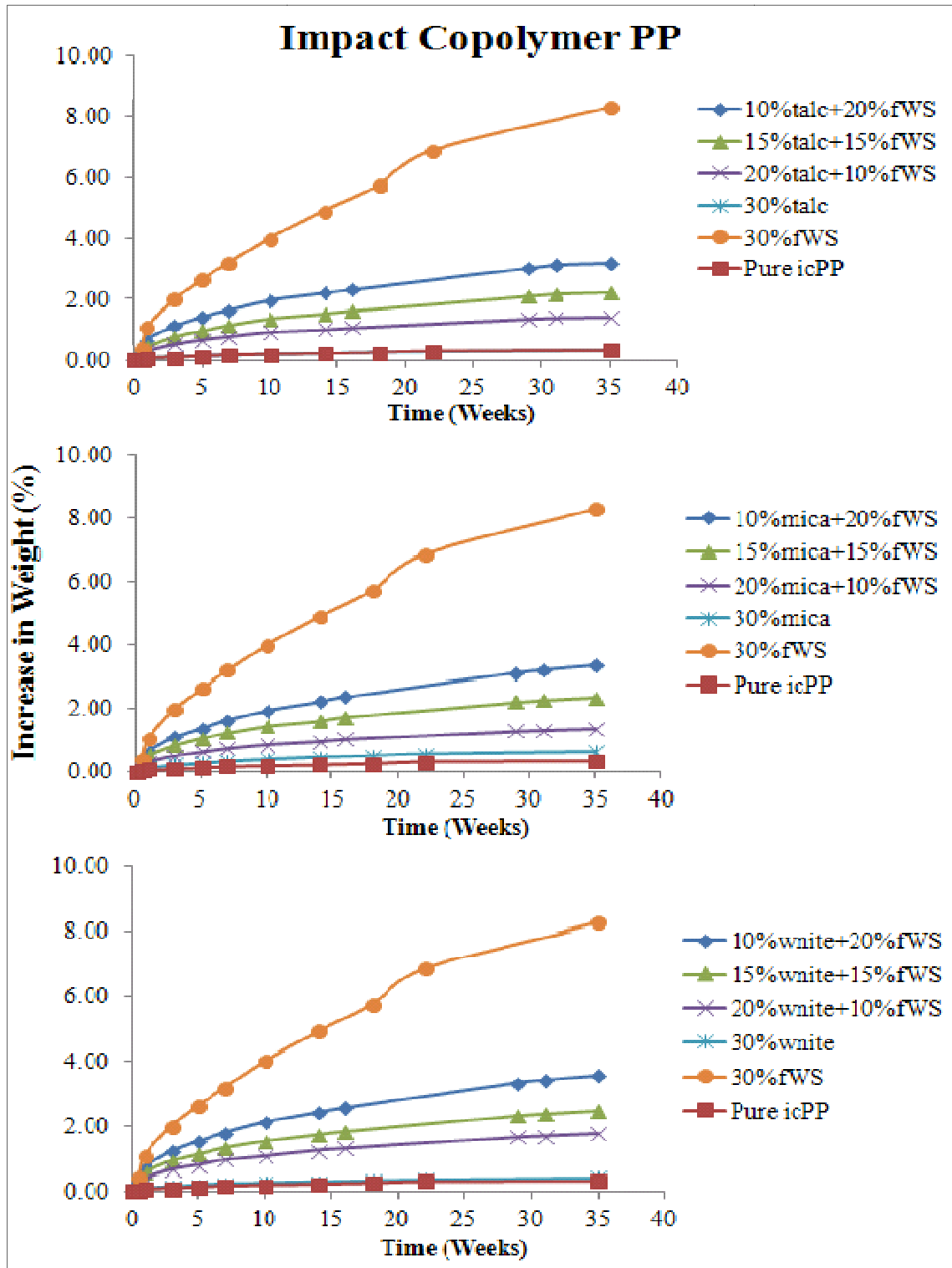


Figure 6.32 Water Absorption Plots for Mineral/fWS icPP Composites

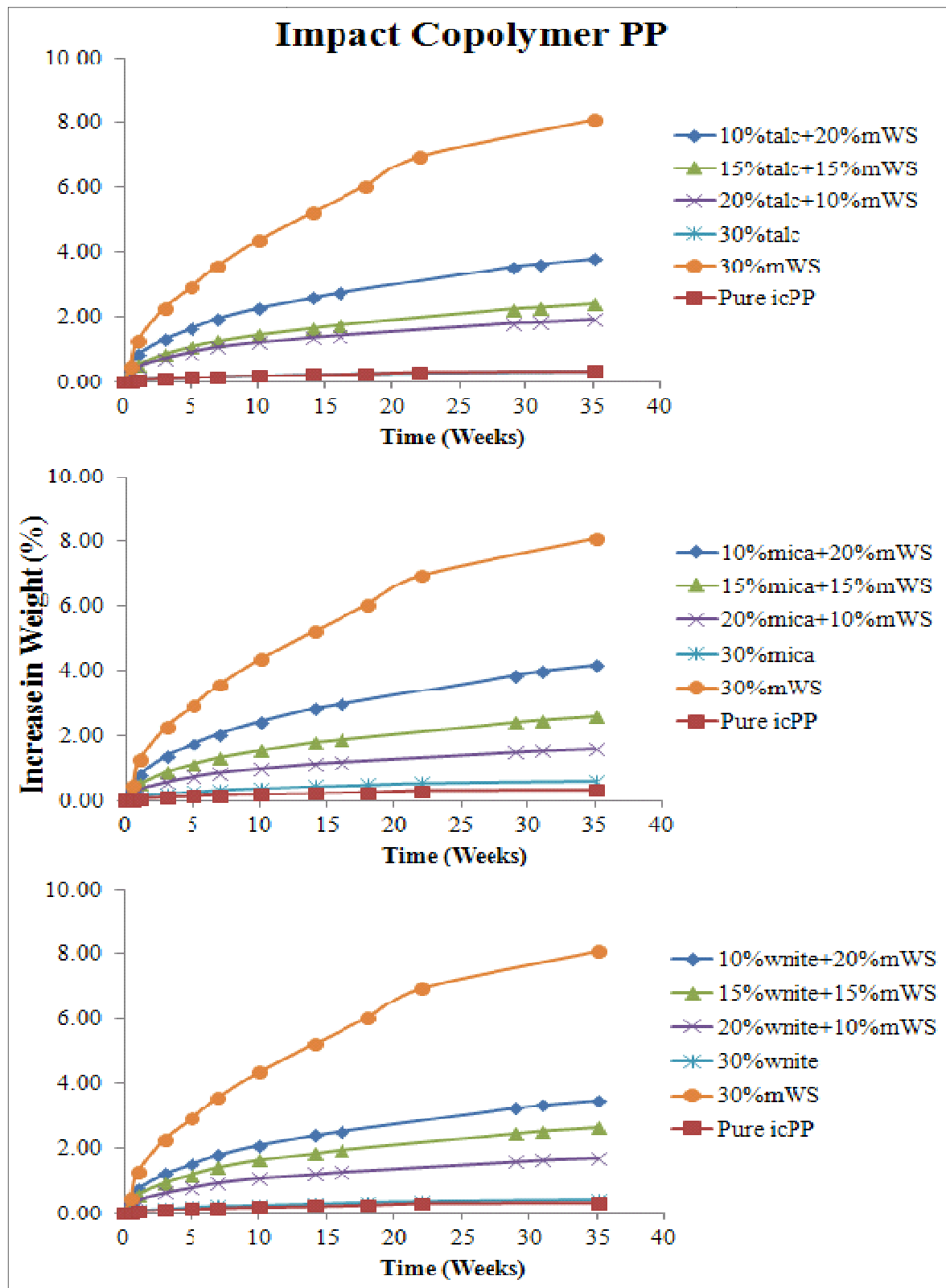


Figure 6.33 Water Absorption Plots for Mineral/*mWS* icPP Composites

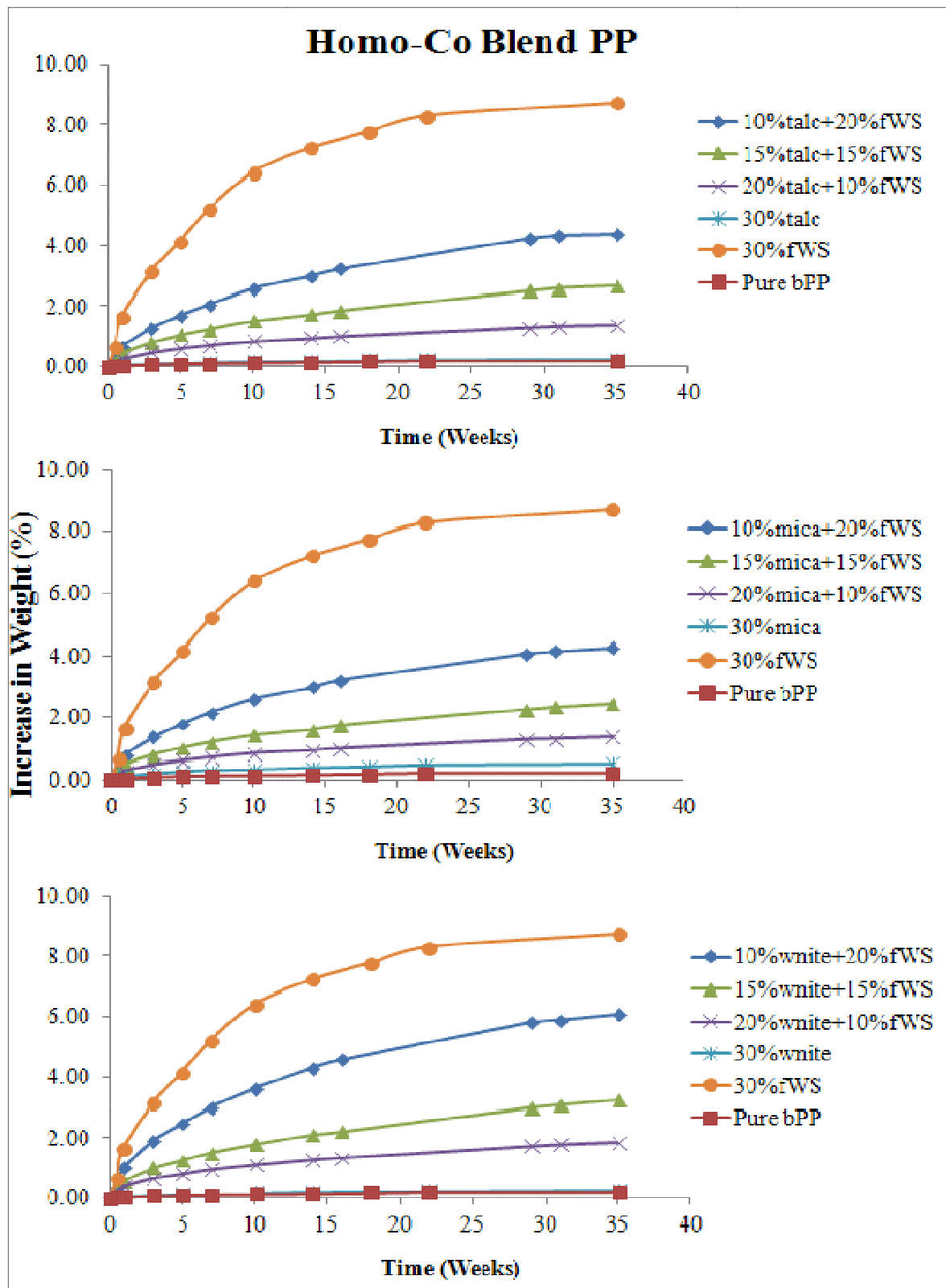


Figure 6.34 Water Absorption Plots for Mineral/fWS bPP Composites

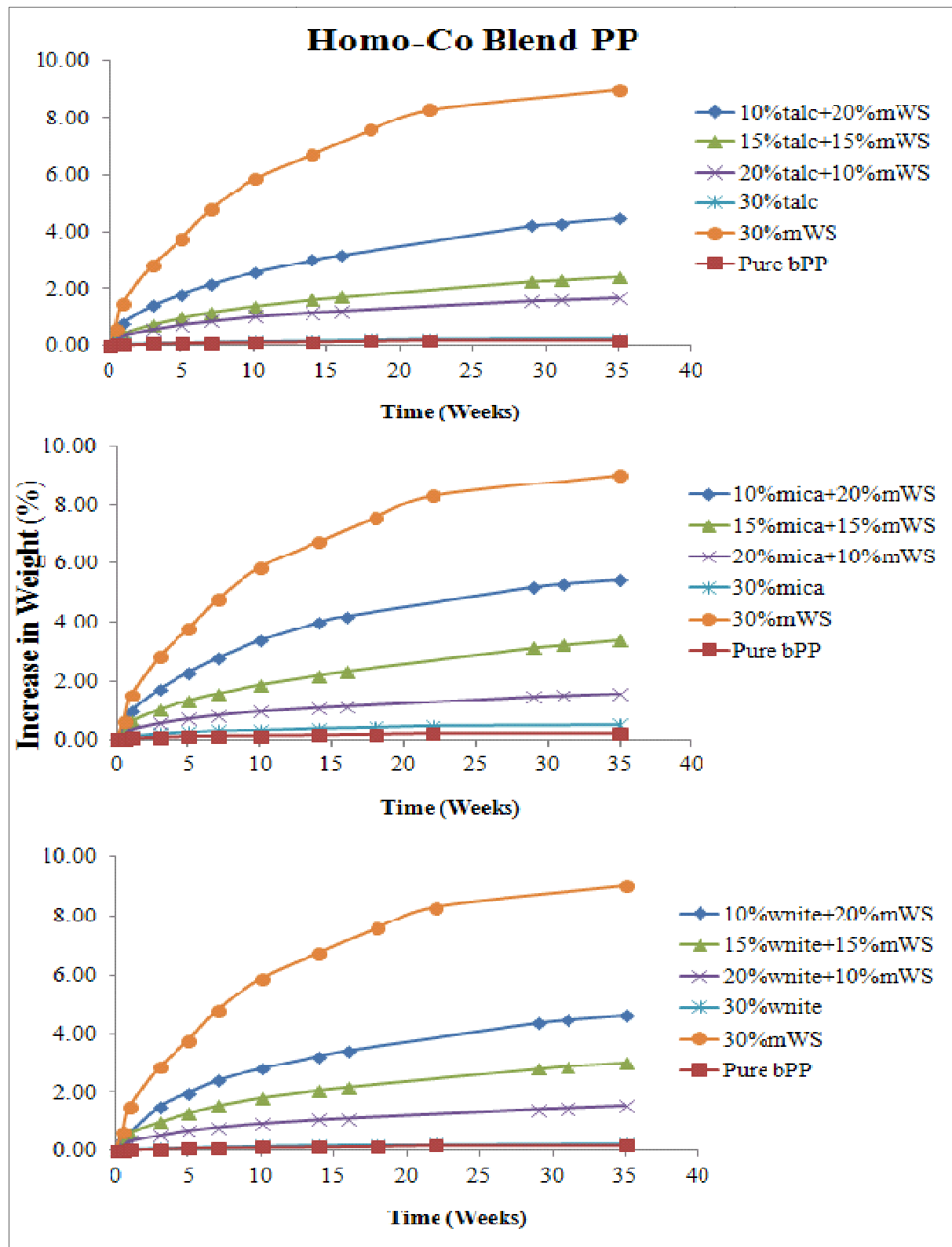


Figure 6.35 Water Absorption Plots for Mineral/mWS icPP Composites

7 CONCLUSIONS AND RECOMMENDATIONS

The mechanical properties and water absorption characteristics of polypropylene composites based on three different PP matrices and five types of fillers at varying filler concentrations were investigated. To the best of the author's knowledge, this is the first time that such comprehensive systematic evaluation was carried out. It allows for benchmarking the performance of wheat straw with three widely used mineral fillers (talc, mica and wollastonite) using three grades of polypropylene (homopolymer, high impact copolymer, and a blend).

The composite formulations were compounded using a co-rotating twin screw extruder and specimens were prepared using an injection mold. The tests revealed that there was a significant effect of filler type and filler content on the properties of homopolymer, copolymer and PP blend composites. The effect of varying loadings of multiple fillers (while keeping the total filler content constant at 30 wt%) on PP matrices was also investigated.

Wollastonite filled PP composites, irrespective of the matrix type, consistently showed higher improvement in flexural strength, flexural modulus, tensile strength and specific flexural modulus at 20, 30 and 40 wt% of loadings. The composite also exhibited enhancement in tensile modulus of homopolymer at 30 wt%. It can be concluded that the incorporation of talc improved the tensile modulus of homopolymer at 20 wt% loading and that of impact copolymer PP composite at all three loading levels. The blend of homopolymer and copolymer PP (bPP) showed positive effect on Young's modulus with the addition of fillers but did not show any dependence on the filler type. There was a significant drop in impact strength of the composites. However an interesting observation was made when the property increased with increasing percentage of wollastonite in homopolymer and at 40 wt% the impact strength of the composite was almost same as that of pure homopolymer. Though the mechanical properties of mica, fWS and mWS composites were enhanced, they did not show any promising results at higher concentrations.

The incorporation of wollastonite/fWS and wollastonite/mWS at 20/10 wt% loadings into the homopolymer matrix provided the highest enhancement in flexural strength, flexural modulus, tensile strength, tensile modulus, impact strength and specific flexural modulus of fWS-hPP and

mWS-hPP composites. The tensile modulus of mica/fWS-hPP at 20/10 wt% and mica/mWS-hPP at 15/15 wt% was also greater than that of pure mica hPP composite at 30 wt%. The same applies to the Young's modulus of talc/mWS at 20/10 wt% with respect to pure talc composite. The summary of formulations providing the best property achievements are summarized in Table 7.1.

The combination of talc and mWS showed highest flexural properties (flexural strength, modulus and specific property) for the talc filled copolymer PP at 10/20 wt% composition. The flexural strength of talc/fWS at 10/20 wt% is higher than pure talc composite whereas the tensile modulus of wollastonite/fWS is higher than 30 wt% wollastonite icPP composite. The 20/10 wt% combination of wollastonite/fWS enhanced the flexural modulus and impact strength of fWS-copolymer PP composite. Similar behaviour is observed with wollastonite/mWS hybrid at that same loadings as well with an exception that the hybrid composite also showed synergy to the impact strength of pure wollastonite icPP composite. The same composition also resulted in higher tensile modulus for wollastonite/mWS compared to pure wollastonite and mica/mWS compared to pure mica and mWS icPP composites. At 15/15 wt% loading, talc/fWS showed an increment in flexural modulus and specific flexural modulus of talc-icPP composite whereas talc/mWS showed synergy effects in impact strength property. At the same loading concentration with copolymer, mica/mWS enhanced the tensile strength of mica icPP composite whereas mica/fWS showed synergy with the tensile modulus of both pure mica and pure fWS composites at 30 wt% loading.

The PP blend composites again showed higher flexural strength, modulus and specific modulus at 15/15 wt% loading of mica/fWS compared to pure mica and pure fWS composites. Talc/mWS improved specific flexural modulus of talc composite whereas mica/mWS improved the tensile modulus of mica bPP composite. Like in homopolymer, the wollastonite/mWS hybrid at 20/10 wt% loading showed increment in flexural modulus and specific flexural modulus against pure mWS composite. At the same loading percentages, talc/mWS showed higher flexural modulus than pure talc bPP composite and higher tensile modulus than its single filler counterparts. Mica/fWS, wollastonite/fWS and talc/fWS improved the tensile modulus, impact strength and specific flexural modulus respectively. All the other formulations did not show synergy effect on

the properties. The hybrid formulations containing 10/20 wt% loadings of mineral/WS combinations were seen to be least beneficial for both homopolymer and blend PP.

The resistance to water absorption decreased with increasing percentage of fillers. Single filler composites based on fine WS and medium WS absorbed the maximum amount of water in a 35 weeks exposure period owing to their inherent hydrophilic nature. Among mineral composites, mica showed the least resistance to moisture, with a value significantly higher than pure resins. An interesting observation is that both talc and wollastonite based icPP and bPP composites showed a water absorption trend similar to that of pure copolymer and pure blend PP. In hybrid composites, the resistance to water absorption decreased with increasing WS (fine or medium) content in the matrix. It was observed that the difference in increase in weight gain with varying filler content was lower for copolymer PP. With hybridization, the water absorption tendency of WS composites could be greatly reduced.

SEM analysis on fWS and mWS single filler composites revealed that the interfacial interaction of the filler and the matrix did have a significant influence on the mechanical performance of the composites. The morphological study showed poor bonding of fillers with the copolymer matrix which can be related to the poor mechanical behaviour observed for icPP composites.

Table 7.1 Summary of Formulation-Property Relationship

Filler Combinations	Homopolymer PP	Impact Copolymer PP	Homo-Co Blend PP	Properties
Mineral/fWS	-Wnite/fWS at 20/10 wt% (compared to pure fWS composite)	-Talc/fWS at 10/20 wt% (compared to pure talc composite)	-Mica/fWS at 15/15 wt% (compared to pure fWS and mica composite)	Flexural Strength
Mineral/mWS	-Wnite/mWS at 20/10 wt% (compared to pure mWS composite)	-Talc/mWS at 10/20 wt% (compared to pure talc composite)		

Mineral/fWS	- Wnite/fWS at 20/10 wt% (compared to pure fWS composite)	- Wnite/fWS at 20/10 wt% (compared to pure fWS composite), - Talc/fWS at 15/15 wt% (compared to pure talc composite)	- Mica/fWS at 15/15 wt% (compared to pure fWS and mica composite)	Flexural Modulus
Mineral/mWS	- Wnite/mWS at 20/10 wt% (compared to pure mWS composite)	- Wnite/mWS at 20/10 wt% (compared to pure mWS composite), - Talc/mWS at 10/20 wt% (compared to pure talc composite)	- Wnite/mWS at 20/10 wt% (compared to pure mWS composite), - Talc/mWS at 20/10 wt% (compared to pure talc composite)	
Mineral/fWS	- Wnite/fWS at 20/10 wt% (compared to pure fWS composite)			Tensile Strength
Mineral/mWS	- Wnite/mWS at 20/10 wt% (compared to pure mWS composite)	- Mica/mWS at 15/15 wt% (compared to pure mica composite)		
Mineral/fWS	- Wnite/fWS at 20/10 wt% (compared to pure fWS composite), - Mica/fWS at 20/10 (compared to pure Mica composite)	- Mica/fWS at 15/15 wt% (compared to pure fWS and mica composite), - Wnite/fWS at 10/20 wt% (compared to pure wnite composite)	- Mica/fWS at 20/10 wt% (compared to pure fWS and mica composite)	Tensile Modulus
Mineral/mWS	- Wnite/mWS at 20/10 wt%	- Mica/mWS at 20/10 wt%	- Talc/mWS at 20/10 wt%	

	(compared to pure mWS composite), -Talc/mWS at 20/10 wt% (compared to pure talc composite), -Mica/mWS at 15/15 wt% (compared to pure mica composite)	(compared to pure mWS and mica composite), - Wnite/mWS at 20/10 wt% (compared to pure wnite composite)	(compared to pure mWS and talc composite), -Mica/mWS at 15/15 wt% (compared to pure mica composite)	
Mineral/fWS	- Wnite/fWS at 20/10 wt% (compared to pure fWS composite)	- Wnite/fWS at 20/10 wt% (compared to pure fWS composite),	- Wnite/fWS at 20/10 wt%	Impact Strength (decreased with the addition of fillers or multiple fillers)
Mineral/mWS		- Talc/mWS at 15/15 wt% (compared to pure talc composite), - Wnite/mWS at 20/10 wt% (compared to pure mWS and wnite composite)		
Mineral/fWS	- Wnite/fWS at 20/10 wt% (compared to pure fWS composite)	- Talc/fWS at 15/15 wt% (compared to pure talc composite)	- Mica/fWS at 15/15 wt% (compared to pure fWS and mica composite), -Talc/fWS at 20/10 wt% (compared to pure talc composite)	Specific Flexural Modulus
Mineral/mWS	- Wnite/mWS at 20/10 wt% (compared to pure mWS composite)	- Talc/mWS at 10/20 (compared to pure talc composite)	- Talc/mWS at 15/15 wt% (compared to pure talc composite), -Wnite/mWS at 20/10 wt% (compared to pure mWS composite)	

The results obtained in this study provide suggestions for future work in order to further analyze the properties of polypropylene composites. Some of them are:

1. Developing mechanical models to better understand and correlate each composite property and fitting those models with related literature data.
2. Studying the effect of filler particle size on PP composites.
3. Varying the type and amount of coupling agent in the composite formulations to study its effect on mechanical properties and water absorption.

REFERENCES

- ASTM International, 2008A, ASTM D 570-98, Standard Test Method for Water Absorption of Plastics.
- ASTM International, 2008B, ASTM D 792-08, Standard Test Methods for Density and Specific Gravity (Relative Density) of Plastics by Displacement.
- ASTM International, 2010A, ASTM D 256-10, Standard Test Methods for Determining the Izod Pendulum Impact Resistance of Plastics.
- ASTM International, 2010B, ASTM D 790-10, Standard Test Methods for Flexural properties of Unreinforced and Reinforced Plastics and Electrical Insulating Materials.
- ASTM International, 2010C, ASTM D 1708-10, Standard Test Method for Tensile Properties of Plastics by use of Microtensile Specimens.
- Bledzki, A.K., Sperber, V.E. and Faruk, O., 2002, *Natural and wood fibre reinforcement in polymers*, Report 152, Rapra Review reports, Rapra Technology Ltd., **13**, Number 8.
- Brydson, J. A., 1999, *Plastics materials*, 7th edition, Butterworth Heinemann, MA.
- CABOT, 'Melt Flow Index', Cabot Corporation, MA, USA.
- Calhoun, A. and Peacock, A.J., 2006, *Polymer chemistry: properties and applications*, Carl Hanser Verlag, Munich.
- Callister, W.D., 2001, *Fundamentals of materials science and engineering: an interactive e.Text*, 5th edition, John Wiley & Sons Inc., NY.
- Chen, M., Wan, C., Shou, W., Zhang, Y., Zhang, Y. and Zhang, J., 2008, 'Effects of interfacial adhesion on properties of polypropylene/wollastonite composites', *Journal of Applied Polymer Science*, **107**, pp.1718-1723.
- Clemons, C.M. and Caulfield, D.F., 2005, *Natural Fibers*, in Functional Fillers for Plastics (ed M. Xanthos), Wiley-VCH Verlag GmbH & Co. KGaA, Weinheim, pp. 195-205.

- Cui, Y.H., Tao, J., Noruziaan, B., Cheung, M. and Lee, S., 2010, 'DSC analysis and mechanical properties of wood plastic composites', *Journal of Reinforced Plastics and Composites*, **29**, pp. 278-289.
- Digabel, F.L., Boquillon, N., Dole, P., Monties, B. and Averous, L., 2004, 'Properties of thermoplastic composites based on wheat-straw lignocellulosic fillers', *Journal of Applied polymer Science*, **93**, pp. 428-436.
- Drake, N., 1998, *Thermoplastics and thermoplastic composites in the automotive industry 1997-2000*, Rapra Industry Analysis Report Series, Rapra Technology Limited, UK.
- El-Midany, A.A. and Ibrahim, S.S., 2011, 'Interfacial role of compatibilizers to improve mechanical properties of silica polypropylene composites', *Physiochemical Problems of Mineral Processing*, **46**, pp. 295-305.
- Eroglu, M., 2007, 'Effect of talc and heat treatment on the properties of polypropylene/EVA composites', *International Journal of Science and Technology*, **2**, pp. 63-73.
- Frank, H.P., 1968, *Polypropylene*, 1st edition, Gordon and Breach Science Publishers, NY.
- Gao, F., 2004, 'Clay/Polymer composites: the story', *Materialstoday*, **7**, pp. 50-55.
- Güttler, B. E., 2009, 'Soy-polypropylene biocomposites for automotive applications', University of Waterloo, Ontario, Canada.
- Hancock, M. and Rethon, R.N., 2003, *Principal types of particulate fillers*, in *Particulate Filled Polymer Composites*, 2nd edition, Smithers Rapra Technology, pp. 53-100.
- Jahani Y., 2010, 'Dynamic rheology, mechanical performance, shrinkage, and morphology of chemically coupled talc-filled polypropylene', *Journal of Vinyl and Additive Technology*, **16**, pp. 70-77.
- Jahani, Y., 2011, 'Comparison of the effect of mica and talc and chemical coupling on the rheology, morphology, and mechanical properties of polypropylene composites', *Polymers for Advanced Technologies*, **22**, pp. 942-950.

Joseph, K., Varghese, S., Kalaprasad, G., Thomas, S., Prasannakumari, L., Koshy, P. and Pavithran, C., 1996, 'Influence of interfacial adhesion on the mechanical properties and fracture behaviour of short sisal fibre reinforced polymer composites', *European Polymer Journal*, **32**, pp. 1243-1250.

Karger-Kocsis, J., 1995A, *Polypropylene structure, blends and composites: Composites*, **3**, 1st edition, Chapman & Hall, London.

Karger-Kocsis, J., 1995B, *Polypropylene structure, blends and composites: Copolymers and blends*, **2**, 1st edition, Chapman & Hall, London.

Karian, H.G., 1999, *Handbook of polypropylene and polypropylene composites*, 2nd edition, Marcel Dekker, Inc., NY.

Karnani, R., Krishnan, M. and Narayanan, R., 1997, 'Bio-fibre reinforced polypropylene composites', *Polymer Engineering and Science*, **37**, pp. 476-483.

Kastner, E., Nardin, M. and Papirer, E., 1988, 'Coupling of mica as filler in polypropylene', *Journal of Materials Science Letters* **7**, pp. 955-957.

Koç, E. and Demiryürek, O., 2009, 'Design basis and hydrodynamic performance analysis of single-screw extruders I – polymer flow behaviour', *Industrial Lubrication and Tribology*, **61**, pp.188 – 196.

Krüger, P.K., 2007, 'Wheat straw - polypropylene composites', University of Waterloo, Ontario, Canada.

Lapcik, L. Jr., Jindrova, P., Lapcikova, B., Tamblyn, R., Greenwood, R. and Rowson, N., 2008, 'Effect of talc filler content on the mechanical properties of polypropylene composites', *Journal of Applied Polymer Science*, **110**, pp. 2742-2747.

Leong, Y.W., Abu Bakar, M.B., Mohd. Ishak, Z. A., Ariffin, A. and Pukanszky, B., 2004, 'Comparison of the mechanical properties and interfacial interactions between talc, kaolin and calcium carbonate filled polypropylene composites', *Journal of Applied Polymer Science*, **91**, pp. 3315-3326.

LongMold Technology Co. Ltd., 2009, "Injection molding of thermoplastics", viewed 10 March 2012, <www.longmold.com/viewnews.php?id=87>

Maier, C. and Calafut, T., 1998, *Polypropylene: The definitive user's guide and databook*, Plastics Design Library, Norwich, NY.

Maiti, S.N. and Sharma, K.K., 1992, 'Studies on polypropylene composites filled with talc particles', *Journal of Materials Science*, **27**, pp. 4605-4613.

Maritomi, S., Watanabe, T., Kanzaki, S., 2010, *Polypropylene compounds for automotive applications*, Sumitomo Kagaku 2010-I, Technical Report, pp. 1-16.

Dr. McKean, W.T. and Jacobs, R.S., 1997, *Wheat straw as a paper fibre source*, The Clean Washington Centre, Seattle and Domtar Inc., University of Washington, Technical Report.

Mengelloglu, F., and Karakus, K., 2008, 'Thermal degradation, mechanical properties and morphology of wheat straw flour filled recycled thermoplastic composites', *Sensors*, **8**, pp. 500-519.

Mohanty, A.K. (ed.), Misra, M. (ed.) and Drzal, L.T. (ed.), 2005, *Natural fibers, biopolymers, and biocomposites*, 1st edition, CRC Press, NW.

Moore, E.P., 1996, *Polypropylene handbook : polymerization, characterization, properties, processing, application*, 1st edition, Hanser Gardner Publications, NY.

Mussig, J., 2010, *Industrial applications of natural fibres: Structure, properties and technical applications*, 1st edition, John Wiley & Sons Ltd., UK.

Nielson, L.E., 1974, *Mechanical properties of polymers and composites*, Marcel Dekker, Inc., NY, vol. **2**.

Nwabunma, D. and Kyu, T., 2008, *Polyolefin composites*, 1st edition, Wiley-Interscience, NJ.

Prof. Pandey, P.C., 2004, *Composite materials*, Web based course material, IISC Bangalore.

Poucke, J.V. and James, A., 2006, *Long glass fibre technology for automotive applications*, Dow Automotive, SPE Automotive Composites Conference 2006.

Racine, G., 2010, 'Composites in Automotive', American Composites Manufacturers Association, Washington DC, video presentation.

Rana, A.K., Mandal, A., Mitra, B.C., Jacobson, R., Rowell, R. and Banerjee, A.N., 1998, 'Short jute fibre reinforced polypropylene composites: Effect of compatibilizer', *Journal of Applied Polymer Science*, **69**, pp. 329-338.

Reddy, C.R., Sardhashti, A. and Simon, L.C., 2010, 'Preparation and characterization of polypropylene-wheat straw-clay composites', *Composites Science and Technology*, **70**, pp. 1674-1680.

Robinson, S., 2006, *High performance fillers 2006, wollastonite: strength in legacy*, R.T. Vanderbilt Company Inc., Technical Report.

Rosato, D.V., Rosato, A.V. and Di Mattia, D.P., 2004, *Blow molding handbook*, 2nd edition, Carl Hanser Verlag, Munich.

Rosato, D.V., Rosato, D.V., Rosato, M.G. and Schott, N.R., 2001, *Plastics Engineering, Manufacturing & Data Handbook*, **1**, Kluwer Academic Publishers, Boston.

Rothon, R.N., 1999, 'Mineral fillers in thermoplastics: Filler manufacture and characterization', *Advances in Polymer Science*, **139**, pp. 69-107

Rothon, R.N. and Hancock, M., 2003, *General Principles Guiding Selection and Use of Particulate Materials*, in *Particulate Filled Polymer Composites*, 2nd edition, Smithers Rapra Technology, pp. 5-51.

Rowell, R.M., Tillman, A.M., Simonson, R., 1986, 'A simplified procedure for the acetylation of hardwood and softwood flaxes for flakeboard production', *Journal of Wood Chemistry and Technology*, **6**, pp. 427-448.

Rowell, R.M., 2007, 'Challenges in biomass-thermoplastic composites', *Journal of Polymers and the Environment*, **15**, pp. 229-235.

"SABIC's molded automotive applications bags awards at 2011 SPE automotive innovation", *Plastic News*, **49**, Issue 12, 2011, pp. 88.

Sannigrahi, P., Pu, Y. and Ragauskas, A., 2010, 'Cellulosic biorefineries—unleashing lignin opportunities', *Current Opinion in Environmental Sustainability*, **2**, pp. 383-393.

Sardhashti, A., 2009, 'Wheat straw clay polypropylene hybrid composites', University of Waterloo, Ontario, Canada.

Sarkar, M., Dana, K., Ghatak, S. and Banerjee, A., 2008, 'Polypropylene–clay composite prepared from Indian bentonite', *Bull. Mater. Sci.*, vol. 31, pp. 23-28.

Seymour, R.B., 1990, *New concepts in polymer science: Polymer composites*, VSP BV, Netherlands.

Shen, J., Ji, G., Hu, B. and Huang, Y., 1993, 'Effect of filler size and surface treatment on impact and rheological properties of wollastonite-polypropylene composite', *Journal of Materials Science Letters* **12**, pp. 1344-1345.

Švab, I., Musil, V. and Leskovac, M., 2005, 'The adhesion phenomena in polypropylene/wollastonite composites', *Acta Chim. Slov.*, **52**, pp. 264-271.

Tajvidi, M. and Ebrahimi, G., 2003, 'Water uptake and mechanical characteristics of natural filler-polypropylene composites', *Journal of Applied Polymer Science*, **88**, pp. 941-946.

"Thermoforming", CustomPartNet, 2008, viewed 10 March 2012, <www.custompartnet.com/wu/thermoforming>

Thomas, S. and Pothan, L., 2009, *Natural fibre reinforced polymer composites—from macro to nanoscale*, 1st edition, Old City Publishing Inc., USA.

Vasile, C. (ed.) and Kulshreshtha, A.K. (ed.), 2003, *Handbook of polymer blends and composites*, **3A**, Rapra Technology Ltd., UK.

White, J.L. and Choi, D.D., 2004, *Polyolefins: processing, structure development, and properties*, Carl Hanser Verlag, Munich.

Wypych, G., 1993, *Fillers*, ChemTec Publishing, Canada.

Zhang, J.G., Jiang, D.D. and Wilkie, C.A., 2005, 'Polyethylene and polypropylene nanocomposites based upon an oligomerically modified clay', *Thermochemica Acta*, **430**, pp. 107-113.

Zhang, Y., Gu, J., Tan, H., Di, M., Zhu, L. and Weng, X., 2011, 'Straw based particle board bonded with composite adhesives', *BioResources*, **6**, pp. 464-476.

Zihlif, A.M., 1991, 'Mechanical properties of talc-polypropylene composites', *Materials Letters*, **11**, number 10, 11, 12.

Zweifel, H., 2001, *Plastics additives handbook*, 5th edition, Carl Hanser Verlag, Munich.

PERMISSIONS PAGE

ELSEVIER LICENSE TERMS AND CONDITIONS

May 17, 2012

This is a License Agreement between Arathi Mohan Sharma ("You") and Elsevier ("Elsevier") provided by Copyright Clearance Center ("CCC"). The license consists of your order details, the terms and conditions provided by Elsevier, and the payment terms and conditions.

All payments must be made in full to CCC. For payment instructions, please see information listed at the bottom of this form.

Supplier	Elsevier Limited The Boulevard, Langford Lane Kidlington, Oxford, OX5 1GB, UK
Registered Company Number	1982084
Customer name	Arathi Mohan Sharma
Customer address	6 Brookfield Cres Kitchener, ON N2E0A7
License number	2910281251004
License date	May 15, 2012
Licensed content publisher	Elsevier
Licensed content publication	Current Opinion in Environmental Sustainability
Licensed content title	Cellulosic biorefineries—unleashing lignin opportunities
Licensed content author	Poulomi Sannigrahi, Yunqiao Pu, Arthur Ragauskas
Licensed content date	December 2010
Licensed content volume number	2
Licensed content issue number	5–6
Number of pages	11
Start Page	383
End Page	393
Type of Use	reuse in a thesis/dissertation
Portion	figures/tables/illustrations
Number of figures/tables/illustrations	1
Format	both print and electronic

Are you the author of this Elsevier article?	No
Will you be translating?	No
Order reference number	
Title of your thesis/dissertation	Mechanical behaviour, water absorption and morphology of wheat straw, talc, mica and wollastonite filled polypropylene composites
Expected completion date	Aug 2012
Estimated size (number of pages)	150
Elsevier VAT number	GB 494 6272 12
Permissions price	0.00 USD
VAT/Local Sales Tax	0.0 USD / 0.0 GBP
Total	0.00 USD
Terms and Conditions	

INTRODUCTION

1. The publisher for this copyrighted material is Elsevier. By clicking "accept" in connection with completing this licensing transaction, you agree that the following terms and conditions apply to this transaction (along with the Billing and Payment terms and conditions established by Copyright Clearance Center, Inc. ("CCC"), at the time that you opened your Rightslink account and that are available at any time at <http://myaccount.copyright.com>).

GENERAL TERMS

2. Elsevier hereby grants you permission to reproduce the aforementioned material subject to the terms and conditions indicated.

3. Acknowledgement: If any part of the material to be used (for example, figures) has appeared in our publication with credit or acknowledgement to another source, permission must also be sought from that source. If such permission is not obtained then that material may not be included in your publication/copies. Suitable acknowledgement to the source must be made, either as a footnote or in a reference list at the end of your publication, as follows:

“Reprinted from Publication title, Vol /edition number, Author(s), Title of article / title of chapter, Pages No., Copyright (Year), with permission from Elsevier [OR APPLICABLE SOCIETY COPYRIGHT OWNER].” Also Lancet special credit - “Reprinted from The Lancet, Vol. number, Author(s), Title of article, Pages No., Copyright (Year), with permission from Elsevier.”

4. Reproduction of this material is confined to the purpose and/or media for which permission is hereby given.

5. Altering/Modifying Material: Not Permitted. However figures and illustrations may be altered/adapted minimally to serve your work. Any other abbreviations, additions, deletions and/or

any other alterations shall be made only with prior written authorization of Elsevier Ltd. (Please contact Elsevier at permissions@elsevier.com)

6. If the permission fee for the requested use of our material is waived in this instance, please be advised that your future requests for Elsevier materials may attract a fee.

7. Reservation of Rights: Publisher reserves all rights not specifically granted in the combination of (i) the license details provided by you and accepted in the course of this licensing transaction, (ii) these terms and conditions and (iii) CCC's Billing and Payment terms and conditions.

8. License Contingent Upon Payment: While you may exercise the rights licensed immediately upon issuance of the license at the end of the licensing process for the transaction, provided that you have disclosed complete and accurate details of your proposed use, no license is finally effective unless and until full payment is received from you (either by publisher or by CCC) as provided in CCC's Billing and Payment terms and conditions. If full payment is not received on a timely basis, then any license preliminarily granted shall be deemed automatically revoked and shall be void as if never granted. Further, in the event that you breach any of these terms and conditions or any of CCC's Billing and Payment terms and conditions, the license is automatically revoked and shall be void as if never granted. Use of materials as described in a revoked license, as well as any use of the materials beyond the scope of an unrevoked license, may constitute copyright infringement and publisher reserves the right to take any and all action to protect its copyright in the materials.

9. Warranties: Publisher makes no representations or warranties with respect to the licensed material.

10. Indemnity: You hereby indemnify and agree to hold harmless publisher and CCC, and their respective officers, directors, employees and agents, from and against any and all claims arising out of your use of the licensed material other than as specifically authorized pursuant to this license.

11. No Transfer of License: This license is personal to you and may not be sublicensed, assigned, or transferred by you to any other person without publisher's written permission.

12. No Amendment Except in Writing: This license may not be amended except in a writing signed by both parties (or, in the case of publisher, by CCC on publisher's behalf).

13. Objection to Contrary Terms: Publisher hereby objects to any terms contained in any purchase order, acknowledgment, check endorsement or other writing prepared by you, which terms are inconsistent with these terms and conditions or CCC's Billing and Payment terms and conditions. These terms and conditions, together with CCC's Billing and Payment terms and conditions (which are incorporated herein), comprise the entire agreement between you and publisher (and CCC) concerning this licensing transaction. In the event of any conflict between your obligations established by these terms and conditions and those established by CCC's Billing and Payment terms and conditions, these terms and conditions shall control.

14. Revocation: Elsevier or Copyright Clearance Center may deny the permissions described in this License at their sole discretion, for any reason or no reason, with a full refund payable to you. Notice of such denial will be made using the contact information provided by you. Failure to receive

such notice will not alter or invalidate the denial. In no event will Elsevier or Copyright Clearance Center be responsible or liable for any costs, expenses or damage incurred by you as a result of a denial of your permission request, other than a refund of the amount(s) paid by you to Elsevier and/or Copyright Clearance Center for denied permissions.

LIMITED LICENSE

The following terms and conditions apply only to specific license types:

15. **Translation:** This permission is granted for non-exclusive world **English** rights only unless your license was granted for translation rights. If you licensed translation rights you may only translate this content into the languages you requested. A professional translator must perform all translations and reproduce the content word for word preserving the integrity of the article. If this license is to re-use 1 or 2 figures then permission is granted for non-exclusive world rights in all languages.

16. **Website:** The following terms and conditions apply to electronic reserve and author websites:
Electronic reserve: If licensed material is to be posted to website, the web site is to be password-protected and made available only to bona fide students registered on a relevant course if:
This license was made in connection with a course,
This permission is granted for 1 year only. You may obtain a license for future website posting,
All content posted to the web site must maintain the copyright information line on the bottom of each image,
A hyper-text must be included to the Homepage of the journal from which you are licensing at <http://www.sciencedirect.com/science/journal/xxxxx> or the Elsevier homepage for books at <http://www.elsevier.com> , and
Central Storage: This license does not include permission for a scanned version of the material to be stored in a central repository such as that provided by Heron/XanEdu.

17. **Author website** for journals with the following additional clauses:

All content posted to the web site must maintain the copyright information line on the bottom of each image, and
the permission granted is limited to the personal version of your paper. You are not allowed to download and post the published electronic version of your article (whether PDF or HTML, proof or final version), nor may you scan the printed edition to create an electronic version,
A hyper-text must be included to the Homepage of the journal from which you are licensing at <http://www.sciencedirect.com/science/journal/xxxxx> , As part of our normal production process, you will receive an e-mail notice when your article appears on Elsevier's online service ScienceDirect (www.sciencedirect.com). That e-mail will include the article's Digital Object Identifier (DOI). This number provides the electronic link to the published article and should be included in the posting of your personal version. We ask that you wait until you receive this e-mail and have the DOI to do any posting.
Central Storage: This license does not include permission for a scanned version of the material to be stored in a central repository such as that provided by Heron/XanEdu.

18. **Author website** for books with the following additional clauses:

Authors are permitted to place a brief summary of their work online only.
A hyper-text must be included to the Elsevier homepage at <http://www.elsevier.com>

All content posted to the web site must maintain the copyright information line on the bottom of each image

You are not allowed to download and post the published electronic version of your chapter, nor may you scan the printed edition to create an electronic version.

Central Storage: This license does not include permission for a scanned version of the material to be stored in a central repository such as that provided by Heron/XanEdu.

19. **Website** (regular and for author): A hyper-text must be included to the Homepage of the journal from which you are licensing at <http://www.sciencedirect.com/science/journal/xxxxx>. or for books to the Elsevier homepage at <http://www.elsevier.com>

20. **Thesis/Dissertation**: If your license is for use in a thesis/dissertation your thesis may be submitted to your institution in either print or electronic form. Should your thesis be published commercially, please reapply for permission. These requirements include permission for the Library and Archives of Canada to supply single copies, on demand, of the complete thesis and include permission for UMI to supply single copies, on demand, of the complete thesis. Should your thesis be published commercially, please reapply for permission.

21. **Other Conditions**:

v1.6

If you would like to pay for this license now, please remit this license along with your payment made payable to "COPYRIGHT CLEARANCE CENTER" otherwise you will be invoiced within 48 hours of the license date. Payment should be in the form of a check or money order referencing your account number and this invoice number RLNK500779947. Once you receive your invoice for this order, you may pay your invoice by credit card. Please follow instructions provided at that time.

Make Payment To:
Copyright Clearance Center
Dept 001
P.O. Box 843006
Boston, MA 02284-3006

For suggestions or comments regarding this order, contact RightsLink Customer Support: customercare@copyright.com or +1-877-622-5543 (toll free in the US) or +1-978-646-2777.

Gratis licenses (referencing \$0 in the Total field) are free. Please retain this printable license for your reference. No payment is required.

SPRINGER LICENSE TERMS AND CONDITIONS

May 17, 2012

This is a License Agreement between Arathi Mohan Sharma ("You") and Springer ("Springer") provided by Copyright Clearance Center ("CCC"). The license consists of your order details, the terms and conditions provided by Springer, and the payment terms and conditions.

All payments must be made in full to CCC. For payment instructions, please see information listed at the bottom of this form.

License Number	2910300583964
License date	May 15, 2012
Licensed content publisher	Springer
Licensed content publication	Journal of Polymers and the Environment
Licensed content title	Challenges in Biomass–Thermoplastic Composites
Licensed content author	Roger M. Rowell
Licensed content date	Oct 1, 2007
Volume number	15
Issue number	4
Type of Use	Thesis/Dissertation
Portion	Figures
Author of this Springer article	No
Order reference number	
Title of your thesis / dissertation	Mechanical behaviour, water absorption and morphology of wheat straw, talc, mica and wollastonite filled polypropylene composites
Expected completion date	Aug 2012
Estimated size(pages)	150
Total	0.00 USD
Terms and Conditions	

Date: Wed, 16 May 2012 13:55:25 +0200 [16/05/2012 07:55:25 EDT]

From: Josiger Gabriele <Gabriele.Josiger@hanser.de>

To: 'amohansh@uwaterloo.ca' <amohansh@uwaterloo.ca>

Subject: AW: Re: AW: Request for permission to use figures from book(2006)

Dear Mr. Arathi,

I am pleased to grant you permission to reprint the figures of this publication as mentioned in your mail. We only require that you quote the complete source of the original illustration (author, title, Carl Hanser Verlag Munich, as well as year of publication).

Sincerely
Gabriele Josiger
Publishing Assistant

-----Ursprüngliche Nachricht-----

Von: amohansh@uwaterloo.ca [mailto:amohansh@uwaterloo.ca]

Gesendet: Mittwoch, 16. Mai 2012 13:47

An: Josiger Gabriele

Betreff: Fwd: Re: AW: Request for permission to use figures from book(2006)

Hi Gabriele,

They are the figure numbers 1.8 "Principal types of tacticity found in polypropylene" and Figure 19.8 "Two phase structure of impact modified polypropylene".

Please could you help me get permission at the earliest?

Thank you
Arathi Sharma
University of Waterloo

Date: Tue, 15 May 2012 09:00:36 +0200 [15/05/2012 03:00:36 EDT]

From: Josiger Gabriele <Gabriele.Josiger@hanser.de>

To: 'amohansh@uwaterloo.ca' <amohansh@uwaterloo.ca>

Subject: AW: Request for permission to use figures from book(2006)

Dear Mr. Sharma,

thank you for your request. Please let me know, which figures do you like to use. We must check if we have the rights.

Best,
Gabriele

-----Ursprüngliche Nachricht-----

Von: amohansh@uwaterloo.ca [mailto:amohansh@uwaterloo.ca]

Gesendet: Montag, 14. Mai 2012 18:34

An: Info

Betreff: Request for permission to use figures from book(2006)

Hello,

I am a Master's Student from the university of Waterloo, Ontario, Canada.

I am currently working on my master's thesis related to my work on Polymer Composites and would like to use figures on stereoregularity and impact modified polypropylene from the book titled "Polymer Chemistry: Properties and Applications" by Andrew Peacock and Allison Calhoun, 2006.

Please could you let me know whom to contact in this regard?

Regards

Arathi Sharma

MASc Candidate

University of Waterloo

APPENDIX

Appendix A: DSC plots for the pure resins – homopolymer PP, copolymer PP and homo-copolymer blend PP.

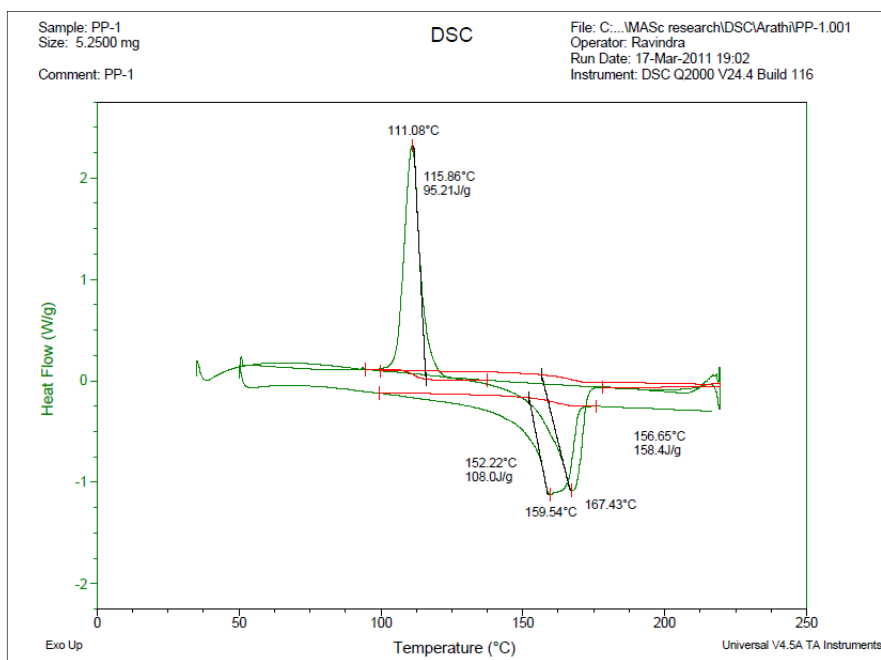


Figure A.1 DSC Plot for Homopolymer PP without Antioxidant

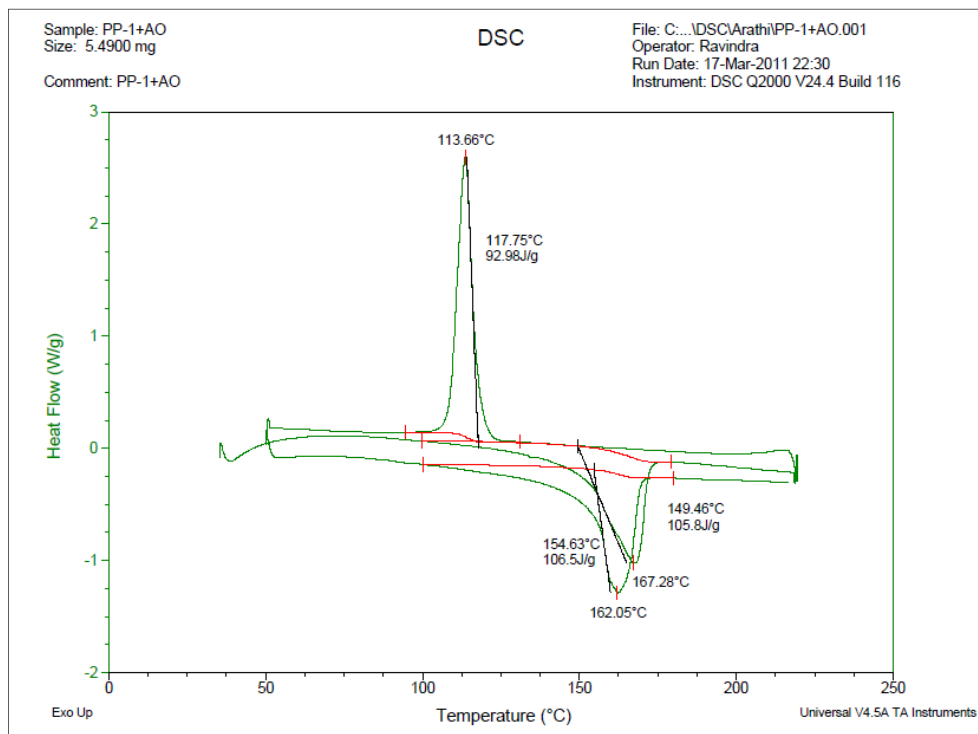


Figure A.2 DSC Plot for Homopolymer PP with Antioxidant

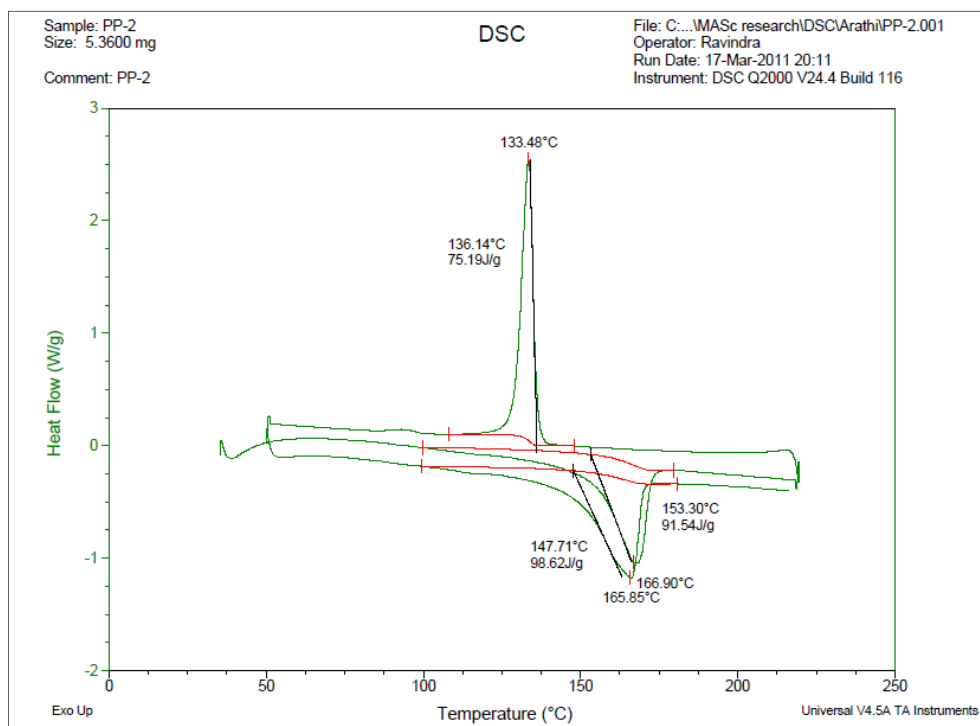


Figure A.3 DSC Plot for Impact Copolymer PP without Antioxidant

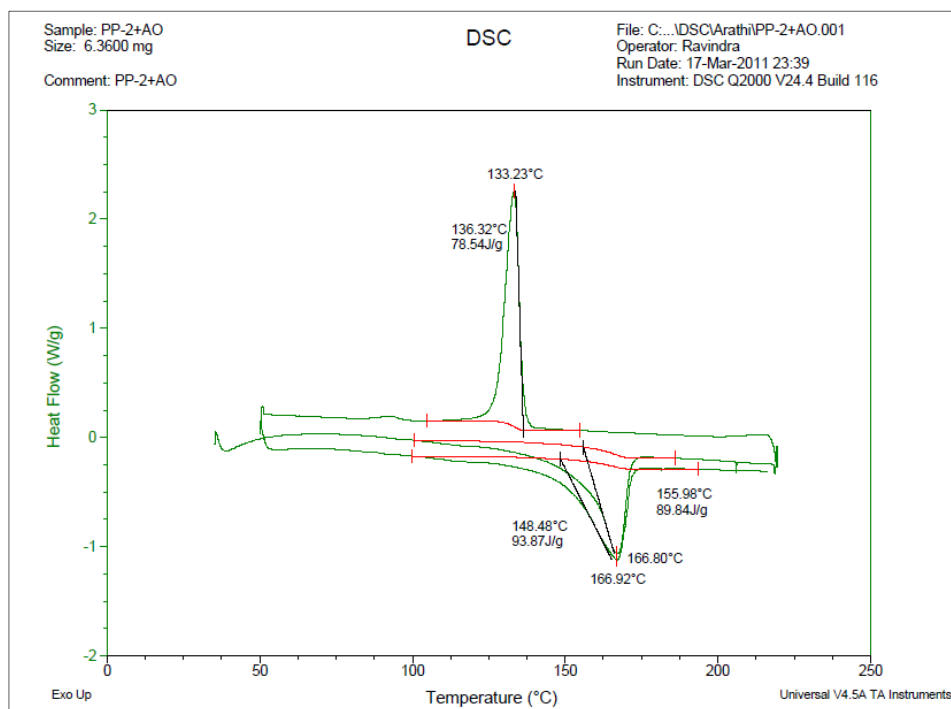


Figure A.4 DSC Plot for Impact Copolymer PP with Antioxidant

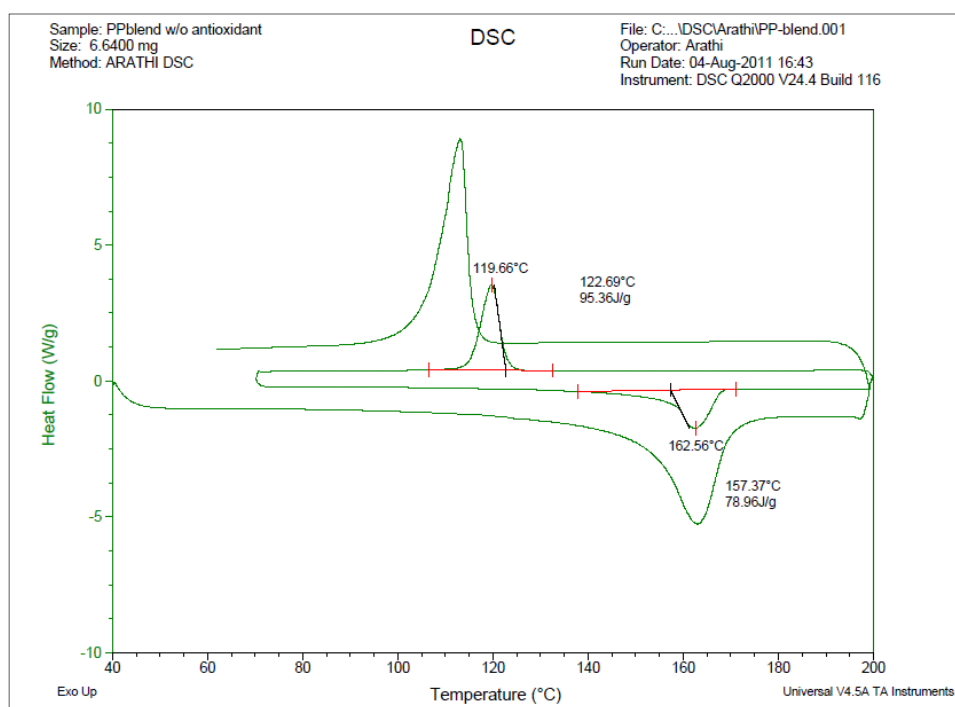


Figure A.5 DSC Plot for Homopolymer-Copolymer Blend PP without Antioxidant

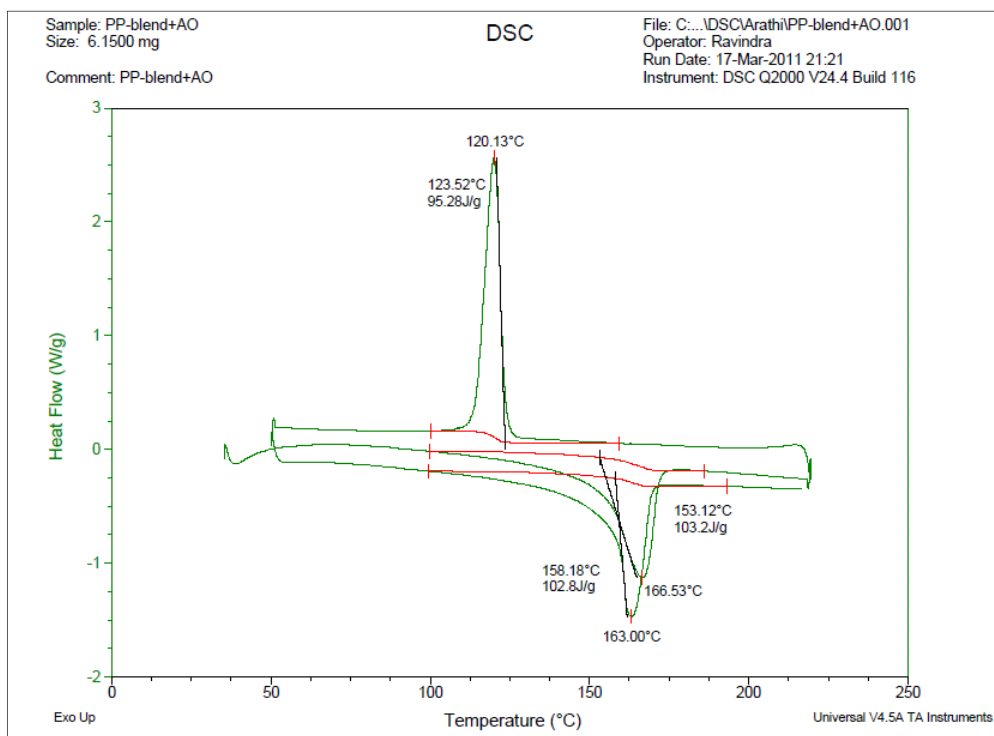


Figure A.6 DSC Plot for Homopolymer-Copolymer Blend PP with Antioxidant

Appendix B:

SEM



Figure A.7 SEM of 30wt% mWS-hPP Composite (100X)

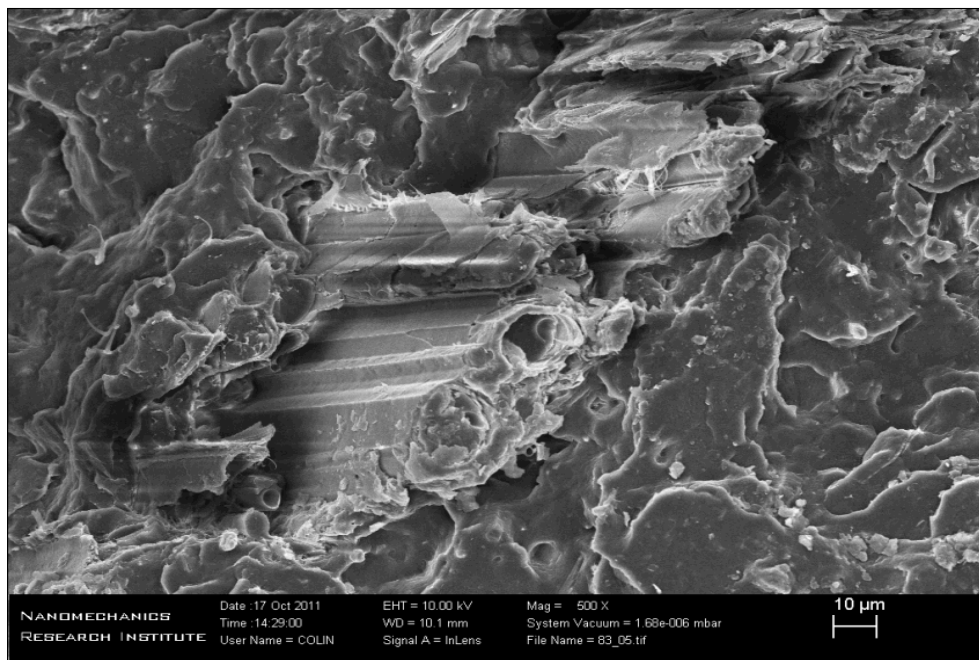


Figure A.8 SEM of 15% wollastonite-15% fWS-hPP Composite (500X)

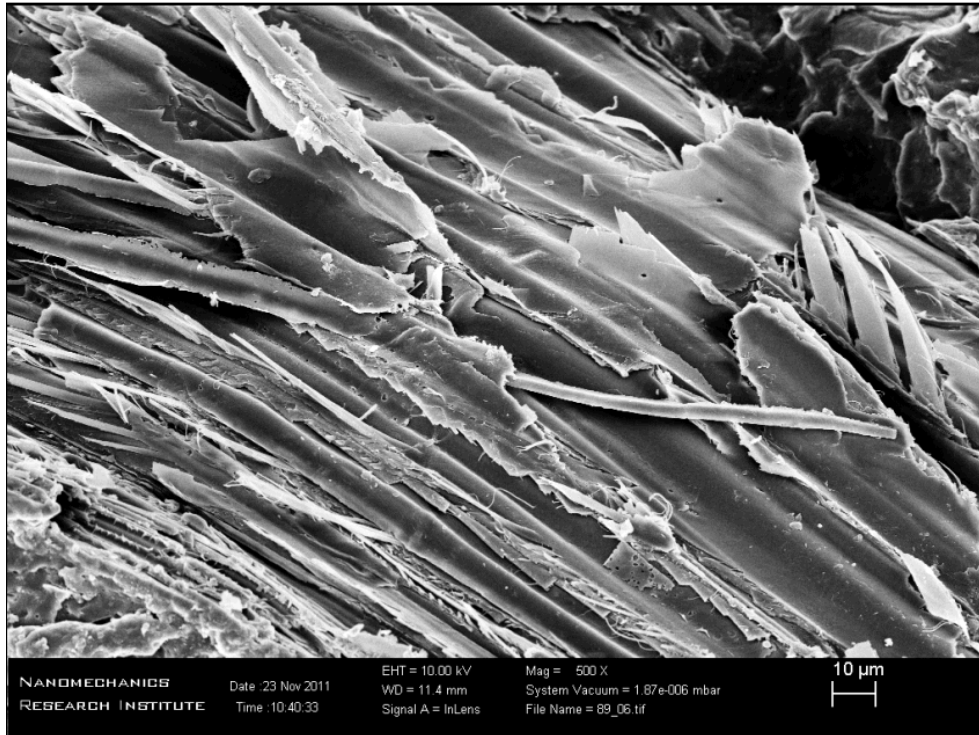


Figure A.9 SEM of 15% wollastonite-15%fWS-bPP Composite (500X)

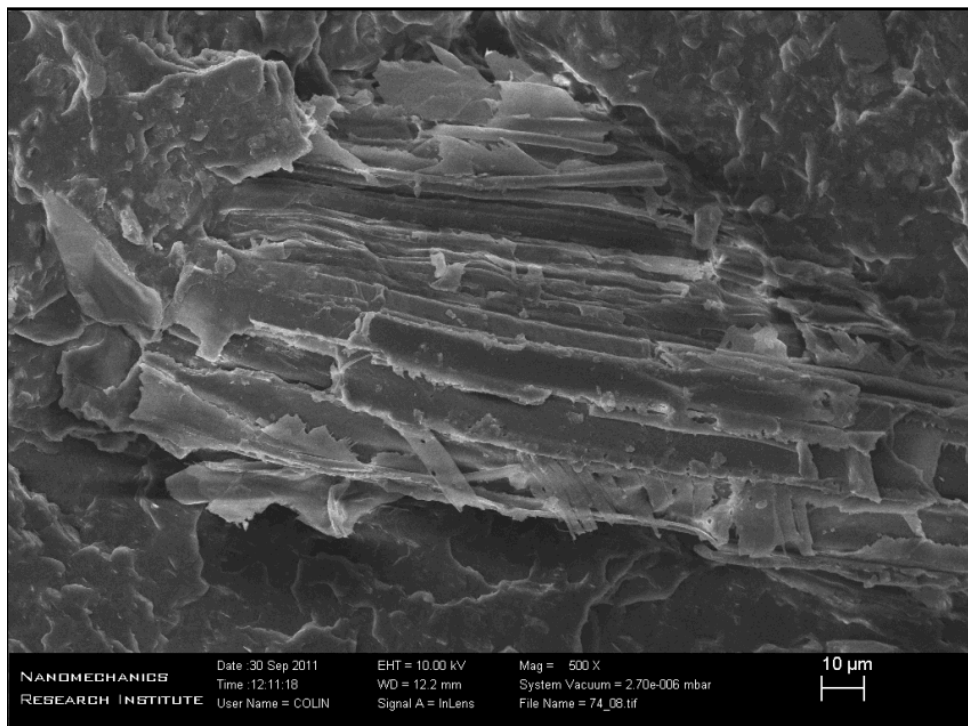


Figure A.10 SEM of 15% mica-15%mWS-hPP Composite (500X)

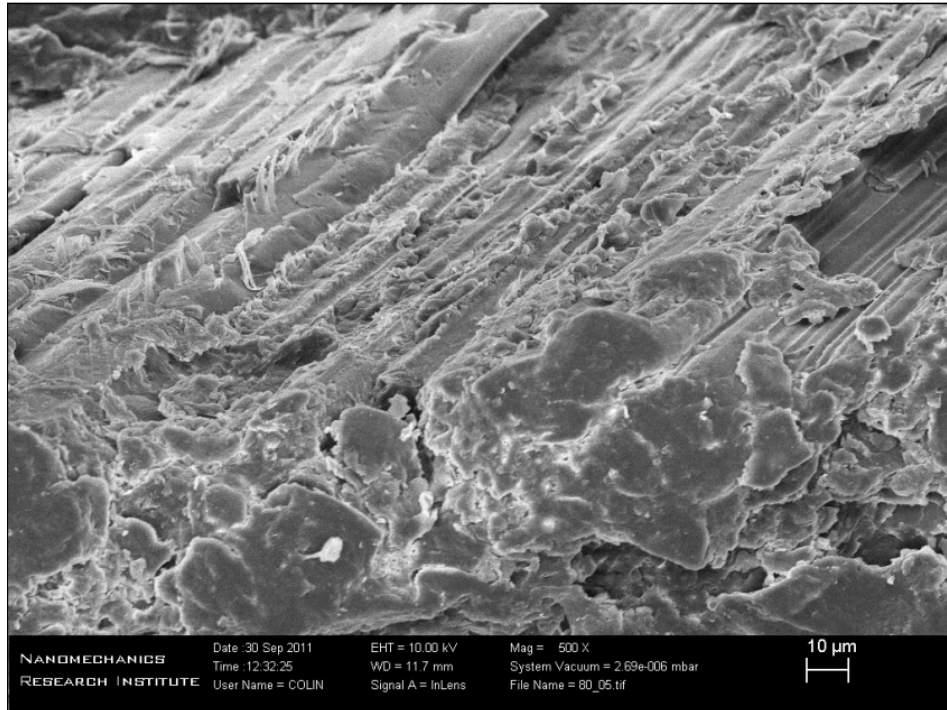


Figure A.11 SEM of 15% mica-15% mWS-bPP Composite (500X)

Appendix C: Material Data Sheets

D180M

Homopolymer Polypropylene

- Low Gas Fade
- Suggested Uses Include BCF Multi-Filaments, High Tenacity Continuous Filament Yarn, Fine Denier Staple Fibers

Property	Units	Typical Value	Test Method
Nominal Melt Flow Rate (230°C/2.16kg)	g/10 min	18	ASTM D1238
Tensile Strength at Yield (2 in/min, 50 mm/min)	psi MPa	5,100 35	ASTM D638
Elongation at Yield (2 in/min, 50 mm/min)	%	9	ASTM D638
Flexural Modulus (0.05 in/min, 1.3 mm/min, 1% secant)	psi MPa	190,000 1,310	ASTM D790A
Notched Izod Impact Strength at 23°C	ft-lbs/in J/m	0.5 27	ASTM D256A
Rockwell Hardness	R	104	ASTM D785
Tenacity of Fibers (3.3 draw ratio, 1,250 m/min roll speed, 225°C spin temperature, D1000/68)	g/denier	2.9	ASTM D2256
Elongation of Fibers (3.3 draw ratio, 1,250 m/min roll speed, 225°C spin temperature, D1000/68)	%	93	ASTM D2256
Suggested Takeup Roll Speed	ft/min m/min	6,561 2,000	Sunoco Chemicals

Information contained herein is considered accurate to our best knowledge. It is offered for your consideration and investigation, and is not to be construed as a representation or warranty, expressed or implied, for which Sunoco Chemicals assumes legal responsibility. Our warranties are limited to those expressly stated in formal contracts or in conditions of sale on our invoices and order acceptances. Conditions and methods of use vary and are beyond the control of Sunoco Chemicals. Sunoco Chemicals, therefore, disclaims any liability incurred as a result of the use of its products in accordance with the data contained herein. No information herein shall be construed as an offer of indemnity for infringement or as a recommendation to use these products in such a manner as to infringe any patent, domestic or foreign.

Material Data Sheet for Homopolymer PP



TI6200N

High Impact Copolymer Polypropylene

- High Impact Copolymer, Superior Stiffness / Impact Balance, Antistatic
- Suggested Uses Include Compounding, Injection Molding, Automotive Applications, Consumer Products, Industrial

Property	Units	Typical Value	Test Method
Nominal Melt Flow Rate (230°C/2.16kg)	g/10 min	18	ASTM D1238
Tensile Strength at Yield (2 in/min, 50 min/min)	psi MPa	2,850 20	ASTM D638
Flexural Modulus (0.05 in/min, 1.3 mm/min, 1% secant)	psi MPa	170,000 1,172	ASTM D790A
Notched Izod Impact Strength at 23°C		No Break	ASTM D256A

Information contained herein is considered accurate to our best knowledge. It is offered for your consideration and investigation, and is not to be construed as a representation or warranty, expressed or implied, for which Sunoco Chemicals assumes legal responsibility. Our warranties are limited to those expressly stated in formal contracts or in conditions of sale on our invoices and order acceptances. Conditions and methods of use vary and are beyond the control of Sunoco Chemicals. Sunoco Chemicals, therefore, disclaims any liability incurred as a result of the use of its products in accordance with the data contained herein. No information herein shall be construed as an offer of indemnity for infringement or as a recommendation to use these products in such a manner as to infringe any patent, domestic or foreign.

For cautions and other information relating to handling of
and exposure to this product, please see material safety
data sheet code number C4004 published by Sunoco Chemicals.

550 Technology Drive
Pittsburgh, PA 15219
1-800-223-8871

Revision Date: Monday,
March 23, 2009
www.sunocochemicals.com

Material Data Sheet for Impact Copolymer PP

DuPont Fusabond® MD353D Random Copolymer Polypropylene		
Categories:	Other Engineering Material ; Additive/Filler for Polymer ; Polymer ; Thermoplastic ; Polypropylene	
Material Notes:	<p>Typical Use:</p> <ul style="list-style-type: none"> • Coupling agent • Long glass filled polypropylene • Coupling agent for nonhalogen, flame retarded wire and cable compounds containing magnesium hydroxide • Adhesion promoter • Natural fiber wood-plastic compounds <p>Availability: North America</p> <p>Information provided by DuPont.</p>	
Vendors:	No vendors are listed for this material. Please click here if you are a supplier and would like information on how to add your listing to this material.	
Physical Properties	Original Value	Comments
Melt Flow	450 g/10 min @Load 2.16 kg, Temperature 190 °C	
Thermal Properties	Original Value	Comments
Melting Point	136 °C	
Descriptive Properties		
MAH Graft Level, wt%	Very High	FTIR (DuPont)
<p>Some of the values displayed above may have been converted from their original units and/or rounded in order to display the information in a consistent format. Users requiring more precise data for scientific or engineering calculations can click on the property value to see the original value as well as raw conversions to equivalent units. We advise that you only use the original value or one of its raw conversions in your calculations to minimize rounding error. We also ask that you refer to MatWeb's terms of use regarding this information. Click here to go back to viewing the property data in MatWeb's normal format.</p>		

Material Data Sheet for Fusabond MD 353D Maleic Anhydride Grafted PP Coupling Agent



®IRGANOX 1010

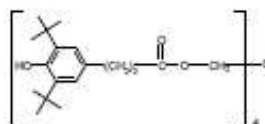
Phenolic Primary Antioxidant for Processing and Long-Term Thermal Stabilization

Characterization [®]IRGANOX 1010 - a sterically hindered phenolic antioxidant - is a highly effective, non discoloring stabilizer for organic substrates such as plastics, synthetic fibers, elastomers, adhesives, waxes, oils and fats. It protects these substrates against thermo-oxidative degradation.

Chemical Name Pentaerythritol Tetrakis(3-(3,5-di-tert-butyl-4-hydroxyphenyl)propionate)

CAS Number 6683-19-8

Structure [®]IRGANOX 1010



Molecular weight 1178

Applications [®]IRGANOX 1010 can be applied in polyolefins, such as polyethylene, polypropylene, polybutene and olefin copolymers such as ethylene-vinylacetate copolymers. Also, its use is recommended in other polymers such as polyacetals, polyamides and polyurethanes, polyesters, PVC, styrene homo- and copolymers, ABS, elastomers such as butyl rubber (IIR), SBS, SEBS, EPM and EPDM as well as other synthetic rubbers, adhesives, natural and synthetic tackifier resins, and other organic substrates.

Features/ Benefits [®]IRGANOX 1010 has good compatibility, high resistance to extraction and low volatility. It is odorless and tasteless.

The product can be used in combination with other additives such as costabilizers (e.g. thioethers, phosphites, phosphonites), light stabilizers and other functional stabilizers. The effectiveness of the blends of [®]IRGANOX 1010 with [®]IRGAFOS 168 ([®]IRGANOX B-blends) or with [®]IRGAFOS 168 and HP-136 ([®]IRGANOX HP products) is particularly noteworthy.

Product Forms

Code:
powder
FF (C)
DD

Appearance:
white, free-flowing powder
white, free-flowing granules
white to slightly green pellets

Distributed by
Wi

Date first Edition:
Printing Date: Aug-88

Product Name: [®]IRGANOX 1010

page 1
[®]Ciba Specialty Chemicals, Inc.

Guidelines for Use Already 500 ppm - 1000 ppm of [®]IRGANOX 1010 provide long-term thermal stability to the polymer. Concentrations up to several percent may be used depending on the substrate and the requirements of the end application.
In polyolefins the concentration levels for [®]IRGANOX 1010 range between 0.05% and 0.4% depending on substrate, processing conditions and long-term thermal stability requirements. The optimum level has to be determined application specific.
Concentration levels of [®]IRGANOX 1010 in hot melt adhesives range from 0.2% to 1%. In synthetic tackifier resins, [®]IRGANOX 1010 concentration ranges between 0.1% and 0.5%. Extensive performance data of [®]IRGANOX 1010 in various organic polymers and applications are available upon request.

Physical Properties

Melting Range (°C)	110-125
Flashpoint (°C)	297
Specific Gravity (20°C)	1.15 g/cm ³
Bulk density	powder: 530 - 630 g/l FF (C): 480 - 570 g/l DD: 450 - 550 g/l
Solubility (20°C)	g/100g solution
Acetone	47
Chloroform	71
Ethanol	1.5
Ethylacetate	47
n-Hexane	0.3
Methanol	0.9
Methylene Chloride	63
Toluene	60
Water	<0.01

Handling & Safety In accordance with good industrial practice, handle with care and prevent contamination of the environment. Avoid dust formation and ignition sources.
For more detailed information please refer to the material safety data sheet.

Registration

[®]IRGANOX 1010 is listed on the following inventories:

Australia: AICS	Canada: DSL	China: First Import
Europe: EINECS	Japan: MITI	Korea: ECL
Philippines: PICCS	USA: TSCA	

[®]IRGANOX 1010 is approved in many countries for use in food contact applications.
For detailed information refer to our Positive List or contact your local sales office.

IMPORTANT: The following supersedes Buyer's documents. SELLER MAKES NO REPRESENTATION OR WARRANTY, EXPRESS OR IMPLIED, INCLUDING OF MERCHANTABILITY OR FITNESS FOR A PARTICULAR PURPOSE. No statements herein are to be construed as inducements to infringe any relevant patent. Under no circumstances shall Seller be liable for incidental, consequential or indirect damages for alleged negligence, breach of warranty, strict liability, tort or contract arising in connection with the product(s). Buyer's sole remedy and Seller's sole liability for any claims shall be Buyer's purchase price. Data and results are based on controlled or lab work and must be confirmed by Buyer by testing for its intended conditions of use. The product(s) has not been tested for, and is therefore not recommended for, uses for which prolonged contact with mucous membranes, abraded skin, or blood is intended, or for uses for which implantation within the human body is intended.

Date first Edition: Product Name: [®]IRGANOX 1010
Printing Date: Aug-08

page 2
©Ciba Specialty Chemicals, Inc.

Material Data Sheet for Irganox 1010 antioxidant

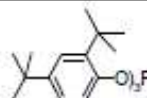


Ciba® IRGAFOS® 168 Processing Stabiliser

General

IRGAFOS 168 is a tris(aryl)phosphite processing stabiliser. It is a highly effective, low-volatile and hydrolysis resistant antioxidant for coating resins. It protects the resin polymer against oxidation during resin synthesis, manufacturing of the paint, processing (thermal curing and overbaking) and the designed life-time of the final coating. IRGAFOS 168 provides excellent protection against discolouration and change of physical properties caused by excessive heat exposure.

Chemical Structure



Tris (2,4-di-tert-butylphenyl)phosphite; Molecular Weight: 646.9
CAS Number: 31570-04-4

Physical Properties (typical values)

IRGAFOS 168 is offered in two different product forms:

Appearance:	white powder	IRGAFOS 168
	white free-flowing powder	IRGAFOS 168 FF

Melting point: 185°C

Solubility (g/100g solution) at 20°C:

Acetone	1
Cyclohexane	10
Hexane	11
Ethanol	0.1
Methanol	< 0.01
Ethyl acetate	4
Toluene	30
Water	< 0.01 (degradation)

Applications

IRGAFOS 168 provides outstanding thermal and colour stability to a variety of coating resins upon exposure to high temperatures during synthesis and subsequent processing. It is particularly suited to stabilise alkyd and polyester resin based coating systems that are used in applications such as:

- industrial powder coatings (electrical and gas oven heating)
- coil coatings
- other industrial high bake coatings

A special feature of the IRGAFOS 168 phosphite stabiliser is its

Ciba® IRGAFOS® 168 Processing Stabiliser



efficiency in presence of NO_x gases and thus its potential to function in critical gas oven curing conditions.

In electrical ovens and gas fired ovens where the coated substrates being exposed to only very low NO_x concentrations, a combination IRGAFOS 168 with hindered phenolic antioxidants such as IRGANOX 1076 or IRGANOX 1010 typically leads to a synergistic performance improvement. In the presence of NO_x, the same combination often exhibits adverse discolouration effects, however. In this case phenol-free synergistic antioxidant systems can be obtained by using IRGAFOS 168 in combination with hindered amine light stabilisers (HALS) such as TINUVIN 111 FD, TINUVIN 292 or TINUVIN 622 LD.

For improved performance IRGAFOS 168 may also be combined with other phosphite or phosphonite co-stabilizers such as IRGAFOS 38, IRGAFOS XP 40 and IRGAFOS XP 60 or with thiosynergists such as IRGANOX PS 800.

The amount of IRGAFOS 168 required for optimum performance should be determined in trials covering a concentration range.

Recommended concentration: (based on resin solids)

<ul style="list-style-type: none">• Industrial powder coatings• coil coatings• other industrial high bake coatings	0.2 - 0.8% IRGAFOS 168 alone or in combination with synergists
--	---

Safety and Handling

IRGAFOS 168 is sensitive to moisture. Commercial quantities are offered in special metallised plastic inner packagings to prevent hydrolysis of the product upon storage. To ensure optimum performance, opened packages and small samples should be used up without delay and care taken to avoid exposure to moist environments.

IRGAFOS 168 should be handled in accordance with good industrial practice. Detailed information is provided in the Safety Data Sheet.

Trademark

IRGAFOS and IRGANOX are registered trademarks.

Important Notice

IMPORTANT: The following supersedes Buyer's documents. SELLER MAKES NO REPRESENTATION OR WARRANTY, EXPRESS OR IMPLIED, INCLUDING OF MERCHANTABILITY OR FITNESS FOR A PARTICULAR PURPOSE. No statements herein are to be construed as inducements to infringe any relevant patent. Under no circumstances shall Seller be liable for incidental, consequential or indirect damages for alleged negligence, breach of warranty, strict liability, tort or contract arising in connection with the product(s). Buyer's sole remedy and Seller's sole liability for any claims shall be

Ciba® IRGAFOS® 168
Processing Stabiliser



Buyer's purchase price. Data and results are based on controlled or lab work and must be confirmed by Buyer by testing for its intended conditions of use. The product(s) has not been tested for, and is therefore not recommended for, uses for which prolonged contact with mucous membranes, abraded skin, or blood is intended; or for uses for which implantation within the human body is intended.

Material Data Sheet for Irgafos 168 Antioxidant



Georgia Industrial Minerals, Inc.

CD-2200 Muscovite Mica

Markets

CD-2200 is a water ground muscovite mica that has optimum delamination and high purity. Our patented process produces a mica product that gives optimum performance in a variety of applications. In addition to excellent color, CD-2200 creates a functional pigment that is very desirable where low bulk density, fineness, high aspect ratio, and excellent coverage are required.

Applications

The major applications for CD-2200 are:

Foundry coatings	Mold releases
Wire & cable	Engineering plastics
Asphalt products	Gaskets
Asbestos replacement	Sealants, caulks
High temp coatings	Industrial primers
Exterior coatings	Marine coatings

Performance Characteristics

The performance characteristics that make CD-2200 an acceptable cost effective additive for these markets are:

- Excellent color
- Ease of dispersion
- Chemical inertness
- Increased coverage
- Superior barrier properties
- High temperature stability
- Superior dielectric properties
- Superior reinforcement properties

Plant Location : Deepstep Community
1132 Veal Road
Sandersville, Ga. 31082
Phone: (478) 553-0048
Fax: (478) 553-0050

<u>Physical Properties</u>	<u>Specifications</u>	<u>Typical</u>
Mean Particle Size, microns	18 - 22	20
Sieve Analysis, % retained		
+100 mesh	0.1 max.	0.08
+200 mesh	1 max.	0.25
+325 mesh	2.0 max.	1.0
Bulk Density (Colgate method)	10 - 14	12
Moisture Loss, 100C °, %	0.5 max.	0.3
Color, L value	90 min.	

Chemical Properties

Mineral	Muscovite mica
Chemical Composition	Potassium aluminum silicate
Specific gravity	2.82
CAS#	12001-26-2
ph	6.0 – 7.5

Regulatory

GIM mica meets the FDA requirements of Title 21 CFR § 175.105.5 Adhesives; §175.300 Resinous & Polymeric coatings; §177.1520(B) Olefin polymers; §177.2800 Rubber articles intended for repeated use; §178.3297 Colorants for polymers. Meets CTFA 73.2498 for use in cosmetics. These mica products are listed on the US TSCA list and Canadian DSL. See MSDS for safety and additional regulatory information.

Contacts

Sales Manager:	Product Manager:
Jim Barton	Jerry Korte
(864) 984-4266	(706) 376-5200
Office & Fax	Office & Fax
jbarton@gimmica.com	jkorte@gimmica.com

The statements herein are based on data which is believed to be reliable. This data is offered in good faith and typical of normal production. GIM makes no warranty or representation, expressed or implied, regarding the accuracy of this data or the use of this product. The user is solely responsible for the use of this product. Updated 11/15/05
Meets: CTFA

Material Data Sheet for Mica CD 2200

NYCO[®]

premium quality wollastonite

NYCO SUPPLIES PREMIUM QUALITY WOLLASTONITE TO THE WORLD

NYCO is not only the foremost supplier
of wollastonite in the world,
we are also the first...

Since our pioneering plant at Willbore,
New York opened in 1953, to our most
recent development of a world class
deposit in the Sonora desert of Mexico,
NYCO has led the world in its growing
acceptance of wollastonite.

- + highest quality ores
- + state-of-the-art processing
- + world class treatment facilities
- + market leading reliability
& technical service
- + 100 plus years of reserves

The data contains general information and describes
typical properties only. It is offered for use by
persons qualified to determine for themselves the
suitability of our products for particular purposes.
No guarantee is made or liability assumed, the
application of this data and the products described
herein being at the sole risk of the user.

TYPICAL PROPERTY	TYPICAL VALUE	METHOD
G.E. Brightness	90	ASTM E97
Oil Absorption (lbs./100 lbs.)	80	ASTM D281
Bulk Density		
Loose (lbs./cu.ft.)	14.0 (17.0)*	ASTM C87
(g/cc)	0.22 (0.27)*	ASTM C87
Tapped (lbs./cu.ft.)	30.0 (35.0)*	ASTM C87
(g/cc)	0.48 (0.56)*	ASTM C87
Median Particle Size (µm)	8	CILAS GRANULOMETER
Surface Area (m ² /g) (BET)	1.2	ASAP 2405 (Micromeritics)
Minus 325 U.S. Mesh Screen (%)	99.0	Alpine Jet Sieve
Moisture (%)	0.10	Karl Fischer
Loss on Ignition (1000°C) (%)	0.42 (0.55)*	ASTM D1208
*Typical values for surface treatments		



NYGLOS[®] 8

CHEMICAL COMPOSITION: CaSiO ₃		
COMPONENT	TYPICAL VALUE (%)	
CaO	46.15	
SiO ₂	51.60	
Fe ₂ O ₃	0.77	
Al ₂ O ₃	0.34	
MnO	0.16	
MgO	0.38	
TiO ₂	0.05	
K ₂ O	0.05	
Wt. Loss (1000°C)	0.50	

NYCO[®]

One Mineral, A World Of Applications

UNITED STATES
P.O. Box 368
803 Mountain View Drive
Willsboro, NY
12996-0368, USA
Tel: (518) 963-4262
Fax: (518) 963-1110

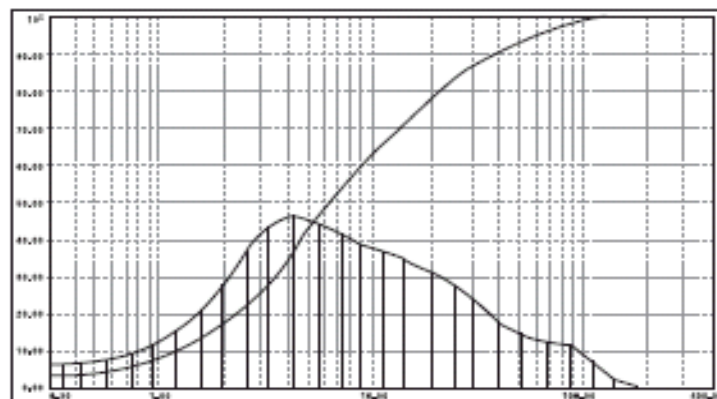
EUROPE
Belgium
Tel: (32) 10 88 13 02
Fax: (32) 10 22 65 99

MEXICO
Hermosillo, Sonora
Mexico CP 83005
Tel: (52) 62 89 10 00
Fax: (52) 62 89 10 90

www.nycominerals.com
info@nycominerals.com

TYPICAL PROPERTIES	VALUE
APPEARANCE	WHITE
MORPHOLOGY	ACICULAR
MOLECULAR WEIGHT	116
SPECIFIC GRAVITY	2.9
REFRACTIVE INDEX	1.63
pH (10% SLURRY)	9.9
WATER SOLUBILITY (g/100cc)	0.0095
DENSITY (lbs./cu.ft.)	181
BULKING VALUE (gal./lbs.)	0.0413
MOHS HARDNESS	4.5
COEFFICIENT OF EXPANSION (mm/mm/°C)	6.5 X 10 ⁻⁶
MELTING POINT (°C) - theoretical	1540
MELTING POINT (°C) -by ASTM D1857	1410

CILAS GRANULOMETER CURVE



Technical data sheets on other wollastonite products and comprehensive health & safety information are available upon request.

NYGLOS[®] 8

Material Data Sheet for Wollastonite (Nyglos 8)